Role of Transient Receptor Potential channels in mammalian oviduct and uterine epithelia.

(PhD)

Maryam Ghavideldarestani

BSc. (Azad University of Tonekabon)

MSc. (University of Hull)

October, 2011

Hull York Medical School

University of Hull

Dedication

This thesis is dedicated to my loving parents

Mahtab Mousavi Darestani and Abbas Ghavidel Darestani

who have always supported me financially and morally

and encouraged me when it was most needed.

Acknowledgments

I would like to express my thanks to my supervisor, Dr Roger G Sturmey, whose scientific and moral support has always been with me throughout the difficult times of my research.

I wish to express my gratefulness to Prof Henry J Leese who always inspired me with his knowledge and humanity.

I would also like to thank Prof Stephen Atkins for supporting me throughout my PhD project.

I would like to express a special word of thanks to my family who have never stopped being supportive. A special thanks to my mother and father who light the path of my life and my siblings Mahmoud, Mehrnoosh and Masoud who tirelessly encouraged me by their word of assurance.

My thanks and appreciation to Mehdi and Fereshteh for their moral support.

I am also grateful to my friends; Vahideh, Negar, Nasim, Smaira, Mehran, Marjan, Mohammad, Nikoleta, Paul, Veerle, Patty and many others who have always been there when they were needed.

Abstract

Calcium is an important secondary messenger and plays a major role in cell function, including proliferation, cell growth, secretion and death .It also plays a critical role in uterine smooth muscle contraction and embryo implantation. This thesis is concerned with calcium homeostasis in epithelial tissue lining the oviduct and uterus which are key players in early reproductive events, being involved in gamete transport, sperm capacitation and providing the micro-environment for the gametes and early embryo. Calcium transport across epithelial cells is either via tight junctions or calcium channels, specifically, members of the transient receptor potential (TRP) channel superfamily and the Na+/Ca2+ exchanger. TRP channels are an important class of calcium channels with more than 28 identified members and their potential involvement in calcium transport in uterus and oviduct epithelia has yet to be determined. The aim of this study was to discover which TRPC isoforms are expressed in epithelial cells lining the female reproductive tract in the bovine and human. Gene expression of TRPC channels changes was measured throughout the estrous cycle in bovine oviduct and uterine epithelial cells using Real-Time PCR, while immunohistochemistry, immunocytochemistry and western blotting were used to discover the localization of TRPC channels in oviduct/uterine epithelium and changes in protein expression of TRPC isoforms induced by sex hormones. . to The physiological role of TRPC isofoms in regulating intracellular calcium concentration in bovine oviduct epithelial cells was determined using a calcium assay approach and finally. the potential clinical relevance of a possible role of TRP channels in female reproduction was investigated.

OF 7 members of TRPC family, TRPC1, 2, 3, 4 and 6 were expressed in bovine oviduct and uterine epithelia. In human endometrium, TRPC1, 6 and 7 genes were detected. Expression levels of all TRPC isoforms present in both bovine oviduct and uterine epithelia changed throughout the estrous cycle. 17β-estradiol, FSH and LH individually and in combination up-regulated gene expression of TRPC isoforms in bovine oviduct epithelial cells. However, progesterone inhibited the up-regulatory effect of 17β-estradiol, FSH and LH on TRPCs gene

expression. TRPC1 and TRPC6 which are the common TRPC isoforms in bovine oviduct/uterine epithelium and human endometrium were localized on the apical, basal and lateral membranes of the epithelial tissue in bovine oviduct/uterus and human endometrium. TRPC isoforms were physiologically active in bovine oviduct epithelial cells (BOEC). SKF96365 which is a general TRP channel blocker inhibited the calcium influx into BOEC. Furthermore, Hyperforin which is a TRPC6 channel activator increased the intracellular calcium concentration in BOEC. TRPC1, 6 and 7 expression in endometrium of patients being treated for infertility by IVF illustrated that gene expression of TRTPC1 and 6 were up regulated in the endometrium of the IVF patients compared to controls. However, gene expression of TRPC7 in IVF patients was down-regulated compared to that of the endometrium of the control group. Gene expression of TRPC6 and 7 in endometrium of women with Poly Cystic Ovarian Syndrome (PCOS) who have higher level of LH and normal FSH level, alongside the absence of the post-ovulatory increase in progesterone secretion, were up -regulated compared to that of the control group. However, the expression level of TRPC1 in endometrium of PCOS patients was not significantly different compared to the control group.

Gene expression of TRPC isoforms in the epithelia lining the female reproductive tract is possibly regulated by sex hormones via nuclear factor-kappa B (NF-KB) signalling pathway. However, further investigation is required to determine the mechanisms underlying the endocrine regulation of TRPC channels.

Publications

- Xu SZ, Zhong W, Ghavideldarestani M, Saurabh R, Lindow SW, and Atkin SL.(2009) Multiple mechanisms of soy isoflavones against oxidative stress-induced endothelium injury. *Free Radical Biology & Medicine*. **47** (2). 167-75

- Maryam Ghavideldarestani, Stephen Atkin, Henry Leese, and Roger Sturmey (2011) Expression of transient receptor potential canonical (TRPC) channels in female bovine reproductive tract. *Human Fertility* (published abstract)

Abbreviations

APS Ammonium Persulfate

BOEC Bovine Oviduct Epithelial Cells

BSA Albumin from Bovine Serum

BUEC Bovine Uterine Epithelial Cells

cDNA complementary Deoxyribonucleic acid

DAPI 4',6-diamidino-2-phenylindole

DBQ 2.5-Di-t-butylhydroquinone

DEPC Diethylpyrocarbonate

dATP Deoxyadenosine Triphosphate

dCTP Deoxycytidine Triphosphate

dGTP Deoxyguanosine Triphosphate

DMEM Dulbecco's Modified Eagle's Medium

DMSO Dimethyl Sulfoxide

DNA Deoxyribonucleic acid

dNTP Deoxyribonucleotide Triphosphate

DTT Dithiothreitol

dTTP Deoxythymidine Triphosphate

ECL Enhanced Chemiluminescence

EGTA Ethylene Glycol Tetraacetic Acid

FBS Foetal Bovine Serum

FCS Foetal Calf Serum

HBSS Hanks' Balanced Salt Solution

HEPES 4-(2-hydroxyethyl)-1-piperazineethanesulfonic acid

HRP Horseradish Peroxidase

IgG Immunoglobulin G

MDB Membrane Desalting Buffer

mRNA messenger Ribonucleic Acid

RNA Ribonucleic acid

PBS Phosphate Buffers Saline

PCR Polymerase Chain Reaction

PFA Paraformaldehyde

PMSF Phenylmethanesulfonyl fluoride

PVDF Polyvinylidene Difluoride

Real-Time PCR Real-Time Polymerase Chain Reaction

RIPA RadioImmuno Precipitation Assay

SDS Sodium Dodecyl Sulfate

SDS-PAGE Sodium Dodecyl Sulfate Polyacrylamide Gel Electrophoresis

TBST Tris Base Saline-Tween

TEMED *N,N,N′,N′*- Tetramethylethylenediamine

Tris Tris(hydroxymethyl)aminomethane

TRP Transient Receptor Potential

TRPA Transient Receptor Potential Ankyrin

TRPC Transient Receptor Potential Canonical

TRPM Transient Receptor Potential Melastatin

TRPML Transient Receptor Potential MucoLipin

TRPN Transient Receptor Potential NOMPC

TRPV Transient Receptor Potential Vanilloid

Contents

List of Figures

List of Tables

Chapter 1

Introduction

1. Reproduction

The reproductive system describes the aspect of physiology involved in the survival and propagation of the species. The reproductive systems of both males and females have broadly similar components that comprise the gonads, a 'reproductive tract' and accessory sex glands. However, unlike other body systems that are largely identical between male and female individuals, the anatomy of the reproductive system is unique to each of the sexes. The female reproductive tract is a complex system which, in eutherian mammals, undergoes periodic physiological changes which relate to functional requirements. The detail of these cyclical changes in female reproductive physiology differs between species of eutherian mammals, and can be categorised as *menstrual* (in humans and higher primates such as gorillas (Nadler *et al.*, 1979) and chimpanzees (Graham *et al.*, 1972) or *estrous* (in other placental mammalian species).

1.1 The oviduct

The anatomy of the oviduct is highly variable among the different species. In general terms, the oviduct is a tube consisting of an internal mucosa, specifically termed the endosalpinx, especially in women, an intermediate muscular layer, also known as the myosalpinx, and an outer serosa. The endosalpinx is lined by three types of cells; ciliated, secretory and peg cells. It is divided into three sections; the infundibulum, the ampulla and the isthmus (Menezo & Guerin, 1997). The infundibulum is the part of the oviduct that is nearest to the ovary and is associated with the fimbriae, a bordering fringe at the ovarian end of the oviduct. The infundibulum is mainly lined with a ciliated simple columnar epithelium that facilitates the movement of the oocyte toward the uterus (Yániz *et al.*, 2000).

The ampulla is a thin-walled part of oviduct and forms more than half of the length of the tube. In woman, the outer diameter of the ampulla is 1-2 cm and the inner diameter is 1-2 mm (Pauerstein & Eddy, 1979). It is in the ampulla that fertilization occurs (Shalgi & Phillips, 1988). The epithelial cells in the ampulla are largely secretory and contain a granular cytoplasm and their endoplasmic reticulum is spread out irregularly. However, ciliated epithelial cells are still apparent (Pauerstein & Eddy, 1979). These secretory cells release secretory

material into the lumen for nourishment of the oocyte and embryo providing an optimal environment for fertilization (Ledger, 2010).

The isthmus is the narrow, proximal portion of the oviduct which connects to the ampulla and terminates in the uterus at the uterotubal junction. The isthmus is 2-3 cm in length and 0.1-1.0 mm in diameter (Pauerstein & Eddy, 1979). There are fewer ciliated cells in the isthmus compared to the infundibulum and ampulla. The increase in the percentage of ciliated cells from the isthmus to the fimbriae is dramatic (Shalgi & Phillips, 1988).

First described by Novak and Everett (1928), the histological appearance of the oviductal epithelium undergoes cyclic changes (Novak & Everett, 1928) that are regulated by the level of estrogens and progesterone during the menstrual/estrous cycle. At the late follicular phase, the height and degree of ciliation of the epithelial cells reach a maximum level in the ampulla and infundibulum. Atrophy and deciliation occurs in the late luteal phase. In the early follicular phase the epithelial cells undergo hypertrophy and re-ciliation. Further atrophy and deciliation occur during pregnancy and the postpartum period (Verhage *et al.*, 1979).

1.2 The uterus

The uterus in women is a pear-shaped organ, made up of the fundus, body and cervix. In the bovine, there are two uterine horns. The endometrium lines the uterus and comprises a single layer of columnar luminal epithelium with glandular epithelial cells which penetrate into the stroma. This epithelial layer is supported by a base of stromal connective tissue (Lawn, 1973).

17-β estradiol and progesterone, two of the major ovarian steroids, regulate the function of the uterus. For instance, a balance of 17-β estradiol and progesterone controls proliferation of the uterine epithelial cells by regulating DNA synthesis, mitogenesis and expression of cell cycle markers such as Ki67 (Martin, 1980; Clarke & Sutherland, 1990). Progesterone inhibits the 17-β estradiol-induced epithelial proliferation (Martin *et al.*, 1973) .

During the follicular phase of the menstrual/estrous cycle, a rise in 17-β estradiol level leads to an increase in both myometrial contractility and excitability to facilitate spermatozoa movement towards the site of fertilization in

the ampulla (Mesiano & Welsh, 2007). Also, in the endometrium, proliferation of the stromal cells contributes to overall stromal thickening. An increase occurs in the surface area and metabolic activity of the surface epithelium which involves an increase in the number and size of the glandular epithelial cells.

Estrogens bind to estrogen receptors ERα, ERβ which are abundant in the uterine tissue. Estrogens induce the synthesis of intracellular progesterone receptor at the proliferation phase ready for ovulation and the transition to the subsequent proliferative phase. In the rat, estradiol increases the mRNA level of ERα in glandular and luminal epithelia, however, the protein level of ERα decreases in glandular epithelium under the influence of estradiol (Sharma & Rao, 1992).

1.3 Menstrual and estrous cycles

The menstrual (human) and estrous (bovine) cycles commence with puberty. The ovaries begin their endocrine activity with the secretion of two key steroid hormones; oestrogen and progesterone. Both menstrual and estrous cycle involve changes in the ovary and uterus. The bovine cycle, summarised in Fig 1, is considered first.

1.3.1 Bovine estrous cycle

The bovine estrous cycle (Fig 1.1) begins with ovulation, when the oocyte(s) is released from the dominant follicle on the ovary as a result of the preovulatory Luteinizing hormone (LH) surge which in turn triggers nuclear and cytoplasmic maturation of the oocyte (Gordon, 2003). After ovulation, the tissue of the recently ovulated follicle consists of theca interna cells, which have LH receptors, and granulosa cells which have both FSH and LH receptors (Boron & Emile, 2005). Under the influence of these hormones, the tissue undergoes transformation under the effect of follicle stimulating hormone (FSH) and Luteinizing hormone (LH) produced in gonadotrophs of the anterior pituitary gland (Channing *et al.*, 1980), and differentiates to form small and large luteal cells respectively. Both small and large luteal cells secrete progesterone. Secretion of LH is regulated by 17-β estradiol concentration (Gordon, 2003) whereas, secretion of FSH is regulated by inhibin in association with 17-β estradiol (Kaneko *et al.*, 1995). Large luteal cells secrete oxytocin and are

responsive to prostaglandin E whereas, small luteal cells are responsive to LH. Formation of a functional CL requires LH. However, the CL maintains its function without LH (Peters *et al.*, 1994). Progesterone, which is secreted from the CL, is the dominant hormone for the major part of the bovine's estrous cycle. The concentration l of progesterone increases from day 3-4 of the estrous cycle, and then, dramatically until day 8 of the estrous cycle when a plateau is reached (Gordon, 2003). A decrease in progesterone concentration, the result of rapid regression of the CL induced by $PGF_{2\alpha}$ secreted by the endometrium (Schramm *et al.*, 1983) is the key event in the estrous cycle. Regression of the CL begins 1-4 days before estrous and is completed within 2 days (Gordon, 2003). Apoptosis is responsible for CL regression (Zheng *et al.*, 1994). $PGF_{2\alpha}$ is secreted from the endometrium as a result of interaction with oxytocin secreted from the CL with its specific receptor on the endometrial cells. The formation of oxytocin is dependent on the 17-β estradiol secreted by the granulosa cells of the follicle using the androstenedione produced in theca cells (Gordon, 2003).

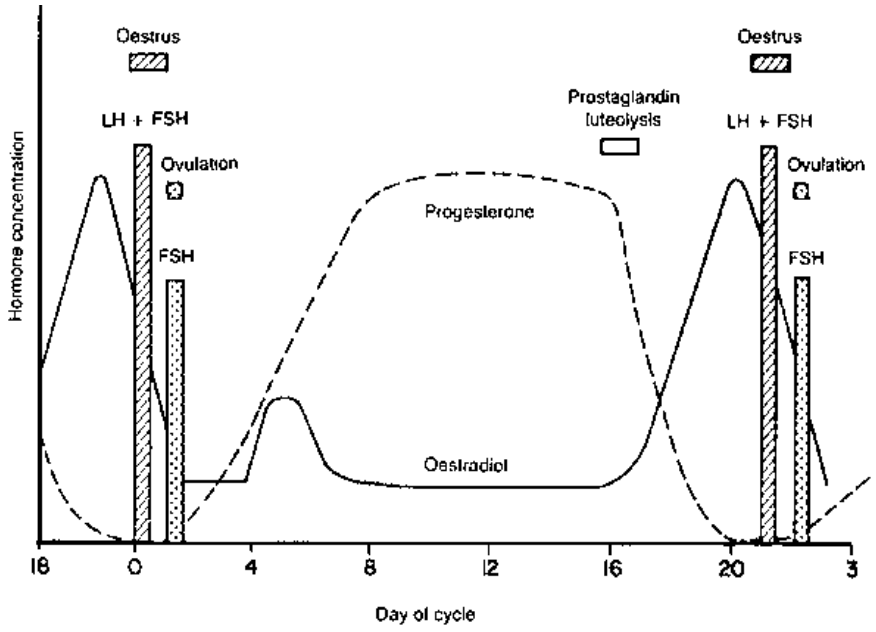

Fig 1.1 Hormonal changes throughout the bovine estrous cycle. Taken from http://www.google.co.uk/imgres?q=hormonal+changes+in+estrous+cycle&um=1&hl=en&sa=N&rlz=1T4GGHP_en-GBGB438GB438&biw=1366&bih=583&tbm=isch&tbnid=B9rlHU3_-jxUBM:&imgrefurl=http://www.fao.org/Wairdocs/ILRI/x5442E/x5442e04.htm&docid=AtGarE7y084EQM&imgurl=http://www.fao.org/Wairdocs/ILRI/x5442E/x5442e09.gif&w=599&h=486&ei=waSyTvWVHcnFtAbM-6ypBA&zoom=1. Accessed on 31/10/2011

1.3.2 The menstrual cycle

The menstrual cycle (Fig 1.2), which usually takes 28 days, is controlled by interaction between the hypothalamus, pituitary gland and ovaries similar to that of the estrous cycle. Gonadotropin-releasing hormone (GnRH) is synthesized, stored and released by neurons in the hypothalamus. GnRH is then carried to the anterior pituitary where it binds to its specific receptors on gonadotrophs (Boron & Emile, 2005) and induces the synthesis and secretion of FSH and LH. FSH and LH in turn induce the synthesis and release of estrogens and progesterone from the ovaries. Furthermore, the ovaries secrete two peptides called inhibins and activins which are also involved in regulation of the menstrual cycle (Boron & Emile, 2005).

The follicular phase, which is the first phase of the ovarian cycle, begins with menstruation. The FSH surge in the late luteal phase of the preceding cycle results in the development of follicles in the ovary. Upon initiation of follicle development, granulosa cells of the follicle start the secretion of 17-β estradiol which is turn triggers continue growth and maturation of endometrium, known as the proliferative phase of the endometrial cycle. Increased levels of 17-β estradiol lead to an LH surge just before ovulation via a positive feedback on the anterior pituitary. An increase in progesterone and activin concentrations then leads to the FSH surge prior to ovulation (Boron & Emile, 2005).

The second phase of the ovarian cycle is known as the luteal phase and begins after ovulation with the formation of the corpus luteum. Luteal cells secrete significant amount of progesterone, and at lower concentrations, 17-β estradiol and inhibin. Progesterone and 17-β estradiol trigger further growth and development of endometrium (Boron & Emile, 2005). This is known as the secretory phase of the endometrial cycle. Increase in estrogen and progesterone leads to a fall in FSH and LH levels via a negative feedback on the hypothalamic-pituitary system. The decrease in FSH and LH levels results in the regression of the corpus luteum which in turn leads to menstrual bleeding known as the menstrual phase of the endometrial cycle and initiation of the next cycle (Boron & Emile, 2005).

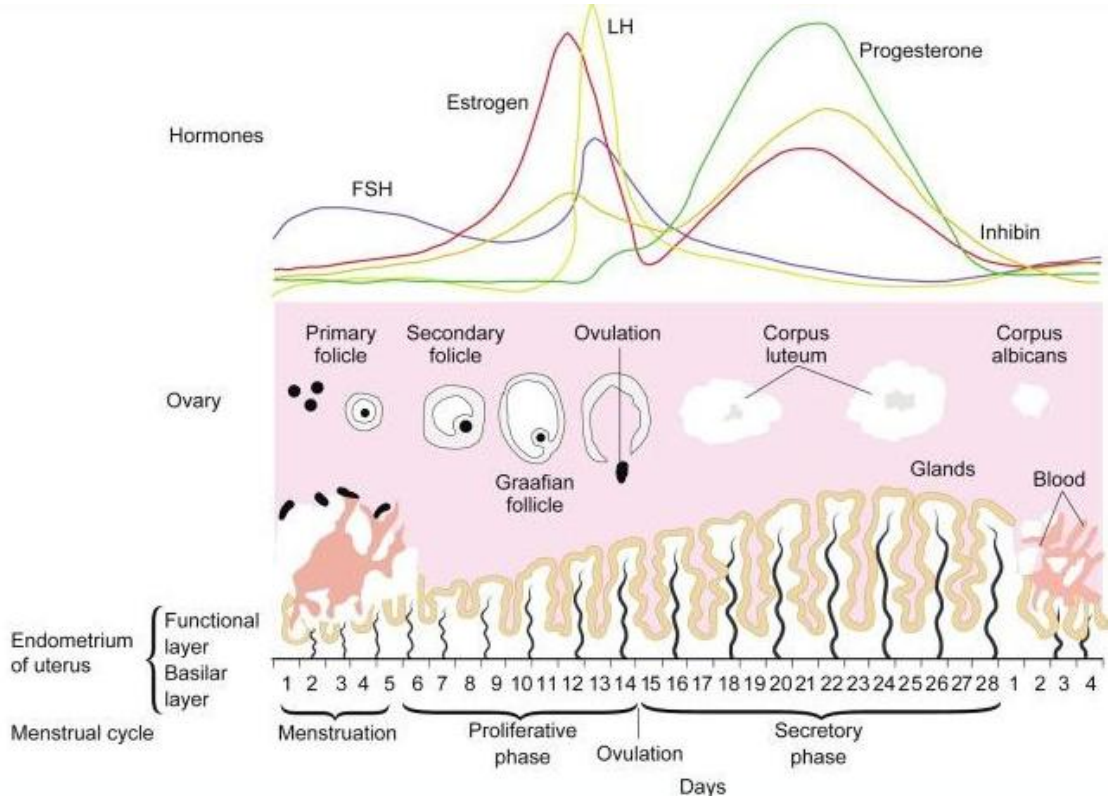

Fig 1.2 Physiological and hormonal changes in endometrium and ovary throughout the menstrual cycle. Taken from

http://www.google.co.uk/imgres?q=hormonal+changes+in+menstrual+cycle&um=1&hl=en&rlz=1T4GGHP_enBGB438GB438&biw=1366&bih=544&tbm=isch&tbnid=6XUkkqokSxQt1M:&imgrefurl=http://www.medscape.com/viewarticle/719473_2&docid=I75DhXyo3QjAmM&imgurl=http://img.medscape.com/article/719/473/719473-fig1.jpg&w=800&h=515&ei=JaayTvquGcv0sgai6u23BA&zoom=1. Accessed on 31/10/2011

1.4 Endocrine control of calcium homeostasis

About 99% of total calcium in the body is stored in crystalline form within the skeleton and teeth. About one tenth of the remaining 1% resides within cells in the soft tissue. Less than 0.1% of the total calcium in the body is found in the extracellular fluid. Approximately half of this extracellular fluid calcium is restricted to the plasma, bound to the plasma proteins or involved in formation of complexes with PO_4^{-3}. Consequently only approximately 0.05% of total body calcium is biologically active and involved in essential physiological activities (Aurbach *et al.*, 1992).

Regulation of Ca^{2+} homeostasis is hormone dependent. Parathyroid hormone (PTH), vitamin D and calcitonin are the three key hormones that regulate Ca^{2+} homeostasis and balance in the body (Mundy & Guise, 1999).

1.4.1 Parathyroid Hormone

PTH is a 84-amino acid peptide hormone secreted from the parathyroid glands. The key function of PTH is to prevent hypocalcemia by increasing Ca^{2+} concentration of plasma by acting on bone, kidneys and intestine. It also reduces plasma PO_4^{-3} concentration, thus raising unbound Ca^{2+} levels (Mundy & Guise, 1999).

PTH secretion from the parathyroid gland is initiated when hypocalcaemia occurs, as the secretory cells of the parathyroid are directly responsive to changes in free plasma Ca^{2+} concentration. PTH can promote either a fast Ca^{2+} efflux into the plasma from bone fluid or a slow increase by triggering bone dissolution and transferring Ca^{2+} and PO_4^{-3} from bone minerals. In the case of rapid Ca^{2+} efflux, PTH first activates a membrane Ca^{2+} pump in osteocytes and osteoblasts. This Ca^{2+} pump in turn promotes Ca^{2+} movement from bone fluid into the cytosol of these cells without movement of PO_4^{-3} (Sherwood, 2008). Osteocytes and osteoblast then release the Ca^{2+} into the plasma. The entire process is dependent on cAMP (Dietrich *et al.*, 1976). The slow PTH-induced transfer of Ca^{2+} from bone to the extracellular fluid occurs through stimulation of osteoblasts to secrete the receptor activator of NF-ᵏß ligand (RANKL), which induces macrophages to differentiate into osteoclasts (Fu *et al.*, 2002). This results in stimulation of osteoclasts to metabolise the bone and further increase

the formation of osteoclasts. In parallel, bone formation by osteoblasts is transiently inhibited. Released PO_4^{-3} during bone dissolution is eliminated by the kidney under the influence of PTH. However, PTH induces reabsorption of filtered Ca^{2+} by the kidneys which leads to an increase in the plasma Ca^{2+} concentration. Furthermore, PTH enhances the activation of vitamin D (cholecalciferol) by the kidney which in turn increases Ca^{2+} and PO_4^{-3} absorption in the intestine. The relationship between PTH secretion and free plasma Ca^{2+} concentration forms a negative-feedback loop similar to that of calcitonin (Mundy & Guise, 1999).

1.4.2 Vitamin D

Vitamin D is a steroid-like compound produced in the skin from 7-dehydrocholestrol when exposed to sunlight (Webb & Holick, 1988). Vitamin D is then released into the blood stream and after conversion to its active metabolite (see below) acts on intestine and bone. In countries close to the poles, with seasonal short periods of sunlight, essential vitamin D should be obtained from dietary sources. Vitamin D produced in the skin or from a dietary source is biologically inactive and must undergo biochemical alteration by addition of two hydroxyl (-OH) groups to become activated. The first hydroxylation step occurs in liver and the second in the kidney (Kawashima *et al.*, 1982). Hydroxylated vitamin D is known as *1,25*-$(OH)_2$-vitamin D_3 or calcitriol. The enzymes that catalyse the second hydrolxylation of vitamin D in kidney are regulated by PTH (Barbour *et al.*, 1981; Gkonos *et al.*, 1984; Zerwekh & Breslau, 1986).

Most of the dietary Ca^{2+} is lost in the faeces. However, when plasma Ca^{2+} level is low, the active form of vitamin D, Calcitriol, increases the absorption of dietary Ca^{2+} as well as PO_4^{-3} into the plasma (Norman *et al.*, 1982). Vitamin D also enhances the effect of PTH on bone. Vitamin D induces its effect by binding to a nuclear vitamin D receptor and regulating gene expression (Takahashi *et al.*, 1988; Suda *et al.*, 1992).

1.4.3 Calcitonin

Calcitonin is a 32-amino acid peptide which is secreted by the C cells of the thyroid gland and acts in contrast to PTH and vitamin D to decrease plasma

Ca^{2+} levels. Calcitonin induces short-term and a long-term effects on plasma Ca^{2+} concentration in a similar but reciprocal manner to that of PTH. The short-term action of calcitonin decreases Ca^{2+} transport from bone fluid into the plasma (Friedman *et al.*, 1968). The long-term effect reduces bone resorption via inhibition of cAMP activity in osteoclasts (Heersche *et al.*, 1974). Inhibition of bone resorption results in hypocalcemia and hypophatemia. Calcitonin inhibits Ca^{2+} and PO_4^{-3} reabsorption from the nephron (Quamme, 1980). However, Ca^{2+} and PO_4^{-3} absorption in intestine is not affected by calcitonin.

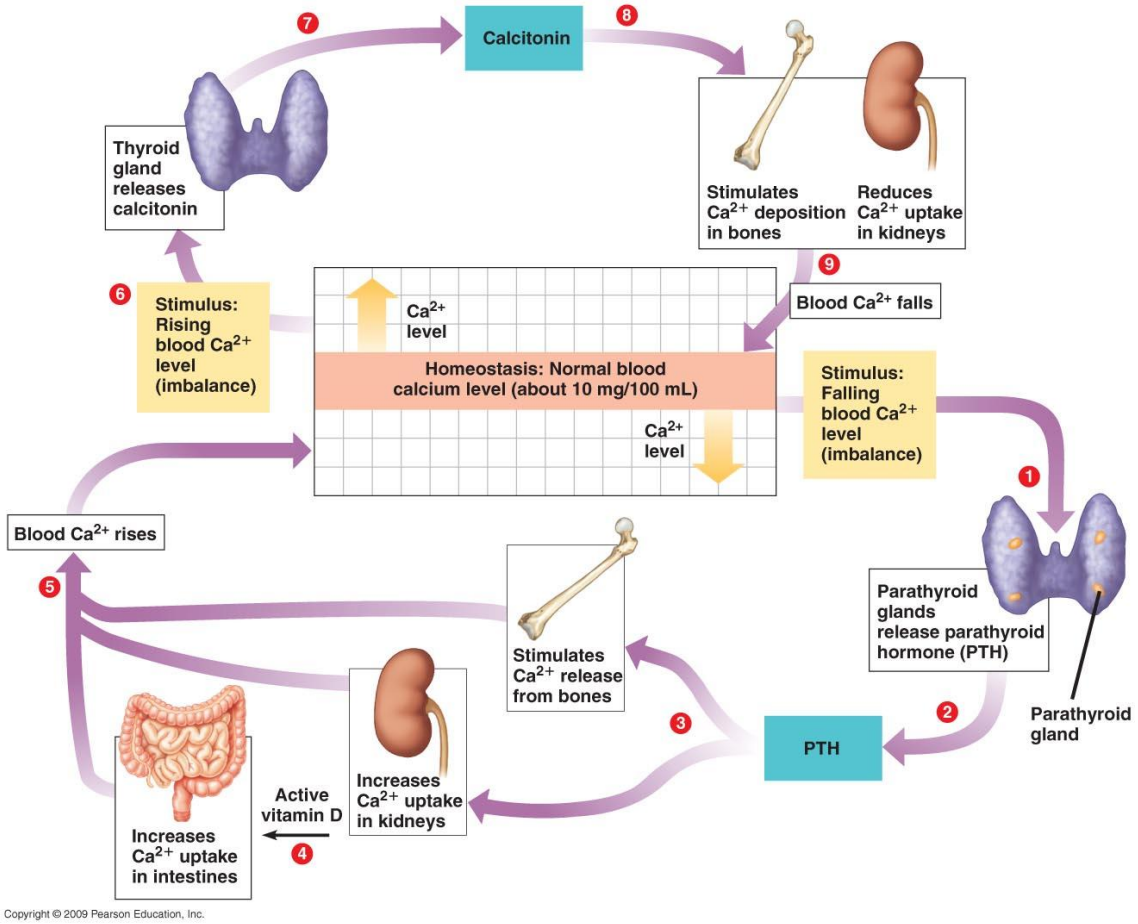

Fig 1.3 Endocrine regulation of calcium homeostasis. Taken form http://mycozynook.com/102RGCh25OH.htm

1.5 Calcium homeostasis in the oviduct and uterus

Calcium acts as an intracellular second messenger and plays a major role in a variety of cell functions, including proliferation, growth, secretion and death (Berridge *et al.*, 1998a). As regards the female reproductive tract, it is useful to distinguish between the role of calcium ions in the outer muscle coats (myometrium of the uterus and myosalpinx in the oviduct) and the mucosal lining (endometrium and endosalpinx respectively). While calcium ions are obviously closely linked with contraction of the myometrium and myosalpinx (Wray *et al.*, 2003), their role in these processes is not considered in this thesis where the focus is on calcium regulation of events in the endosalpinx and endometrium. Here the main emphasis is on the epithelial cells lining the oviduct and uterus, rather than the stroma, though in some cases, localisation of calcium transporters in stroma has been examined. The epithelial cells are ultimately responsible for regulating the passage of calcium ions into the lumen compartment where they are required by the gametes and cleavage stages of the preimplantation embryo and by the blastocyst during implantation (Sanborn, 2000). The movement of calcium from the blood across the epithelial cells is therefore vital for gamete and embryo survival and requires calcium transporters but this process has been little studied in female tract epithelia. Similarly, intracellular calcium homeostasis is obviously essential for the survival of the endosalpinx and endometrium but the mechanisms involved have yet to be determined.

In general, calcium movement across epithelia has to be considered alongside calcium exchange between epithelial cells, which is either via tight junctions or calcium channels which are voltage-dependent calcium channels (VDCCs), members of either transient receptor potential (TRP) channels, or $Na+/Ca^{2+}$ exchangers (NCXS) (Linck *et al.*, 1998). VDCCs have been categorised into two major groups; high voltage-activated (HVA) channels which are activated at voltages higher than -40 mV (depolarized potential) and low voltage-activated (LVA) channels which are activated at voltages between -80mV and -60mV (relatively small depolarisation) (Huguenard, 1998).

Many events related to mammalian reproduction, such as gamete transport, fertilization, early embryonic development and embryo transport take place in

the oviduct. By virtue of its importance as an intracellular second messenger, calcium is likely to play a key role in morphological and functional changes in the oviduct epithelium. Alterations in ciliary activity of oviduct, ampullary transport of the oocyte and early embryo, are controlled by estrogen and progesterone (Nozaki & Ito, 1987) and cytokines such as Platelet-Activating Factor (PAF), which is produced by preimplantation embryos (Velasquez *et al.*, 1995; Downing *et al.*, 2002). PAF induces a transient increase in intracellular calcium concentration $[Ca^{2+}]_i$ in bovine oviduct epithelial cells (Tiemann *et al.*, 1996) and increases the proliferation rate in human endometrial HEC-1B cells (Ahmed *et al.*, 1994), bovine endothelial cells (Lin & Rui, 1994) and bovine endometrial stromal cells (Tiemann & Hansen, 1995). It has been shown that PAF-dependent increases in $[Ca^{2+}]_i$ in bovine oviduct epithelial cells are dependent on Ca^{2+} influx from the extracellular environment (Tiemann *et al.*, 1996). Treatment of these cells with verapamil which is a voltage-gated Ca^{2+} channels inhibitor does not affect the PAF-dependent increase in $[Ca^{2+}]_i$ (Tiemann *et al.*, 1996). Flufenamic acid reduces the PAF-dependent increase in $[Ca^{2+}]_i$ (Wangemann *et al.*, 1986; Gögelein *et al.*, 1990). Furosemide which is a Na^+-K^+-$2Cl^-$ cotransporter, reduces the effect of PAF on the potential difference and short-circuit current (I_{SCC}) across human fallopian tubal epithelial cells (Downing *et al.*, 2002).

1.6 Calcium homeostasis in the endometrium

The human endometrium is a regenerative tissue which remodels during each menstrual cycle by going through phases of growth, proliferation, differentiation, breakdown and shedding. There are several calcium transport-related proteins expressed in endometrium at different levels depending on the stage of the endocrine cycle indicating the importance of this molecule in endometrial activity during both the menstrual cycle and pregnancy.

Ovarian hormones, estrogen and progesterone, play an important role in calcium homeostasis in endometrium by altering the expression of calcitonin, a short peptide hormone (Ding *et al.*, 1994; Dong *et al.*, 2003). Expression of P2X1–3,6,7, a ligand-gated ion channel which is activated by extracellular ATP is also up-regulated, on the apical side of epithelium at the time of implantation.

This has been interpreted as an important role of this receptor in supplying increased $[Ca^{2+}]_i$ in the endometrial epithelium (Slater *et al.*, 2000).

For example, in RL95-2, a human uterine epithelial cell line, increase in intracellular calcium ($[Ca^{2+}]_i$) is related to adhesion of trophoblast-like JAR cells to the apical surface of these cells in culture. Pretreatment of RL95-2 cells with diltiazem, a voltage-activated calcium channel blocker, results in a reduction in intracellular calcium concentration. Furthermore, separation of established bonds between RL95-2 and trophoblast-like JAR cells induces an increase in $[Ca^{2+}]_i$ which is reduced by SKF-96365, a blocker of transient receptor potential (TRP) channels; mainly receptor-activated Ca^{2+} channels and voltage-gated Ca^{2+} channels, but not by application of nifedipin or diltiazem, both of which are specific blockers of voltage-gated Ca^{2+} channels (Tinel *et al.*, 2000).

Studies such as these on human endometrium calcium homeostasis have mainly been carried out on primary cell lines or animal models due to the ethical and experimental difficulties of in vivo studies.

In conclusion, this survey of the literature indicates there are very few studies on the mechanisms underlying calcium homeostasis in the endosalpinx and endometrium and how these may be linked to the transport of calcium across the epithelial cells.

The aim of this thesis is to address this general lack of knowledge, focussing on the potential role of TRP channels in these processes. In order to devise a suitable experimental approach, it is necessary to summarise the role of TRP channels in epithelial cells and the mechanisms involved in their action.

1.7 Epithelial cell connections and calcium homeostasis

The term *Epithelium* refers to a layer of connected individual cells which form a functional barrier between external and internal environments. The fundamental functions of epithelial cells are twofold: a) to maintain separation of different compartments within the organism and b) to regulate exchange of the ions and nutrients between these compartments (Weinstein & Windhager, 2001; González-Mariscal *et al.*, 2003). (Goodenough, 1999). Exchange of ions and nutrients can be via passage between the cells (paracellular transport) or ‘through’ the cells (transcellular) in epithelial tissues.

An important feature of epithelial cells is tight junctions which are specialized intracellular structures where the plasma membranes of adjacent epithelial cells are in very close contact. Several integral membrane proteins complex to form the tight junction. These include occludin, claudins and immunoglobulin superfamily members (Martìn-Padura. I. *et al.*, 1998; Goodenough, 1999; Ebnet. K. *et al.*, 2003).

Gap junctions (Fig 1.4) are another cell connection mediator which allow direct communication between adjacent cells. Molecular exchange via gap junctions occurs by passive diffusion. Metabolites, ions, second messengers with molecular mass of up to 1000 Da, water and electrical impulses are exchanged through gap junctions (Kumar & Gilula, 1996; Alexander & Goldberg, 2003). Gap junctions are composed of two connexons, each of which consists of six connexin subunits. These subunits contain four transmembrane region, two extracellular loops, one cytoplasmic loop and cytoplasmic N and C termini (Söhl & Willecke, 2004).

Desmosomes are another group of intracellular junctions in epithelial cells which are also present in myocardium. Intermediate filaments are bound to the plasma membrane by means of desmosomes. The desmosome is morphologically divided into three zones; the extracellular core region (desmoglea), the outer dense plaque (ODP) and the inner dense plaque (IDP) (Kowalczyk *et al.*, 1994; Schmidt *et al.*, 1994; Green & Jones, 1996; North *et al.*, 1999; Garrod & Chidgey, 2008). Desmosomes bind the adjacent cells to one another and provide the resiliency of the epithelium (Garrod *et al.*, 1996).

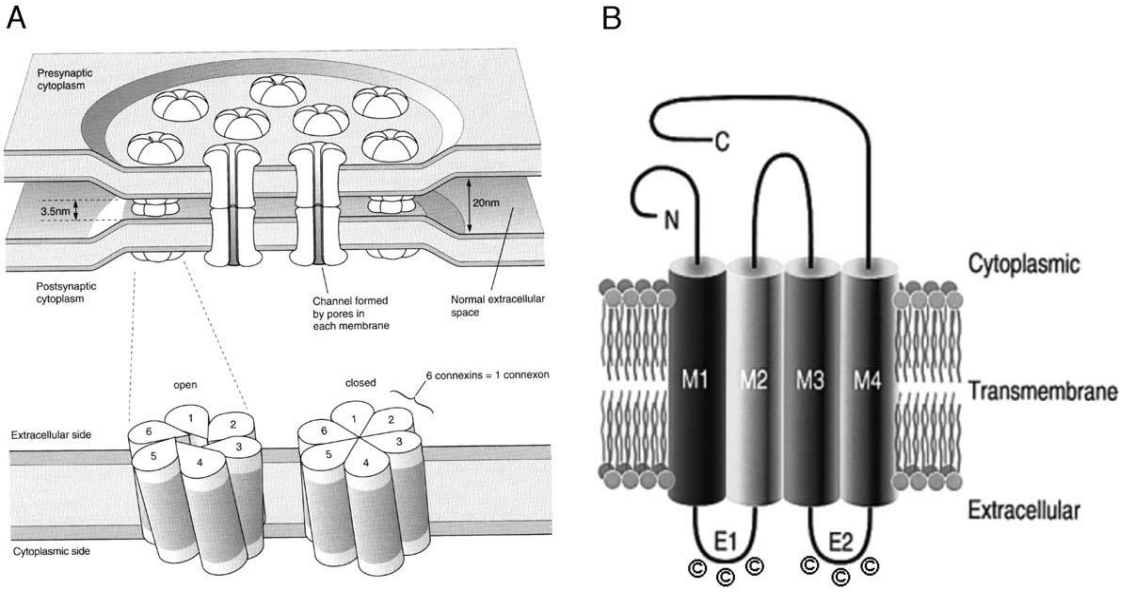

Fig 1.4 Schematic drawing of gap junction and its subunits, connexins. A: Each of the adjacent cell contributes a hemi-channel to the gap junction. Changes in the configuration of subunits lead to opening and closing of the gap junction channels [Adapted from (Kandel *et al.*, 1995)]. B: Topology of a connexin with four teansmembrane domains (M1-M4), two extracellular loop, one cytosolic and cytosolic N and C termini [Adapted from (Kumar & Gilula, 1996)].

Ions can traverse an epithelium though the tight junctions. Movement of ions via tight junction depends on the electrical and concentration gradients across the epithelium and is described as *passive transport* since energy is not required to drive transport. However, hormones and other factors affecting the electrochemical gradient indirectly control the passive ion flow through tight junctions (Pappenheimer, 1987; Goodenough, 1999). Growth factors, cytokines, bacterial toxins, hormones and other factors modulate tight junction permeability (Garcia *et al.*, 1998; Gopalakrishnan *et al.*, 2002; Benais-Pont *et al.*, 2003; Wang *et al.*, 2004).

Many cells express specific pathways for the transport of ions across their membranes and into the cell. Once internalised, these ions can either exit through the opposing membrane or can be affect the behaviour of the cell.

One ion which has special importance is calcium due to its crucial role in many physiological events such as reproduction (Tesarik & Sousa, 1996; Jimenez-Gonzalez *et al.*, 2006). The maintenance of extracellular and intracellular calcium concentration is vital for many physiological functions in the body and as a consequence, exchange between the extracellular and intracellular environments is tightly controlled. Calcium entry into the epithelial cells is through calcium selective channels. Absorption of calcium in epithelial cells via calcium channels has been the subject of various studies (Lajeunesse *et al.*, 1994; Yu *et al.*, 1995; Moreau *et al.*, 2002). Several voltage-dependent like calcium channels are present in the epithelium of distal part of the nephron (Yu *et al.*, 1995). PTH-induced calcium influx in the renal distal tubule via calcium channels is thought to be stimulated by both protein kinase A (PKA) and C (PKC) (Friedman *et al.*, 1996; Hoenderop JG, 1999). Furthermore, it has been shown that 1,225-$(OH)_2D_3$- induced calcium channel activation in mammalian intestinal cells is via cAMP/PKA-pathway (Massheimer *et al.*, 1994). Further studies and the discovery of Transient Receptor Potential (TRP) channel superfamily led to recognition of the critical role of TRP channels, more specifically TRPV5 and 6, in epithelial cell calcium transport (Peng *et al.*, 1999; Hoenderop *et al.*, 2002; Montell *et al.*, 2002; Peng *et al.*, 2003).

Calcium efflux across the basolateral membrane of absorptive epithelia which occurs against the electrochemical gradient, is mediated by two calcium transporters; the Na^+/Ca^{2+} exchangers (NCX) and Ca^{2+}- ATPase (PMCA).

1.7.1 Na^+/Ca^{2+} exchangers

In mammals, three isoforms of NCX have been identified: NCX1, NCX2 and NCX3. NCX1 is distributed widely in many different mammalian tissue, and in the rabbit kidney, expression is restricted to the distal part of the nephron where it localizes mainly on the basolateral (basal) membrane (Hoenderop *et al.*, 2000; Loffing *et al.*, 2001; Biner *et al.*, 2002). By contrast, NCX2 and NCX3 expression is restricted to brain and skeletal muscle (Li *et al.*, 1994; Nicoll *et al.*, 1996). NCXs are activated by the membrane potential, protein kinase C (PKC) activation, nucleotides, calciotropic hormones and protons (Blaustein & Lederer, 1999). Several functional studies suggest that calcium is extruded via the basal membrane of the kidney epithelium. However, this mechanism seems to play a minor role in the small intestine.

K^+ -dependent Na^+/Ca^{2+} exchangers (NCKX), (Blaustein & Lederer, 1999; Philipson & Nicoll, 2000) are expressed in the epithelium of small intestine and kidney (Li *et al.*, 2002; Cai & Lytton, 2004). The abundant expression of these channels in various tissues indicates their vital role in regulating the intracellular calcium concentration in mammalian cells. However, their exact role in epithelial calcium transport is yet to be determined.

1.7.2 Ca^{2+}- ATPases

PMCAs are widely expressed in all eukaryotic cells where they maintain the resting intracellular calcium concentration (Blaustein *et al.*, 2002). Each of the the four isoforms of PMCA (PMCA1-4) are encoded by four separate genes and each isoform has various splice variants which mainly differ in their carboxy-terminal (Stauffer *et al.*, 1993; Strehler & Zacharias, 2001). Unlike NCX, PMCA is expressed throughout the nephron segment although it is more abundant on the basal membrane of the epithelium lining the distal part of the nephron (Doucet & Katz, 1982; Borke *et al.*, 1989). PMCA1 and PMCA4 have been proposed as ‘housekeeping genes’ which are crucial in the maintenance of cellular calcium homeostasis due to their abundant expression. However,

PMCA2 and PMCA3 are more tissue specific (Stauffer *et al.*, 1993). Of various isoforms of PMCA, PMCA4b is a significant extruder of basolateral (basal) calcium in Madin-Darby Canine Kidney (MDCK) cells. Furthermore, in the small intestine PMCA1b is the predominant isoform of PMCAs (Kip & Strehler, 2003, 2004).

1.8 Transient Receptor Potential Superfamily Channels

Transient Receptor potential (TRP) channels were first discovered through studying a mutation in photoreceptor cells of Drosophila melanogaster that alters eye responses to light by increasing cell membrane permeability to Ca^{2+} (Hardie, 1992), (Pak, 1970; Suss-Toby E, 1991). Since then, 28 members of this superfamily have been identified. All the TRP members have a unique structure of six transmembrane domains, one intracellular N- terminal, one intracellular C-terminal and a pore domain which is located between the fifth (S5) and sixth (S6) segment (Fig 1.5). Despite their unique morphology, members of this superfamily differ widely in terms of their selectivity (Padinjat & Andrews, 2004) and specific activation mechanism (Venkatachalam K & Montell C, 2007). Members of the mammalian TRP superfamily are divided into seven families based on amino acid homologies; the TRPC (*C*anonical) family, the TRPV (*V*anilloid) family, the TRPM (*M*elastatin) family, the TRPP (*P*olycystin) family, the TRPML (*M*uco*L*ipin) family, the TRPA (*A*nkyrin) family, and the TRPN (*N*OMPC) family (Montell C *et al.*, 2002a; Montell C *et al.*, 2002b; Clapham, 2003a; Corey DP, 2003; Delmas P, 2004; Pedersen SF *et al.*, 2005) (Fig 1.6).

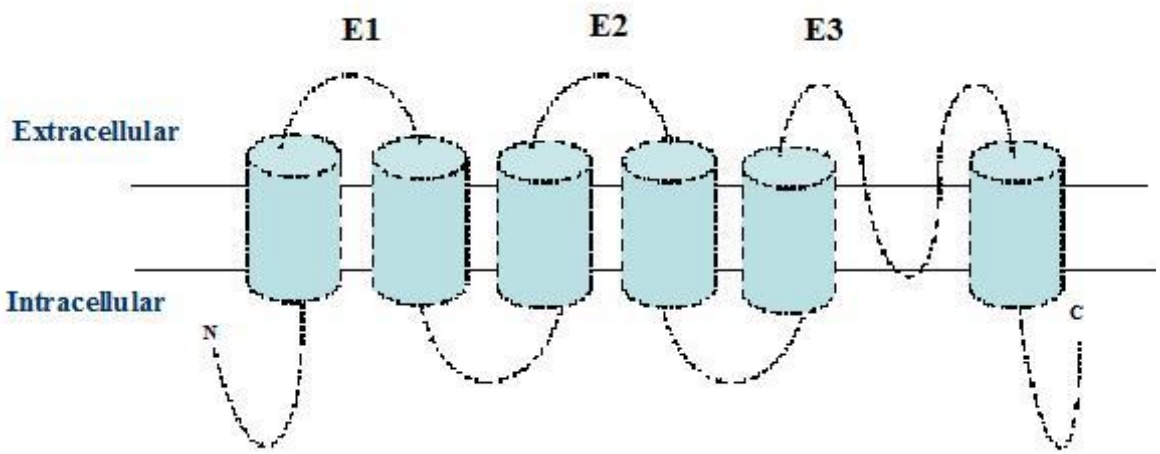

Figure 1.5 TRP channel topology with six transmembrane domains. E1, E2 and E3 (the extracellular loops) are located between segments1 and 2, 3 and 4, 5 and 6 respectively.

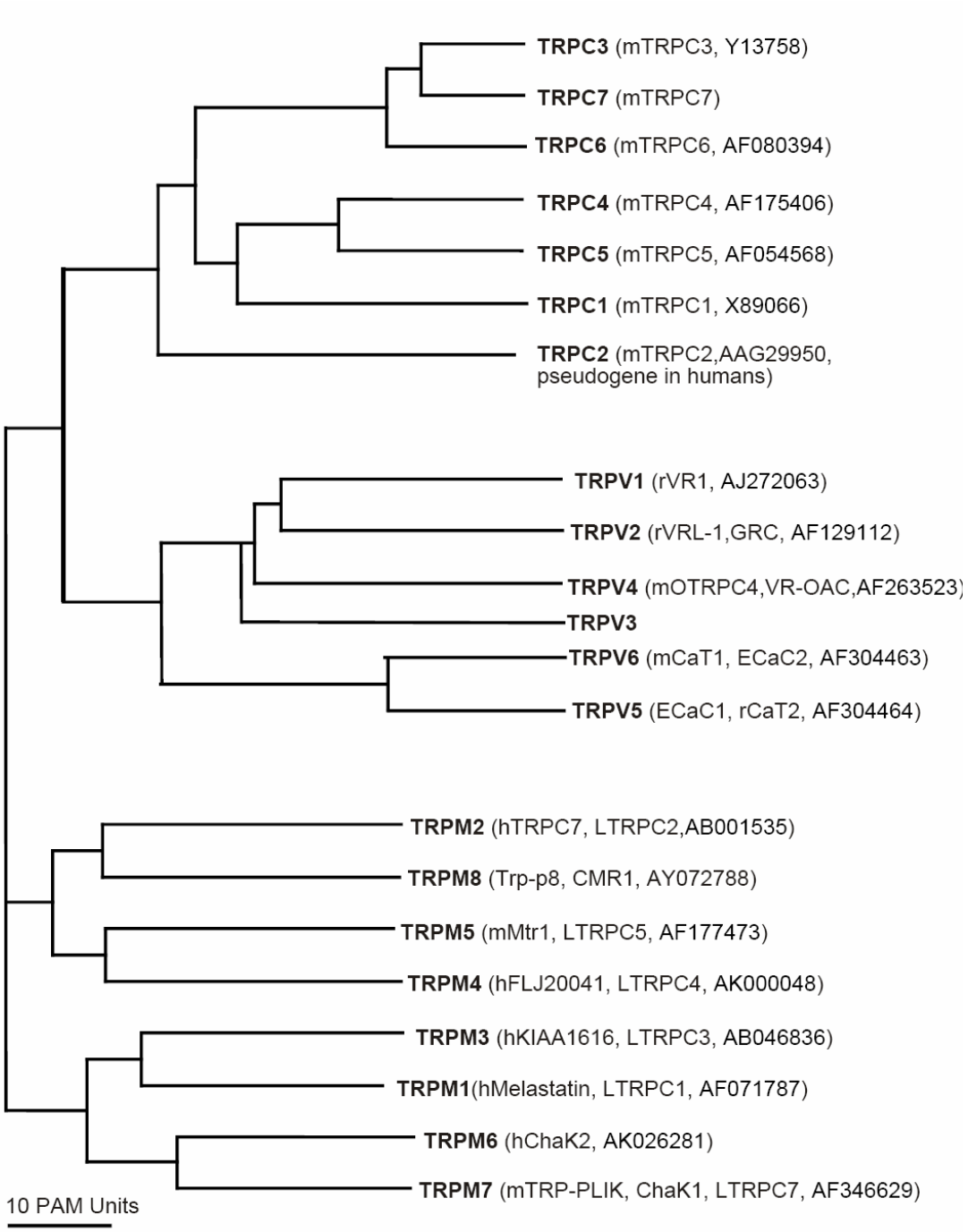

Figure 1.6 Phylogenetic tree of the TRP family. The evolutionary tree is calculated using the neighbour joining method. The total branch length in Point Accepted Mutations units (PAM units) demonstrates the evolutionary distance. PAM units are the mean number of substitutions per 100 residues (Clapham DE *et al.*, 2001).

1.8.1 Transient Receptor Potential Canonical (TRPC)

The identification of TRPC1 as the first recognized member of mammalian TRP channels has led to the establishment of the TRPC subfamily (Wes PD *et al.*, 1995). On the basis of their sequence alignment and functional properties, the TRPC subfamily is further sub-divided into three groups; TRPC1-4-5 , TRPC3-6-7, and TRPC2 (Clapham, 2003a).

The TRPC1 gene is located on chromosome 3, q22-q24, and its full length polypeptide is composed of about 790 amino acids (Wes PD *et al.*, 1995). Its structure is similar to the other TPC family members and contains three ankyrin repeat motifs, which mediate protein-protein interaction via its N-terminal (Lussier MP *et al.*, 2005a; Rychkov G & Barritt GJ, 2007).

TRPC2 is nonfunctional truncated protein (Vannier b *et al.*, 1999), and as such is considered a pseudogene in the human. The human TRPC2 gene, which is located on chromosome 11, lacks the sequence of exon 16, which encodes the fifth transmembrane segment and half of the pore region in comparison to the functional rodent TRPC2 Yildirim E *et al.* (2003).

Human **TRPC3** is located on chromosome 4 and consists of 11 exons (Riccio A *et al.*, 2002). The expression of TRPC3 is more noticeable in embryonic and developing tissues (Stru¨bing C *et al.*, 2003). Human TRPC3 comprises 848 amino acids which have 94% homology to mouse TRPC3 (Preuss KD *et al.*, 1997). A short splice variant of TRPC3 with a truncated N-terminus which is named Trp3sv has been isolated from a rat heart complementary DNA (cDNA) and comprises 736 amino acids (Ohki G *et al.*, 2000). By contrast, an extended splice variant has been detected in human, mouse and rat with one additional exon which leads to an extension at the N-terminus of the protein (hTRPC3a: 921aa; mTRPC3a: 911aa; rTRPC3a: 910 aa) (Yildirim E *et al.*, 2005).

TRPC4 cDNA was first cloned from bovine adrenal gland (Philipp S *et al.*, 1996). This was followed by the identification of various orthologues from mouse, rat and human(Mori Y *et al.*, 1998; Mizuno N *et al.*, 1999; McKay RR *et al.*, 2000). To date, ten different splice variants have been reported of which TRPC4α has the longest sequence. In one group of these splice variants the C-terminal region is deleted, while the six transmembrane segments are

conserved. TRPC4β is another splice variant that lacks 84 amino acids in the C-terminal region. This deleted domain is the suggested region for calmodulin and inositol 1,4,5 triphosphate (IP3) receptors in TRPC4α. In another TRPC4 splice variant group, truncated channels at the second transmembrane segment (S2) are encoded (Plant TD & Schaefer M, 2003).

The **TRPC5** gene was initially known as CCE2 and was first cloned from rabbit and mouse brain (Philipp S *et al.*, 1998). The human *TRPC5* gene is located at Xq23 and consists of 11 exons with a length of about 308 Kb and the transcript length of 5.84 Kb (Sossey-Alaoui K *et al.*, 1999) There are no splice variants reported for this member of TRPC family. TRPC5 protein is made of 973-975 amino acids and its molecular weight has been predicted to be 111.4 kDa. Structural comparison of TRPC5 protein and voltage-gated potassium channels suggest four TRPC5 proteins form a tetrameric structure that act as a single channel. Over-expression of TRPC5 leads to the formation of functional channels which confirm the activity of homomeric TRPC5 (Greka A *et al.*, 2003). However, several studies have shown that TRPC5 interacts with TRPC1 and TRPC4 (Strubing C *et al.*, 2001; Goel M *et al.*, 2002; Hofmann T *et al.*, 2002; Strubing C *et al.*, 2003). Furthermore, TRPC3 may be involved in this interaction in the presence of TRPC1(Strubing C *et al.*, 2003). Wide expression of the other TRPC family members alongside with TRPC5 strongly suggests the heterotetrameric arrangement of endogenous TRPC5.

TRPC5 channel is active at any voltage between -100 to +100 mV. Although TRPC5 is not considered as a “voltage-gated channel” its activity is voltage-dependent (Zeng F *et al.*, 2004). The current-voltage relationship,I-V of TRPC5 is a double-rectification which is specific to this channel (Xu SZ *et al.*, 2005). The permeability of the TRPC5 channel to sodium, caesium and potassium is equal, while it is impermeable to chloride and the large cationic molecules such as *N*-methyl-D- glucamine (Okada T *et al.*, 1998; Schaefer M *et al.*, 2000; Strubing C *et al.*, 2001; Lee YM *et al.*, 2003; Obukhov AG & Nowycky MC, 2004; Xu *et al.*, 2005). TRPC5 is also permeable to divalent cations such as calcium, barium, manganese and strontium (Okada T *et al.*, 1998; Schaefer M *et al.*, 2000; Venkatachalam K *et al.*, 2003).

TRPC6 gene was first isolated from mouse brain (Boulay G *et al.*, 1997). The human gene is located on chromosome 11q21-q22 and contains 13 exons (D'Esposito M *et al.*, 1998; Hofmann T *et al.*, 1999). The full length human and mouse TRPC6 proteins differ by just one amino acid (931 and 930 respectively). TRPC6 contains two glycosylation sites that control the receptor-operated behaviors of the channel. These have been located in the first and second extracellular loops of the channel using glycosylation scanning (Asn^{473}; Asn^{561}) (Dietrich A *et al.*, 2003). Application of different approaches such as cellular co-trafficking of TRPC subunits; fluorescence resonance energy transfer (FRET), differential functional suppression using dominant-negative subunits and co-immunoprecipitation has demonstrated that TRPC6 in its native environment form homo and heteromeric channel complexes (Hofmann T *et al.*, 2000).

The amino acid sequence of TRPC6 contains three ankyrin domains in the amino terminus; an EWKFAR TRP box motif; two inositol 1, 4, 5 triphosphate (IP_3) receptor binding domains and a calmodulin site which overlaps with the second IP_3 receptor binding domain (Boulay G *et al.*, 1999; Zhang L & SaffenD, 2001; Zhang Z *et al.*, 2001; Lussier MP *et al.*, 2005b).

Four splice variants (TRPC6B,C,D,E) of TRPC6 have been cloned from rat lung and human airway smooth muscle cells (Zhang L & SaffenD, 2001).

The **TRPC7** gene is located on chromosome 5q31.1 and consists of 12 exons. Translation of human and mouse TRPC7 gene results a protein of 862 amino acids (Okada T *et al.*, 1999; Riccio A *et al.*, 2002).

Two splice variants have been reported for mTRPC7. In splice variant 1, a 345bp domain, encoding 115 amino acids (261-376) of transmembrane segment 1(S1) is deleted. In variant 2, 165bp of the same region of the channel encoding 55amino acids(321-376) is deleted (Okada T *et al.*, 1999; Walker RL *et al.*, 2001).

1.9 Aims

The aims of this research project were :

- To discover which TRPC isoforms are expressed in epithelial cells lining the female reproductive tract (oviduct/uterus) in the bovine (addressed in Chapter 3) and human (addressed in Chapter 6).
- To discover if gene expression of TRPC channels changes throughout the estrous cycle in bovine oviduct and uterine epithelial cells (addressed in chapter 3)
- To discover the localization of TRPC channels in oviduct/uterine epithelium and changes in protein expression of TRPC isoforms induced by sex hormones in the bovine (addressed in chapter 4) and in the human (addressed in chapter 6)
- To discover the physiological role of TRPC isofoms in regulating intracellular calcium concentration in bovine oviduct epithelial cells (addressed in chapter 5)
- To examine the clinical relevance of a possible role of TRP channels in female reproduction (addressed in chapter 6)

Chapter 2

Materials and Methods

2.1 Materials

2- Methylbutan, Sigma Aldrich

2-mercaptoenol, Sigma Aldrich

2.5-Di-t-butylhydroquinone (DBQ), Sigma Aldrich

30% Arylamide solution, Sigma Aldrich

4-(2-hydroxyethyl)-1-piperazineethanesulfonic acid (HEPES), Gibco Invitrogen

8-well strips, Applied Biosystems

Adhesive film, Applied Biosystems

Albumin from Bovine Serum, Sigma Aldrich

Alexa Four 647 donkey anti goat, Invitrogen

Alexa Flour 488 donkey anti rabbit, Invitrogen

Ammonium Persulfate (APS), Sigma Aldrich

Amphotericin B, Gibco Invitrogen

Aprotinin, Sigma Aldrich

Bio-Rad Protein Assay Kit, Bio Rad

Blotting sheets, Sigma Aldrich

Bromophenol blue, Sigma Aldrich

$CaCl_2$, Sigma Aldrich

Cryomatrix, Shadon-Thermal Scientific

D- Glucose, Sigma Aldrich

Dimethyl sulfoxide (DMSO), Sigma Aldrich

Donkey pAb to Rabbit IgG- HRP, Abcam

Donkey serum, Sigma Aldrich

Dulbecco's Modified Eagle's Medium (DMEM), Sigma Aldrich

Ethylene Glycol Tetraacetic Acid (EGTA), Sigma Aldrich

EZ-First Strand cDNA Synthesis Kit, Geneflow, Isreal

EZ-Run™ Pre-Stained Protein Ladder, Fisher BioReagents

Foetal Calf Serum, Gibco Invitrogen

Fura PE 3-AM, Sigma Aldrich

Glycerol, Sigma Aldrich

Glycine, Sigma Aldrich

Hank's Balanced Salt solution without CaCl and MgCl (HBSS), Gibco Invitrogen

Hyperfilm ECL, GE Healthcare, Amersham Hybound™-P

Hyperforin, Sigma Aldrich

KCl, Sigma Aldrich

PenStrep, Gibco Invitrogen

L-Glutamine, Sigma Aldrich

Lauryl sulfate, Sigma Aldrich

Leupeptin, Sigma Aldrich

Luminol, Sigma Aldrich

$MgCl_2$, Sigma Aldrich

Mouse mAb to β Actin-HRP, Abcam

NaCl, Sigma Aldrich

Newborn Calf Serum, Sigma Aldrich

N,N,N′,N′- Tetramethylethylenediamine (TEMED), Sigma Aldrich

Non-Idet P-40, Sigma Aldrich

NucleoSpin® RNA II isolation kit, Macherey- Nagel

Nutrient Mixture F-12 Ham, Sigma Aldrich

P-Coumoric, Sigma Aldrich

Pancreatin, Sigma Aldrich

Paraformaldehyde (PFA), Sigma Aldrich

PCR Master Mix (2X), Fermentas, Life Science

Phenylmethanesulfonyl fluoride (PMSF), Sigma Aldrich

PVDF transfer membrane, GE Healthcare, Amersham Hybound™-P

Rabbit anti TRPC1, Alomone Labs

Rabbit anti TRPC6, Alomone Labs

Real-Time PCR optical 96 well plate, Applied Biosystems

SKF96365, Sigma Aldrich

Sodium deoxycholate, Sigma Aldrich

Sodium orthovanadate, Sigma Aldrich

strips of caps, Applied Biosystems

SYBR Green Master Mix (2X), Applied Biosystems

Tris base, Sigma Aldrich

Tris HCl, Sigma Aldrich

Triton X-100, Sigma Aldrich

TRPC1 goat polyclonal IgG, Santa Cruz

TRPC6 rabbit polyclonal IgG, Abcam

Trypsin, Sigma Aldrich

Tween-20, Sigma Aldrich

Vectashield with DAPI, Vector Laboratories

2.2 Methods

2.2.1 Staging the female bovine reproductive tract

Fresh female bovine reproductive tracts were obtained from a local abattoir and transported to the laboratory immediately in Hans Balanced Salt solution without $CaCl_2$ and $MgCl_2$ (HBSS-Gibco Invitrogen) containing 10 mM HEPES (4-(2-hydroxyethyl)-1-piperazineethanesulfonic acid)(Gibco Invitrogen) which is a zwitterionic organic chemical buffering agent and 1 µM Aprotinin (Sigma Aldrich) which is a competitive serine protease inhibitor that inhibits trypsin, chymotrypsin, kallikrein and plasmin. The stage of estrous was determined according to the ovary characteristics shown in table 2.1 (Ireland *et al.*, 1980).

Characteristics	**I**	**II**	**III**	**IV**
Estimated day of cycle	1-4	5-10	11-17	18-20
External appearance of corpus luteum (CL)	Red, recently ovulated, point of rupture not covers by epithelium	Point of rupture covered over, apex of CL red or brown	Tan or orange	Light yellow or white
Internal appearance of corpus luteum	Red, occasionally filled with blood, cells loosely organised	Red or brown at apex only, remainder of CL is orange	Orange	Orange to yellow
Diameter of corpus luteum	0.5-1.5cm	1.6-2.0cm	1.6-2.0cm	<1cm
Vasculature on surface of corpus luteum	Not visible	Generally limited to periphery	Will cover the apex of CL late in this stage	Not visible
Follicles >10mm in diameter	Absent	Present	May be absent or present	Present

Table 2.1 Staging the female bovine reproductive tract. Taken from Ireland *et al,.* (1980).

2.2.2 Harvesting and culturing bovine oviduct epithelial cells

The oviduct was dissected from the tract and connective tissue carefully removed. Epithelial cells were harvested by squeezing the oviduct from isthmus to infundibulum. Cells were collected into HBSS and centrifuged at 2500 x *g* for 5 minutes. The supernatant was removed and the cells were washed twice by being re-suspended in 10 ml HBSS and re-centrifuged at 2500 x *g* for 5 minutes. The cell pellet was then re-suspended in 1 ml of cell culture medium and counted on a hemocytometer. The cells were seeded into a T25 culture flask at a density of $5x10^6$/ml Cells were maintained at 39˚C in a 5%CO_2 incubator. The culture medium (Table 2.2) was first changed after 24 hours and then every 48 hours until the cells reached the confluence stage after 7-10 days.

Culturing the epithelial cells in a cell culture flask does not replicate the *in vivo* condition due to lack of permeability in the surface to which the cells are attached . Permeable transwell could be used to address this issue. However, using the permeable transwell membrane in this research project would have been extremely expensive. Furthermore, the number of cells that can be cultured on each transwell membrane would not have provided enough material for the proposed experiments in this research, notably, the western blots.

Compound	**Concentration**
Dulbecco's Modified Eagle's Medium	500 ml
Nutrient Mixture F-12 Ham	500 ml
Penicillin	270 U/ml
Streptomycin	270 µg/ml
Amphotericin B	20 µg/ml
L-Glutamine	2 mM
Newborn Calf Serum	2.5% v/v
Foetal Calf Serum	2.5% v/v
Albumin from Bovine Serum (essentially fatty acids free)	0.1% w/v

Table 2.2. Bovine oviduct and uterine epithelial cell culture medium

2.2.3 Harvesting and culturing bovine uterine epithelial cells

Fresh female bovine reproductive tracts were obtained as described in section 2.1. The uterine epithelium was dissected and cut into 1 x 1 cm pieces and incubated at 4˚C for 1 hour in enzyme medium (Table 2.3). Samples were then incubated at room temperature for a further hour. The enzyme solution was removed and 10 ml HBSS was added to the pieces of tissue and vortexed vigorously for 1 minute. HBSS containing dissociated cells was gently transferred to a clean 50 ml centrifuge tube. The bovine uterine epithelial cells were then centrifuged at 2500 x *g* for 5 minutes and washed twice by resuspending the cell pellet in HBSS and re-centrifuging. Cells were treated as described in section 2.2.2 after this step.

Compound	**Concentration**
HBSS	200 ml
Trypsin	0.05% w/v
Pancreatin	2.7% w/v

Table 2.3 Enzyme Medium

2.2.4 RNA extraction

Total RNA was isolated from epithelial cells using a NucleoSpin® RNA II isolation kit (Macherey- Nagel). Cells were harvested as described in Section 2.2.2 and 2.2.3, and the cell pellet was used for RNA isolation according to the manufacturer's manual. In order to lyse the cells, 350µl buffer RA1 and 3.5µl β-mercaptoethanol were added to the cell pellet and this was vortexed until the cells were completely re-suspended. The cell lysate was then filtered, to reduce viscosity, using a NucleoSpin® filter. The lysate was poured onto the filter which was placed in a 2ml collection tube and centrifuged for 1 minute at 11,000x *g*. To adjust RNA binding to the silica membrane, 350µl 70% ethanol was added to the homogenized lysate and mixed by repeatedly pipetting up and down after discarding the NucleoSpin® filter. The cell lysate was then loaded onto the NucleoSpin® RNA II column (silica membrane) and centrifuged for 30 seconds at 11,000 X *g*. To desalt the silica membrane 350µl of membrane desalting

buffer (MDB) was added to each NucleoSpin® RNA II column and subjected to a further centrifugation step at 11,000 x *g* for 1 minute.

In order to digest any contaminating genomic DNA from the lysate, 90µl of Reaction buffer for rDnase which was provided by the manufacturer and 10µl of reconstituted rDnase were mixed and 95 µl of this mixture was applied directly onto the centre of the silica membrane of each column. The silica membrane was then incubated at room temperature for 15 min. Following this, the silica membrane was washed by adding 200µl Buffer RA2 to the column and centrifuging for 30 seconds at 11,000 x *g*. This wash step was followed by adding 600µl Buffer RA3, which desalts the solution containing RNA, to the column which was placed into a fresh 2ml collection tube and centrifuged for 30 seconds at 11,000x *g*. To complete washing of the silica membrane, 250µl Buffer RA3 was added to the NucleoSpin® RNA II column and centrifuged for 2min at 11,000x *g* to dry the membrane completely. The RNA was eluted from the column by adding 40µl RNase-free H_2O to the centre of the silica tube and then centrifuged for 1min at 11,000x g.

RNA concentration and purity were assessed by measuring 260/280 nm absorbance on a nanospectrophotometer (Implen, Germany). RNA was then stored at -80˚C until further use.

2.2.5 Reverse transcription

Isolated total RNA was reverse transcribed to cDNA using the EZ-First Strand cDNA Synthesis Kit (Geneflow, Isreal) according to the manufacturer's directions. These consisted of mixing 1 µg RNA and 2 µM Oligo (dT) Primer in a 0.25 ml nuclease free eppendorf tube. DEPC-Treated water was used to bring the volume up to 10 µl. The mixture was then gently mixed and heated at +70˚C for 10 min in a thermocycler. Eppendorf tubes were placed rapidly on ice, 8 µl Reaction Mix (2.5X) and 2 µl DTT (100 mM) added to each tube and mixed gently by pipetting up and down. Samples were incubated at +42˚C for 60 min followed by a 15 minutes incubation at +70˚C to stop the cDNA synthesis reaction. cDNA was then stored at -20˚C until further use.

2.2.6 Solution Polymerase Chain Reaction (PCR)

Expression of TRPCs genes was confirmed by solution PCR. PCR Master Mix (2X) (Fermentas, Life Science), which consisted of 0.05 units/µl *Taq* DNA polymerase in reaction buffer, 4 mM $MgCl_2$, and dNTPs (0.4 mM dGTP, 0.4 mM dATP, 0.4 mM dCTP, and 0.4 mM dTTP) was used. All reagents were thawed on ice, gently vortexed and pulse-spun prior to mixing in a 0.25 ml thin walled eppendorf tube. 12.5 µl PCR Master Mix was mixed with 0.1 µM of each forward and reverse primers, 1 µg template DNA, and nuclease-free H_2O to bring the volume up to 25 µl. The mixture was then vortexed and pulse-spun before being placed in an Applied Biosystem thermocycler. The thermal stages of PCR are shown in table 2.4.

Temperature (°C)	**Time**	**Description**	**Cycle**
95	10 minutes	Hot start	1
95	30 seconds	Denaturation	35
60*	30 seconds	Annealing	35
72	30 seconds**	Extension	35
72	7 minutes	Final extension	1
4	infinite	-	-

Table2.4 The steps of solution PCR. * All primers were designed with the same annealing temperature. ** Extension time varies depending on the PCR product size. However, in this case all PCR products were smaller than 500 bp and the extension time was the same for all the primers.

Primers were designed using Primer Blast from the NCBI website. Each primer was ‘blasted’ to check for its specificity. Details of the primers are given in Table 2.5 and 2.6.

Target Gene	Primer	Sequence	Tm (˚C)
Bovine β actin	β actin F	TTCAACACCCCTGCCATG	59.64
	β actin R	TCACCGGAGTCCATCACGAT	59.73
Bovine cytokeratin 18	bCytkr18E3E4F	TGAGATCGAGGCTCTCAAGG	60.63
	bCytkr18E3E4R	TGAGCCAGCTCGTCATACTG	60.16
Bovine TRPC1	bTRPC1E5E7F	CTCGTGGAGGTGGAATTCAG	60.65
	bTRPC1E5E7R	TGGACTGGGAAACAAACTCC	59.94
Bovine TRPC2	bTRPC2E3E4F	TCATCCTGACTGCCTTCCTC	60.35
	bTRPC2E3E4R	ATGAGCATGTTGAGCAGCAC	60.02
Bovine TRPC3	bTRPC3E2E4F	CAAAAAGTTCGTGGCTCACC	60.67
	bTRPC3E2E4R	GCCCAGGAAGATGATGAAAG	59.63
Bovine TRPC4	bTRPC4E6E7F	GACCAATGTCAAAGCACAGC	59.30
	bTRPC4E6E7R	CATTGAAGGGGGTAGGAAGG	60.67
Bovine TRPC5	bTRPC5E6E7F	TGATCGCCATGATGAACAAC	60.49
	bTRPC5E6E7R	TTGTTGAACCAGTTGCCAAG	59.73
Bovine TRPC6	bTRPC6E6E7F	TGCTTGATTTTGGAATGCTG	59.81
	bTRPC6E6E7R	AGGGGTCCCACTTTATCCTG	60.18
Bovine TRPC7	bTRPC7E3E4F	TCCTGGCTGTCTTTGGAGTC	60.39
	bTRPC7E3E4R	CTGATGCGTTCACAACCAAC	60.16

Table 2.5 Primers for the solution PCR and their sequence for the gene detected in bovine oviduct and uterine epithelia. "E" in the primer's name indicates the exon that the primer is designed for.

Gene	Primer	Sequence	Tm (˚C)
Human β actin	hβ actin F	ACAGAGCCTCGCCTTTGC	59.70
	hβ actin R	GGAATCCTTCTGACCCATGC	59.73
Human cytokeratin 18	H Cytkr18E1 F	CAGCATGAGCTTCACCACTC	59.58
	H Cytkr18E1 R	CTCCTTCTCGTTCTGGATGC	59.95
Human TRPC1	hTRPC1E11E12F	TGCTTACCAAACTGCTGGTG	59.90
	hTRPC1E11E12R	AACTGTTTTGCCGTTTGACC	60.02
Human TRPC3	hTRPC3E3E4F	GCAGCTCTTGACGATCTGGT	60.56
	hTRPC3E3E4R	CCTGTCTGAGGCATTGAACA	59.83
Human TRPC4	hTRPC4E6E7F	CTCTGGGAAGAATGCTCCTG	59.94
	hTRPC4E6E7R	ATGCTGTGCTTTGACATTGG	59.72
Human TRPC5	hTRPC5E4E5F	ACCTTGGGCTGTTCATCAAG	60.11
	hTRPC5E4E5R	CATCCATTCCACGACAGTTG	59.96
Human TRPC6	hTRPC6E4E5F	GCCAACAGCAACTTCTCTCC	60.00
	hTRPC6E4E5R	TCCCAGAAAAATGGTGAAGG	59.90
Human TRPC7	hTRPC7E5E6F	AGTACGTGCTGCACTTGTGG	59.97
	hTRPC7E5E6R	CGTAGAGCCCTTCCGATATG	59.69

Table 2.6 Solution PCR primers and their sequence for the gene detected in human endometrium.

2.2.7 Real-Time PCR

Relative TRPC gene expression level was determined by quantitative real-time PCR using SYBR green, an asymmetrical cyanine dye which absorbs blue light (λmax = 497 nm) and emits green light (λmax = 520 nm). SYBER green binds to double-stranded DNA. However, it also binds to single-stranded DNA with a lower performance and to RNA at a rate lower than that of single-stranded DNA. All experiments were carried out in triplicate. For each sample, 50 µl SYBR Green Master Mix (2X) (Applied Biosystems) was added to 300 nM of each forward and reverse primer (Table 2.7 and 2.8), 100 ng cDNA. Finally, nuclease-free H_2O was used to bring the final volume up to 100 µl. This was mixed in a sterile 0.25 ml eppendorf tube. The mixture was then vortexed and gently centrifuged for 1 minute in a bench centrifuge. For each sample, 25 µl of the above mixture was transferred in triplicate into a Real-Time PCR optical 96 well plate (Applied Biosystems) which was sealed with adhesive film (Applied Biosystems), or into 8 well strips (Applied Biosystems) which were sealed with the strips of caps (Applied Biosystems). The 96 well plate or the 8 well strips were then centrifuged before being loaded into a Step-one Real-Time PCR machine (Applied Biosystems). For Real-Time PCR, cycles consisted of 95°C for 10 minutes (Hot start) followed by 40 cycles of 95°C for 15 seconds (Denaturation), 60°C for 1 minute (Annealing/ extension) and a cycle of melt curve consisted of 95°C for 15 seconds, 60ºC for 1minutes and 95°C for 15 seconds. In all samples studied, β actin, was measured to act as a comparator 'house-keeping' gene in parallel with the control which varied depending on the experiment. The relative gene expression was analyzed using StepOne software V2.0 and the baseline and threshold were set manually. $\Delta\Delta$Ct method (section 2.8) was used to analyse the RT-PCR data.

The primers that were used in this research were not designed to detect the splice variants of each TRPC isoforms. This might affect the data interpretation as the exact amount of mRNA which are used for protein synthesis (translation) might not have been measured.

Gene	Primer	Sequence	Tm (˚C)
Bovine TRPC1	QbTRPC1E6E7F	CCGGCAGTGTAAAATGTTTGC	59
	QbTRPC1E6E7R	CATTGGATGTATGGTTTAGGATAACTTC	58
Bovine TRPC2	QbTRPC2E4F	GGCCGGGCCCTCTATG	58
	QbTRPC2E4R	GAGCATGTTGAGCAGCACAATC	59
Bovine TRPC3	QbTRPC3E8F	ACAGTGATGTAGAGTGGAAGTTTGCT	59
	QbTRPC3E8R	GGAGGTAATGTTTTTCCATCATCAA	59
Bovine TRPC4	QbTRPC4E6F	TGGTCAATATTTGGGCTCATCA	59
	QbTRPC4E6R	CGGTGAATTCATGCTGTGCTT	60
Bovine TRPC6	QbTRPC6E4F	CCCATCCAAACTGCCAACAG	60
	QbTRPC6E4R	GCGAGGACCACAAGGAACTT	59

Table 2.7 Primers for Real-Time PCR and their sequence for the TRPC genes detected in bovine oviduct and uterine epithelium.

Gene	Primer	Sequence	Tm (˚C)
Human TRPC1	QhTRPC1E11F	CATTGGCACCTGCTTTGCT	58
	QhTRPC1E11R	AAGATTGCCACATGCGCTAA	58
Human TRPC6	QhTRPC6E5 F	CGCAGCCTCCTTCACCATT	60
	QhTRPC6E5 R	TCAAATCTGTCAGCTGCATTCA	58
Human TRPC7	QhTRPC7E6F	ACATTCTGCCAGCCAACGA	59
	QhTRPC7E6R	TCACAGTTCTCCCTAGCGAGAT	58

Table 2.8 Primers for Real-Time PCR and their sequence for the TRPC genes detected in human.

2.2.8 Analysing Real-Time PCR using ΔΔCt method

ΔΔCt is a relative quantification method to analyse the data from Real-Time quantitative PCR. Changes in expression of the target gene are measured relative to a reference gene (a housekeeping gene) in the control group. A series of equations and assumptions are required to analyse the RT-PCR data using the ΔΔCt method (Livak & Schmittgen, 2001). The exponential amplification of PCR is described in the equation below :

$$\boldsymbol{X_n} = \boldsymbol{X_0} \times (\mathbf{1} + \boldsymbol{E_X})^{\boldsymbol{n}}$$

$\boldsymbol{X_n}$ represents the number of target genes at cycle $\boldsymbol{n}$ of the reaction, $\boldsymbol{X_0}$ is the initial number of target genes. The efficiency of target amplification is represented by $\boldsymbol{E_X}$ and $\boldsymbol{n}$ is the number of cycles.$\boldsymbol{C_T}$ which is the threshold cycle and indicates the fractional cycle number at which the amount of amplified target is a fixed threshold. Therefore,

$$\boldsymbol{X_T} = \boldsymbol{X_0} \times (\mathbf{1} + \boldsymbol{E_X})^{\boldsymbol{C_{T,X}}} = \boldsymbol{K_X}$$

$\boldsymbol{X_T}$ represents the threshold number of target genes, the threshold cycle for target amplification is shown by $\boldsymbol{C_{T,X}}$ and $\boldsymbol{K_X}$ is a constant.

The equation for the endogenous gene (internal control reference) is

$$\boldsymbol{R_T} = \boldsymbol{R_0} \times (\mathbf{1} + \boldsymbol{E_R})^{\boldsymbol{C_{T,R}}} = \boldsymbol{K_R}$$

$\boldsymbol{R_T}$ represents the threshold number of the reference gene, the initial number of reference genes and the efficiency of reference amplification are shown by $\boldsymbol{R_0}$ and $\boldsymbol{E_R}$ respectively. $\boldsymbol{C_{T,R}}$ represents the threshold cycle for reference amplification. $\boldsymbol{K_R}$ is a constant.

Expression is derived from dividing $\boldsymbol{X_T}$ by $\boldsymbol{R_T}$

$$\frac{\boldsymbol{X_T}}{\boldsymbol{R_T}} = \frac{\boldsymbol{X_0} \times (\mathbf{1}+\boldsymbol{E_X})^{\boldsymbol{C_{T,X}}}}{\boldsymbol{R_0} \times (\mathbf{1}+\boldsymbol{E_R})^{\boldsymbol{C_{T,R}}}} = \frac{\boldsymbol{K_X}}{\boldsymbol{K_R}}$$

Assuming efficiencies of the target and the reference are the same,

$$\boldsymbol{E_X} = \boldsymbol{E_R} = \boldsymbol{E}$$

$$\frac{\boldsymbol{X_0}}{\boldsymbol{R_0}} \times (\mathbf{1} + \boldsymbol{E})^{\boldsymbol{C_{T,X}} - \boldsymbol{C_{T,R}}} = \boldsymbol{K}$$

or

$$\boldsymbol{X_N} \times (\mathbf{1} + \boldsymbol{E})^{\Delta \boldsymbol{C_T}} = \boldsymbol{K}$$

$\boldsymbol{X_N}$ represents the normalized amount of target $\frac{\boldsymbol{X_0}}{\boldsymbol{R_0}}$ and the difference in threshold and cycle ($\boldsymbol{C_{T,X}} - \boldsymbol{C_{T,R}}$) is shown by $\Delta \boldsymbol{C_T}$.

The expression is derived by rearranging the equation

$$\boldsymbol{X_N} = \boldsymbol{K} \times (\mathbf{1} + \boldsymbol{E})^{-\Delta \boldsymbol{C_T}}$$

Finally $\boldsymbol{X_N}$ for any target gene (*q*) is divided by $\boldsymbol{X_N}$ for the calibrator (*cb*)

$$\frac{\boldsymbol{X_{N,q}}}{\boldsymbol{X_{N,cb}}} = \frac{\boldsymbol{K} \times (\mathbf{1}+\boldsymbol{E})^{-\Delta \boldsymbol{C_{T,q}}}}{\boldsymbol{K} \times (\mathbf{1}+\boldsymbol{E})^{-\Delta \boldsymbol{C_{T,cb}}}} = (\mathbf{1} + \boldsymbol{E})^{-\Delta\Delta \boldsymbol{C_T}}$$

$$-\Delta\Delta \boldsymbol{C_T} = -\left(\Delta \boldsymbol{C_{T,q}} - \Delta \boldsymbol{C_{T,cb}}\right)$$

When amplicons designed to be less than 150 bp and the RT=PCR reaction are optimized, the efficiency is close to one. Thus, the amount of target gene when normalized to an endogenous reference gene and to a calibrator is

Amount of target gene $= 2^{-\Delta\Delta \boldsymbol{C_T}}$

2.2.9 Cell Lysate preparation for Western Blot

Confluent bovine oviduct epithelial cultured cells were first washed twice with PBS. 40 µl of RIPA (RadioImmuno Precipitation Assay) buffer which consists of 1% non-Idet P-40, 0.5% sodium deoxycholate, 0.1% SDS, 10µg/ml Phenylmethanesulfonyl fluoride (PMSF dissolved in isopropanol), 1nM Sodium orthovanadate, 10ng/ml Leupeptin and 30ul/ml Aprotinin (Sigma Aldrich) made up in PBS were added to each T25 cell culture flask and incubated on ice for 20 minutes. Cells were then scraped and transferred into a fresh pre-chilled eppendorf and centrifuged at 4˚C for 10 minutes at 11,000 x *g*. The supernatant containing the whole cell protein was then transferred into a fresh eppendorf tube and stored at -80˚C.

2.2.10 Protein assay

In order to measure the concentration of protein in the cell lysates prepared for western blot, a commercial colorimetric assay, based on that of Lowry (1951) was used (DC Protein Assay Reagents Package, BioRad). The reaction between the protein, an alkaline copper tartrate solution and Foiln reagent forms the basis of the protein assay. The colour development is a result of the reaction of protein with the copper in an alkaline medium which is followed by reduction of Folin reagent by the copper-treated protein. The main amino acids involved in this process are tyrosine and tryptophan, and to a lesser extent, cystine, cysteine, and histidine (Lowry *et al.*, 1951; Peterson, 1979). Reduction of the Folin reagent occurs by loss of 1, 2, or 3 oxygen atoms leading to the production of one or more possible reduced species which produce blue colour with maximum absorbance at 750 nm and minimum absorbance at 405 nm.

To measure the protein concentration in a microplate (Nalge Nunc, Fisher Scientific), 20 µl of reagent 'S' a proprietary component of the kit was added to each ml of reagent 'A' (the alkaline copper tratrate solution). To obtain a standard curve, 4 different concentrations of Bovine Serum Albumin (BSA) (0.2, 0.5, 1 and 1.5 mg/ml) were prepared. 5µl of BSA and samples were added into wells of a 96 well plate with a flat bottom followed by the addition of 25 µl of reagent 'A'. 200 µl of reagent 'B' which is a dilute Folin reagent was then added to each well. The microplate was gently agitated to mix the reagents. Absorbance was measured using a plate reader after 15 minutes incubation of the microplate at room temperature in the dark. There was less than 5% change in the absorbance after an hour.

2.2.11 SDS-Page

According to the size of proteins of interest 10% Acrylamide gel was adequate for protein separation. SDS-page is a term used for Sodium Dodecyl Sulfate PolyAcrylamide Gel Electrophoresis. In this technique separation of proteins occurs based on their molecular weight. Polymerization of acrylamide and *N,N,N',N'*- Tetramethylethylenediamine (TEMED) results in formation of SDS-page gel which is a hydrophilic, neutral, three-dimensional networks of long hydrocarbons crosslinked by methylene groups. The size of the pore within the gel determine the separation of proteins according to their molecular weight.

The amount of acrylamide and crosslinker determines the size of the pore within the gel. The increase in the amount of the acrylamide results in the decrease in the pore size. The total acrylamide present in the gel is given as a percentage (w/v). The percentage of the gel determines the rate of migration and separation of proteins (Table 2.9).

Protein size (kDa)	**Gel percentage (%)**
4-40	20
12-45	15
10-70	12.5
15-100	10
25-200	8

Table 2.9 Percentage of SDS-page Gel.

6.48 ml dH_2O, 5.3ml 30% Acrylamide solution and 4 ml buffer I (Table 2.10), 65 µl of 10% Ammonium Persulfate (APS) and 5.3 µl *N,N,N′,N′*-Tetramethylethylenediamine (TEMED) were added to the above solution to polymerise the gel. Acrylamide gel (resolving gel) was poured into the sandwich assembly. To ensure a level interface was obtained, the resolving gel was overlaid with 100% methanol.

Compound	**Concentration**	**g/L**
Tris base	1.5 M	181.5
Lauryl sulfate	0.4% w/v	4
pH was adjusted to 8.8 using HCl		

Table 2.10 Composition of Buffer I, used for making resolving gel.

The resolving gel was left at room temperature to set for 45 minutes. The methanol was then removed completely before addition of 3.1% stacking gel on top of the resolving gel. The 3.1% stacking gel was prepared for two mini size SDS-Page gel by mixing 4.87 ml dH_2O, 0.75 ml 30% Acrylamide solution and 1.87 ml buffer II (table 2.11). Similar to the resolving gel, 75 µl of 10% APS and 10 µl of TEMED were added to the mixture just before pouring it in the sandwich cassette. Combs were rinsed with 100% methanol and placed into the sandwich cassette.

Compound	**Concentration**	**g/L**
Tris base	0.5 M	60.5
Lauryl sulfate	0.4% w/v	4
pH was adjusted to 6.8 using HCl		

Table 2.11 Composition of Buffer II, used for making stacking gel.

SDS-Page gels were maintained at room temperature for 20-30 minutes to be polymerized. The SDS-Page gel was then placed into a tank chamber which was filled with SDS-Page running buffer (Table 2.12).

Compound	**Concentration**	**g/L**
Glycine	0.192 M	14.4
Tris base	0.025 M	3.03
Lauryl sulfate	0.1% w/v	1

Table 2.12 SDS-Page running buffer.

Cell lysates were boiled alongside Laemmli buffer containing 2-mercaptoethanol (Table 2.13) to linearise the proteins for 5 minutes before being loaded on to the gel. The linearised protein binds the SDS giving it a negative charge. This then leads to the separation of protein on the resolving gel solely based on molecular weight and not electrical charge.

Compound	**Concentration**
Lauryl sulfate	12% w/v
2-mercaptoenol	30% v/v
Glycerol	60% w/v
bromophenol blue	0.012% v/v
Tris HCl	0.375 M
pH was adjusted to 6.8	

Table 2.13 Composition of Laemmli buffer.

35 µg of cell lysate was loaded into each well. In order to detect the size of each band on the gel, 10µl of 10 kDa to 170 kDa protein marker ladder (EZ-Run™ Pre-Stained Protein Ladder, Fisher BioReagents) was also loaded into a well. SDS-Page gel was then electrophoresed at 120 v for 150minutes.

2.2.12 Western Blot

PVDF transfer membrane (GE Healthcare, Amersham Hybound™-P) was primed before protein transfer. PVDF transfer membrane was cut into 10 x 10 cm pieces which were slightly larger than the gel size, and placed into 100% methanol for 1min at room temperature. PVDF transfer membrane was then washed for 10min in dH_2O before being soaked in transfer buffer (Table 2.14) for a minimum of 5 minutes.

Compound	**Concentration**	**g/L**
Tris base	25 mM	3
Glycine	0.2 M	75.07
Methanol	20% v/v	200 ml

Table 2.14 Transfer buffer.

Filter paper (Blotting sheets, 3MM- Sigma Aldrich) and fibre pads were cut to the dimensions of the transfer cassette (10 x 10 cm) and then soaked in transfer buffer for a minimum of 5 minutes.

The transfer cassette was placed into a tray containing transfer buffer; two fibre pads were placed on the transfer cassette and two filter papers were placed onto the fibre pads. SDS-Page was removed from the cassette by separating the glass plates. The stacking gel was then cut away, the gel was gently placed onto the filter paper, and then covered fully with transfer buffer. The PVDF membrane was placed on the gel and any air bubbles removed by rolling over with a serological pipette. Two filter papers and two fibre pads were placed on the PVDF membrane. Any further air bubbles were removed before closing the cassette and placing it in the tank chamber for electrophoresis. The tank chamber, containing the transfer cassette and filled with transfer buffer, was placed on ice and electrophoresed at 100 V for 150 minutes.

2.2.13 Immunodetection

The transfer cassette was disassembled and the PVDF membrane was cut into the approximate dimensions of the gel. The membrane was washed with Tris Base Saline-Tween (TBST) (Table 2.14) buffer for 5 minutes. The PVDF membrane was then incubated with TBST containing 10% BSA for 30 minutes at room temperature to block the non-specific binding sites for the antibody. The PVDF membrane was then rinsed for 5 minutes with TBST.

Compound	**Concentration**	**g/L**
NaCl	150 mM	8.28
Tris base	20 mM	2.42
Tween-20	0.1%	1ml/L
pH was adjusted to 7.6 before addition of Tween-20 using HCl		

Table 2.15 Tris Base Saline-Tween (TBST) Buffer

Primary antibodies were diluted 1:200 (0.2 µg/ml for both TRPC1 and TRPC6) Both TRPC1 and TRPC6 antibodies were raised in rabbit (Alomone Labs). TBST buffer containing 2% BSA. Primary antibodies were then added to the protein-bound surface of the PVDF membrane which was incubated with the primary antibodies at 4°C overnight. Primary antibodies were removed and PVDF membrane was washed with TBST buffer three times each for 10 minutes.

Donkey pAb to Rabbit IgG- HRP (Abcam) was used as the secondary antibody. It was diluted 1:10000 (2 *µg*/ml) in TBST buffer containing 2% BSA. The transfer membrane was incubated with the secondary antibody for 60 minutes at room temperature before being washed three times with TBST buffer at 10 minutes intervals. To develop the PVDF membrane, a 1:1 ratio of ECL1 (Table 2.15) and ECL2 (Table 2.16) was mixed and added to the membrane which was then shaken in the dark at room temperature for 5 minutes. Excess ECL solution was removed and membrane wrapped in cling film and placed in a developing cassette. In a dark room, a Hyperfilm ECL (Amersham) was exposed to the PVDF membrane for an appropriate length of time depending on the amount of detected protein on the PVFD membrane. The exposed Hyperfilm ECL was then placed into a tray containing 1:5 dilution of Kodak® processing chemicals for autoradiography films/developer (Sigma Aldrich) and shaken vigorously for 1 minute. Hyperfilm ECL was then transferred to another tray containing 1:5 dilution Kodak® processing chemicals for autoradiography films/fixer (Sigma Aldrich) and shaken for 1-2 minutes. Hyperfilm ECl was washed in H_2O for 2-3 minutes.

Compound	Concentration
Luminol (dissolved in DMSO)	2.5 mM
P-Coumoric (dissolved in DMSO)	0.45 mM
Tris base	0.1 M
H_2O	To adjust the volume
Stored at 4˚ C	

Table 2.16 Composition of ECL1 reagent.

Compound	Concentration
H_2O_2	0.1% v/v
Tris base	0.1 M
H_2O	To adjust the volume
Stored at 4˚ C	

Table 2.17 Composition of ECL2 reagent.

The PVDF membrane was washed four times with TBST buffer at 30 minutes intervals and was then blocked with TBST containing 10% BSA for 30 minutes at room temperature. To detect β actin protein as the control for the experiment the membrane was incubated with 1:500 (2*μg*/ml) of Mouse mAb (Abcam) to β Actin-HRP in TBST containing 2% BSA for 60 minutes at room temperature. The antibody was removed and the PVDF membrane was washed with TBST buffer three times at 10 minutes intervals. The membrane was developed as described in section 2.13.

2.2.14 Paraffin embedding and sectioning of the bovine uterus and oviduct

Fresh tissue was obtained from the local abattoir and staged according to section 2.1.

The oviduct and the uterine horns were dissected and cut into approximately 0.5 x 0.5 cm sections. Tissue sections were placed into a labelled embedding cassette that was immersed in 10% formalin overnight. The embedding cassettes containing the tissue section were then washed in 70% ethanol on a shaker for 10 minutes. Ethanol was replaced with fresh 70% ethanol for a further 10 minutes wash step. The embedding cassettes were then placed into absolute ethanol for 10 minutes; this step was repeated three times. Tissue sections in the embedding cassettes were then placed into isopropanol for 10 minutes on a shaker. Isopropanol was replaced with xylene or histoclear for a further 30 minutes on shaker, refreshing the xylene or histoclear at 10 minutes intervals. Excess xylene or histoclear was removed by blotting the embedding cassette thoroughly with a tissue. The embedding cassettes containing the

tissue sections were then placed into three consecutive wax pots melted in a 60˚C incubator. The time of incubation in melted wax differed depending on the thickness and dimensions of the tissue. The sections of uterus were incubated in the first wax pot overnight and for one hour in each of the two subsequent wax pots, while the oviduct sections were incubated for 1 hour in each of the three wax pots. After this time, tissue sections were removed from the embedding cassettes and placed in a sectioning frame before being covered with melted wax and left at room temperature till the wax was solidified. Paraffin embedded tissue was then cut into 10 micron sections using a Microm HM 3555 microtome (Thermo Scientific).

2.2.15 Deparaffinization of paraffin embedded tissue sections

The paraffin embedded tissue was placed on a Super Frost plus slide (Thermo Scientific) and washed twice with xylene, each time for 3 minutes. The tissue sections were then washed with 1:1 dilution of xylene in absolute ethanol for 3 minutes followed by three washing steps of three minutes with 95%, 70%, and 50% ethanol in turn. The tissue sections were finally rinsed with running cold tap water.

2.2.16 Frozen sectioning of bovine uterus and oviduct

Fresh tissue was obtained from the local abattoir and staged according to section 2.1.

The oviduct and the uterine horns were dissected and cut into approximately 0.5 x 0.5 cm sections. Each specimen was placed on a 1cm x 1cm square shaped cork with thickness less than 0.5 cm which was covered with 1-2 drops of Cryomatrix (Shadon, Thermal Scientific). After adjusting the position of the specimen, it was completely covered with Cryomatrix. A scalpel with a plastic handle was used to hold the cork which was dipped in a container filled with 2-Methylbutan (Sigma Aldrich) and then placed in liquid nitrogen. As the tissue freezes and Cryomatrix solidifies, it was placed directly into liquid nitrogen for 1-2 minutes. Frozen tissue was either cut into 10 micron sections using a Microm HM 505E cryostat (Thermo Scientific) or was stored at -80˚C.

2.2.17 Immunohistochemistry

Immunohistochemistry was used to determine the localization of TRPC1 and TRPC6 in bovine oviduct and uterine epithelia and human endometrium.

The tissue sections were either permeabilized to detect intracellular localization of TRPC1 and TRPC6, or were used for localization of the TRPC1 and TRPC6 channels on the cell membrane (non- permeabilized).

To permeabilize the tissue sections, slides were first placed in a Coplin jar containing ice cold Methanol for 5 minutes then incubated in PBS with 0.1% Triton X-100 for an hour at room temperature. Triton X-100 ($C_{14}H_{22}O(C_2H_4O)_n$) is a non-ionic surfactant. 0.1% Triton X-100 PBS was removed and the slides were washed three times with 0.25% Tween 20 in PBS each time for 5 minutes.

To block the non specific binding sites, slides were placed in a humidifier chamber and tissue sections were covered with PBS containing 2% donkey serum (Sigma Aldrich), the host for the secondary antibodies, for 30 minutes at room temperature. PBS containing 2% donkey serum was replaced with 1:250 (1*μg*/ml) dilution of each of TRPC1 goat polyclonal IgG (Santa Cruz) and TRPC6 rabbit polyclonal IgG (Abcam) primary antibodies diluted in PBS containing 1% FCS. Slides in the humidified chamber were then incubated at 4°C overnight. Primary antibodies were removed and the slides washed three times, each time for 5 minutes, with PBS containing 0.25% Tween 20 (Sigma Aldrich). Secondary antibodies, 4*μg*/ml Alexa Four 647 donkey anti goat (Invitrogen) (against TRPC1 primary) and 4*μg*/ml Alexa Flour 488 donkey anti rabbit (Invitrogen) (against TRPC6 primary), were diluted 1:500 in PBS containing 1% FCS. Tissue sections were wrapped in foil paper in a humidified chamber and incubated with secondary antibodies for an hour at room temperature. Secondary antibodies were removed, the slides were placed in a Coplin jar and washed three times with 0.25% Tween 20 in PBS each time for 5 minutes.

Excess wash solution was removed and 1 to 2 drops of Vectashield containing 1.5 *μg*/ml 4',6-diamidino-2-phenylindole (DAPI) (Vector Laboratories) used to cover each specimen. DAPI counterstains DNA and is used to visualise the cell

nucleus. Tissue sections were then covered with a coverslip which was sealed with nail polish and stored at 4°C. until visualisation

Non permeabilized staining was done according to the method above with the omission of the first two steps of permeabilization with ice cold Methanol and PBS containing 0.1% Triton X-100.

Similarly to the primers used in this research, primary antibodies used for TRPC1 and TRPC6 might not be capable to detect the splice variant of these isoforms. Furthermore, there is always the possibility of non-specific binding of antibodies. Moreover, in immunohistochemistry unlike to the western blot intact proteins are the target of the antibodies. Configuration of the proteins within the cells and tissue as well as interaction of the target protein with other proteins might affect the efficiency of the antibodies.

2.2.18 Immunocytochemistry

Confluent bovine oviduct epithelial cells cultured in T25 culture flasks were trypsinised then seeded into 8 well chambered coverglass (Nalge Nunc, Thermo Scientific). Cells were seeded at a density of $2x10^5$/ml. The oviduct epithelial cells regained confluency 7 to 10 days after being seeded into the chambers.

In order to fix the cells, the culture medium was removed using a vacuum aspirator and cells were washed with PBS. The epithelial cells were then incubated with 4% Paraformaldehyde (PFA) for 15 minutes at room temperature. Cells were either immediately stained or stored covered with PBS and placed in a humidifier chamber at 4°C.

Other than the fixation step, immunocytochemistry followed the same procedure as described in section 2.2.17. However, cells were not covered with coverslips after counterstaining of DNA with DAPI and were stored in humidifier chamber at 4°C.

2.2.19 Image Acquisition

a Zeiss LSM 710 confocal microscope and Zen software was used for image acquisition. Details for wavelength used is given in the figure legend.

2.2.20 Measuring Fluorescent Intensity

Fluorescent Intensity was measured using Image analysing software, ImageJ. Integrated density was divided by the measured area. The value obtained was in Fluorescence per μm^2. Fluorescent Intensity in epithelial tissues was measured from 3 parts of tissue; apical, basal and lateral membrane as shown in Fig 2.1. Epithelial cells are assymmetrical due to their polarity and epithelial specific connections, such as tight junctions, connexins/gap junctions and desmosomes. To analyse the data, the epithelial tissue was therefore divided into basal, apical and lateral sections so that the possible role of TRPC1 and TRPC6 could be detected, for example, the possible involvement of the TRPC channels in tight junctions which are located on the facing membranes of adjacent cells.

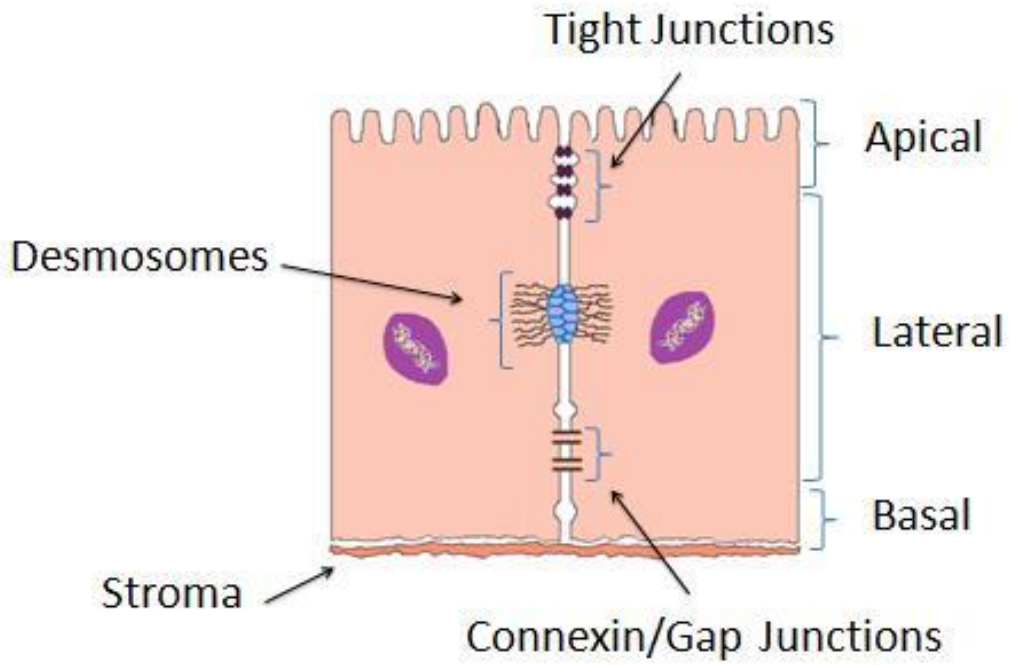

Fig 2.1 Area used for fluorescent intensity measurements of epithelial tissue.

.

2.2.21 Calcium assay

Confluent bovine oviduct epithelial cells cultured in T25 culture flasks were trypsinised then seeded at a density of $2x10^5$ cells/ml into sterile black polystyrene 96 well plates (Nalge Nunc, Fisher Scientific). The oviduct epithelial cells regained confluency 7 days after being seeded into the 96 well plates.

Culture medium was removed from the wells and confluent bovine oviduct epithelial cells were washed with calcium free solution (Table 2.17). Cells were then incubated with calcium free solution containing 10µM Fura PE 3-AM (Sigma Aldrich) for 30 minutes at 39˚C in a 5% CO_2 incubator. Fura PE 3-AM was removed from the well and the cells washed 2-3 times with calcium free solution. Cells were kept in the dark after treatment with Fura PE 3-AM to avoid non-specific bleaching. The 96 well plate containing the BOECs was placed in an Infinite M200 Tecan plate reader (Tecan). i-Control 1.6 software was used to control the experiment. Cells were kept at 37˚ C in the plate reader. After measuring the basal intracellular calcium, calcium free solution was replaced with calcium solution (Table 2.18). Depending on the number of agonists and antagonists used and their required time of action, different numbers of kinetic cycle without intervals were used for each experiment.

Fura PE 3-AM is a Cell permeable fluorescent probe for Ca^{2+} that provides a ratiometric readout which reduces effects caused by leaking or bleached dyes or varying assay conditions. The emission wavelength for Fura PE 3-AM is 380nm which shifts to 340nm when bound to calcium. Cells were first excited at 510 nm and the absorbance measured at 380 and 340 nm. For each emission wavelength, multiple readings were carried out per well (2x2 circle with border of 450 µm). The ratio of absorbance at 340 nm and 380 nm was used to determine the changes in intracellular calcium. Agonist and antagonist used in this study are shown in table 2.19.

Compound	Concentration
NaCl	130 mM
KCl	5 mM
$MgCl_2$	1.2 mM
HEPES	10 mM
Glucose	8 mM
EGTA	0.4 mM
pH 7.4	

Table 2.18 Calcium free solution.

Compound	Concentration
NaCl	130 mM
KCl	5 mM
$MgCl_2$	1.2 mM
HEPES	10 mM
Glucose	8 mM
$CaCl_2$	1.5 mM
pH 7.4	

Table 2.19 Calcium solution.

Compound	Concentration	Function
2.5-Di-t-butylhydroquinone (DBQ)	15 µM	SERCA channel blocker
Hyperforin	25 µM	TRPC6 channel activator
SKF96365	25 µM	General TRPC channel blocker

Table 2.20 Agonist and antagonist used in calcium assay.

Chapter 3

Gene expression of TRPC channels in female reproductive tract epithelia

3. Transient Receptor Potential Canonical (TRPC) genes in female bovine reproductive tract

The role of TRPC channels in the female bovine reproductive tract is largely unknown although a number of research groups have reported the presence of some of the TRPC isoforms in human and rat myometrium (Babich *et al.*, 2004). However, the presence and role of these channels in the epithelium of the female reproductive tract has yet to be investigated. Experiments in this chapter were designed to identify the TRPC isoforms in bovine oviduct and uterine epithelial tissue and to determine the expression pattern of these genes throughout the estrous cycle. Further experiments were conducted to discover possible regulator molecules or pathways in these tissues. The bovine was used as a model for the human due to the difficulties in obtaining human biopsies and the numerous similarities in human and bovine female reproductive systems (Navara *et al.*, 1995; Anderiesz *et al.*, 2000).

3.1 Expression of the TRPC family in bovine oviduct epithelium

Fig 3.1 indicates that the genes that encode TRPC 1 (Lane 2), 2 (Lane 3) , 3 (Lane 4), 4 (Lane 5) and 6 (Lane 7) are expressed in bovine oviduct epithelium. These results were collected from cDNA generated from total mRNA extracted from bovine oviduct epithelial tissue. Expression of β actin confirmed that PCR conditions were optimised (Lane 1, Fig 3.1). Positive expression of Cytokeratin18 (Lane 9, Fig 3.1), a marker specific to epithelial cells, confirmed that template cDNA was from epithelial cells. The expected size of the PCR products were β actin 100 bp, TRPC1 232 bp, TRPC2 233 bp, TRPC3 244 bp, TRPC4 227 bp, TRPC5 179 bp, TRPC6 183 bp, TRPC7 168 bp and Cytokeratin18 181 bp.

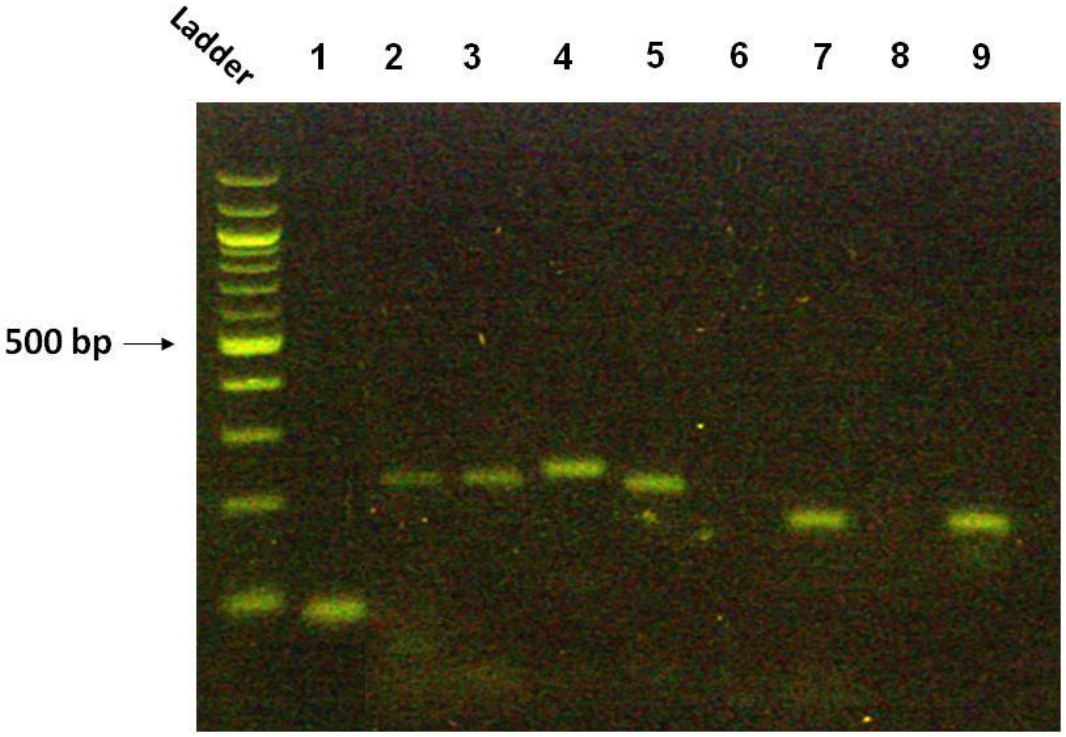

Fig 3.1 TRPC isofoms expressed in bovine oviduct epithelium. PCR Products eletrophoresed on a 2% agarose gel, indicating positive expression of TRPC 1, 2, 3, 4 and 6 in bovine oviduct tissue. Expression of TRPC5 and TRPC7 was not detected. PCR products were loaded on the gel as following: lane 1; β actin (100 bp), lane 2; TRPC1 (232 bp), lane 3; TRPC2 (233bp), lane 4; TRPC3 (244 bp), lane 5; TRPC4 (227 bp), lane 6 ; TRRPC5 (179 bp), lane 7; TRPC6 (183 bp), lane 8; TRPC7 (168 bp) and lane 9; Cytokeratin18 (181 bp).

3.2 Expression of TRPC genes in bovine oviduct epithelium throughout the estrous cycle

Relative gene expression of members of the TRPC family in bovine oviduct epithelial tissue is shown in Fig 3.2. In general, the expression patterns of all the TRPC family members showed remarkable similarity throughout the estrous cycle. Expression level of TRPC1 was decreased by 0.24 ($p= 0.0006$) and 0.35 ($p= 0.0007$) fold at stage 2 and 4 respectively relative to stage 1 of the estrous cycle. However, at stage 3, expression of TRPC1 was up-regulated by 1.49 fold ($p= 0.01$) compared to stage 1 of the estrous cycle (Fig 3.2, A). Expression of TRPC2 was down regulated by 0.10 ($p= 8.95 \times 10^{-6}$), 0.72 ($p= 0.01$) and 0.28 ($p= 0.01$) fold at stage 2, 3 and 4 respectively compared to stage 1 of the estrous cycle (Fig 3.2, B). Expression level of TRPC3 was decreased by 0.069 ($p= 7.6 \times 10^{-5}$), 0.65 ($p= 0.007$) and 0.17 ($p= 0.0005$) fold at stages 2, 3 and 4 respectively relative to stage 1 of the estrous cycle (Fig 3.2, C). TRPC4 expression was down regulated by 0.065 ($p= 3.97 \times 10^{-5}$), 0.63 ($p= 0.01$) and 0.17 ($p= 8.79 \times 10^{-5}$) fold at stage 2, 3 and 4 respectively compared with stage 1 of the estrous cycle (Fig 3.2, D). Furthermore, expression level of TRPC6 was decreased by 0.51 ($p= 0.01$), 0.79 ($p= 0.01$) and 0.41 ($p= 0.006$) fold at stages 2, 3 and 4 of the estrous cycle respectively compared to the stage 1 (Fig 3.2, E).

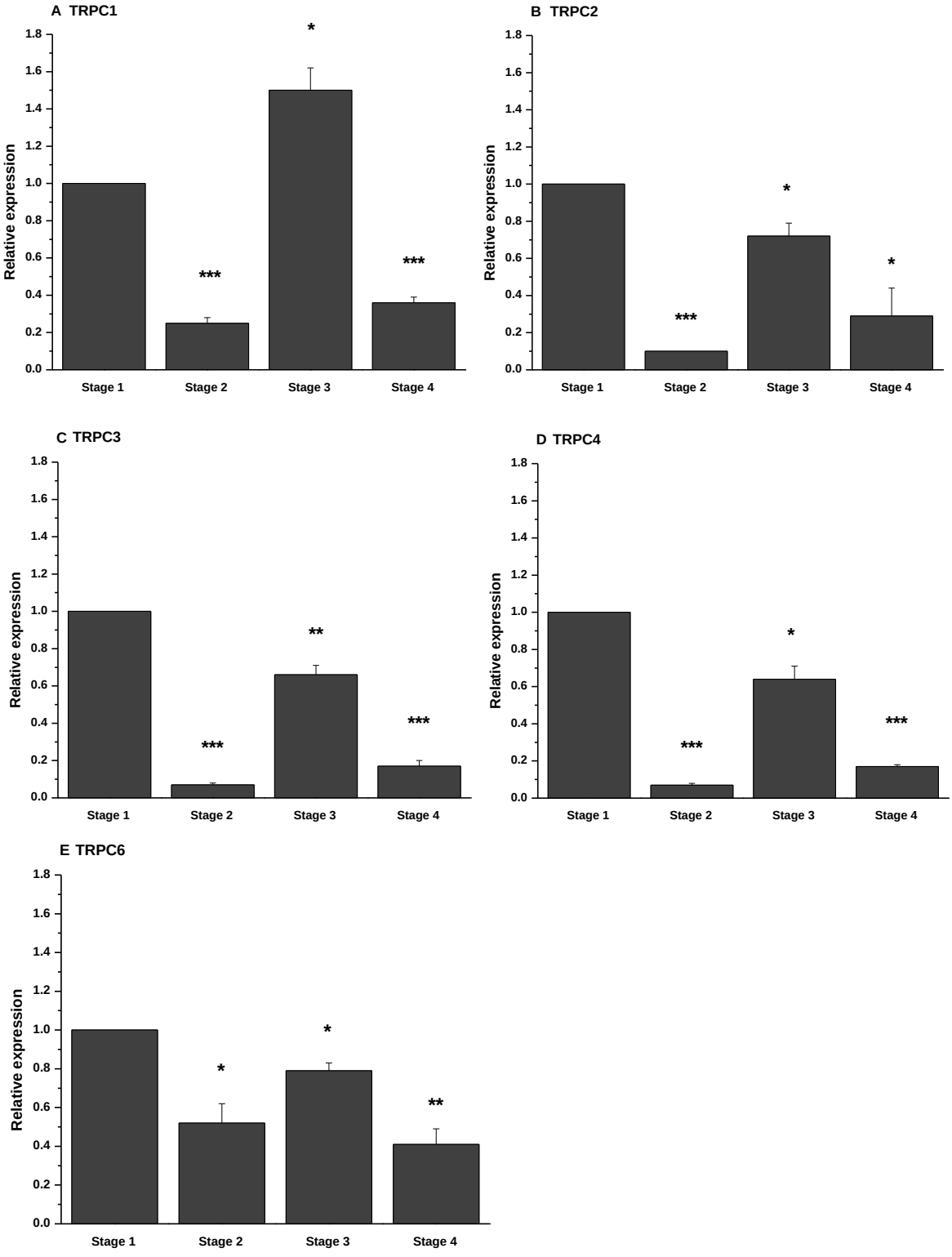

Fig 3.2 Changes in expression of TRPC genes in bovine oviduct epithelium throughout the estrous cycle. Expression of each TRPC isoforms throughout the estrous cycle was normalized to stage 1 of the cycle as a comparator. Expression level of TRPC2 (3.2, B), TRPC3 (3.2, C), TRPC4 (3.2, D) and TRPC6 (3.2, E) was lower at stage 2, 3 and 4 of the estrous cycle compared of that of the stage 1. However, unlike other TRPC isoforms, expression of TRPC1 gene (3.2, A) was higher at stage 3 of the estrous cycle compared to the stage 1. All data are expressed as a mean of 3 experiments ± 1 standard deviation. (* = $p<0.05$; ** = $p<0.01$; *** = $p<0.001$).

3.3 Differences in gene expression of TRPC isoforms in bovine oviduct epithelial tissue and cultured cells

The pattern of expression of TRPC isoforms by bovine oviduct epithelial cells collected from tissue representative of the different phases of the estrous cycle and cultured in vitro differed markedly to that observed in intact tissue (Fig 3.3). The expression of TRPC1 at stage 2 (p= 0.08) in the Bovine Oviduct Cultured Cells (BOEC) was not significantly different to that of the stage 1. However, at stage 3 and 4 of the estrous cycle TRPC1 was up regulated by 1.98 (p= 0.02) and 10.98 (p= 0.004) fold respectively compared to stage 1. Comparing the expression level of TRPC1 between the bovine oviduct epithelial tissue and BOEC indicates that although the pattern of expression at stage 2 and 4 of the cycle in BOEC was similar to that of the tissue, expression of TRPC1 at stage 2 in BOEC was 1.68 fold (p= 0.004) higher than that of the tissue. However, expression of TRPC1 at stage 4 in BOEC was lower by 0.48 fold (p= 0.002) compared to that of the tissue. At stage 3, expression of TRPC1 was up regulated in tissue compared to that of the stage 1 but in BOEC there was no significant difference in expression of TRPC1 at stage 3 compared to that of the BOEC at stage 1(Fig 3.3, A).

Expression of TRPC2 at stage 2 in BOEC was not significantly different (p= 0.6) compared to that of the stage 1. However, expression of TRPC2 at stage 2 of the estrous cycle in BOEC was higher by 10.76 fold (p= 0.03) compared to that of the tissue. Expression of TRPC2 at stage 3 of the estrous cycle was down regulated by 0.64 fold (p= 0.04) relative to the stage 1.There was no significant difference (p= 0.4) in expression of TRPC2 at stage 3 in BOEC compared to that of the tissue. Expression of TRPC 2 at stage 4 of the estrous cycle was up regulated by 1.96 fold (p= 0.002) compared to that of the stage 1 in BOEC. Expression of TRPC2 at stage 4 in BOEC was 6.86 fold (p= 0.0004) higher than that of the tissue (Fig 3.3, B).

With regard to TRPC3, expression at stage 2 of the estrous cycle was down regulated by 0.44 fold (p= 0.01) in BOEC compared to stage 1. Expression of TRPC3 at stage 2 was higher by 6.35 fold (p= 0.02) compared to that of the tissue. TRPC3 was down regulated by 0.62 fold (p= 0.03) at stage 3 in BOEC relative to the stage 1. There was no significant difference (p= 0.7) in

expression of TRPC3 at stage 3 in BOEC and the tissue. At stage 4 of the estrous cycle, expression of TRPC3 was down regulated by 0.16 fold (p= 0.002) relative to the stage 1. There was no significant difference (p= 0.9) in expression of TRPC3 at stage 4 in BOEC and the tissue (Fig 3.3, C). Expression level of TRPC4 in BOEC at stage 2 was down regulated by 0.07 fold (p= 0.0001) compared to the stage 1. No significant difference (p= 0.5) was observed in expression of TRPC4 at stage 2 in BOEC compared to the tissue. At stage 3 expression of TRPC4 in BOEC was down regulated by 0.33 fold (p= 0.001) relative to that of the stage 1. In BOEC expression of TRPC4 at stage 3 of the estrous cycle was lower by 0.52 fold (p= 0.007) compared to that of the tissue. At stage 4 of the estrous cycle, expression of TRPC4 was down regulated by 0.07 fold ($p= 5.68 \times 10^{-5}$) relative to the stage 1. Expression of TRPC4 in BOEC at stage 4 was lower by 0.41 fold (p= 0.001) compared to that of the tissue (Fig 3.3, D).

Expression of TRPC6 at stage 2 of the estrous cycle in BOEC was reduced by 0.25 fold (p= 0.005) compared to stage 1. In BOEC at stage 2 of the estrous cycle, expression of TRPC6 was lower by 0.49 fold (p= 0.02) compared to that of the tissue. Expression of TRPC6 in BOEC at stage 3 (p= 0.6) was not significantly different to that of the stage 1. Furthermore, there was no significant difference (p= 0.6) in expression of TRPC6 at stage 3 in BOEC compared to that of the tissue. At stage 4 expression of TRPC6 was down regulated by 0.29 fold (p= 0.01) relative to that of the TRPC6 at stage 4 of the estrous cycle was not significantly different (p= 0.3) in BOEC compared to the tissue (Fig 3.3, E).

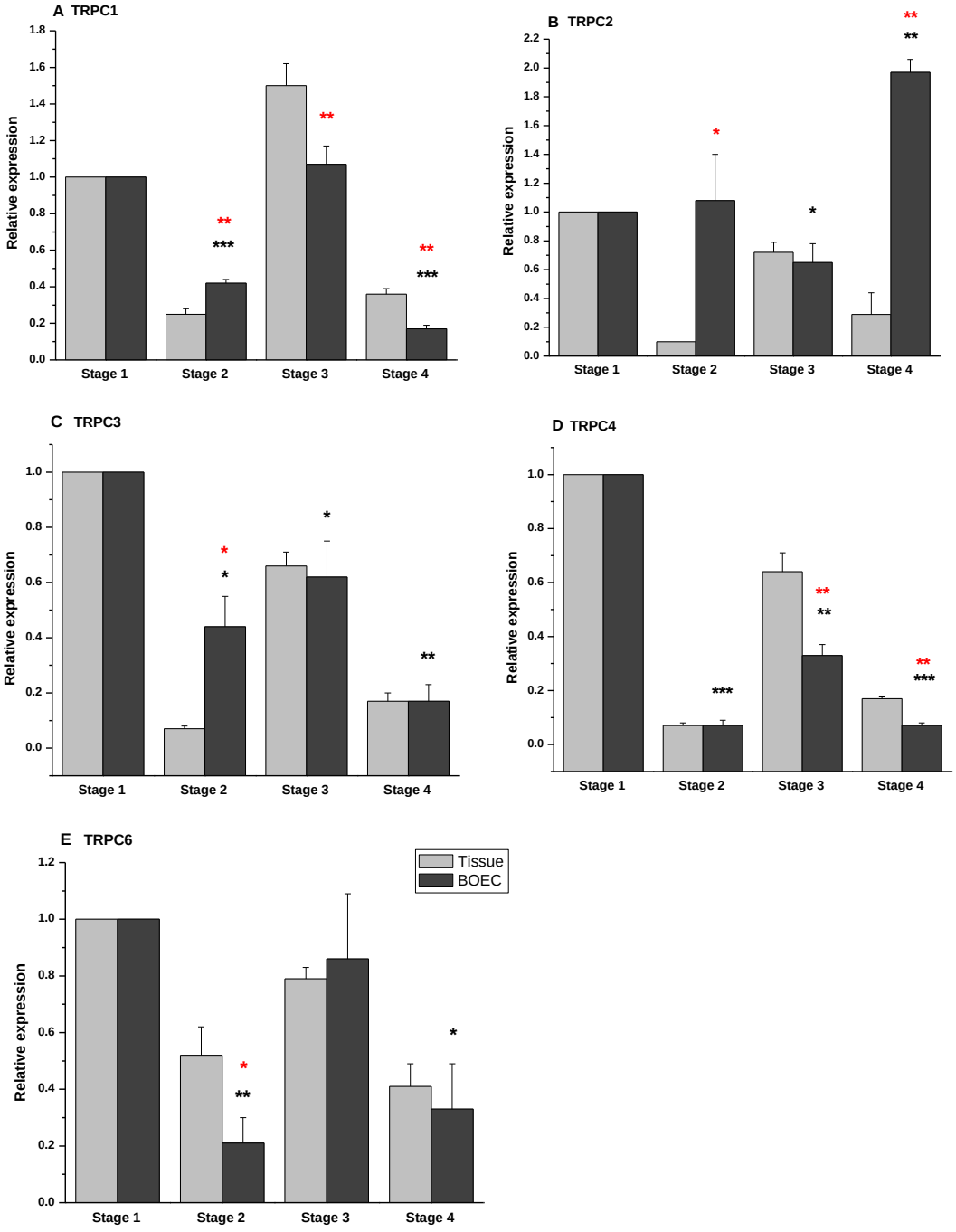

Fig 3.3 Gene expression of TRPC isoforms in bovine oviduct epithelial cultured cells differ compared with that of tissue throughout the estrous cycle. Expression of TRPCs at stages 2,3 and 4 is normalized to stage 1 of the estrous cycle. In cultured bovine oviduct epithelial cells expression of TRPC1 (3.3, A) at stage 2, 3 and 4, TRPC2 (3.3, B) at stage 2 and 4, TRPC3 (3.3, C) at stage 2, TRPC4 (3.3, D) at stage 3 and 4 and TRPC6 (3.3, E) at stage 2 were significantly different compared to the tissue. Data are expressed as mean 3 experiments ± 1 standard deviation. (* = $p<0.05$; ** = $p<0.01$; *** = $p<0.001$). * represents the P value, comparing the changes in the gene expression at different stage of the estrous cycle to the stage 1 in BOEC. * represents the P value, comparing the changes in the gene expression at each stage of the estrous cycle in BOEC to that of the same stage in the tissue.

3.4 Effect of Sex Steroids, Follicle Stimulating Hormone (FSH) and Luteinizing Hormone (LH) on gene expression of TRPC isoforms in cultured bovine oviduct epithelial cells

Acute 24 hour treatment with Progesterone, 17β- estradiol, Follicle Stimulating Hormone (FSH) and Luteinizing Hormone (LH) induced significant changes in expression of TRPC isoforms BOEC (Fig 3.4). The effect of sex hormones on expression of each member of the TRPC family is described in turn. As FSH and LH act synergistically and their circulating levels throughout the estrous cycle mirror each other, BOEC cultures were treated with 0.5 International Unit (IU) of FSH and LH simultaneously. The concentrations of sex steroids used in this experiment chosen were 2 pg/ml of 17β- estradiol (Est) and 10 nM of progesterone (Prog) (Ginther *et al.*, 2010).

3.4.1 TRPC1

Expression of TRPC1 at stage 1 was 0.60 fold (p= 0.01) lower in response to Est when compared to BOEC cultured in the absence of hormonal supplementation. However, expression of TRPC1 in FSH/LH-treated BOEC was up regulated by 8.12 fold (p= 0.02) relative to the control group. Treatment of BOEC with Prog caused a modest, 0.40 fold (p= 0.008) fall in the expression of TRPC1 at stage 1 of the estrous cycle. However concurrent treatment of BOEC with Prog and Est (p= 0.6) and Prog, FSH and LH (p= 0.3) did not cause any change in the expression of TRPC1 at stage 1 of estrous cycle compared to that of untreated BOEC. Synchronous treatment of BOEC with Est, Prog, FSH and LH promoted a dramatic increase in the expression of TRPC1; a greater than 32 fold (p= 0.003) increase compared to that of the untreated BOEC. When Prog was combined with the other hormones, no significant changes (p= 0.05) were observed in expression of TRPC1 relative to the control group (Fig 3.4, A).

In cells harvested from stage 2 of the estrous cycle, Est treated BOEC displayed a 1.39 fold (p= 0.01) increase in the gene expression of TRPC1 compared to untreated BOEC. Expression of TRPC1 in FSH and LH treated BOEC at stage 2 of the estrous cycle was 3.49 fold (p= 0.02) higher than control cells and also greater than that of the effect seen in BOEC treated with Est alone. Treatment of stage 2 BOEC with Prog increased TRPC1 expression

by 1.50 fold (p= 0.02). A combination of Prog and Est induced a 2.70 fold (p= 0.01) increase in expression of TRPC1 in BOEC harvested from stage 2 of the estrous cycle relative to the control group. Prog, FSH and LH combined, increased the expression level of TRPC1 2.63 fold (p= 0.001) compared to that of untreated BOEC. A mixture of Est, FSH and LH increased TRPC1 expression by 16.82 fold (p= 0.02) relative to the untreated group. However, treating BOEC with Prog, Est, FSH and LH led to only a modest 3.24 fold (p= 0.01) increase of TRPC1 expression in relation to that of untreated BOEC (Fig 3.4, B).

In BOEC harvested from stage 3 of the estrous cycle, the expression TRPC1 fell 0.72 (p= 0.03) fold in response to Est compared to the untreated group. FSH and LH treatment led to a 3-fold (p= 0.01) increase in the expression of TRPC1 relative to the control group whereas Prog down-regulated the TRPC1 expression level by 0.55 fold (p= 0.02) compared to untreated stage 3 BOEC. TRPC1 expression was not significantly different (p= 0.1) in stage 3 BOEC in response to treatment with Prog and Est in combination compared to that of the control group. Furthermore, treatment of stage 3 BOEC with a mixture of Prog, FSH and LH or with Prog, Est, FSH did not induce any significant change (p= 0.1) in expression of TRPC1 compared to the untreated group. However, a combination of Est, FSH and LH increased the expression of TRPC1 in stage 3 BOEC by 61.31 fold (p= 0.004) relative to the controls. When Prog was added to the mixture of Est, FSH and LH, expression of TRPC1 fell to 0.53 fold (p= 0.01) compared to the control group (Fig 3.4, C).

At stage 4 of the estrous cycle, a general up-regulation in the expression of TRPC1 was observed in response to exposure to each of Est, FSH, LH, Prog and their combinations. Est treatment increased the expression level of TRPC1 by 3.44 fold (p= 0.004) in stage 4 BOEC compared to that of the untreated group. TRPC1 expression in stage 4 BOEC in response to FSH and LH was 22.12 fold (p= 0.01) higher compared to the control group. Prog-treated BOEC showed a 5.44 fold (p= 0.004) increase in TRPC1 expression relative to the untreated BOEC. When added in combination, Prog and Est up-regulated TRPC1 gene expression 20.0 fold (p= 0.002) whereas the up-regulation of TRPC1 in response to the mixture of Prog, FSH and LH was only 5.03 fold (p= 0.02) compared to the control BOEC. Simultaneous treatment of BOEC with Est, FSH and LH led to a dramatic 86 fold (p= 0.02) increase in TRPC1 gene

expression compared to untreated BOEC. However, addition of Prog to the above mixture reduced this extensive up-regulation to a more modest 2.4 fold (p= 0.03) increase in expression compared to control cells (Fig 3.4, D).

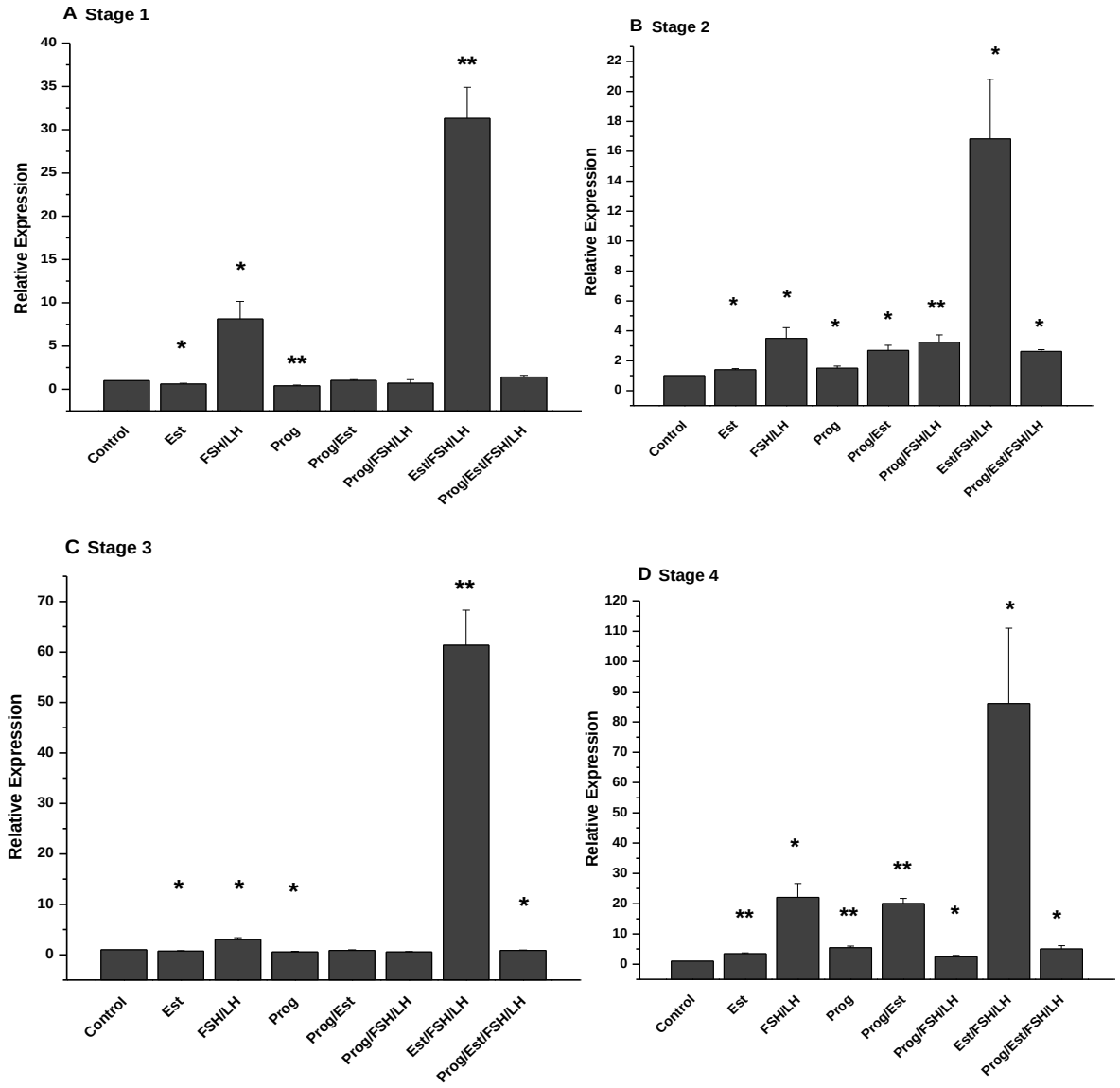

Fig 3.4 Effect of sex hormones on the expression of TRPC1 throughout the estrous cycle. Expression of TRPC1 in BOEC at stage 1 (3.4, A), 2 (3.4, B), 3 (3.4, C) and 4 (3.4, D) of the estrous cycle was altered by each of the sex hormones individually and combined. However, combination of Est/Prog and Prog/FSH/LH did not induce any significant effect on the expression of TRPC1 in stage 3 BOEC. Changes induced in expression of TRPC1 in BOEC was introduced as a fold of that of the untreated BOEC. Data are expressed as mean 3 experiments ± 1 standard deviation. (* = $p<0.05$; ** = $p<0.01$; *** = $p<0.001$).

3.4.2 TRPC2

In cells harvested from oviducts at stage 1 of the estrous cycle, treatment with Est had no significant effect (p= 0.1) on expression of TRPC2 compared to untreated cells. Treatment with FSH and LH led to an 11.47 fold (p= 0.002) increase in TRPC2 expression. However at stage 1, BOEC treated with Prog, expression of TRPC2 was reduced by 0.49 fold (p= 0.01) of that of the untreated BOEC. A combination of Prog and Est did not change (p= 0.8) the expression of TRPC2 in cells from stage 1 of the estrous cycle compared to that of untreated BOEC. When treated with a mixture of Prog, FSH and LH expression of TRPC2 was unchanged (p= 0.4) compared to the control group. In stage 1 BOEC treated with Est, FSH and LH, expression of TRPC2 was greatly increased by 194 fold (p= 0.04) compared to that of untreated BOEC. However, expression of TRPC2 in stage 1 BOEC treated with Prog, Est, FSH and LH combined was not significantly different (p= 0.3) to that of the control group (Fig 3.5, A).

At stage 2 of the estrous cycle, treatment of BOEC with Est did not significantly (p= 0.2) alter the expression of TRPC2 relative to the control group. Treatment of stage 2 BOEC with FSH and LH produced a more marked response as TRPC2 expression was 4.64 fold (p= 0.01) higher than that in untreated BOEC. Treatment with Prog alone reduced TRPC2 expression by 0.31 fold (p= 0.01) compared to the control group. Simultaneous treatment of stage 2 BOEC with Prog and Est did not significantly (p= 0.06) affect the expression of TRPC2 compared to untreated BOEC. Furthermore, a mixture of Prog, FSH and LH did not elicit a significant (p= 0.5) response, however concurrent treatment of BOEC with Est, FSH and LH dramatically up-regulated TRPC2 expression by 138 fold (p= 0.04) relative to untreated BOEC. When Prog was added to the mixture of Est, FSH and LH, up-regulation of TRPC2 expression was not significantly (p= 0.1) different compared to that of control group (Fig 3.5, B).

Fig 3.5,C shows the expression of TRPC2 at stage 3 of the estrous cycle in response to the sex hormones. Treatment of BOEC with Est did not result in any significant difference (p= 0.2) in expression of TRPC2 compared to the control group. TRPC2 expression was significantly increased by 93 fold (p= 0.03) in response to FSH and LH treatment. Prog induced a 16.1 fold (p= 0.02) increase in the expression level of TRPC2, furthermore, when combined with

Est, expression of TRPC2 was up-regulated 18.8 fold (p= 0.002) relative to the untreated group. Together, Prog, FSH and LH increased the expression level of TRPC2 by 10.2 fold (p= 0.04) compared to the control group whereas simultaneous treatment of BOEC with Est, FSH and LH led to an extensive increase in expression of TRPC2 by 1702 fold (p= 0.04) relative to that of untreated BOEC. When Est, FSH and LH were combined with Prog expression of TRPC2 was merely 15.23 fold (p= 0.02) higher than untreated cells (Fig 3.5, C).

As shown in Fig 3.5,D at stage 4 of the estrous cycle, Est induced a 14.2 fold (p= 0.01) increase in expression of TRPC2 in BOEC. The effect of FSH and LH was stronger than Est as TRPC2 was up-regulated by 30.93 fold (p= 0.008) relative to the untreated BOEC. Expression of TRPC2 in BOEC treated with Prog was not significantly different (p= 0.07) compared to the control. A combination of Prog and Est increased the expression level of TRPC2 by 55 fold (p= 0.03), whereas combined Prog, FSH and LH down regulated TRPC2 expression by 0.55 fold (p= 0.02) relative to that of untreated BOEC. Simultaneous treatment of BOEC with Est, FSH and LH resulted in a greater than 420-fold (p= 0.008) increase in TRPC2 expression however addition of Prog to Est, FSH and LH reduced this up-regulation and no significant difference (p= 0.09) was observed compared to the untreated BOEC (Fig 3.5, D).

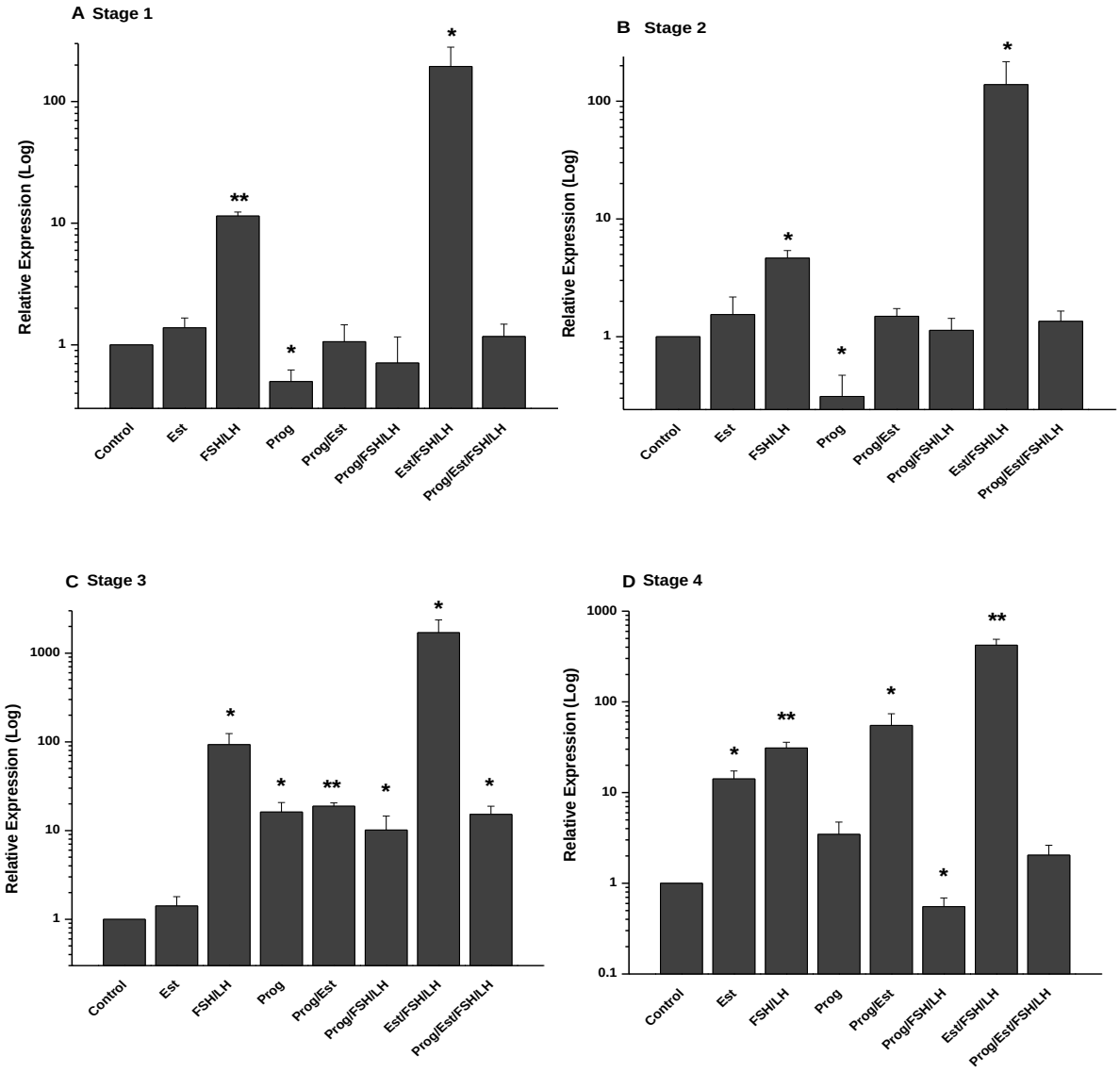

Fig 3.5 Effect of sex hormones on the expression of TRPC2 throughout the estrous cycle. Expression of TRPC2 in BOEC at stage 1 (3.5, A), 2 (3.5, B), 3 (3.5, C) and 4 (3.5, D) of the estrous cycle was altered by sex hormones. At stage 1 and 2 of the estrous cycle, TRPC2 expression was changed in BOEC treated with FSH/LH, Prog and the mixture of Est, FSH/LH (3.5, A and B). Expression of TRPC2 at stage 3 was altered in BOEC treated with each of the sex hormones individually and their combination. However, Est did not induce any significant change on the expression of TRPC2 in stage 3 BOEC (3.5, C). At stage 4, expression of TRPC2 in BOEC was not affected by Prog and the mixture of Prog, Est, FSH/LH (3.5, D). The graphs are plotted on a logarithmic scale for ease of interpretation. Data are expressed as mean 3 experiments ± 1 standard deviation. (* = $p<0.05$; ** = $p<0.01$; *** = $p<0.001$).

3.4.3 TRPC3

Figure 3.6 shows expression of TRPC3 in response to sex hormone treatment. At stage 1 of the estrous cycle, expression of TRPC3 was not changed (p= 0.7) in response to Est in BOEC compared to the control group. By contrast, FSH and LH induced an 11.6 fold (p= 0.04) increase in expression of TRPC3 in stage 1 BOEC relative to the untreated BOEC. However, treatment of stage 1 BOEC with Prog resulted in a 0.49 fold (p= 0.003) down-regulation in expression of TRPC3. Treatment of stage 1 BOEC with Prog and Est together did not induce any significant effect (p= 0.1) in expression of TRPC3 compared to the control group. Prog, FSH and LH together, up-regulated the expression of TRPC3 in stage 1 BOEC by 1.79 fold (p= 0.002) relative to the untreated group. When combined, Est, FSH and LH increased the expression of TRPC3 by 91.5 fold (p= 0.0001) at stage 1 of the estrous cycle relative to the untreated BOEC. However, addition of Prog to the mixture of Est, FSH and LH decreased this up-regulation from 91.48 fold the same expression level (p= 0.8) observed in untreated BOEC (Fig 3.6 ,A).

In cells harvested from oviducts at stage 2 of the estrous cycle, treatment with Est prompted a 1.59 fold (p= 0.03) increase in expression of TRPC3 relative to the control group. Treatment of stage 2 BOEC with FSH and LH also induced an increase in the expression of TRPC3 by 2.42 fold (p= 0.01). However, treatment with Prog did not have any significant effect (p= 0.3) on the expression level of TRPC3 in BOEC at stage 2 of the estrous cycle. A similar result was observed in BOEC treated with Prog and Est (p= 0.09). Furthermore, simultaneous treatment of BOEC with Prog, FSH and LH did not induce any significant effect (p= 0.3) in expression of TRPC3 relative to the untreated BOEC. Expression of TRPC3 at stage 2 of the estrous cycle in BOEC treated with Est, FSH and LH was 56 fold ($p= 3.42 \times 10^{-5}$) higher than the control group. However, addition of Prog to the mixture of Est, FSH and LH abolished this increase and up-regulated the TRPC3 expression by 3.47 fold (p= 0.03) relative to the control group (Fig 3.6 ,B).

At stage 3 of the estrous cycle, expression of TRPC3 in BOEC treated with Est was not significantly different (p= 0.5) from that of the control group. However, FSH and LH together caused a 35.59 fold (p= 0.02) increase in TRPC3

expression compared to the control group. Expression of TRPC3 in BOEC treated with Prog was not significantly different (p= 0.05) compared to that of the untreated BOEC. Furthermore, Prog and Est did not alter (p= 0.1) the expression level of TRPC3 in stage 3 BOEC compared to the control group. Treatment of stage 3 BOEC with the mixture of Prog, FSH and LH resulted in no significant difference (p= 0.1) in expression of TRPC3 relative to the control group. As seen in each of the other groups studied, Est, FSH and LH together resulted in a large rise in expression of TRPC3; 483 fold (p= 0.0006) increase compared to the untreated BOEC. This dramatic effect was not reduced?? (p= 0.7) by the addition of Prog to the hormone mixture (Fig 3.6 ,C).

At stage 4 of the estrous cycle, Est treated BOEC displayed a 7.83 (p= 0.007) fold increase in the gene expression of TRPC3. When BOEC were treated with FSH and LH, a 17.2 fold (p= 0.0001) increase was detected in expression of TRPC3 compared to the control group. Furthermore, Prog up-regulated the expression of TRPC3 in BOEC by 7.43 fold (p= 0.004) compared to the control group. Expression of TRPC3 in BOEC treated with Prog and Est was 29.6 fold (p= 0.007) higher than the control group. However, a combination of Prog, FSH and LH resulted in only a modest 2.76 fold (p= 0.02) increase in expression of TRPC3 in BOEC. By contrast, simultaneous treatment of BOEC with Est, FSH and LH led to a 182 fold (p= 0.003) increase of TRPC3 compared to the untreated group. When Prog was added to the mixture of Est, FSH and LH, the expression of TRPC3 was up regulated by 1.71 fold (p= 0.03) relative to the control BOEC (Fig 3.6 ,D).

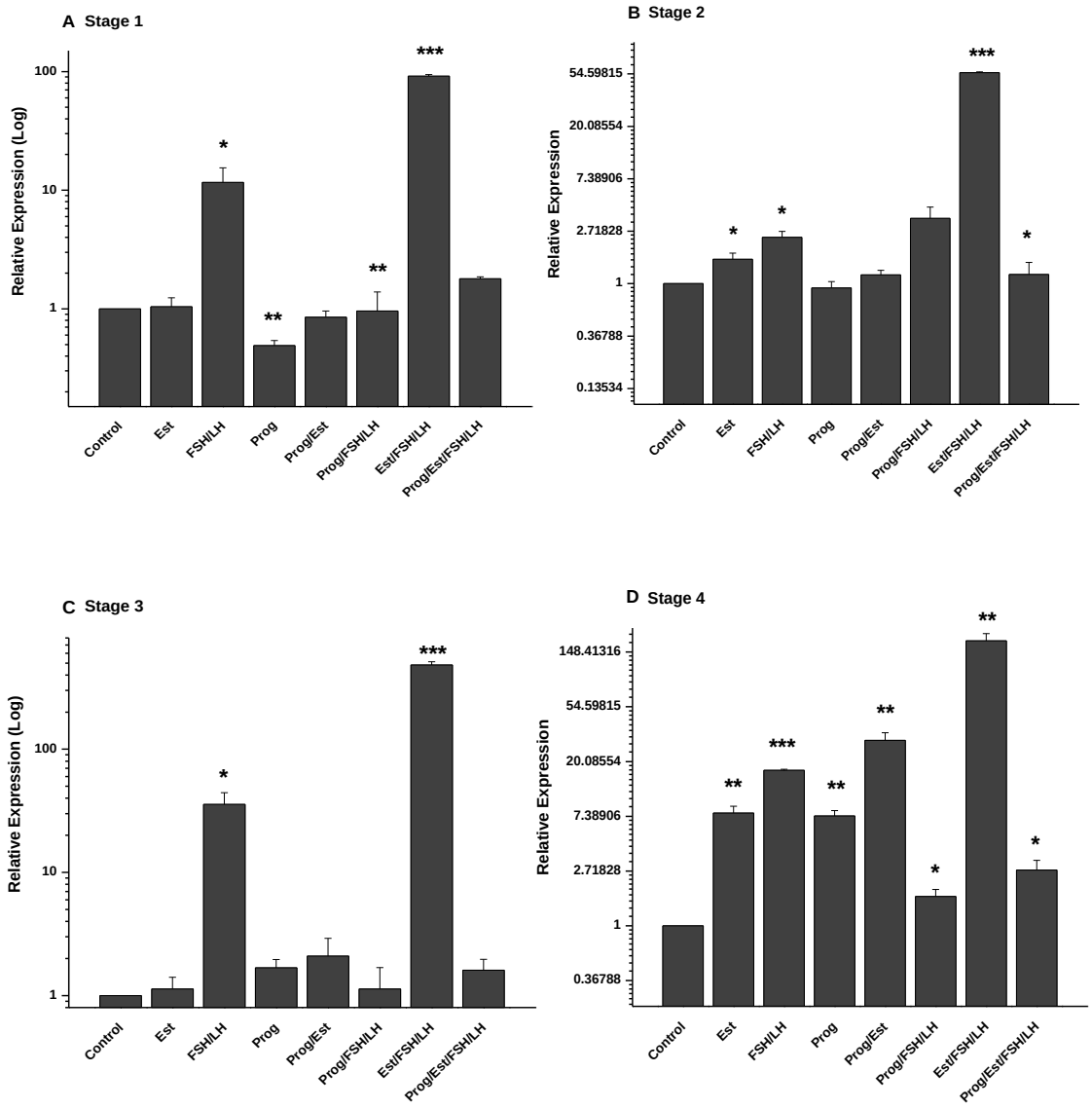

Fig 3.6 Changes of expression of TRPC3 in BOEC throughout the estrous cycle in response to sex hormones. Expression of TRPC3 in BOEC at stage 1 (3.6, A), 2 (3.6, B), 3 (3.6, C) and 4 (3.6, D) of the estrous cycle was altered by sex hormones. At stage 1, TRPC3 expression was changed in BOEC treated with FSH/LH, Prog, combination of Prog, FSH/LH and the mixture of Est, FSH/LH (3.6, A).At stage 2, expression of TRPC3 was altered in BOEC treated with Est, FSH/LH, mixture of Est,FSH/LH and combination of Prog, Est, FSH/LH (3.6, B).Expression of TRPC3 in stage 3 BOEC was affected only by FSH/LH and mixture of Est, FSH/LH (3.6, C). At stage 4, expression of TRPC3 was altered by each of the sex hormones individually and their combination (3.6, D). The graphs are plotted on a logarithmic scale for ease of interpretation. Data are expressed as mean 3 experiments ± 1 standard deviation. (* = $p<0.05$; ** = $p<0.01$; *** = $p<0.001$).

3.4.4 TRPC4

In cells harvested from oviducts at stage 1 of the estrous cycle, expression of TRPC4 was marginally down regulated by 0.62 fold (p= 0.001) in response to the treatment with Est. Furthermore, expression of TRPC4 was 0.43 fold (p= 0.02) lower in BOEC treated with FSH and LH. Similarly, treatment of BOEC with Prog resulted in small 0.36 fold (p= 0.005) down regulation in expression of TRPC4 at stage 1 of the estrous cycle compared to the control group. When added in combination, Prog and Est did not alter (p= 0.6) the TRPC4 gene expression compared to the control cells. Furthermore, when combined, Prog, FSH and LH resulted in no significant difference (p= 0.3) in expression of TRPC4 relative to the control group. In contrary, treatment of BOEC with Est, FSH and LH up regulated the expression of TRPC4 by 3.79 fold (p= 0.003) at stage 1 of the estrous cycle. The expression of TRPC4 in BOEC treated with the combination of Prog, Est, FSH and LH was the same as (p= 0.7) the untreated BOEC (Fig 3.7, A).

At stage 2 of the estrous cycle, supplementation of the culture medium with Est did not caused any significant difference (p= 0.07) in expression of TRPC4 compared to the control group. Furthermore, there was no real change (p= 0.1) in TRPC4 expression when BOEC were treated with FSH and LH. However Prog up regulated the expression of TRPC4 by 21.2 fold (p= 0.004) in BOEC at stage 2 compared to the untreated group. This increase in expression was enhanced to 39 fold (p= 0.004) by a combination of Prog and Est. Furthermore, a 51 fold (p= 0.002) increase in expression of TRPC4 was detected when BOEC was treated with the combination of Prog, FSH and LH compared to the control group. Treatment of stage 2 BOEC with Est, FSH and LH also up regulated TRPC4 expression in BOEC by 33.9 fold (p= 0.009) relative to the untreated group. Treatment of BOEC with the mixture of Prog, Est, FSH and LH all together resulted in a 46 fold (p= 0.02) increase in expression of TRPC at stage 2 of the estrous cycle (Fig 3.7, B).

At stage 3 of the estrous cycle, Est-treatment of BOEC had a 0.30 fold (p= 0.0005) decrease in TRPC4 expression. By contrast, FSH and LH dramatically up regulated the gene expression of TRPC4 in BOEC by 115.4 fold (p= 0.001) compared to the control group, while Prog induced only a modest 4.7 fold (p=

0.002) increase in expression of TRPC4 at stage 3. When Prog was combined with Est TRPC4 expression was increased by 5.39 fold (p= 0.01) compared to the control. Prog, FSH and LH together up regulated the expression of TRPC4 in stage 3 BOEC by 3.59 fold (p= 0.04). Synchronous treatment of BOEC with Est, FSH and LH led to an extensive up regulation of TRPC4 expression by more than 2380 fold (p= 0.01) compared to the untreated group. However, combining Prog with the mixture of Est, FSH and LH resulted in a modest 3.25 fold (p= 0.003) increase of TRPC4 expression relative to that of the control group at stage 3 of the estrous cycle (Fig 3.7, C).

At stage 4 of the estrous cycle, Est induced a 2.02 fold (p= 0.004) increase in expression of TRPC4 in BOEC compared to the untreated cells. Treatment of BOEC with FSH and LH in combination also resulted in a 5.62 fold (p= 0.01) up regulation of TRPC4. Furthermore, Prog treated BOEC displayed a 32.18 fold (p= 0.003) increase in the expression of TRPC4 at stage 4 of the estrous cycle. When Prog was combined with Est, expression of TRPC4 was 86 fold (p= 0.005) higher than that of the control group. However, BOEC treated with the combination of Prog, FSH and LH displayed a more modest 14.5 fold (p= 0.005) increase in expression of TRPC4. Simultaneous treatment of BOEC with Est, FSH and LH caused a dramatic 281 (p= 0.0005) fold increase in TRPC4 expression relative to the control group. This up regulation was decreased by addition of Prog to the mixture of Est, FSH and LH by a 16.45 fold (p= 0.002) increase in expression level of TRPC4 at stage 4 of the estrous cycle (Fig 3.7, D).

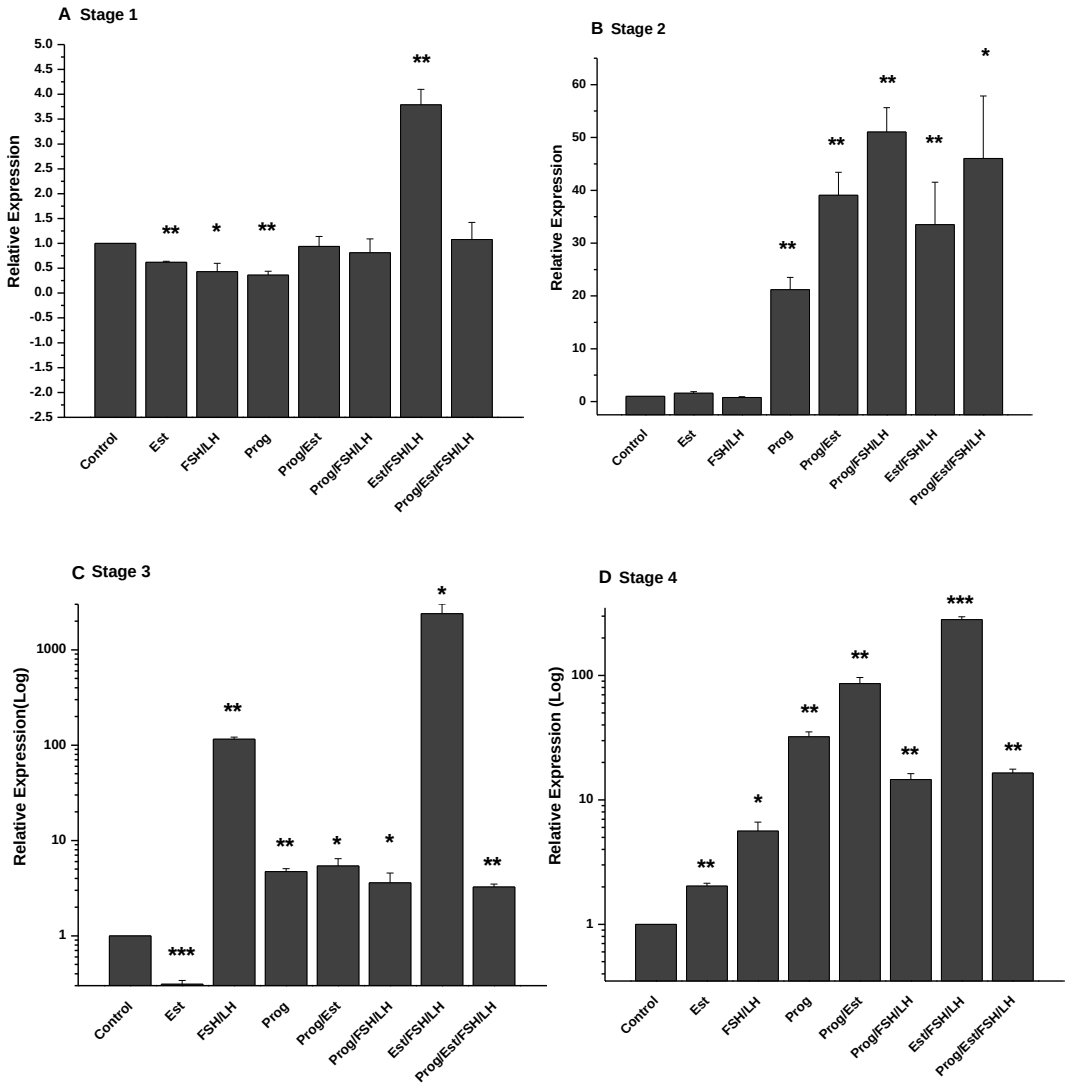

Fig 3.7 Sex hormones alter the TRPC4 in BOEC throughout the estrous cycle. Expression of TRPC4 in BOEC at stage 1 (3.7, A), 2 (3.7, B), 3 (3.7, C) and 4 (3.7, D) of the estrous cycle was altered by sex hormones. At stage 1, TRPC4 expression was changed in BOEC treated with Est, FSH/LH, Prog and combination of Est, FSH/LH (3.7, A).At stage 2, expression of TRPC4 was altered in BOEC treated with Prog and different mixtures of sex hormones but not with Est and FSH/LH (3.7, B).Expression of TRPC4 in stage 3 and 4 BOEC was affected by each of the sex hormones individually and the mixture of them (3.7, C and D). The graphs in Fig 3.7 C and D are plotted on a logarithmic scale for ease of interpretation. Data are expressed as mean 3 experiments ± 1 standard deviation. (* = $p<0.05$; ** = $p<0.01$; *** = $p<0.001$).

3.4.5 TRPC6

Expression of TRPC6 at stage 1 of the estrous cycle was largely independent of hormone treatment when provided individually [Est (p= 0.2), FSH/LH (p= 0.1), Prog (p= 0.1) and Prog/FSH/LH(p= 0.08)]. Only a combination of Est and Prog promoted a 9.18 fold (p= 0.04) increased in expression of TRPC6 in stage 1 BOEC. Furthermore, mixture of Est, FSH and LH up regulated the expression level of TRPC6 by 175 fold (p= 0.0007). When Prog was added to the mixture of Est, FSH and LH a 27.1 fold (p= 0.02) increase was observed in expression of TRPC6 in stage 1 BOEC (Fig 3.8, A).

Est did not produce a significant change (p= 0.3) in gene expression of TRPC6 in BOEC at stage 2 of the estrous cycle compared to the control group. However, a 14.43 fold (p= 0.03) increase in expression of TRPC6 was detected in BOEC treated with FSH and LH at stage 2 relative to the untreated group. Prog supplementation led to a 8.1 fold (p= 0.01) up-regulation in expression of TRPC6 in BOEC compared to the control group. A mixture of Prog and Est caused a 14.2 fold (p= 0.0004) rise in expression of TRPC6; an effect similar to that of FSH and LH. When combined, Prog, FSH and LH up-regulated the expression of TRPC6 by 65.6 fold (p= 0.005) at stage 2 of the estrous cycle; lower than the 382 fold (p= 0.002) increase in TRPC6 expression that was seen in response to the combination of Est, FSH and LH. However, treating BOEC with Pro, Est, FSH and LH led to a 31.4 fold (p= 0.02) increase in expression TRPC6 at stage 2 of the estrous cycle (Fig 3.8, B).

At stage 3 of the estrous cycle, no changes (p= 0.9) were detected in expression level of TRPC6 in BOEC treated with Est compared to the control group. However, treatment of BOEC with FSH and LH resulted in a 70.4 fold (p= 0.001) increase in gene expression of TRPC6 and Prog treated BOEC displayed an 8.6 fold (p= 0.002) increase in expression of TRPC6. Prog and Est together induced a 9.71 fold (p= 0.04) increase in expression of TRPC6 compared to the control group. When combined, Prog, FSH and LH up regulated the expression of TRPC6 in BOEC by more than 13 fold (p= 0.01) at stage 3 of the estrous cycle. Synchronous treatment of BOEC with Est, FSH and LH dramatically up regulated the expression of TRPC6; a greater than 933 fold (p= 0.006) increase was seen in comparison to that of the untreated BOEC.

However, treating BOEC with Prog, Est, FSH and LH led to a 10.5 fold (p= 0.02) increase of TRPC6 expression at stage 3 of the estrous cycle (Fig 3.8, C).

At stage 4 of the estrous cycle, Est treated BOEC displayed an 11.5 fold (p= 0.005) increase in expression of TRPC6 compared to the untreated BOEC. The increase in gene expression of TRPC6 was higher in FSH and LH treated BOEC; a greater than 74 fold (p= 0.002) up-regulation. Furthermore, treating BOEC with Prog resulted in a 17 fold (p= 0.02) increase in expression of TRPC6 relative to the control group. BOEC treated with Pro and Est together displayed a greater than 183 fold (p= 0.01) up regulation in TRPC6 expression. However, combination of Prog, FSH and LH induced only a slight, 2.4 fold (p= 0.02) increase in TRPC6 expression. By contrast, BOEC treated with combination of Est, FSH and LH dramatically up regulated expression of TRPC6 by 726 fold ($p= 9.6 \times 10^{-5}$) compared to the control group. However, when Prog was added to the mixture of Est, FSH and LH the massive increase in expression of TRPC6 was abolished and only a 3.39 fold (p= 0.007) increase in expression of TRPC6 was detected in stage 4 BOEC compared to the untreated BOEC (Fig 3.8, D).

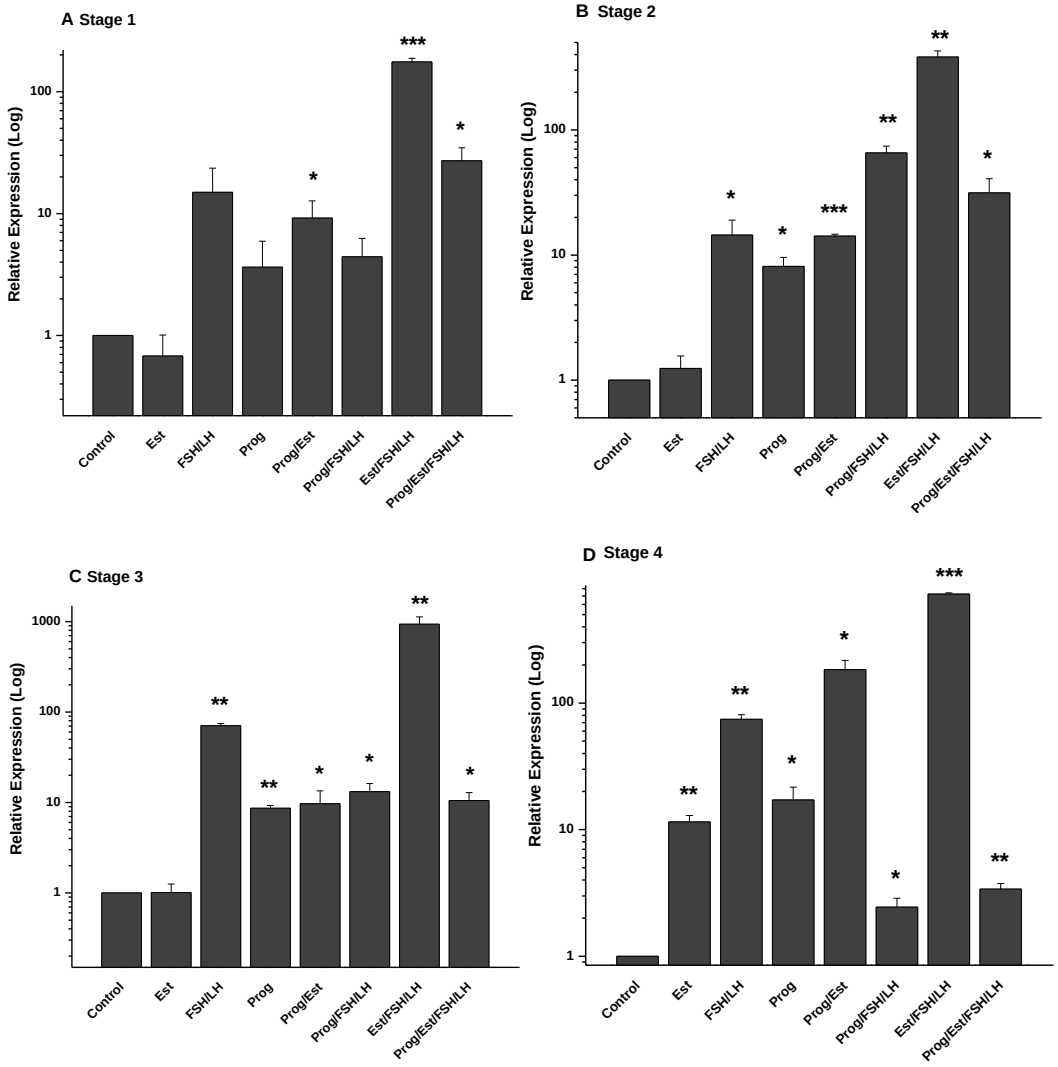

Fig 3.8 Effect of sex hormones on TRPC6 expression in BOEC throughout the estrous cycle. Expression of TRPC6 in BOEC at stage 1 (3.8, A), 2 (3.8, B), 3 (3.8, C) and 4 (3.8, D) of the estrous cycle was altered by sex hormones. At stage 1, TRPC6 expression was changed in BOEC treated with combination of Prog/Est, Est/FSH/LH and Prog/Est/FSH/LH (3.8, A).At stage 2 and 3, expression of TRPC6 was altered in BOEC treated with each of the sex hormones individually, other than Est, and their combination (3.8, B and C).Expression of TRPC6 in stage 4 BOEC was affected by each of the sex hormones individually and the mixture of them (3.8, D). The graphs are plotted on a logarithmic scale for ease of interpretation. Data are expressed as mean 3 experiments ± 1 standard deviation. (* = $p<0.05$; ** = $p<0.01$; *** = $p<0.001$).

3.5 Expression of TRPC genes in bovine uterine epithelial tissue

Fig 3.9 indicates that the genes encoding TRPC 1 (Lane 2), 2 (Lane 3), 3 (Lane 4), 4 (Lane 5) and 6 (Lane 7) were expressed in bovine uterine epithelium. The cDNA was generated from total mRNA extracted from bovine uterine epithelial tissue. Expression of β actin confirmed that the PCR conditions were optimised (Lane 1, Fig 3.9). Positive expression of Cytokeratin18 (Lane 9, Fig 3.9), a marker specific to epithelial cells, confirmed that the template cDNA was from epithelial cells. The expected size of the PCR products were β actin 100 bp, TRPC1 232 bp, TRPC2 233 bp, TRPC3 244 bp, TRPC4 227 bp, TRPC5 179 bp, TRPC6 183 bp, TRPC7 168 bp and Cytokeratin18 181 bp.

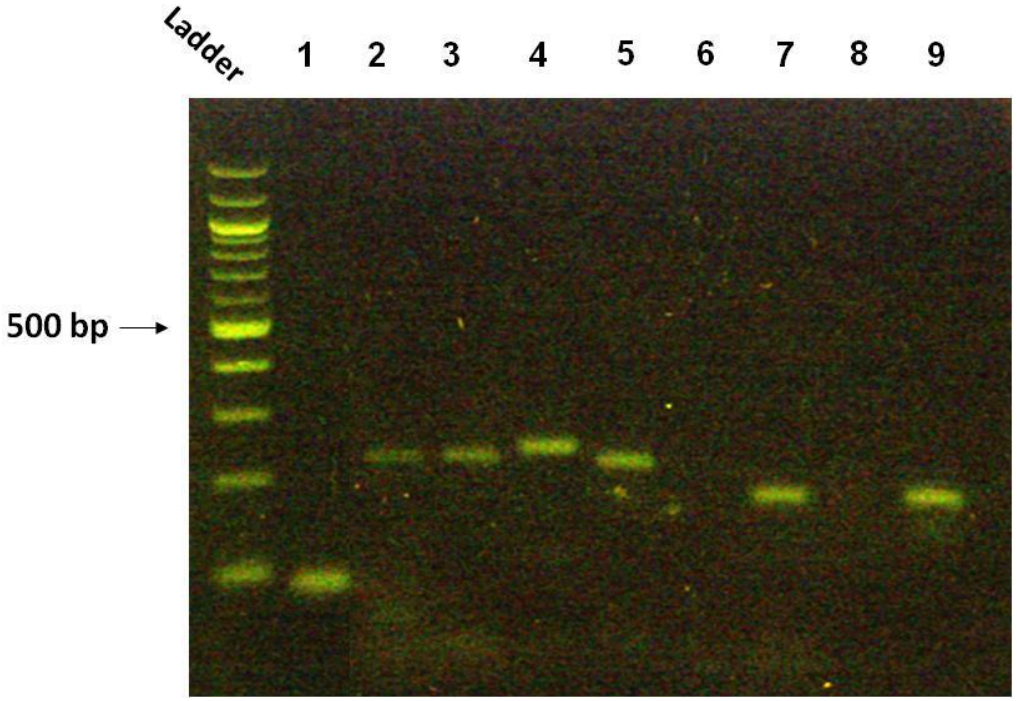

Fig 3.9 TRPC isoforms expressed in bovine uterine epithelium. PCR Products eletrophoresed on a 2% agarose gel, indicating positive expression of TRPC 1, 2, 3, 4 and 6 in bovine uterine tissue. Expression of TRPC5 and TRPC7 was not detected in the bovine uterine epithelial tissue. PCR products were loaded on the gel as following: lane 1; β actin (100 bp), lane 2; TRPC1 (232 bp), lane 3; TRPC2 (233bp), lane 4; TRPC3 (244 bp), lane 5; TRPC4 (227 bp), lane 6 ; TRRPC5 (179 bp), lane 7; TRPC6 (183 bp), lane 8; TRPC7 (168 bp) and lane 9; Cytokeratin18 (181 bp).

3.6 Expression of TRPC genes in bovine uterine epithelial tissue throughout the estrous cycle

Relative gene expression of TRPC family members throughout the estrous cycle in bovine uterine epithelial tissue is shown in Fig 3.10 Changes in expression level of TRPCs throughout the estrous cycle was measured relative to stage 1 of the cycle. In general, the expression patterns of all the TRPC family members show similarity at stage 4 of the estrous cycle.

In bovine uterine epithelial tissue, expression of TRPC1 was not significantly different ($p= 0.08$) at stage 2 compared to that of stage 1. At stage 3, expression of TRPC1 was slightly up-regulated, by 1.29 fold ($p= 0.001$) relative to the stage 1. Expression of TRPC1 at stage 4 was up-regulated by 10.98 fold ($p= 0.004$) compared to stage 1 of the estrous cycle (Fig 3.10, A).

TRPC2 gene expression was down-regulated by 0.48 fold ($p= 0.01$) at stage 2 of the estrous cycle relative to that of the stage 1. However, at stage 3, a 2.41 fold ($p= 0.02$) increase was detected in expression level of TRPC2 in bovine uterine epithelium. This increase was greater by 39.9 fold ($p= 0.005$) at stage 4 of the cycle relative to stage 1 (Fig 3.10, B).

Expression of TRPC3 appeared to be suppressed in bovine uterine epithelial tissue at stage 2 of the estrous cycle by 0.3 fold ($p= 0.003$). However, at stage 3, expression of TRPC3 was not significantly different ($p= 0.2$) to that of the stage 1. By contrast, at stage 4 of the cycle, expression of TRPC3 was increased by 6.40 fold ($p= 0.004$) compared to stage 1 of the estrous cycle (Fig 3.10, C).

The expression of TRPC4 at stage 2 of the estrous cycle was not significantly different ($p= 0.2$) compared to stage 1. By contrast, a 2.7 fold ($p= 0.02$) increase in expression of TRPC4 was detected at stage 3 of the estrous cycle. This increase was followed by a further 31.2 fold ($p= 0.01$) up-regulation at stage 4 of the estrous cycle relative to the stage 1 (Fig 3.10, D).

Similar to TRPC4, the expression level of TRPC6 was not significantly different ($p= 0.4$) at stage 2. Furthermore, at stage 3 of the estrous cycle, no significant change ($p= 0.07$) was detected in expression of TRPC6 compared to that of the

stage 1. However, at stage 4 of the cycle, expression of TRPC6 was up-regulated by 11.67 fold (p= 0.01) relative to that of the stage 1 (Fig 3.10, E).

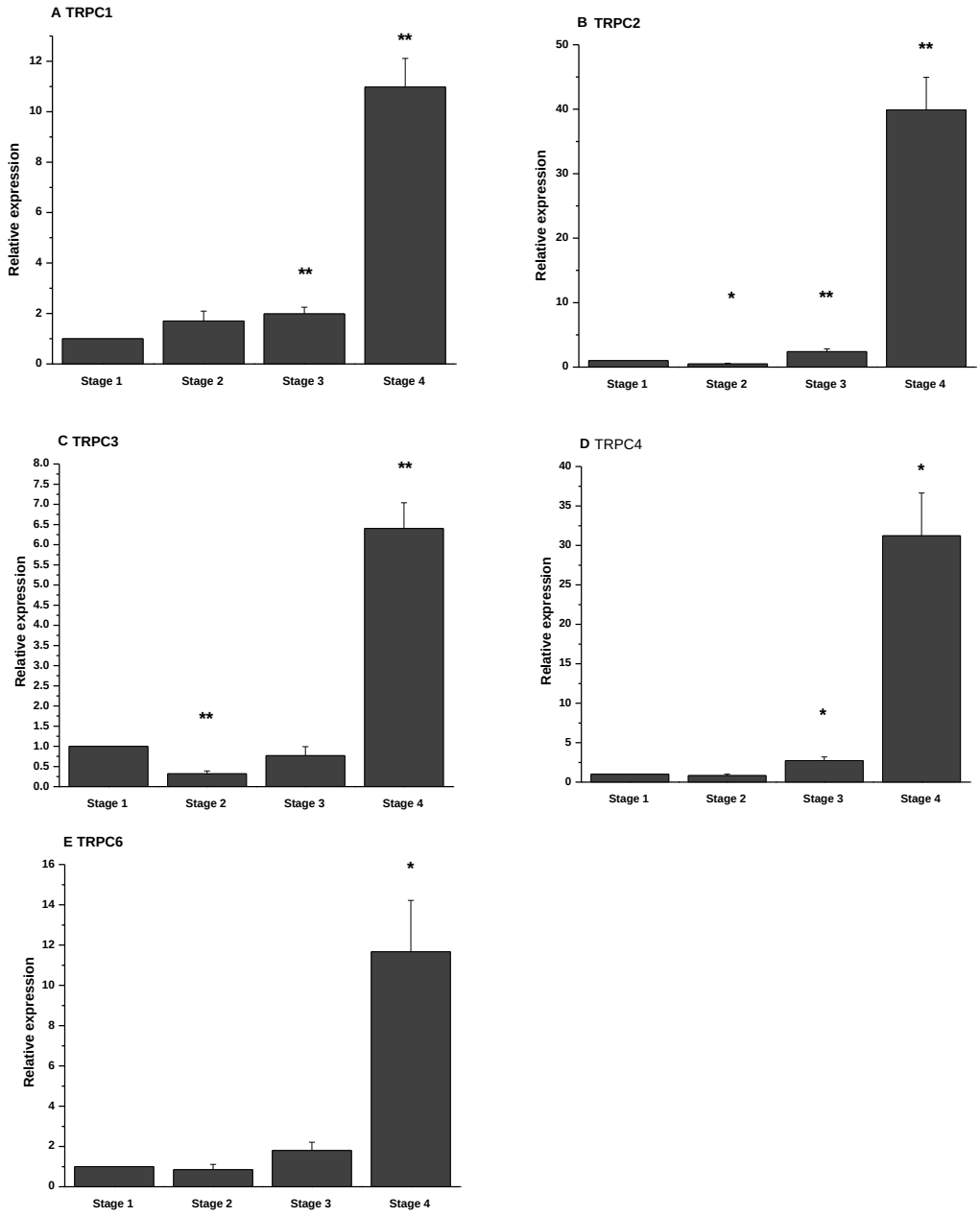

Fig 3.10 Changes in expression of TRPC genes in bovine uterine epithelial tissue throughout the estrous cycle. The expression level of TRPC genes at different stages of the estrous cycle was measured relative to the stage 1. Expression of TRPC1 (3.10, A) was not significantly changed at stage 2 but up regulated at stage 3 and 4 of the cycle in comparison to that of the stage 1. Expression level of TRPC2 (3.10, B) was down regulated at stage 2 but up regulated at stage 3 and 4 of the estrous cycle. TRPC3 expression (3.10, C) was decreased at stage 2 compared to stage 1. However, no significant difference in expression of TRPC3 was observed at stage 3. TRPC3 expression was increased at stage 4 compared to that of the stage1. Expression of TRPC4 (3.10, D) was not significantly different at stage 2 but was up regulated at stage 3 and 4 of the estrous cycle in relation to that of stage 1. Expression level of TRPC6 (3.10, E) in bovine uterine epithelial tissue at stage 2 and 3 was similar to that of the stage 1. However, an up regulation in TRPC6 expression was observed at stage 4 of the estrous cycle comparing to that of stage 1. Data are expressed as mean 3 experiments ± 1 standard deviation. (* = $p<0.05$; ** = $p<0.01$; *** = $p<0.001$).

3.7 Differences in gene expression of TRPC isoforms in bovine uterine epithelial tissue and cultured cells

The pattern of expression of TRPC isoforms in cultured bovine uterine epithelial cells (BUEC) throughout the estrous cycle differed markedly to that observed in the tissue. The changes in expression level of TRPCs in both bovine uterine epithelial tissue and cultured cells at different stages of the estrous cycle were measured in relation to the stage 1 of the cycle and are presented in Fig 3.11.

The expression level of TRPC1 in stage 2 BUEC was not significantly different to that of stage 1 BUEC (p= 0.1) and stage 2 bovine uterine tissue (p= 0.07). The change in expression of TRPC1 at stage 3 of the estrous cycle in BUEC and tissue was similar and 1.29 fold higher than that of the stage 1 (p= 0.001). At stage 4 of the estrous cycle, expression of TRPC1 was down-regulated in BUEC by 0.62 fold (p= 0.0004) and lower by 0.05 fold (p= 0.003) compared to that of the tissue relative to the stage 1 (Fig 3.11, A).

Expression of TRPC2 in BUEC at stage 2 of the estrous cycle was higher by 1.88 fold (p= 0.001) relative to stage 1 which was 3.89 fold (p= 0.0002) higher than that of the tissue at stage 2 of the estrous cycle. Similar to the bovine uterine epithelial tissue, expression of TRPC2 at stage 3 of the estrous cycle was up-regulated by 2.23 fold (p= 0.003) compared to the stage 1. This change was close to that observed in the tissue (p= 0.5). Expression of TRPC2 in BUEC at stage 4 was not significantly different (p= 0.1) to that of the stage 1 and was lower than that of the tissue by 0.02 fold (p= 0.005) (Fig 3.11, B).

While expression of TRPC3 was down-regulated in the tissue at stage 2, it was up-regulated by 2.07 fold (p= 0.009) in stage 2 BUEC compared to stage 1.Changes in expression of TRPC3 at stage in the BUEC was higher by 6.55 fold (p= 0.0005) compared to that of the tissue. At stage 3 of the estrous cycle, expression of TRPC3 in BUEC was slightly up-regulated by 1.33 fold (p= 0.03) compared to that of the stage 1 and was 1.73 fold (p= 0.02) higher than that of the tissue. Expression of TRPC3 in stage 4 BUEC was not significantly different (p= 0.1) to that of the stage 1, and was lower by 0.19 fold (p= 0.005) compared to that of the uterine epithelial tissue at stage 2 of the estrous cycle (Fig 3.11, C).

Expression of TRPC4 at stage 2 was not significantly in tissue compared to stage 1, although it was down-regulated by 0.56 fold (p= 0.002) in stage 2 BUEC. However, this change was not significantly different (p= 0.1) to that of the tissue. When TRPC4 was up-regulated at stage 3 in the bovine uterine epithelial tissue, it was down-regulated by 0.22 fold (p= 4.87 $x10^{-5}$) in stage 3 BUEC. The change in the expression of TRPC4 in stage 3 BUEC was 0.08 fold (p= 0.01) lower than that of the tissue. At stage 4 of the estrous cycle, TRPC4 was down-regulated in the BUEC by 0.43 fold (p= 0.0009) while it was up-regulated in the tissue. Expression of TRPC4 in stage 4 BUEC was 0.01 fold (p= 0.01) lower than that of the tissue (Fig 3.11, D).

Expression of TRPC6 in bovine uterine epithelial tissue was not significantly different at stage 2 and 3, however it was up-regulated by 3.96 (p= 0.002) and 5.92 (p= 0.01) fold in stage2 and 3 BUEC respectively. Expression of TRPC6 was up-regulated in stage 4 BUEC similar to that of the tissue. Up-regulation of TRPC6 in stage 4 BUEC was 3.32 fold (p= 0.007) relative to that of the stage 1 and 0.28 fold (p= 0.03) lower than that of the tissue (Fig 3.11, E).

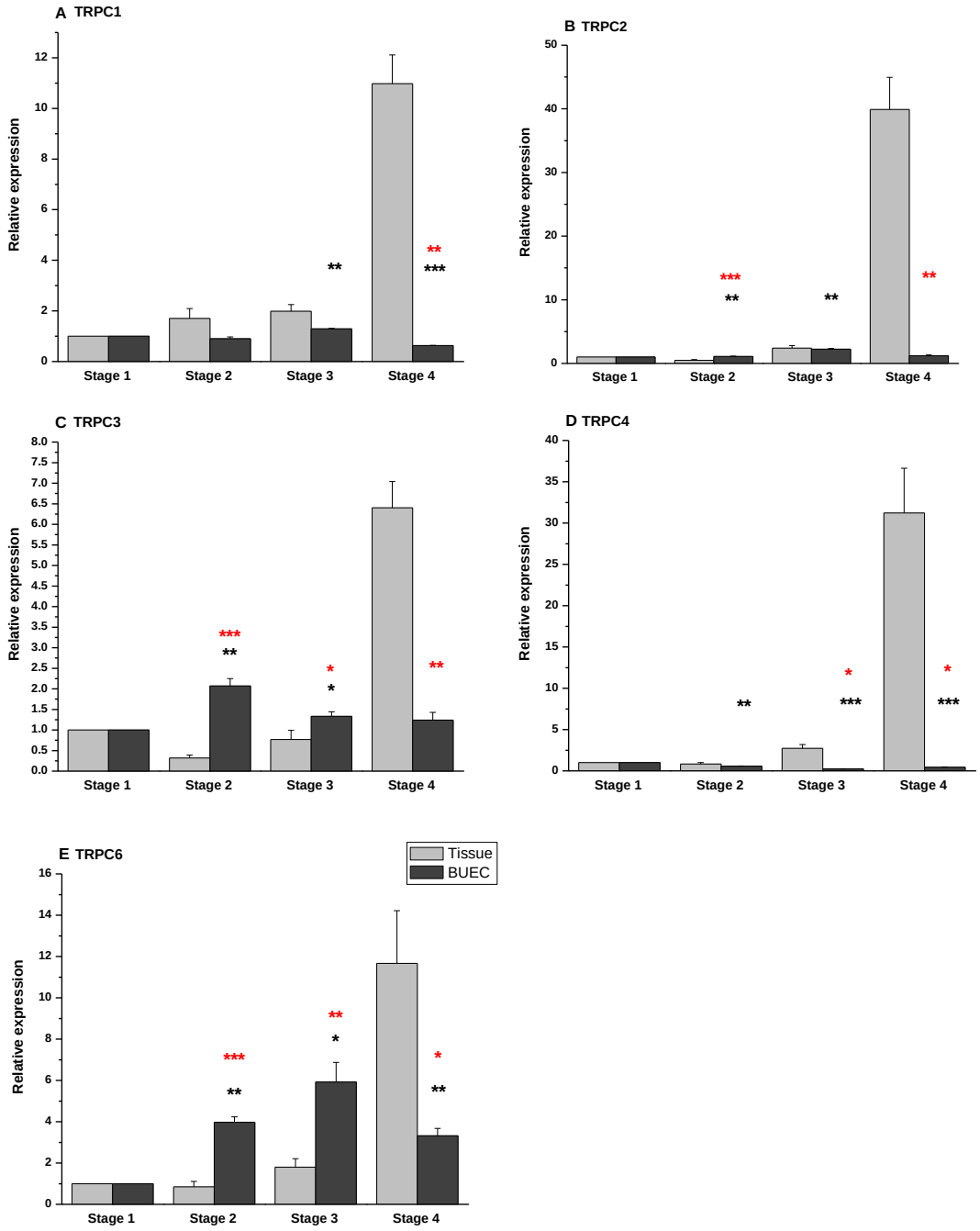

Fig 3.11 Expression of TRPC isoforms in bovine uterine epithelial cultured cells differs to that of the tissue throughout the estrous cycle. Data are expressed as mean 3 experiments ± 1 standard deviation. (* = p<0.05; ** = p<0.01; *** = p<0.001). ***** represents the P value, comparing the changes in the gene expression at different stages of the estrous cycle to the stage 1 in BOEC. ***** represents the P value, comparing the changes in TRPCs gene expression between tissue and cultured cells at each stage of the estrous cycle.

3.8 Discussion

The objective of this chapter was to investigate whether the genes encoding for members of Transient Receptor Potential Canonical channels (TRPC) are expressed in bovine oviduct and uterine epithelia. Once this had been established, the secondary aim was to discover whether the pattern of gene expression, at the mRNA level, differed varied throughout the estrous cycle. Gene expression of TRPC family proteins in bovine oviduct and uterine epithelial tissue was investigated due to their importance in calcium homeostasis in a variety of tissues since calcium plays vital roles in a plethora of fundamental cellular physiological functions including proliferation, growth, contraction, secretion and death (Berridge *et al.*, 1998b). TRPC channels, a subfamily of Transient Receptor Potential channels, are a novel class of calcium permeable cationic channels and it has been proposed they are G protein-coupled receptor-operated Ca2+ channels (ROCs) or internal Ca2+ store-operated channels (SOCs) (Xu & Beech, 2001; Clapham, 2003b).

In the present research, of 7 members of TRPC family; TRPC1, 2, 3, 4 and 6 genes were expressed in both bovine oviduct and uterine epithelial tissue (Fig 3.1 and 3.9).. It was also apparent that the expression levels of all TRPC gene isoforms in both bovine oviduct and uterine epithelial tissue changed throughout the estrous cycle (Fig 3.2 and 3.10). Moreover, the pattern of expression in the oviduct epithelium was different to that of the uterus. Such cyclical regulation suggests a possible role(s) of these channels in the female bovine reproductive tract during the cyclical physiological remodelling associated with estrous.

In general, expression of all the TRPC isoforms present in the bovine oviduct epithelium was the highest at stage 1 of the estrous cycle where progesterone is the dominant hormone and 17β- estradiol, FSH and LH are at their lowest concentration (Fig 3.2). A notable exception to this was TRPC1 whose expression was the highest at stage 3. By contrast, expression of uterine levels of all the TRPC isoforms was highest at stage 4 of the estrous cycle where 17β-estradiol is the dominant hormone and progesterone is at its lowest level. It is also notable that the concentrations of FSH and LH peak at stage 4 of the estrous cycle.

At stage 1 (day 1-4) of the estrous cycle, the production of 17β-estradiol from the corpus luteum (CL) is reduced which leads to a dramatic fall in concentration of 17β estradiol as the CL increases secretion of progesterone. At stage 2 (day 5-10), the concentration of progesterone remains high and 17β-estradiol rises slightly at day 4 before falling to its lowest level throughout the cycle at day 7 (Echternkamp & Hansel, 1973; Randel, 1980). At stage 3 (day 11-17), progesterone is the dominant hormone present in the blood stream (Adeyemo & Heath, 1980; Eduvie & Dawuda, 1986; Llewelyn *et al.*, 1987). However, by stage 4 of the cycle prostaglandin F2α (PGF2α) which is secreted from the uterine epithelium suppresses the secretion of progesterone (LaVoie *et al.*, 1975). Secretion of $PGF_{2\alpha}$ is a consequence of oxytocin binding to its specific receptor in the uterine epithelium. Oxytocin induces an increase in inositol phosphates (IPs) which are involved in store-operated calcium entry (Clapham, 2003b) and regulation of intracellular calcium concentration in bovine uterine epithelial cultured cells (Asselin *et al.*, 1997). Secretion of $PGF_{2\alpha}$ from uterine epithelium starts at the end of stage 3 and beginning of stage 4 of the estrous cycle where the expression of TRPC isoforms are at their highest level in the uterine epithelium. This suggests a possible role of TRPC isoforms in regulating intracellular calcium concentration required for physiological events in bovine uterine epithelium. Oxytocin is synthesized in the CL (Abdelgadir *et al.*, 1994). Secretion of $PGF_{2\alpha}$ occurs at the end of mid luteal phase (stage 3) and increases at the beginning of the late luteal phase (stage 4) where TRPC isoforms are at their highest level in bovine uterine epithelial tissue (Fig 3.10). Furthermore, at this stage, the newly recruited follicle will initiate secretion of 17β- estradiol. Hence, release of Gonadotropin-releasing hormone (GnRH) from the hypothalamus leads to secretion of FSH and LH from the pituitary (Kaltenbach *et al.*, 1974; Schams *et al.*, 1974). It has been reported that progesterone triggers secretion of dipeptidyl peptidase-IV by endometrium of ewe and cow (Liu & Hansen, 1995; Gregoraszczuk *et al.*, 2001). Therefore, progesterone could possibly induce its effect by regulating the intracellular concentration via TRPC channels. Increasing levels of plasma progesterone leads to the secretion of nutrients and electrolytes from oviduct epithelium to provide the microenvironment for spermatozoa, mature oocyte, fertilization and early embryo. Furthermore, after ovulation, the number of ciliated epithelial cells increases to help transport the oocyte from the infundibulum to the site of

fertilization in the ampullary-isthmus junction (AIJ) and to facilitate the movement of the early embryo to the uterus (Hunter, 1994; Croxatto, 2002b). Both the secretion (Richardson *et al.* (1985); (Sharma & Rao, 1992; Dickens *et al.*, 1996) and motility of ciliated cells (Salathe, 2006) are dependent on changes in intracellular calcium concentration. It has been reported that TRP channels are involved in the secretion (Uchida & Tominaga, 2011) and motility of ciliated cells (Lorenzo *et al.*, 2008) and so it may be the case that the TRPC expression pattern is important in regulating the physiology of the epithelia of the female reproductive environment. As demonstrated in this chapter, expression of TRPC isoforms in oviduct epithelium at stage 1 (day 1-4) of the estrous cycle ,which is the most eventful time of the cycle in oviduct (oocyte pick up by infundibulum (Talbot *et al.*, 1999), fertilization and early embryo transport), is higher than the other stage of the estrous cycle suggesting the possible role of these channels in this process. Moreover, such changes in expression of TRPC isoforms in bovine oviduct and uterine epithelial tissue may result from, hormonal changes throughout the estrous cycle and the different expression patterns in uterus and oviduct; possibly due to the different expression pattern and level of estrogen receptors (α and β as well as progesterone receptor in these tissues (Tibbetts *et al.*, 1998; Wang *et al.*, 2000; Mendoza-Rodriguez *et al.*, 2003).

Due to the necessity of using cultured cells for a significant part of this project, changes in the expression level of the TRPC isoforms present in the bovine oviduct and uterine epithelium were studied in both Bovine Oviduct Epithelial Cultured cells (BOEC) and Bovine Uterine Epithelial Cultured Cells (BUEC) throughout the estrous cycle. Furthermore, these changes were compared to those of fresh tissue at equivalent stages of the estrous cycle. It was found that expression levels of TRPC isoforms present in bovine oviduct and uterine epithelium were different in at least one or all the stages of the estrous cycle in both BOEC and BUEC compared to tissue at equivalent stages of the estrous cycle (Fig 3.3 and 3.11). For instance, at stage 4 of the estrous cycle TRPC2 expression was down-regulated in bovine oviduct epithelial tissue, whereas an increase was detected in TRPC2 expression in BOEC (Fig 3.3, B).

The differences in the pattern of gene expression of TRPC isoforms between bovine oviduct and uterine epithelium and BOEC/BUEC highlight a possible role

for the sex hormones since their concentrations change periodically throughout the estrous cycle. These hormones were absent from the basic epithelial cell culture medium (Table 2.2), but have been shown previously to have regulatory effects on gene expression; for instance, the role of progesterone on gene expression regulation in the endometrium of rhesus monkey (Okulicz & Ace, 1999), role of 17β estradiol in gene regulation in breast cancer (Charpentier *et al.*, 2000), FSH-induced gene regulation in pig granulosa primary cells (Bonnet *et al.*, 2006) and LH-induced gene regulation in mouse granulosa cells (Carletti & Christenson, 2009). To determine if the sex hormones had a regulatory role in the expression of TRPC isoforms, BOEC cultures were treated acutely with physiological concentrations(Ginther *et al.*, 2010) of 17β estradiol (Est), Progesterone (Prog) and Follicle-Stimulating Hormone (FSH) and Luteinizing hormone (LH). In general, an up-regulation in expression of all the TRPC isoforms was induced at all 4 stages of the estrous cycle in BOEC treated with FSH and LH. This effect was boosted by the addition of Est to a mixture FSH and LH. When Prog was combined with the mixtures of either FSH and LH or Est, FSH and LH, the up-regulatory effect on expression level of TRPC isoforms throughout the estrous cycle was not seen, with modest exceptions. The FSH/LH-induced increase in the expression level of TRPC3 and 6 at stage 2 of the estrous cycle was not inhibited by addition of Prog (Fig 3.6 and 3.8, B). Furthermore, the FSH/LH-induced up-regulation of TRPC4 was not inhibited at stage 1 of the estrous cycle (Fig 3.7, A) when Prog was present. At stage 2 of the estrous cycle, Prog promoted an increase in expression of TRPC4 individually and in combination with each or all of Est, FSH and LH (Fig 3.7, B). In BOEC treated with Est solely, expression of TRPC1 and 4 was down-regulated at stage 1 and 3 of the estrous cycle. Similarly, an inhibitory effect of Est on expression of TRPC4 was reported in Bovine Aortic Endothelial Cell (Chang *et al.* (1997). However, Est up-regulated the expression of TRPC 1 and 3 at stage 2 and 4 and TRPC2 and 4 and 6 at stage 4 of the estrous cycle.

The apparent regulatory effect of Prog on TRPC4 at stage 1 and 2 and Est on TRPC1 and 4 at stage 1 and 3 compared to stage 2 and 4 could either be due to different expression levels of receptor of these hormone or the presence of TRPC1 (Dedman *et al.*, 2004; Dedman *et al.*, 2005) and 4 (Schaefer *et al.*, 2002) splice variants which might have a different regulation pathway.

Furthermore, the up-regulatory effect of a mixture of FSH/LH on expression of TRPC isoforms throughout the estrous cycle could be related to the FSH receptor which is a member of the rhodopsin-like subfamily of G-protein-coupled receptors (Marion *et al.*, 2002). Rhodopsin-like receptor could be involved in TRPC activation by stimulation of phospholipase C (PLC) through $G\alpha_{q/11}$ activation (Grasberger *et al.*, 2007; Kero *et al.*, 2007; Kleinau *et al.*, 2010). Furthermore, activation of LH receptor induces its effect on steroid biosynthesis and secretion via G-protein $G\alpha_s$ (Dufau, 1998). As was mentioned above, TRPCs are G-protein coupled receptors- channels (Clapham, 2003b). Therefore, activation of TRPC channels by FSH/LH could have a positive impact on their gene expression level. It has also been reported that Tumor Necrosis Factor α (TNF α) up regulates the mRNA expression of TRPC1 in Human Umbilical Vein Endothelial Cells (HUVEC) via activation of Nuclear Factor-Kappa B (NF-κB)(Paria *et al.*, 2003). Both FSH (Wang *et al.*, 2002b) and LH (Gründker *et al.*, 2000) are involved in activation of NF-κB which could be related to the regulatory effect of FSH and LH on TRPC genes expression.

These finding suggest that TRPC gene expression is regulated by sex hormone(s) in Bovine Oviduct Epithelial cells and that Est, Prog, FSH and LH interact with each other to regulate the expression of TRPC genes in this tissue.

Chapter 4

Localization and abundance of TRPC channels in female reproductive tract epithelia

4.1 Localization of TRPC1 and TRPC6 in female bovine reproductive tract

Localization of TRPC1 and TRPC6 in female bovine reproductive tract was studied using immunohistochemistry, immunochytochemistry and confocal microscopy techniques. Specific TRPC1 and TRPC6 antibodies were used to determine the localization of these cation channels in epithelial tissue lining the bovine oviduct and uterus.

4.1.1 Localization of TRPC1 and TRPC6 in bovine oviduct throughout the estrous cycle

The oviduct consists of three sections; infundibulum, ampulla and isthmus. Various physiological events occur in each part of the oviduct. Localization and abundance of TRPC1 and TRPC6 was studied in each section of the oviduct throughout the estrous cycle.

4.1.1.1 Localization and abundance of TRPC1 and TRPC6 in non-permeabilized bovine oviduct epithelium at stage 1 of the estrous cycle

TRPC1 channels were equally located on the apical and basal sides of the bovine infundibulum epithelial tissue and at a lower level on the lateral side of the epithelium in non-permeabilized immunostained tissue (Fig 4.1, A). However, in bovine ampulla epithelium theTRPC1 channel was equally distributed on the apical and lateral sides of the epithelium but its localization was lower on the basal side of the epithelium (Fig 4.1, B). In bovine isthmus epithelial tissue, the TRPC1 channel was located on the lateral side of the epithelial tissue at a higher level compared to the apical and basal side at stage 1 of the estrous cycle (Fig 4.1, C). At stage 1 of the estrous cycle, localization of TRPC6 channel was higher on the apical side of the non-permeabilized bovine infundibulum epithelial tissue compared to that of the basal side. On the lateral side of the bovine infundibulum localization of TRPC6 was lower than that of the apical and basal sides (Fig 4.1, A). Localization of TRPC6 channels in non-permeabilized bovine ampulla tissue was highest on the lateral and the lowest on basal side of the epithelium (Fig 4.1, B). Localization of TRPC6 was slightly greater on the lateral side of the non-permeabilized bovine isthmus epithelial tissue compared to that of the apical and basal sides where equal distribution was observed (Fig 4.1,c.

0

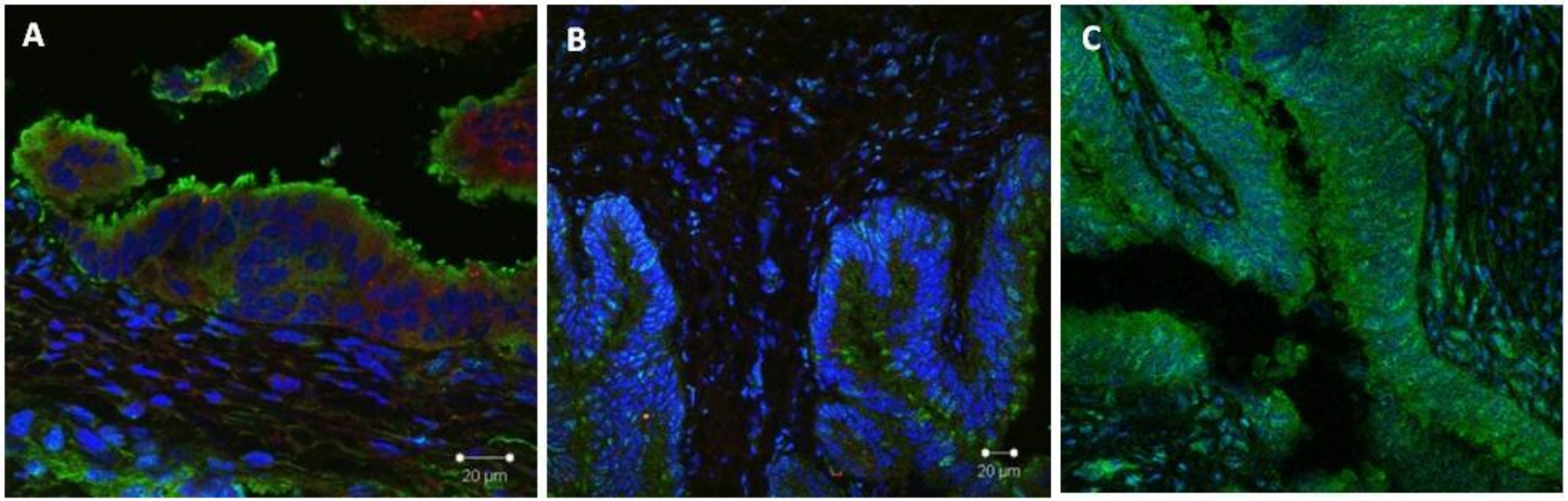

Fig 4.1 Localization of TRPC1 and TRPC6 at stage 1 of the estrous cycle in non-permeabilized epithelial tissue of bovine Infundibulum (4.1,A), Ampulla (4.1, B) and Isthmus (4.1,C). Nuclei are labelled with DAPI (Blue), TRPC1 with Alexa Four 647 FITC conjugated (Red) and TRPC6 with Alexa Flour 488 (Green).

Measuring the fluorescence intensity (FI) indicated that the abundance of TRPC1 on the apical side of the non-permeabilized bovine oviduct epithelium was higher by 9.9 fold (p= 0.01) compared to that of the infundibulum. Furthermore, abundance of TRPC1 in isthmus was 16.5 fold (p= 0.0001) higher relative to the infundibulum (Fig 4.2, A). On the basal side of the tissue, abundance of the TRPC1 channel was 9.6 fold (p= 0.01) higher in ampulla compared to the infundibulum. In isthmus, TRPC1 was more abundant by 23.3 fold (p= 0.0006) compared to the infundibulum (Fig 4.2, B). On the lateral side of the non-permeabilized bovine oviduct epithelium at stage 1 of the estrous cycle abundance of TRPC1 was higher by 15.3 fold (p= 0.009) in ampulla and 41.4 fold (p= 0.0002) in isthmus compared to the infundibulum (Fig 4.2, C).

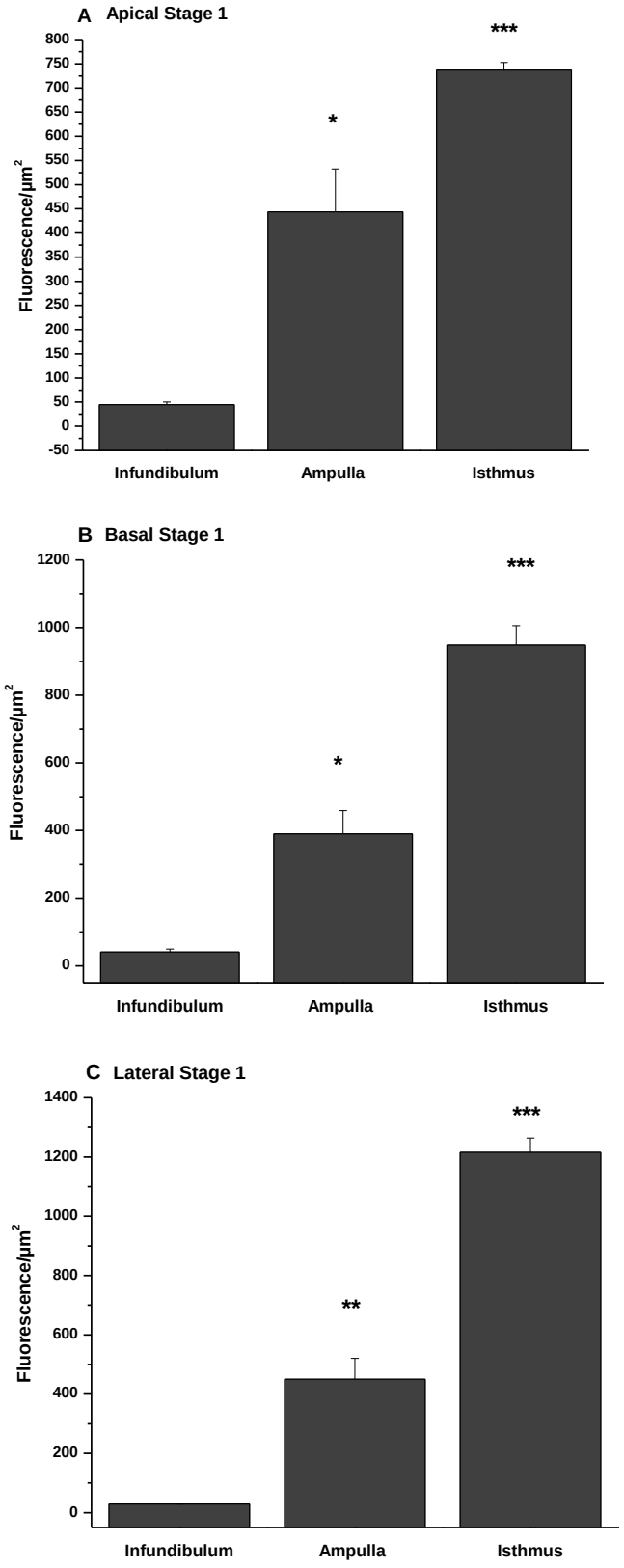

Fig 4.2 Abundance of TRPC1 in non-permeabilized bovine oviduct epithelium at stage 1 of the estrous cycle in apical (4.2,A), Basal (4.2,B) and the lateral (4.2,C) side of the tissue. Abundance of the TRPC1 was higher in ampulla and isthmus on apical, basal and lateral side of the epithelium compared to that of the infundibulum. All data are expressed as a mean of 3 replicates ± 1 standard deviation. (* = $p<0.05$; ** = $p<0.01$; *** = $p<0.001$).

FI measurements of the apical side indicated that the abundance of TRPC6 channels was higher by 10 fold (p= 0.003) in ampulla and 135 fold (p= 0.03) higher in isthmus compared to that of the infundibulum at stage 1 of the estrous cycle in non-permeabilized immunostained tissue (Fig 4.3, A). Abundance of TRPC6 protein on the basal side of the bovine oviduct epithelium was higher by 14 fold (p= 0.008) in ampulla and 280 fold (p= 0.004) in isthmus compared to that of the infundibulum (Fig 4.3, B). The abundance of TRPC6 on the lateral side of the bovine oviduct epithelial tissue at stage 1 of the estrous cycle in non-permeabilized tissue was higher by 38 fold (p= 0.001) in ampulla epithelium and 425 fold (p= 0.02) in isthmus compared to that of the (Fig 4.3, C).

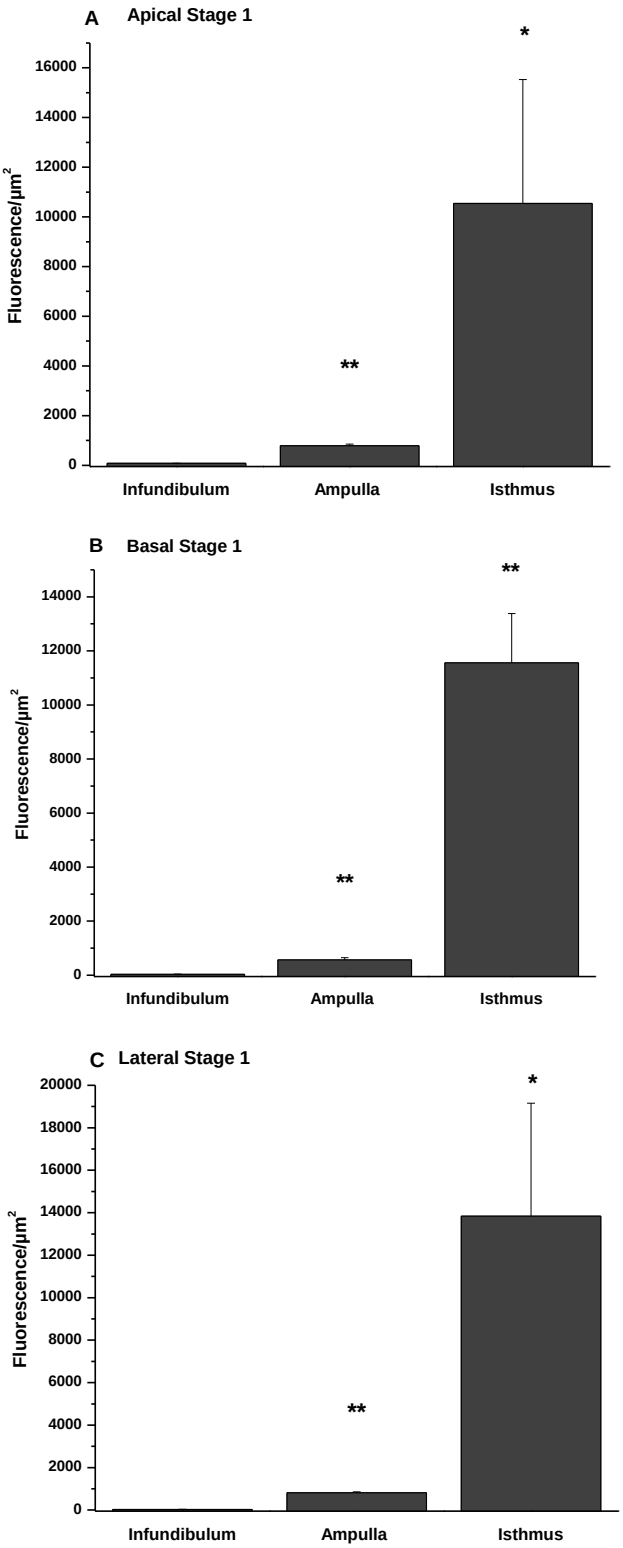

Fig 4.3 Abundance of TRPC6 in non-permeabilized bovine oviduct epithelium at stage 1 of the estrous cycle in apical (4.3,A), Basal (4.3,B), the lateral (Fig 4.3, C) side of the tissue. Abundance of TRPC6 was higher in ampulla and isthmus of the oviduct epithelium in non-permeabilized tissue at stage 1 of the estrous cycle compared to that of the infundibulum. All data are expressed as a mean of 3 replicates ± 1 standard deviation. (* = $p<0.05$; ** = $p<0.01$; *** = $p<0.001$).

4.1.1.2 Localization and abundance of TRPC1 and TRPC6 in permeabilized bovine oviduct epithelium at stage 1 of the estrous cycle

At stage 1 of the estrous cycle, TRPC1 channel was localized on the apical, basal and lateral sides of the bovine infundibulum permeabilized tissue (Fig 4.4, A). However, its localization was lower on the lateral side of the epithelium. Localization of TRPC1 channel in bovine ampulla epithelium was higher on the apical side compared to the basal side of the permeabilized tissue. Distribution of the TRPC1 channel on the lateral side of ampulla epithelium was less than that on apical and basal side permeabilized tissue (Fig 4.4, B). In permeabilized bovine isthmus epithelial tissue, more TRPC1 channel was present on the apical side of the tissue compared to that of the basal and lateral sides where equal distribution of TRPC1 protein was observed (Fig 4.4, C).

At stage 1 of the estrous cycle, the TRPC6 channel was equally distributed on the basal, apical and lateral sides of the permeabilized bovine infundibulum epithelial tissue (Fig 4.4, A). In bovine ampulla, localization of TRPC6 was slightly greater on the lateral side of the epithelium compared to the apical and basal side (Fig 4.4, B). However, in isthmus epithelial tissue, localization of TRPC6 channel was highest on the lateral side and lowest on the basal side of the epithelium (Fig 4.4, C).

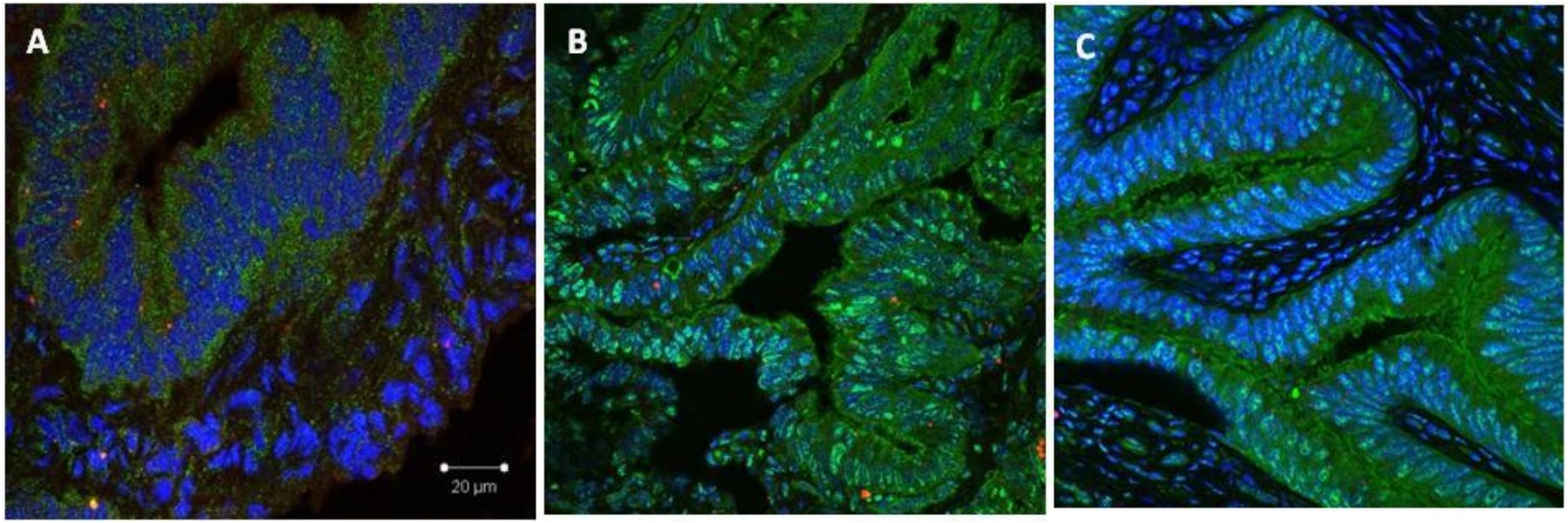

Fig 4.4 Localization of TRPC1 and TRPC6 at stage 1 of the estrous cycle in permeabilized epithelial tissue of bovine Infundibulum (4.4, A), Ampulla (4.4, B) and Isthmus (4.4, C). Nuclei are labelled with DAPI (Blue), TRPC1 with Alexa Four 647 FITC conjugated (Red) and TRPC6 with Alexa Flour 488 (Green).

Measuring the fluorescence intensity indicated that at stage 1 of the estrous cycle, abundance of TRPC1 channel on the apical side of permeabilized immunostained bovine ampulla and isthmus epithelial tissue was 8 (p= 0.02) and 7 (p= 0.001) fold higher than that of infundibulum respectively (Fig 4.5, A). On the basal side of the epithelial tissue, abundance of TRPC1 channel was 9.6 fold (p= 0.02) higher on bovine ampulla epithelium compared to bovine infundibulum. Abundance of TRPC1 channel was highest in isthmus epithelium where the FI was 23.4 fold (p= 0.004) higher than that of the infundibulum (Fig 4.5, B). Abundance of TRPC1 channel on the lateral side of the bovine oviduct epithelial tissue was 6 fold (p= 0.02) higher in ampulla compared to the infundibulum. This is slightly higher in the isthmus by 6.43 fold (0.0004) increase in comparison to the infundibulum (Fig 4.5, C).

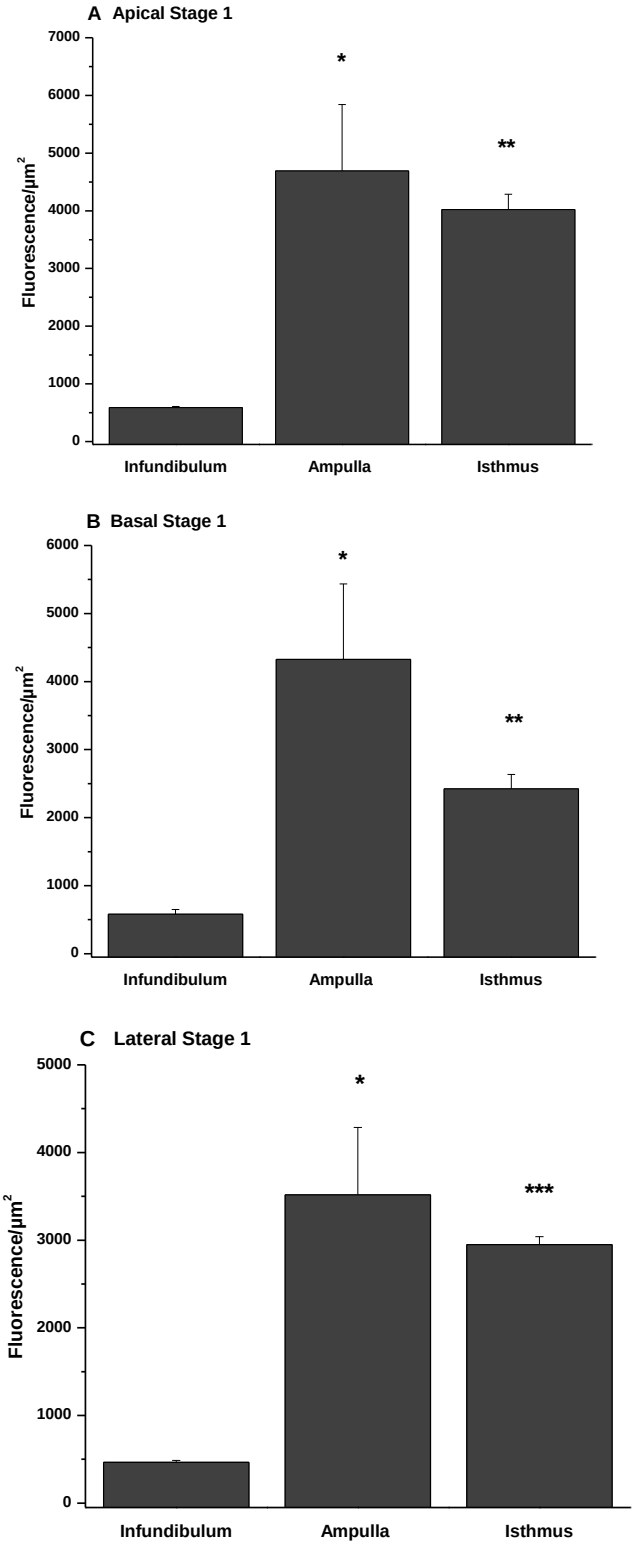

Fig 4.5 Abundance of TRPC1 in permeabilized bovine oviduct epithelium at stage 1 of the estrous cycle in apical (4.5, A), Basal (4.5, B) and lateral (4.5, C) side of the tissue. Abundance of TRPC1 on apical, basal and lateral sides of the tissue in infundibulum was lower than that of ampulla and isthmus. On the apical, basal and lateral sides of the epithelium, abundance of TRPC1 in isthmus was lower than that of ampulla and higher than that of the infundibulum. All data are expressed as a mean of 3 replicates ± 1 standard deviation. (* = $p<0.05$; ** = $p<0.01$; *** = $p<0.001$).

At stage 1 of the estrous cycle on the apical side of the permeabilized bovine oviduct epithelial tissue, TRPC6 channel was 15.5 fold (p= 0.02) more abundant in the ampulla compared to the infundibulum. This was higher in isthmus by 23 fold (p= 0.003) compared to that of the infundibulum (Fig 4.6, A). On the basal side of the bovine oviduct epithelium, abundance of TRPC6 channel was 18.6 fold (p= 0.004) higher in ampulla compared to the infundibulum. Abundance of TRPC6 in isthmus was 21.45 fold (p= 0.001) higher than that of the infundibulum (Fig 4.6, B). Abundance of TRPC6 channels on the lateral side of bovine ampulla epithelium was 19 fold (p= 0.01) higher than that of bovine infundibulum epithelial tissue. This was higher in isthmus by 30.19 fold (p= 0.001) compared to the infundibulum (Fig 4.6, C).

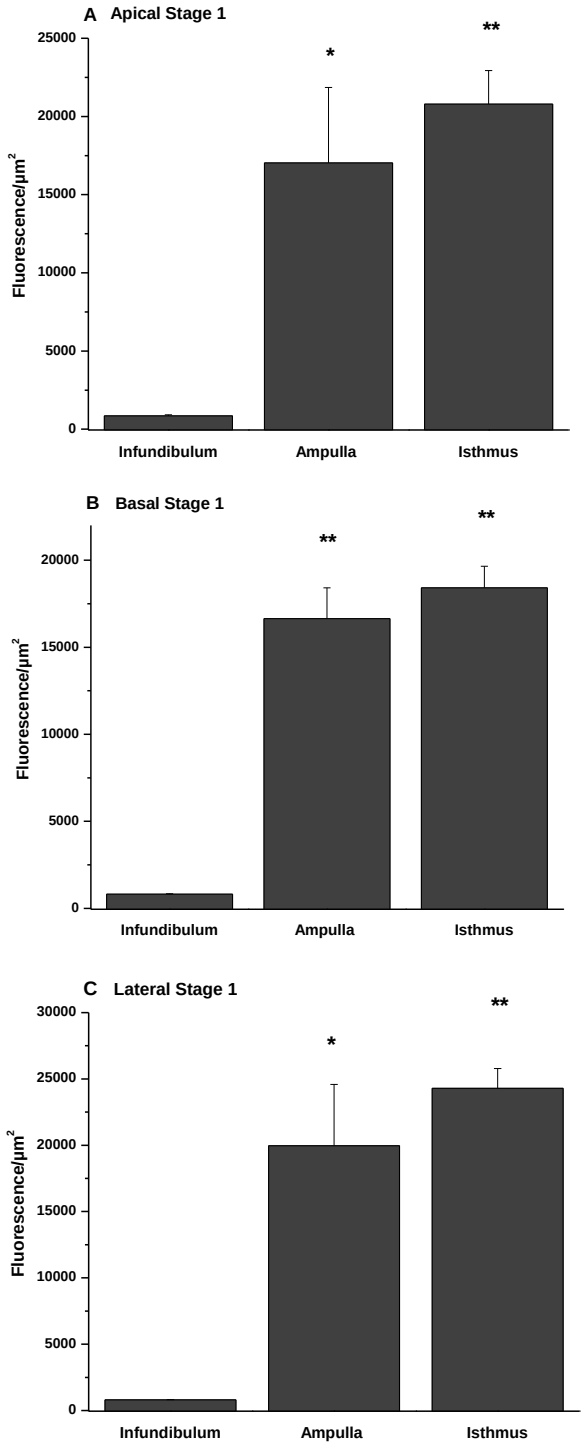

Fig 4.6 Abundance of TRPC6 in permeabilized bovine oviduct epithelium at stage 1 of the estrous cycle in apical (4.6, A), basal (4.6, B), and the lateral (4.6, C) side of the tissue. Abundance of TRPC6 was higher in both ampulla and isthmus on the apical, basal and lateral sides of the permeabilized bovine oviduct epithelium at stage 1 of the estrous cycle compared to that of the infundibulum. All data are expressed as a mean of 3 replicates ± 1 standard deviation. (* = $p<0.05$; ** = $p<0.01$; *** = $p<0.001$).

4.1.1.3 Localization and abundance of TRPC1 and TRPC6 in non-permeabilized bovine oviduct epithelium at stage 2 of the estrous cycle

At stage 2 of the estrous cycle, the TRPC1 channel was distributed equally on apical, basal and lateral sides of the non-permeabilized bovine infundibulum epithelial cells (Fig 4.7, A). Similar to the infundibulum region of the bovine oviduct, TRPC1 was localized equally on the apical, basal and the lateral sides of the ampulla and isthmus epithelial tissue (Fig 4.7, B and C).

Localization of TRPC6 channel in non-permeabilized bovine oviduct epithelium at stage 2 of the estrous cycle, was higher on the apical side compared to the basal and the lateral sides in infundibulum, ampulla and isthmus (Fig 4.7 , A, B and C).

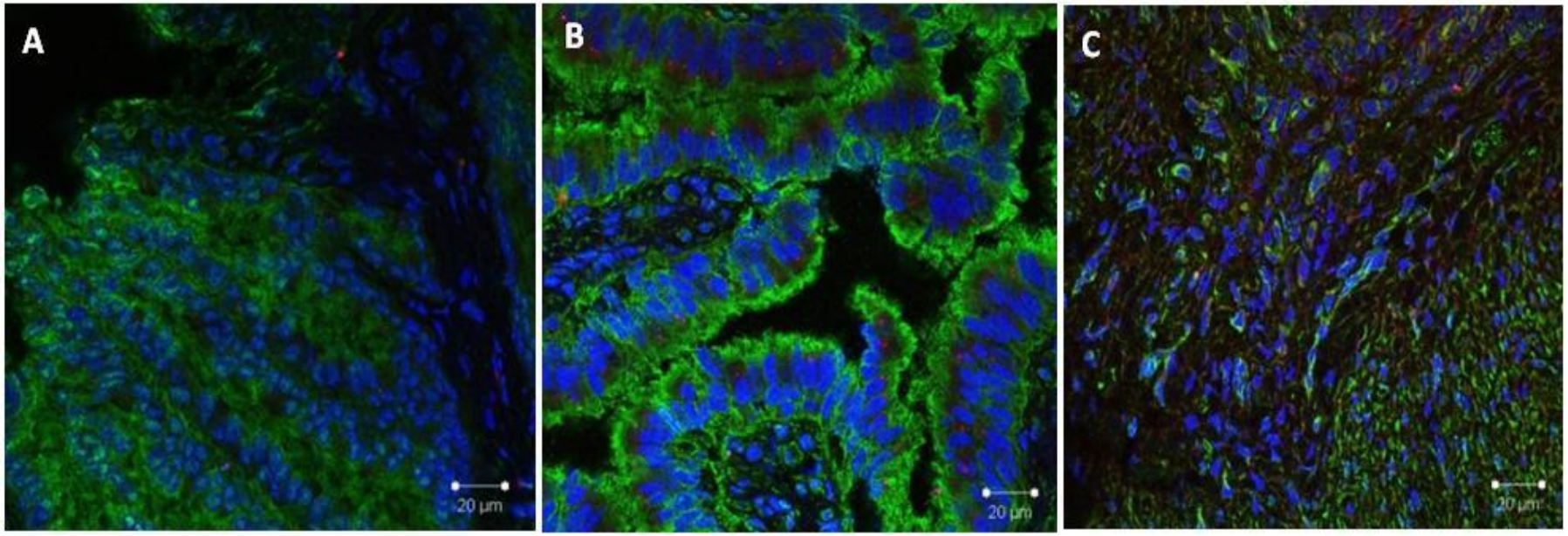

Fig 4.7 Localization of TRPC1 and TRPC6 at stage 2 of the estrous cycle in non-permeabilized epithelial tissue of bovine Infundibulum (4.7, A), Ampulla (4.7, B) and Isthmus (4.7, C). Nuclei are labelled with DAPI (Blue), TRPC1 with Alexa Four 647 FITC conjugated (Red) and TRPC6 with Alexa Flour 488 (Green).

Abundance of TRPC1 channel on the apical side of the non-permeabilized bovine oviduct epithelium at stage 2 of the estrous cycle was 3 fold (p= 0.04) and 6 fold (p= 0.01) higher on ampulla and isthmus epithelium respectively compared to that of the infundibulum (Fig 4.8, A). On the basal side of the tissue, abundance of TRPC1 channels in ampulla was higher by 1.95 fold (p= 0.02) compared to the infundibulum. Abundance of the TRPC1 was 4.15 fold (p= 0.0006) higher in isthmus relative to the infundibulum (Fig 4.8, B). On the lateral side of the bovine oviduct epithelium, abundance of TRPC1 was higher by 1.74 fold (p= 0.03) and 1.84 fold (p= 0.02) in ampulla and isthmus epithelium respectively compared to that of the infundibulum (Fig 4.8, C).

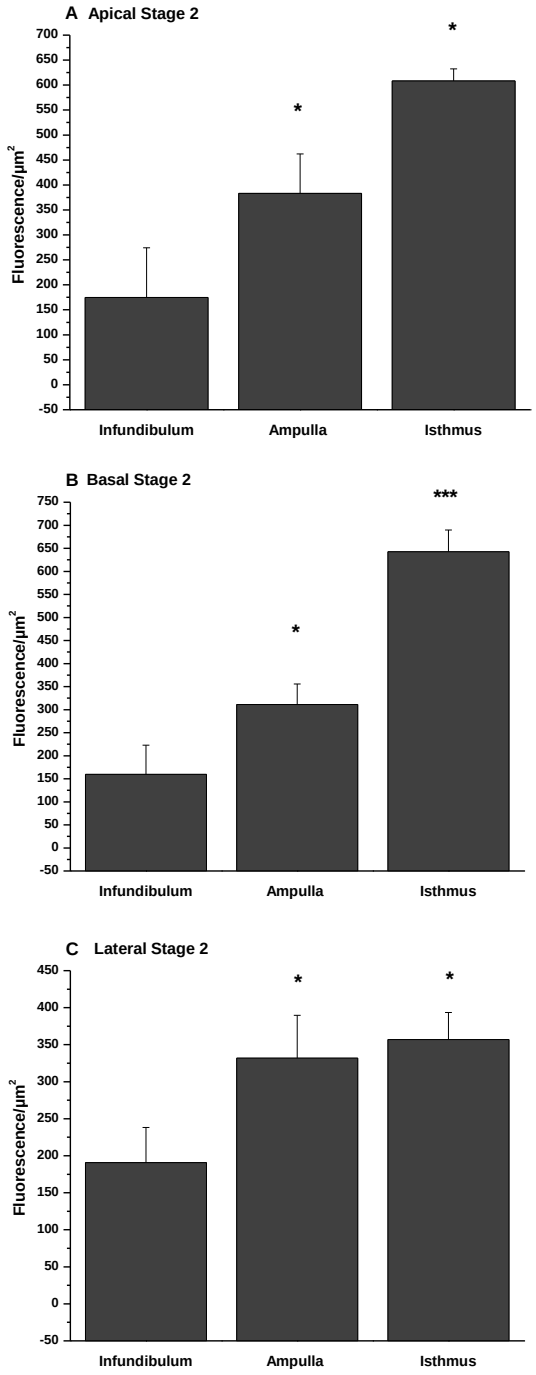

Fig 4.8 Abundance of TRPC1 in non-permeabilized bovine oviduct epithelium at stage 2 of the estrous cycle in apical (4.8, A), Basal (4.8, B), and the lateral (4.8, B) side of the tissue. Abundance of TRPC1 was higher in ampulla and isthmus on the apical, basal and the lateral sides of the non-permeabilized bovine oviduct epithelium at stage 2 of the estrous cycle compared to that of the infundibulum. All data are expressed as a mean of 3 replicates ± 1 standard deviation. (* = $p<0.05$; ** = $p<0.01$; *** = $p<0.001$).

At stage 2 of the estrous cycle on the apical side of the non-permeabilized bovine ampulla epithelial tissue, there was not a significant difference in abundance of TRPC6 channel compared to the infundibulum ($p= 0.4$). Similarly in isthmus ($p= 0.1$) abundance of TRPC6 channel was equal to that of the infundibulum (Fig 4.9, A). Furthermore, on the basal side of the tissue, abundance of TRPC6 in ampulla ($p= 0.1$) was not significantly different to that of the infundibulum. However, in isthmus, abundance of TRPC6 was higher by 1.92 fold ($p= 0.002$) compared to that of the infundibulum (Fig 4.9, B). On the lateral side of the non-permeabilized bovine oviduct epithelial tissue at stage 2 of the estrous cycle, TRPC6 channel was 2.4 fold ($p= 0.008$) more abundant in ampulla region compared to the infundibulum. In contrast, in isthmus epithelium, abundance of TRPC6 channel was not significantly different ($p= 0.2$) to that of infundibulum (Fig 4.9, C).

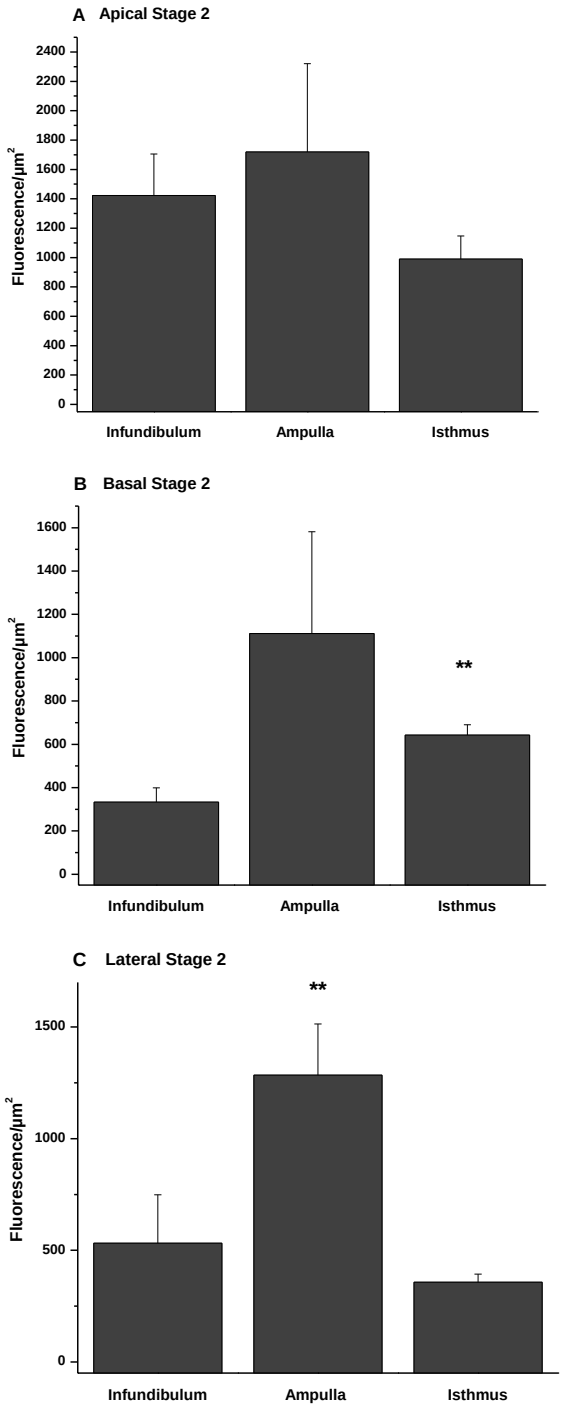

Fig 4.9 Abundance of TRPC6 in non-permeabilized bovine oviduct epithelium at stage 2 of the estrous cycle in apical (4.9, A), basal (4.9, B), the lateral side of the tissue. On the apical side of the tissue there was not a significant difference in abundance of the TRPC6 in ampulla and isthmus compared to the infundibulum. Furthermore, on the basal side of the tissue abundance of TRPC6 was not significantly different in ampulla compared to the infundibulum. However, in isthmus, abundance of TRPC6 was higher than that of the infundibulum. On the lateral side abundance of TRPC6 was higher in ampulla compared to infundibulum. In the contrary, abundance of TRPC6 in isthmus was lower than that of the infundibulum. All data are expressed as a mean of 3 replicates ± 1 standard deviation. (* = $p<0.05$; ** = $p<0.01$; *** = $p<0.001$).

4.1.1.4 Localization and abundance of TRPC1 and TRPC6 in permeabilized bovine oviduct epithelium at stage 2 of the estrous cycle

In permeabilized bovine oviduct epithelium at stage 2 of the estrous cycle, TRPC1 channel was localized on the apical side of the tissue more than basal and lateral side in the infundibulum region (Fig 4.10, A). In the ampulla region of the oviduct, localization of TRPC1 was highest on the apical side and lowest on the lateral side of the tissue (Fig 4.10, B). However, in the isthmus region of the oviduct TRPC1 distribution was highest on the basal side and equal on apical and lateral sides of the epithelium (Fig 4.10, C).

Similar to TRPC1 channel, TRPC6 was localized on the apical side of the infundibulum and ampulla epithelium to a greater extent than the basal and the lateral sides of the epithelium where the channel was distributed equally (Fig 4.10, A and B). However, in isthmus epithelium TRPC6 channel was distributed equally on the apical, basal and lateral sides of the epithelium (Fig 4.10, C).

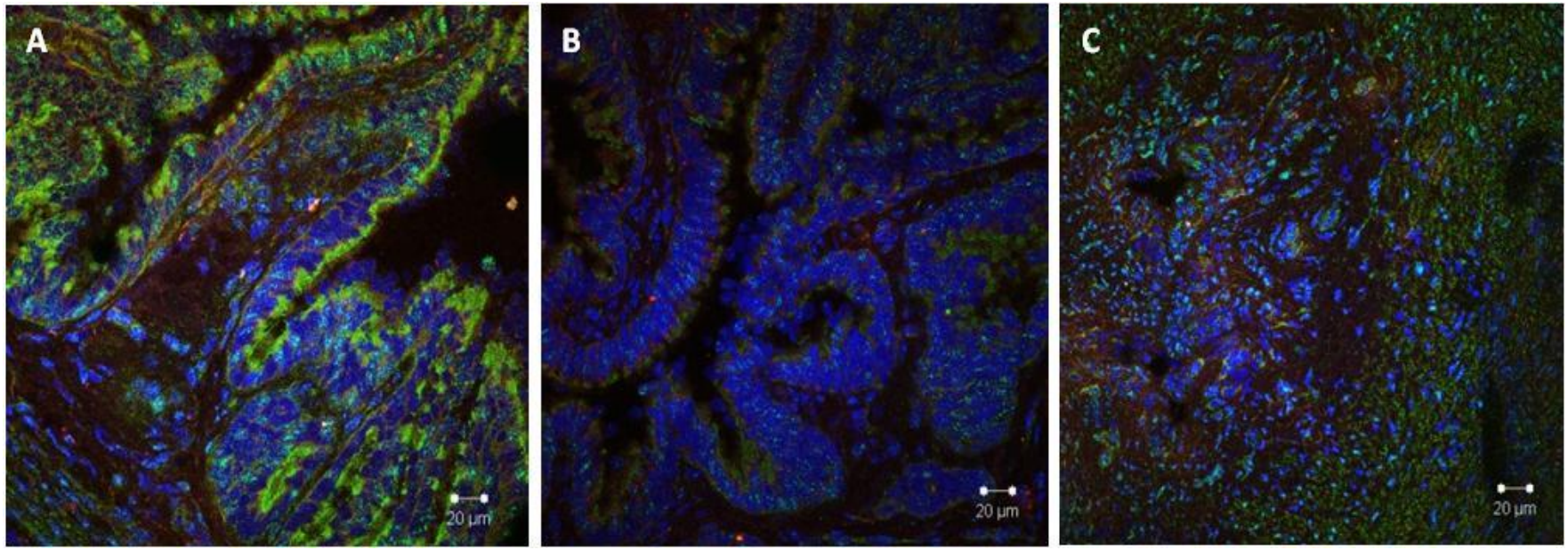

Fig 4.10 Localization of TRPC1 and TRPC6 at stage 2 of the estrous cycle in permeabilized epithelial tissue of bovine Infundibulum (4.10, A), Ampulla (4.10, B) and Isthmus (4.10, C). Nuclei are labelled with DAPI (Blue), TRPC1 with Alexa Four 647 FITC conjugated (Red) and TRPC6 with Alexa Flour 488 (Green).

In the permeabilized bovine oviduct epithelium at stage 2 of the estrous cycle, abundance of TRPC1 channel on apical side of the tissue was 0.53 fold (p= 0.007) lower in ampulla compared to the infundibulum. Furthermore, abundance of TRPC1 channel was 0.6 fold (p= 0.03) less in isthmus epithelium compared to the infundibulum (Fig 4.11, A). On the basal side of permeabilized bovine oviduct epithelium, abundance of TRPC1 channel was not significantly different in ampulla (p= 0.1) compared to the infundibulum. Furthermore, there was no significant difference in abundance of TRPC1 in the isthmus region (p= 0.8) of the oviduct compared to the infundibulum (Fig 4.11, B). On the lateral side of bovine oviduct epithelial tissue, abundance of TRPC1 was 2.56 fold (p= 0.003) higher in infundibulum compared to the ampulla. Hence, abundance of TRPC1 channel was 1.4 fold (p= 0.04) higher on the lateral side of the infundibulum in comparison to that of the isthmus (Fig 4.11, C).

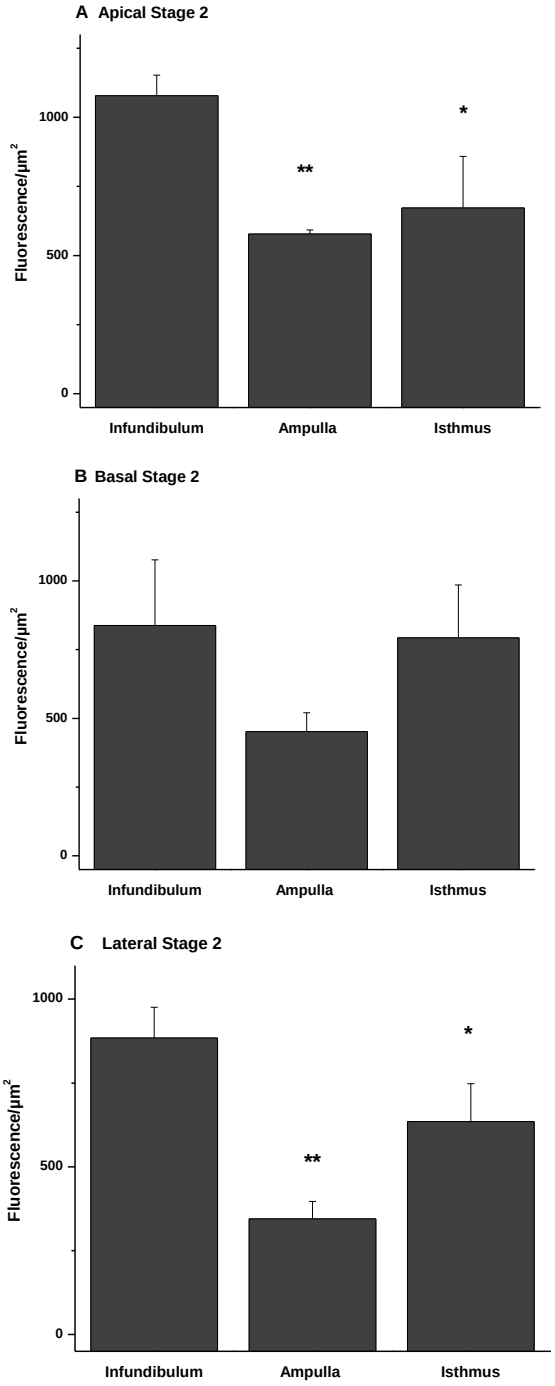

Fig 4.11 Abundance of TRPC1 in permeabilized bovine oviduct epithelium at stage 2 of the estrous cycle in apical (4.11,A), Basal (4.11, B), and the lateral (4.11, C) of the tissue. On the apical side of the tissue, abundance of TRPC1 was lower in both ampulla and isthmus compared to the infundibulum. However, on the basal side abundance of TRPC1 was not significantly different nor in ampulla neither in isthmus compared to the infundibulum. On the lateral side of the tissue abundance of TRPC1 was lower in both ampulla and isthmus compared to the infundibulum. All data are expressed as a mean of 3 replicates ± 1 standard deviation. (* = $p<0.05$; ** = $p<0.01$; *** = $p<0.001$).

Abundance of TRPC6 channels in permeabilized bovine infundibulum epithelial tissue at stage 2 of the estrous cycle was 2.25 fold (p= 0.005) higher on the apical side compared to that of the ampulla. Abundance of TRPC6 on the apical side of isthmus epithelium was 0.5 fold (p= 0.03) less than that of infundibulum (Fig 4.12, A). Abundance of TRPC6 channel on the basal side of permeabilized oviduct ampulla at stage 2 of the estrous cycle was lower by 0.4 fold (p= 0.04) relative to that of the infundibulum. Furthermore, abundance of TRPC6 in isthmus (p= 0.6) was not significantly different to the infundibulum on the basal side of the tissue (Fig 4.12, B). Abundance of TRPC6 on the lateral side of the bovine oviduct epithelium was higher by 2.6 fold (p= 0.01) in ampulla compared to the infundibulum. However, abundance of TRPC6 in isthmus (p= 0.3) was not significantly different to that of the infundibulum region (Fig 4.12, C).

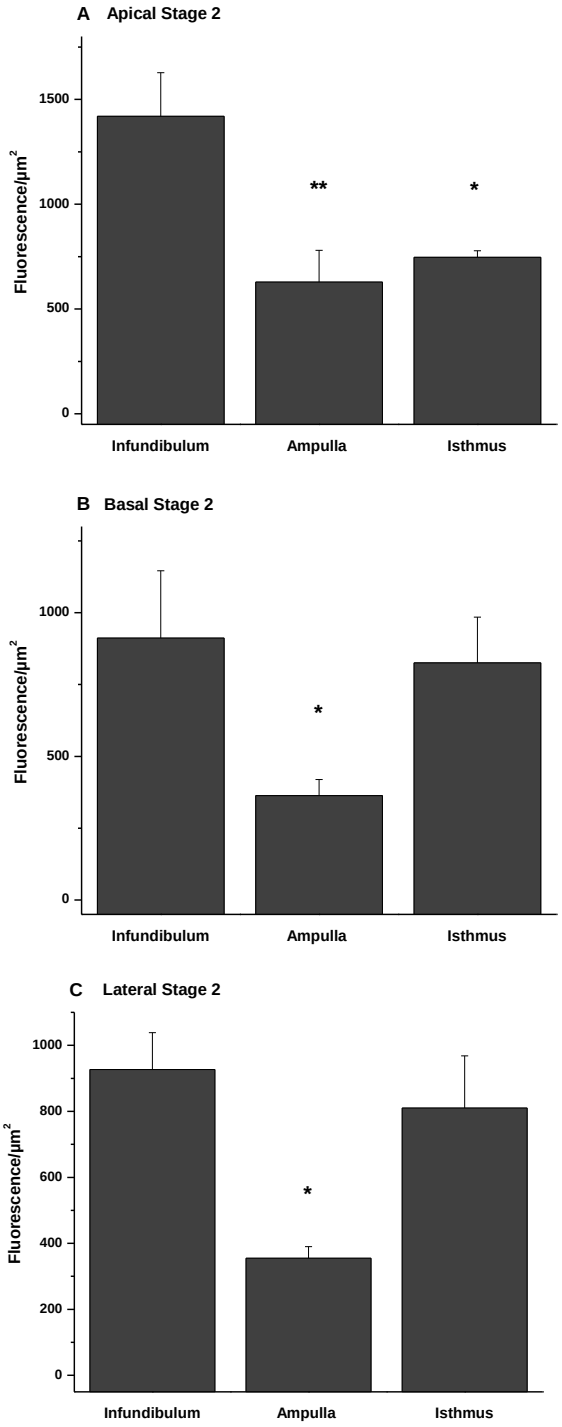

Fig 4.12 Abundance of TRPC6 in permeabilized bovine oviduct epithelium at stage 2 of the estrous cycle in apical (4.12, A), basal (4.12, B) and the lateral side of the tissue. On the apical side of the tissue, abundance of TRPC6 was lower in both ampulla and isthmus compared to that of the infundibulum. On the basal and lateral side of the epithelium, abundance of TRPC6 was lower in ampulla relative to the infundibulum. However, abundance of TRPC6 on the basal and lateral sides of the isthmus epithelium was equal to that of the infundibulum. All data are expressed as a mean of 3 replicates ± 1 standard deviation. (* = $p<0.05$; ** = $p<0.01$; *** = $p<0.001$).

4.1.1.5 Localization and abundance of TRPC1 and TRPC6 in non-permeabilized bovine oviduct epithelium at stage 3 of the estrous cycle

In non-permeabilized bovine infundibulum epithelium at stage 3 of the estrous cycle, localization of TRPC1 was slightly greater on the apical side, and its distribution was equal on basal and lateral sides of the tissue (Fig 4.13, A). In the ampulla region of the oviduct epithelium, TRPC1 channel was equally localized to the apical and basal sides of the tissue while its distribution was lower on the lateral side of the ampulla epithelium (Fig 4.13, B). Localization of TRPC1 channel in the isthmus region of the bovine oviduct epithelium was higher on the apical side compared to the basal side and the lateral side where TRPC1 was localized evenly (Fig 4.13, C).

Localization of TRPC6 channels was higher on the apical side of the non-permeabilized bovine infundibulum compared to the basal and lateral sides of the epithelial tissue at stage 3 of the estrous cycle (Fig 4.13, A). In bovine ampulla epithelum the localization of TRPC6 was highest on the apical side and lowest on the lateral side of the tissue (Fig 4.13, B). In the isthmus region of the oviduct, the localization of TRPC6 channel was highest on the apical side and lowest on the basal side of the epithelium (Fig 4.13, C).

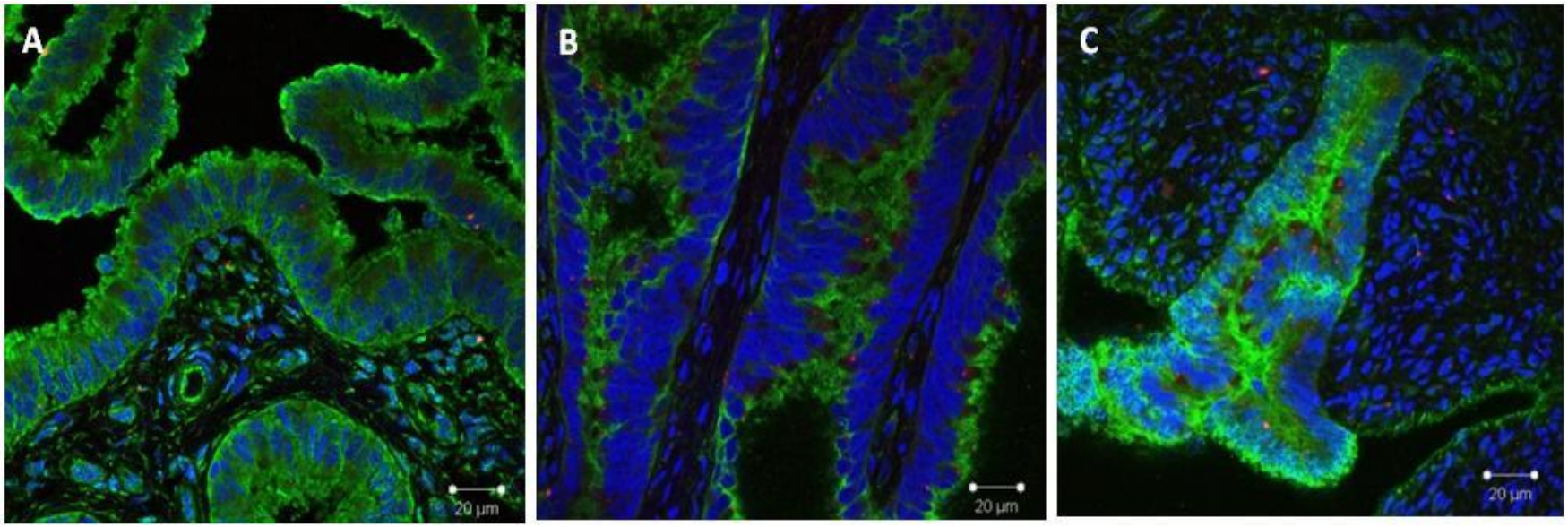

Fig 4.13 Localization of TRPC1 and TRPC6 at stage 3 of the estrous cycle in non-permeabilized epithelial tissue of bovine Infundibulum (4.13, A), Ampulla (4.13, B) and Isthmus (4.13, C). Nuclei are labelled with DAPI (Blue), TRPC1 with Alexa Four 647 FITC conjugated (Red) and TRPC6 with Alexa Flour 488 (Green).

In non-permeabilized bovine oviduct epithelium at stage 3 of the estrous cycle on apical side of the tissue, the abundance of TRPC1 in ampulla (p= 0.2) was not significantly different to that of the infundibulum. However, in isthmus, abundance of TRPC1 was higher by 1.95 fold (p= 0.003) compared to the infundibulum (Fig 4.14, A). On the basal side of the bovine oviduct epithelium, abundance of TRPC1 was not significantly different in ampulla (p= 0.07) compared to that of the infundibulum. However, in the isthmus region of the oviduct abundance of TRPC1 was higher by 1.4 fold (p= 0.02) compared to that of the infundibulum (Fig 4.14, B). On the lateral side of the bovine oviduct epithelium, the abundance of TRPC1 channel in ampulla (p= 0.2) and isthmus (p= 0.1) was equal to that of the infundibulum (Fig 4.14, C).

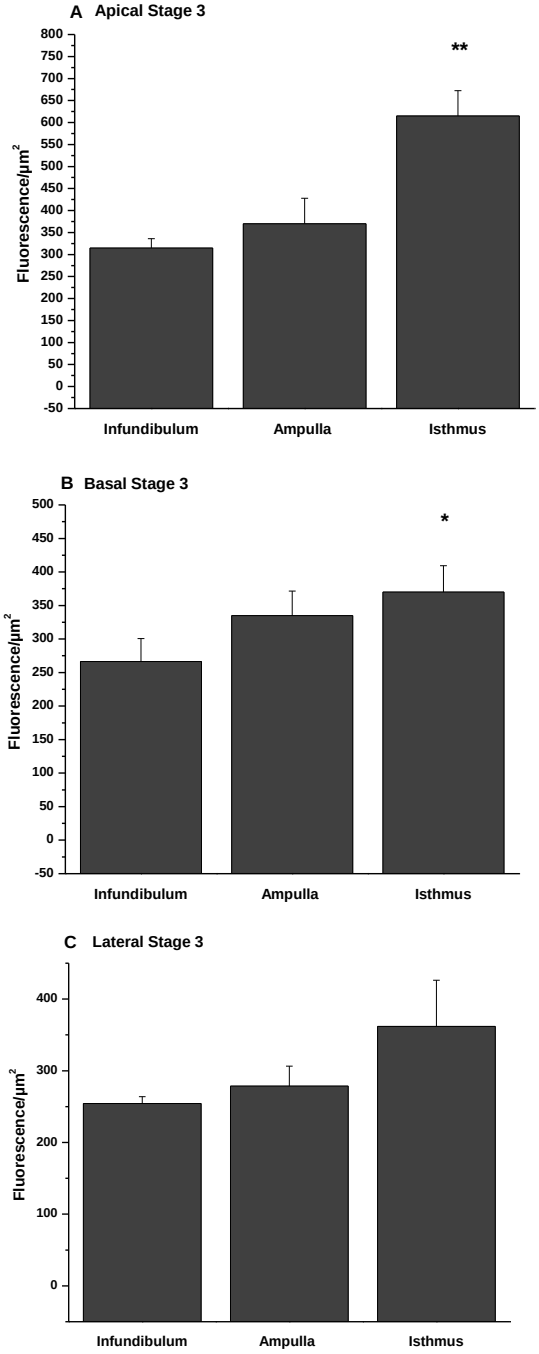

Fig 4.14 Abundance of TRPC1 in non-permeabilized bovine oviduct epithelium at stage 3 of the estrous cycle in apical (4.14, A), basal (4.14, B) and the lateral (4.14, C) side of the tissue. On the apical and basal side of the tissue, abundance of TRPC1 in ampulla was equal to that of the infundibulum. However, on the apical and basal sides of the isthmus the abundance of TRPC1 was higher than that of the infundibulum. Abundance of TRPC1 on the lateral side of the non-permeabilized bovine oviduct epithelium at stage 3 of the estrous cycle was even in infundibulum, ampulla and isthmus region. All data are expressed as a mean of 3 replicates ± 1 standard deviation. (* = $p<0.05$; ** = $p<0.01$; *** = $p<0.001$).

On the apical side of the non-permeabilized bovine oviduct epithelium at stage 3 of the estrous cycle, abundance of TRPC6 channel was 1.5 fold (p= 0.001) higher in infundibulum compared to the ampulla. However, abundance of TRPC6 in isthmus (p= 0.2) was not significantly different to that of the infundibulum (Fig 4.15, A). On the basal side of bovine oviduct epithelium, abundance of TRPC6 was 1.8 fold (p= 0.006) higher in infundibulum compared to the ampulla. However, abundance of TRPC6 on the basal side of the isthmus (p= 0.08) epithelium was not significantly different to that of the infundibulum (Fig 4.15, B). On the lateral side of the bovine oviduct epithelium, TRPC6 abundance was 2.75 fold (p= 0.004) higher in the infundibulum region compared to the ampulla. In contrast, abundance of TRPC6 on the lateral side of the isthmus epithelium was 1.7 fold (p= 0.002) higher than that of the infundibulum (Fig 4.15, C).

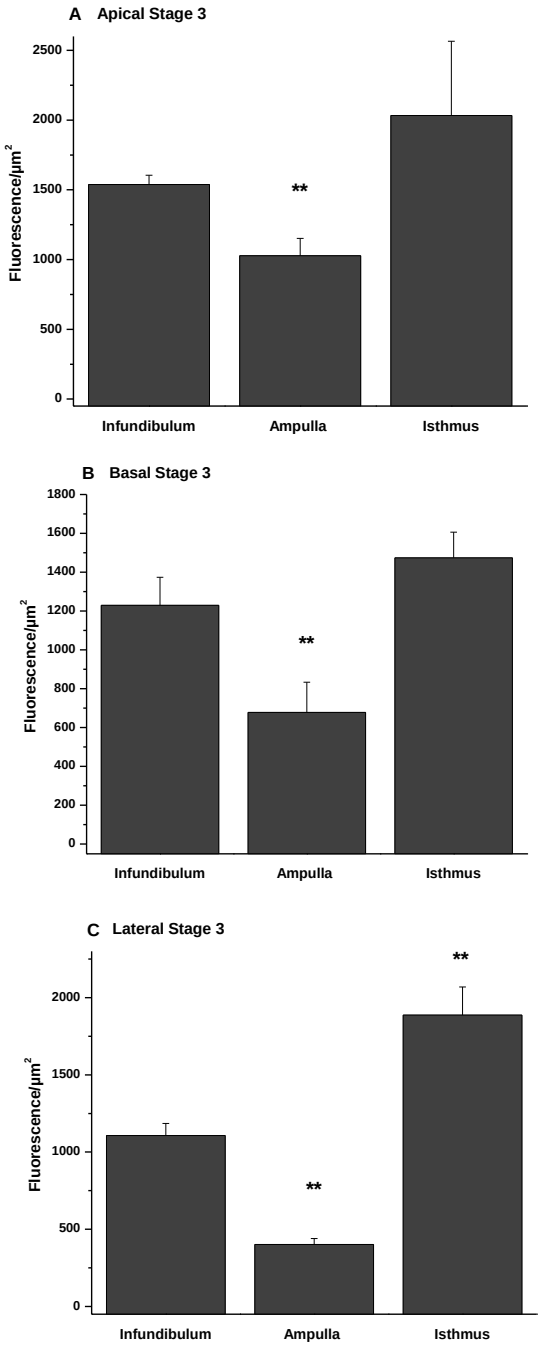

Fig 4.15 Abundance of TRPC6 in non-permeabilized bovine oviduct epithelium at stage 3 of the estrous cycle in apical (4.15, A), basal (4.15, B) and the lateral (4.15, C) side of the tissue. On the apical and basal sides of the non-permeabilized bovine oviduct epithelial tissue at stage 3 of the estrous cycle, abundance of TRPC6 was lower in ampulla compared to the infundibulum. However, that of the isthmus was not significantly different to the infundibulum. On the lateral side of the tissue, abundance of TRPC6 was lower in ampulla and higher in isthmus compared to the infundibulum. All data are expressed as a mean of 3 replicates ± 1 standard deviation. (* = $p<0.05$; ** = $p<0.01$; *** = $p<0.001$).

4.1.1.6 Localization and abundance of TRPC1 and TRPC6 in permeabilized bovine oviduct epithelium at stage 3 of the estrous cycle

In permeabilized oviduct epithelium at stage 3 of the estrous cycle, the TRPC1 channel was equally localized on the apical, basal and lateral sides of the infundibulum epithelial tissue (Fig 4.16, A). In the ampulla region of the oviduct localization of TRPC1 channel was slightly higher on the apical side of the epithelium compared to the basal and lateral sides (Fig 4.16, B). Localization of TRPC1 was highest on the apical side and lowest on the lateral side of the isthmus epithelium (Fig 4.16, C).

Localization of TRPC6 in permeabilized bovine infundibulum epithelial tissue at stage 3 of the estrous cycle was highest on the basal side and lowest on apical side (Fig 4.16, A). In the ampulla region of the oviduct, localization of TRPC6 channel was at its highest level on the apical side and its lowest level on the lateral side of the epithelial tissue (Fig 4.16, B). Localization of TRPC6 in isthmus was similar to that of the ampulla and was the highest on the apical side and lowest on the lateral side of the tissue (Fig 4.16, C).

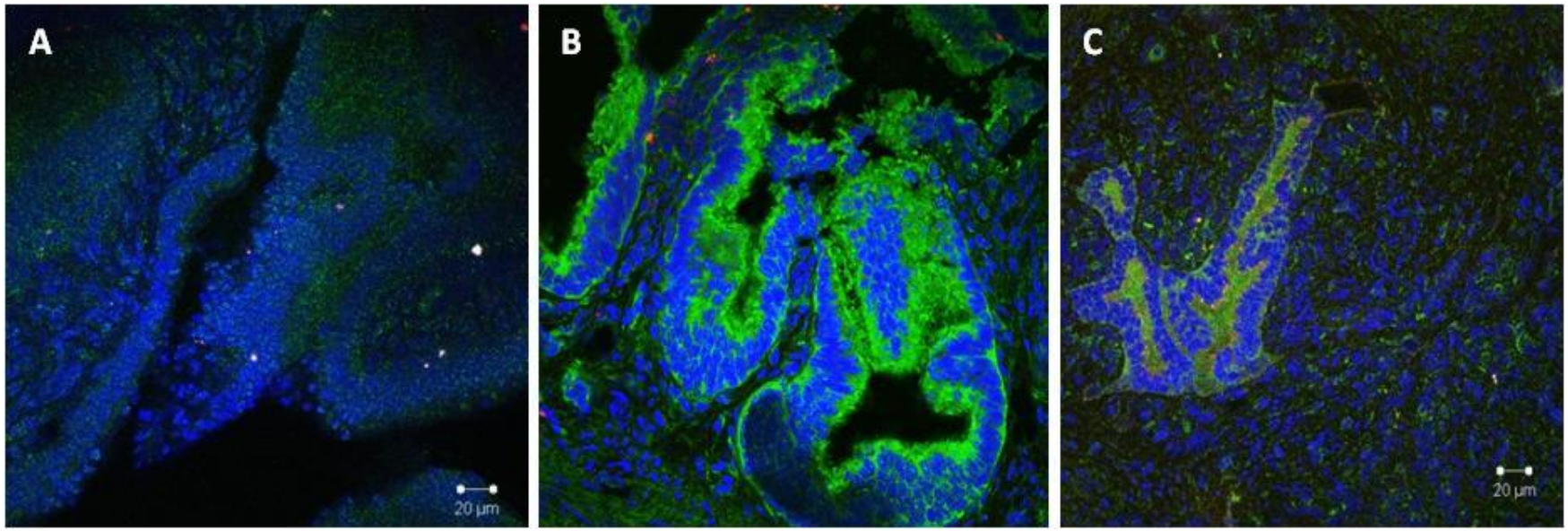

Fig 4.16 Localization of TRPC1 and TRPC6 at stage 3 of the estrous cycle in permeabilized epithelial tissue of bovine Infundibulum (4.16, A), Ampulla (4.16, B) and Isthmus (4.16, C). Nuclei are labelled with DAPI (Blue), TRPC1 with Alexa Four 647 FITC conjugated (Red) and TRPC6 with Alexa Flour 488 (Green).

At stage 3, abundance of TRPC1 in the permeabilized bovine oviduct epithelium on the apical side was 32.7 fold (p= 0.0005) higher in ampulla compared to the infundibulum and 7.8 fold (p= 0.01) higher in the isthmus region relative to the infundibulum (Fig 4.17, A). On the basal side of the epithelium, TRPC1 channel was 29.5 fold (p= 0.01) higher in the ampulla compared to the infundibulum. Furthermore, abundance of TRPC1 was 5.65 fold (p= 0.02) higher in the isthmus compared to the infundibulum (Fig 4.17, B). On the lateral side of the epithelium, abundance of the TRPC1 channel was 21.4 fold (p= 0.005) higher in ampulla compared to the infundibulum and 4.8 fold (p= 0.009) higher in isthmus compared to the infundibulum (Fig 4.17, C).

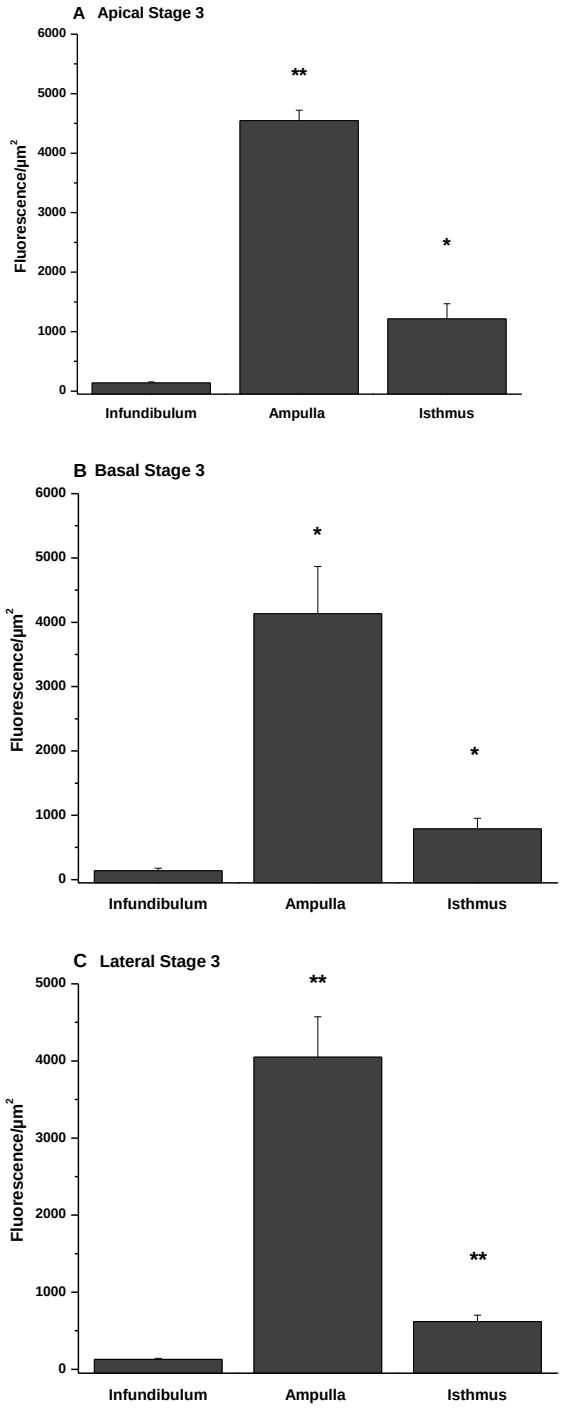

Fig 4.17 Abundance of TRPC1 in permeabilized bovine oviduct epithelium at stage 3 of the estrous cycle in apical (4.17, A), basal (4.17, B), and the lateral (4.17, C) side of the tissue. Abundance of TRPC1 on the apical, basal and lateral sides of the epithelium was the highest in ampulla and the lowest in infundibulum. All data are expressed as a mean of 3 replicates ± 1 standard deviation. . (* = $p<0.05$; ** = $p<0.01$; *** = $p<0.001$).

Abundance of TRPC6 on the apical side of the permeabilized bovine oviduct epithelium at stage 3 of the estrous cycle was higher by 58 ($p= 0.004$) and 3.45 fold ($p= 0.00003$) in ampulla and isthmus respectively compared to that of the infundibulum (Fig 4.18, A). On the basal side of the epithelium, TRPC6 was 38 fold ($p= 0.02$) and 1.95 fold ($p= 0.001$) higher in ampulla and isthmus region respectively compared to the infundibulum (Fig 4.18, B). Abundance of TRPC6 on the lateral side of the oviduct epithelium was 29.6 ($p= 0.005$) and 1.4 fold ($p= 0.02$) higher in ampulla and isthmus respectively compared to that of the infundibulum (Fig 4.18, C).

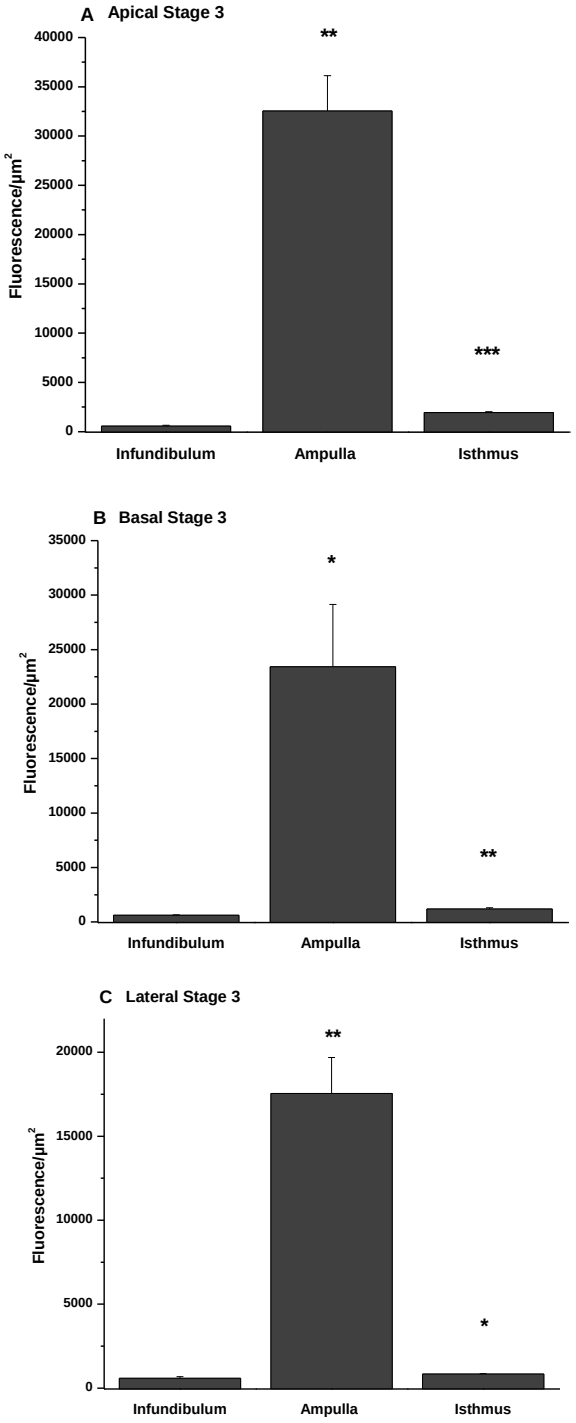

Fig 4.18 Abundance of TRPC6 in permeabilized bovine oviduct epithelium at stage 3 of the estrous cycle in apical (4.18, A), basal (4.18, B), and the lateral (4.18, C) side of the epithelium tissue. On the apical, basal and lateral side of the permeabilized bovine oviduct epithelium abundance of TRPC6 was dramatically higher in ampulla compared to the infundibulum and isthmus region. A modest increase was observed in abundance of TRPC6 in isthmus on apical, basal and lateral side of the tissue compared to the infundibulum. All data are expressed as a mean of 3 replicates ± 1 standard deviation. (* = $p<0.05$; ** = $p<0.01$; *** = $p<0.001$).

4.1.1.7 Localization and abundance of TRPC1 and TRPC6 in non-permeabilized bovine oviduct epithelium at stage 4 of the estrous cycle

In non-permeabilized bovine oviduct epithelial tissue at stage 4 of the estrous cycle, TRPC1 was localized equally on the apical, basal and lateral sides of the infundibulum epithelium (Fig 4.19, A). In the ampulla, localization of TRPC1 channel was highest on the apical side and lowest on the lateral side of the epithelium (Fig 4.19, B). Localization of TRPC1 channel was highest on the apical side and similar on the basal and lateral sides of the epithelium (Fig 4.19, C).

The TRPC6 channel was localized equally on the apical and basal sides of the non-permeabilized epithelial tissue of infundibulum at stage 4 of the estrous cycle. However, localization of TRPC6 was lower on the lateral side of the infundibulum epithelium compared to the apical and basal sides of the tissue (Fig 4.19, A). In the ampulla and isthmus, localization of TRPC6 was slightly greater on the basal side of the epithelium compared to the apical side. Localization of TRPC6 was lowest on the lateral side of the epithelium compared to the apical and basal sides in both ampulla and isthmus (Fig 4.19, B and C).

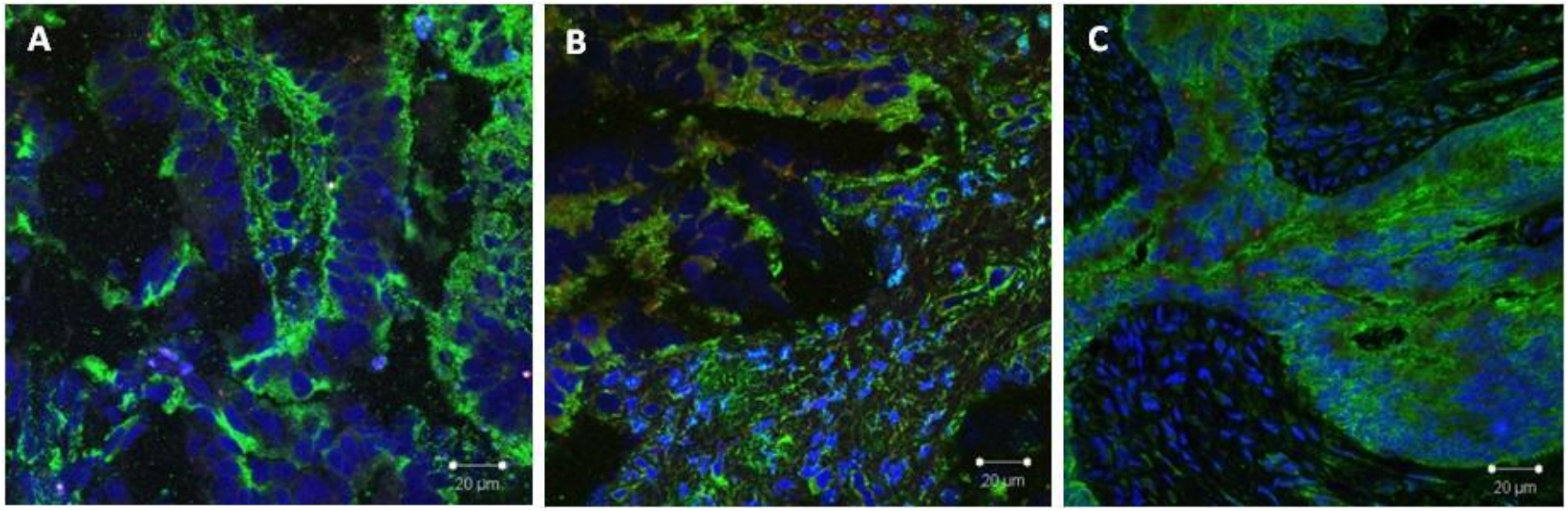

Fig 4.19 Localization of TRPC1 and TRPC6 at stage 4 of the estrous cycle in non-permeabilized epithelial tissue of bovine Infundibulum (4.19, A), Ampulla (4.19, B) and Isthmus (4.19, C). Nuclei are labelled with DAPI (Blue), TRPC1 with Alexa Four 647 FITC conjugated (Red) and TRPC6 with Alexa Flour 488 (Green).

Abundance of TRPC1 channel on the apical side of the non-permeabilized bovine oviduct epithelium was not significantly different in ampulla (p= 0.05) and isthmus (p= 0.7) compared to that of the infundibulum (Fig 4.20, A). On the basal side of the bovine oviduct epithelium, abundance of TRPC1 in ampulla (p= 0.08) was equal to that of the infundibulum. However, abundance of TRPC1 was 0.5 fold (p= 0.03) less in the isthmus compared to the infundibulum (Fig 4.20, B). On the lateral side of the bovine oviduct epithelium, abundance of TRPC1 was equal in infundibulum and ampulla (p= 0.9). TRPC1 was 0.4 fold less abundant in isthmus (p= 0.01) compared to both infundibulum and ampulla (Fig 4.20, C).

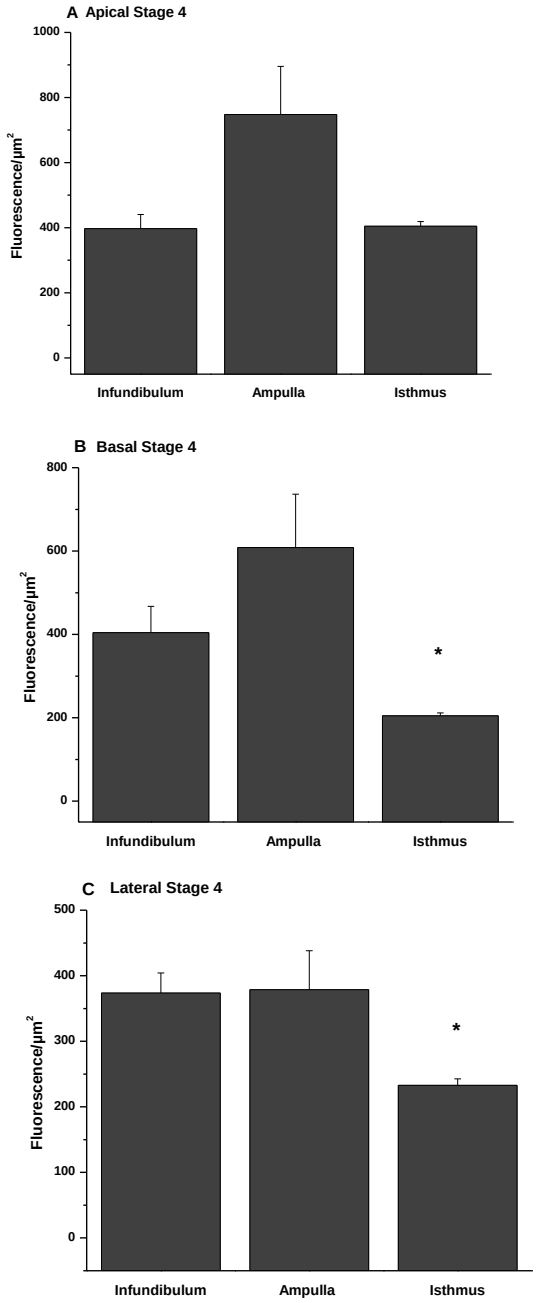

Fig 4.20 Abundance of TRPC1 in non-permeabilized bovine oviduct epithelium at stage 4 of the estrous cycle in apical (4.20, A), basal (4.20, B) and the lateral (4.20, C) side of the tissue. On the apical, basal and lateral sides of the tissue abundance of TRPC1 was equal in infundibulum and ampulla in non-permeabilized bovine oviduct epithelium at stage 4 of the estrous cycle. There was no significant difference in abundance of TRPC1 on the apical side of the isthmus compared to that of the infundibulum. However, on the basal and lateral sides of the tissue abundance of TRPC1 was lower in isthmus relative to the infundibulum. All data are expressed as a mean of 3 replicates ± 1 standard deviation.

Abundance of TRPC6 channels on the apical side of non-permeabilized bovine oviduct epithelium at stage 4 of the estrous cycle was not significantly different in ampulla (p= 0.5) and isthmus (p= 0.6) compared to the infundibulum (Fig 4.21, A). Furthermore, on the basal side of the non-permeabilized bovine oviduct epithelium at stage 4 of the estrous cycle, abundance of TRPC6 was equal in ampulla (p= 0.8) and isthmus (p= 0.1) relative to the infundibulum (Fig 4.21, B). On the lateral side of the tissue, abundance of TRPC6 in ampulla (p= 0.3) was equal to that of the infundibulum. However, TRPC6 was more abundant by 1.27 fold (p= 0.02) on the lateral side of the isthmus relative to the infundibulum (Fig 4.21, C).

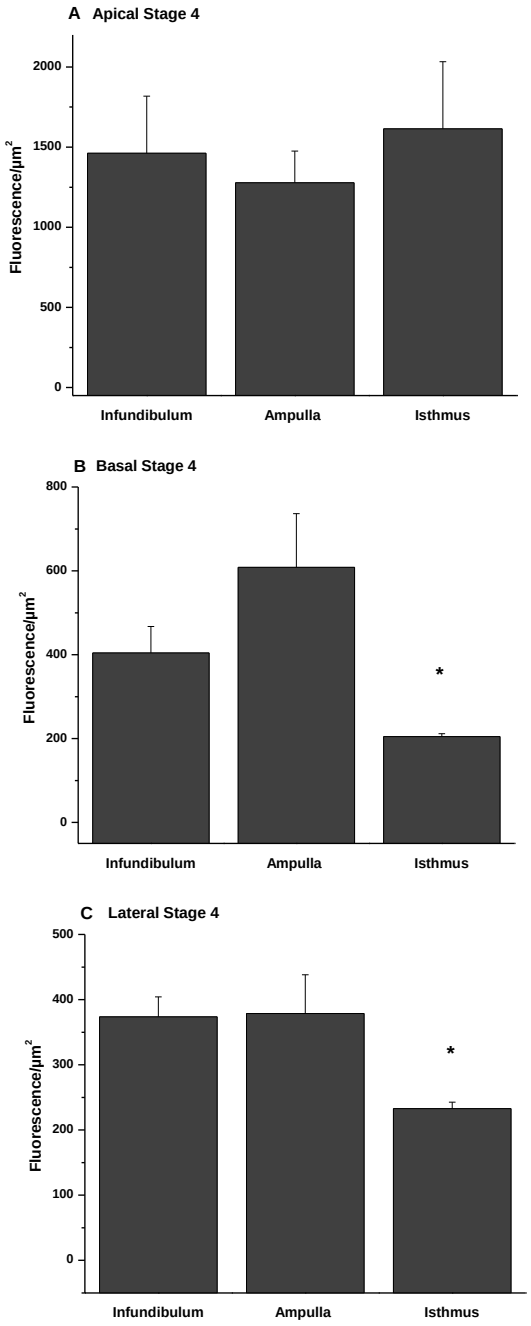

Fig 4.21 Abundance of TRPC6 in non-permeabilized bovine oviduct epithelium at stage 4 of the estrous cycle in apical (4.21, A), basal (4.21, B), and the lateral (4.21, C) side of the tissue. On the apical and basal side of the non-permeabilized bovine oviduct epithelial tissue at stage 4 of the estrous cycle, abundance of TRPC6 was equal in infundibulum, ampulla and isthmus region. Furthermore, abundance of the TRPC6 in ampulla on the lateral side of the tissue was not significantly different to that of the infundibulum. however, on the lateral side of the isthmus abundance of the TRPC6 was higher than that of both infundibulum and ampulla. All data are expressed as a mean of 3 replicates ± 1 standard deviation. (* = $p<0.05$; ** = $p<0.01$; *** = $p<0.001$).

4.1.1.8 Localization and abundance TRPC1 and TRPC6 in permeabilized bovine oviduct epithelium at stage 4 of the estrous cycle

In permeabilized bovine oviduct epithelium at stage 4 of the estrous cycle, TRPC1 channel was equally localized on the apical, basal and lateral sides of the infundibulum region (Fig 4.22, A). Distribution of TRPC1 in ampulla was similar to that of the infundibulum and TRPC1 was equally localized on the apical, basal and lateral sides of the tissue (Fig 4.22, B). In the isthmus region of the oviduct epithelium, localization of TRPC1 was highest on the apical side and lowest on the lateral side of the tissue (Fig 4.22, C).

TRPC6 was localized equally on the apical and lateral sides of the permeabilized infundibulum epithelial tissue at stage 4 of the estrous cycle, and its localization was higher on the basal side of the epithelium compared to both apical and lateral sides (Fig 4.22, A). Localization of TRPC6 was similar on the apical and basal sides of the ampulla but less on the lateral side compared to both the apical and basal sides of the epithelium (Fig 4.22, B). In the isthmus region, localization of TRPC6 was highest on the apical side and lowest on the lateral side of the epithelium (Fig 4.22, C).

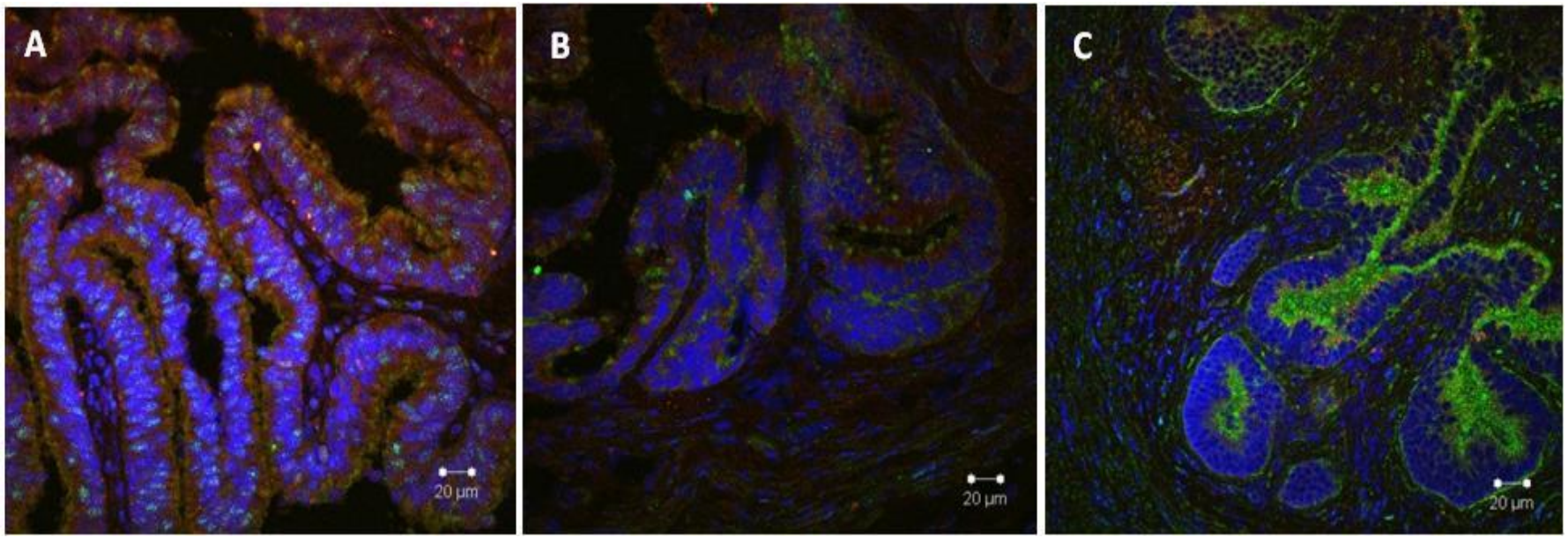

Fig 4.22 Localization of TRPC1 and TRPC6 at stage 4 of the estrous cycle in permeabilized epithelial tissue of bovine Infundibulum (4.22, A), Ampulla (4.22, B) and Isthmus (4.22, C). Nuclei are labelled with DAPI (Blue), TRPC1 with Alexa Four 647 FITC conjugated (Red) and TRPC6 with Alexa Flour 488 (Green).

On the apical side of permeabilized bovine oviduct epithelium at stage 4 of the estrous cycle, abundance of TRPC1 was 1.9 fold (p= 0.01) higher than that of ampulla. However, abundance of TRPC1 in the isthmus region (p= 0.2) of the tissue was equal to that of the infundibulum (Fig 4.23, A). On the basal side of the epithelium, abundance of TRPC1 in infundibulum was 1.94 (p= 0.01) and 2.1 fold (p= 0.02) higher than that of ampulla and isthmus respectively (Fig 4.23, B). Abundance of TRPC1 on the lateral side of the bovine oviduct epithelium in infundibulum was 2.15 fold (p= 0.001) higher than that of ampulla and 2.6 fold (p= 0.006) higher than that of isthmus (Fig 4.23, C).

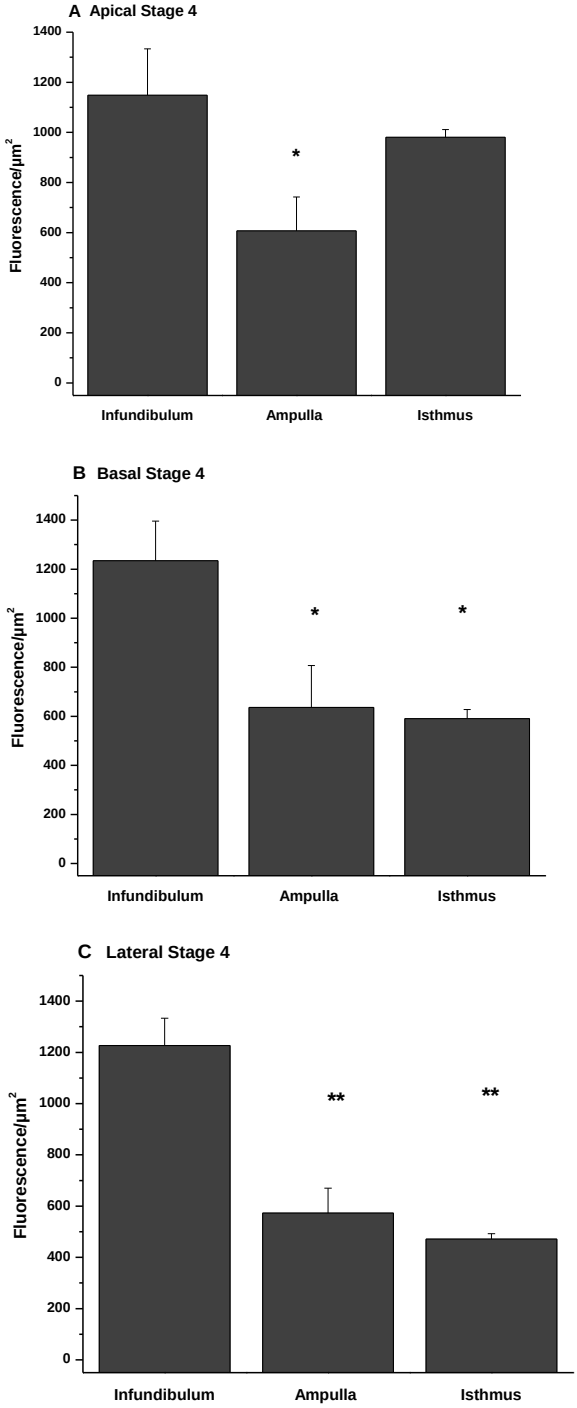

Fig 4.23 Abundance of TRPC1 in permeabilized bovine oviduct epithelium at stage 4 of the estrous cycle in apical (4.23, A), basal(4.23, B), and lateral (4.23, C) side of the tissue. On the apical side of the tissue abundance of TRPC1 was the highest in infundibulum and the lowest in ampulla. On the basal side of the tissue TRPC1 was most abundant in infundibulum and less abundant in ampulla and isthmus where equal abundance was observed. Abundance of TRPC1 on the lateral side was lower in ampulla and isthmus compared to the infundibulum. All data are expressed as a mean of 3 replicates ± 1 standard deviation. (* = $p<0.05$; ** = $p<0.01$; *** = $p<0.001$).

Abundance of TRPC6 on the apical side of permeabilized bovine oviduct epithelial tissue at stage 4 of the estrous cycle was equal in infundibulum and ampulla (p= 0.6) and 2 fold (p= 0.002) higher in isthmus compared to the infundibulum (Fig 4.24, A). Similar to the apical side, on the basal side of the oviduct epithelium, abundance of TRPC6 was equal in infundibulum and ampulla (p= 0.5) and higher by 1.33 fold (p= 0.004) in isthmus relative to the infundibulum (Fig 2.24, B). Furthermore, abundance of TRPC6 on the lateral side of the ampulla (p= 0.2) was not significantly different to that of the infundibulum. In isthmus, abundance of TRPC6 was decreased by 0.61 fold (p= 0.03) on the lateral side of the tissue compared to the infundibulum (Fig 4.24, C).

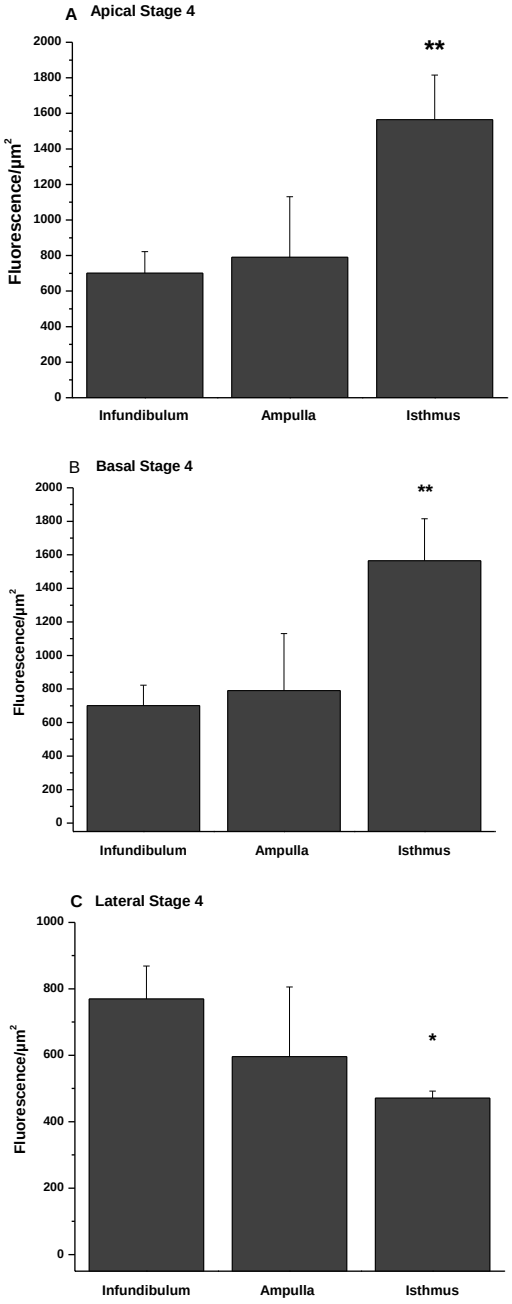

Fig 4.24 Abundance of TRPC6 in permeabilized bovine oviduct epithelium at stage 4 of the estrous cycle in apical (4.24, A), basal (4.24, B) and the lateral (4.24, C) side e of the tissue. On apical, basal and lateral side of the permeabilized bovine oviduct epithelium at stage 4 of the estrous cycle, abundance of TRPC6 was equal in infundibulum and ampulla. On the apical and basal side of the isthmus epithelial tissue, abundance of TRPC6 was higher than that of the infundibulum. However, on the lateral side of the isthmus abundance of the TRPC6 was lower than that of infundibulum. All data are expressed as a mean of 3 replicates ± 1 standard deviation. (* = $p<0.05$; ** = $p<0.01$; *** = $p<0.001$).

4.1.1.9 Changes in localization and abundance of TRPC1 and TRPC6 in non-permeabilized bovine infundibulum epithelium throughout the estrous cycle

The localization pattern of TRPC1 and TRPC6 channels changed in bovine infundibulum epithelial tissue throughout the estrous cycle (Fig 4.25).

In non-permeabilized tissue, there was no significant difference in abundance of TRPC1 on apical side of the infundibulum at stage 2 ($p= 0.1$) compared to stage 1 of the estrous cycle.. Abundance of TRPC1 on the apical side of the tissue was increased by 7 fold ($p= 0.002$) at stage 3 relative to stage 1. Abundance of TRPC1 was 8.9 fold ($p= 0.005$) higher at stage 4 compared to stage 1(Fig 4.26, A). On the basal side of the infundibulum epithelial tissue, abundance of TRPC1 channels at stage 2 ($p= 0.08$) was not significantly different compared to that of stage 1. At stage 3 of the estrous cycle a 6.6 fold ($p= 0.007$) increase in abundance of TRPC1 was observed on the basal side of the infundibulum epithelial tissue compared to stage 1. This increase was higher at stage 4 by 10 fold ($p= 0.009$) (Fig 4.26, B). On the lateral side of the non-permeabilized bovine infundibulum epithelial tissue, abundance of TRPC1 was higher by 6.5 fold ($p= 0.02$) at stage 2 compared to stage 1. At stage 3, abundance of TRPC1 was 8.67 fold ($p= 0.0005$) higher than that of stage 1. Abundance of TRPC1 channel on the lateral side of the tissue was increased by 12.75 fold ($p= 0.002$) at stage 4 compared to the stage 1 (Fig 4.26, C).

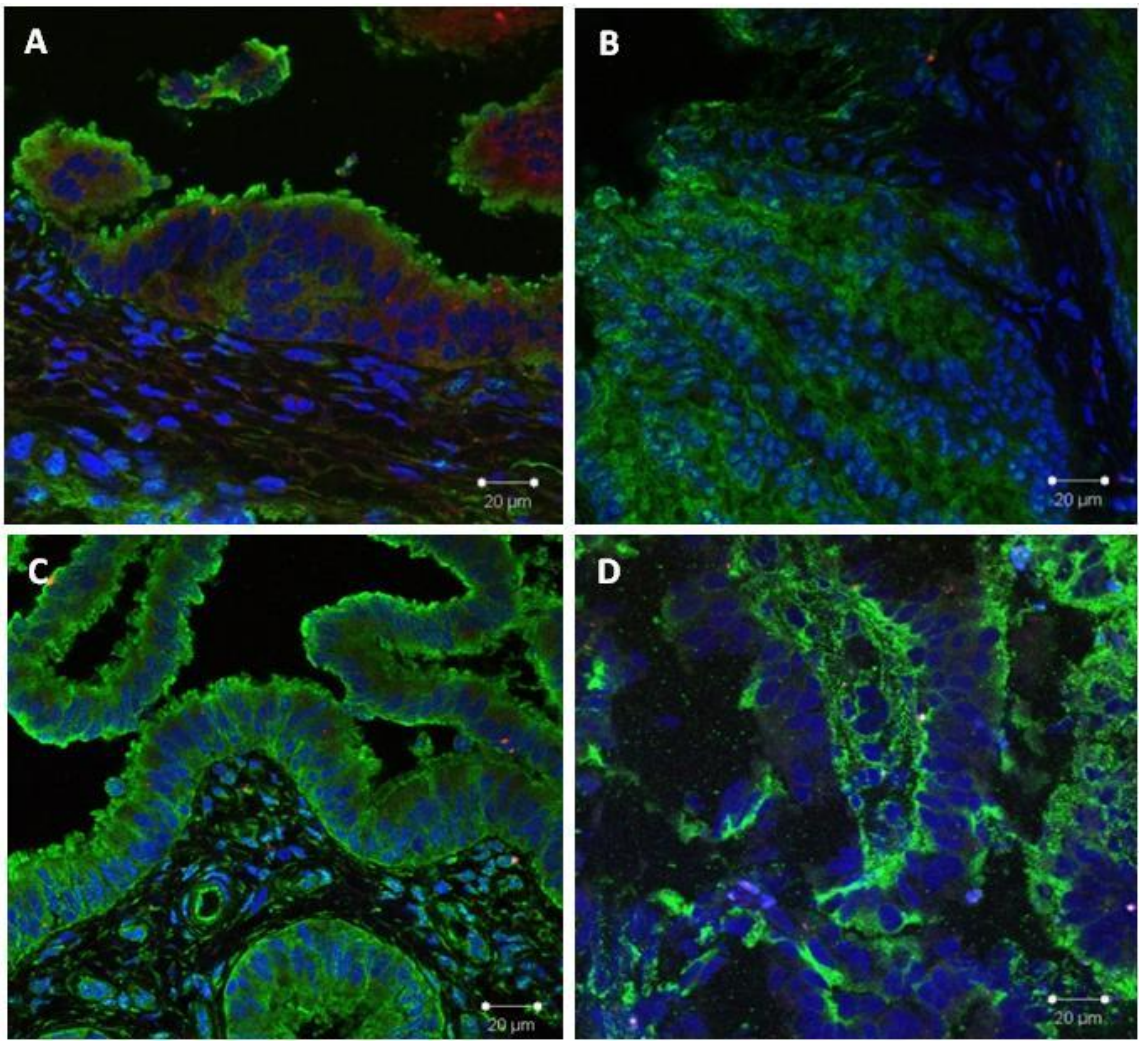

Fig 4.25 Localization of TRPC1 and TRPC6 in non-permeabilized bovine infundibulum epithelial tissue at stage 1 (4.25, A), stage 2 (4.25, B), stage 3 (4.25, C) and stage 4 (4.25,D) of the estrous cycle. nuclei are labelled with DAPI (Blue), TRPC1 with Alexa Four 647 FITC conjugated (Red) and TRPC6 with Alexa Flour 488 (Green).

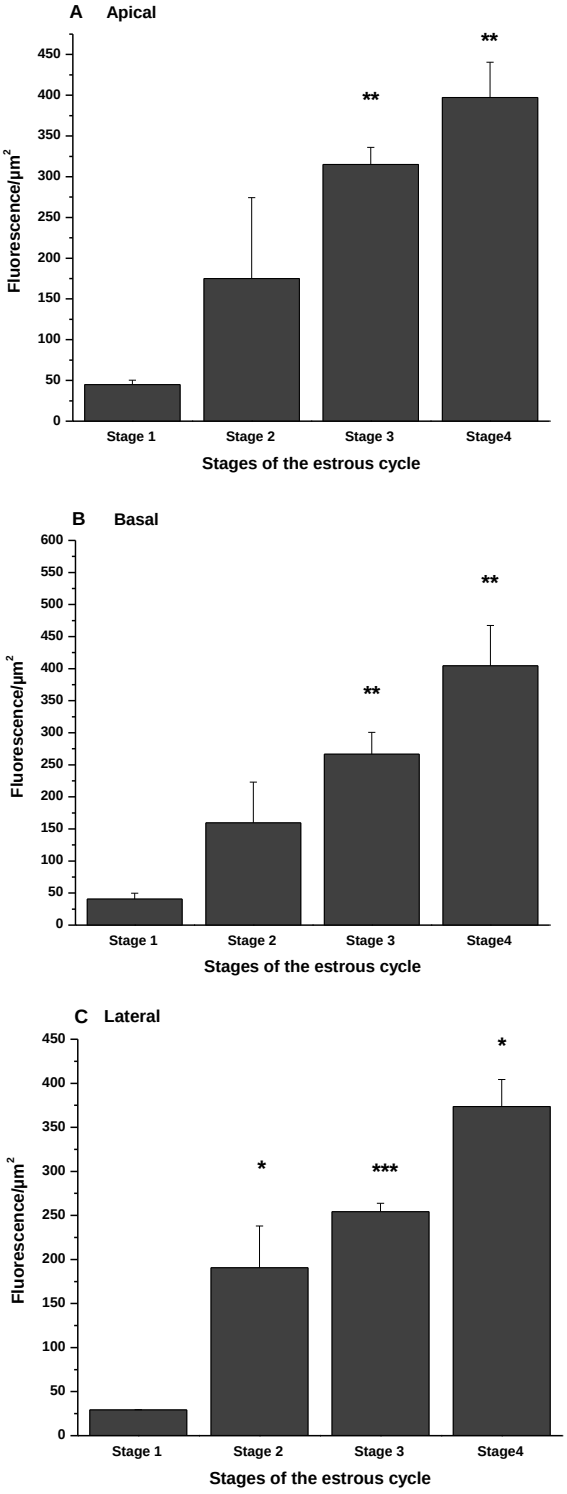

Fig 4.26 Abundance of TRPC1 in non-permeabilized bovine infundibulum epithelium throughout the estrous cycle on apical (4.26, A), basal (4.26, B) and the lateral (4.26, C) side of the tissue. Abundance of TRPC1 on both apical and basal side of the tissue at stage 2 was not significantly different to that of the stage 1. However, abundance of TRPC1 at stage 3 and 4 was higher than that of the stage 1 on both apical and basal side of the tissue. On the lateral side of the tissue, abundance of TRPC1 was the lowest at stage 1 and the highest at stage 4 of the estrous cycle. Abundance of TRPC1 at stage 2, 3 and 4 of the estrous cycle was higher than that of the stage 1. All data are expressed as a mean of 3 replicates ± 1 standard deviation. (* = $p<0.05$; ** = $p<0.01$; *** = $p<0.001$).

At stage 2 of the estrous cycle on the apical side of the non-permeabilized bovine infundibulum epithelial tissue, abundance of TRPC6 was higher by 18.17 fold (p= 0.01) relative to stage 1. Furthermore, abundance of TRPC6 on the apical side of the tissue was higher by 19.64 (p= 0.0007) and 18.67 (p= 0.02) fold at stage 3 and 4 respectively compared to that of the stage 1 (Fig 4.27, A). On the basal side of the epithelium, abundance of TRPC6 was 9.27 fold (p= 0.01) higher at stage 2 compared to that of stage 1. TRPC6 was 34.22 (p= 0.004) and 36.64 (p= 0.01) fold more abundant at stage 3 and stage 4 of the estrous cycle respectively compared to stage 1 (Fig 4.27, B). On the lateral side of the bovine infundibulum epithelial tissue, abundance of TRPC6 was 19.87 fold (p= 0.04) higher at stage 2 compared to that of stage 1. At stage 3 of the estrous cycle, TRPC6 was more abundant by 41.36 fold (p= 0.001) on the lateral side of the epithelium compared to stage1. Abundance of TRPC6 on the lateral side of non-permeabilized bovine infundibulum epithelium was 21.4 fold (p= 0.003) higher than that of stage 1 (Fig 4.27, C).

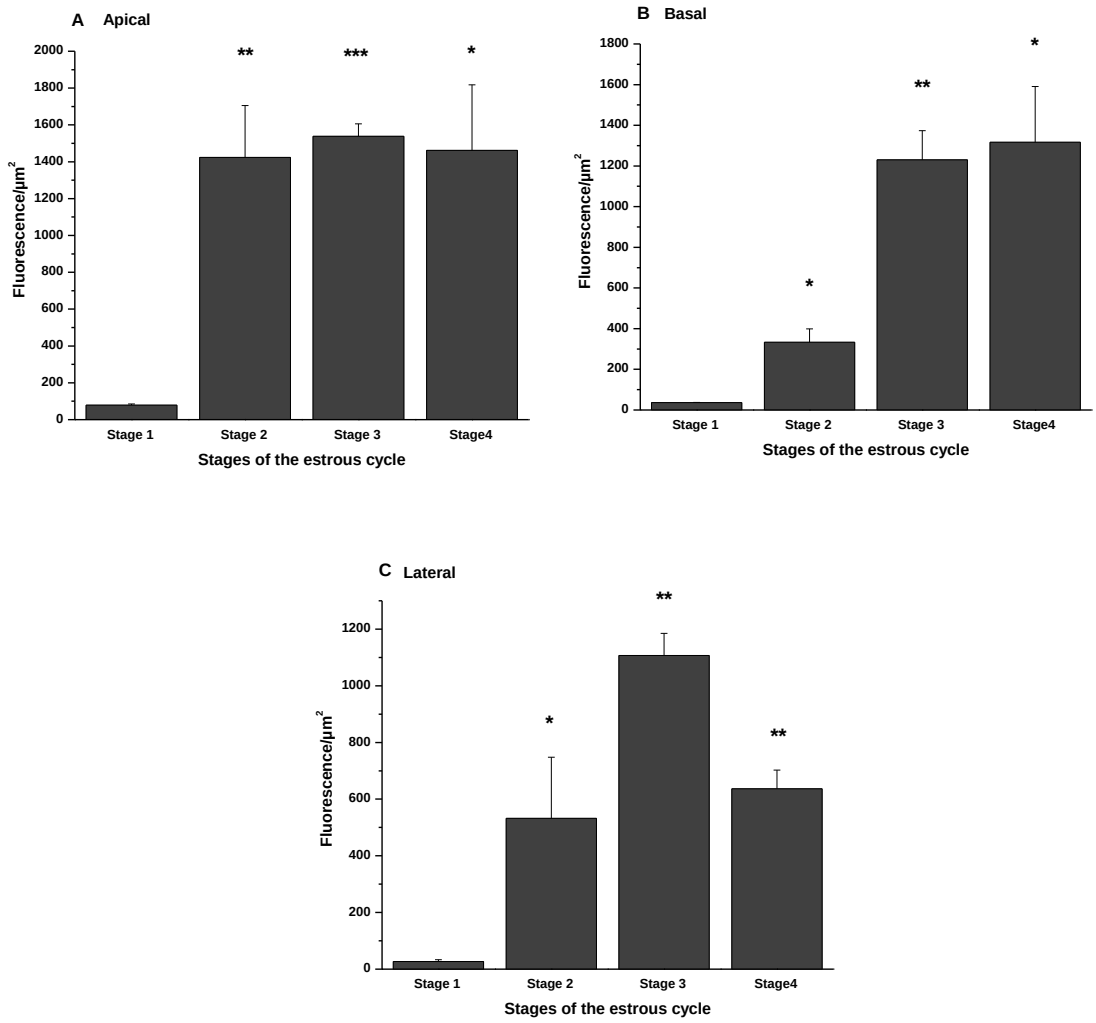

Fig 4.27 Abundance of TRPC6 in non-permeabilized bovine infundibulum epithelium throughout the estrous cycle on apical (4.27, A), basal (4.27, B) and the lateral (4.27, C) side of the tissue. On the apical side of the tissue, abundance of TRPC6 was equal at stage 2, 3 and 4 where it was higher than the stage 1. On basal side of the epithelium, abundance of TRPC6 was equal at stage 3 and 4 where it was higher than stage 2 and 1. Abundance of TRPC6 on the basal side was the lowest at stage 1 of the estrous cycle. On the lateral side of the non-permeabilized infundibulum epithelium, abundance of TRPC6 was equal at stage2 and stage 4 of the estrous cycle. The highest abundance of TRPC6 on the lateral side was observed at stage 3 and the lowest abundance was observed at stage 1 of the estrous cycle. All data are expressed as a mean of 3 replicates ± 1 standard deviation. (* = $p<0.05$; ** = $p<0.01$; *** = $p<0.001$).

4.1.1.10 Changes in localization and abundance of TRPC1 and TRPC6 in permeabilized bovine infundibulum epithelium throughout the estrous cycle

Abundance of TRPC1 on the apical side of the epithelium at stage 2 of the estrous cycle in permeabilized bovine infundibulum epithelial tissue was 1.82 fold (p= 0.008) higher than that of stage 1. However, abundance of TRPC1 was reduced by 0.23 fold (p= 5.32 x 10^{-5}) at stage 3 of the estrous cycle compared to stage1. A 1.95 fold (p= 0.03) increase in abundance of TRPC1 was observed on the apical side of permeabilized bovine infundibulum epithelial tissue at stage 4 of the estrous cycle compared to that of stage 1 (Fig 4.29, A). On the basal side of the permeabilized bovine infundibulum epithelial tissue, abundance of TRPC1 at stage 2 (p= 0.2) was equal to that of stage 1. In contrast, at stage 3 of the estrous cycle abundance of TRPC1 channel was reduced by 0.24 fold (p= 0.001) compared to stage 1. At stage 3 of the estrous cycle, abundance of the TRPC1 was increased by 2.12 fold (p= 0.007) relative to that of stage 1 (Fig 4.29, B). Abundance of TRPC1 channels on the lateral side of the permeabilized bovine infundibulum epithelial tissue, was 1.9 fold (p= 0.01) higher at stage 2 of the estrous cycle compared to stage1. However, abundance of TRPC1 at stage 3 of the estrous cycle was reduced by 0.27 fold (p= 0.0001) compared to stage 1 of the estrous cycle. At stage 4 abundance of TRPC1 was increased by 2.6 fold (p= 0.006) compared to stage 1 (Fig 4.29, C).

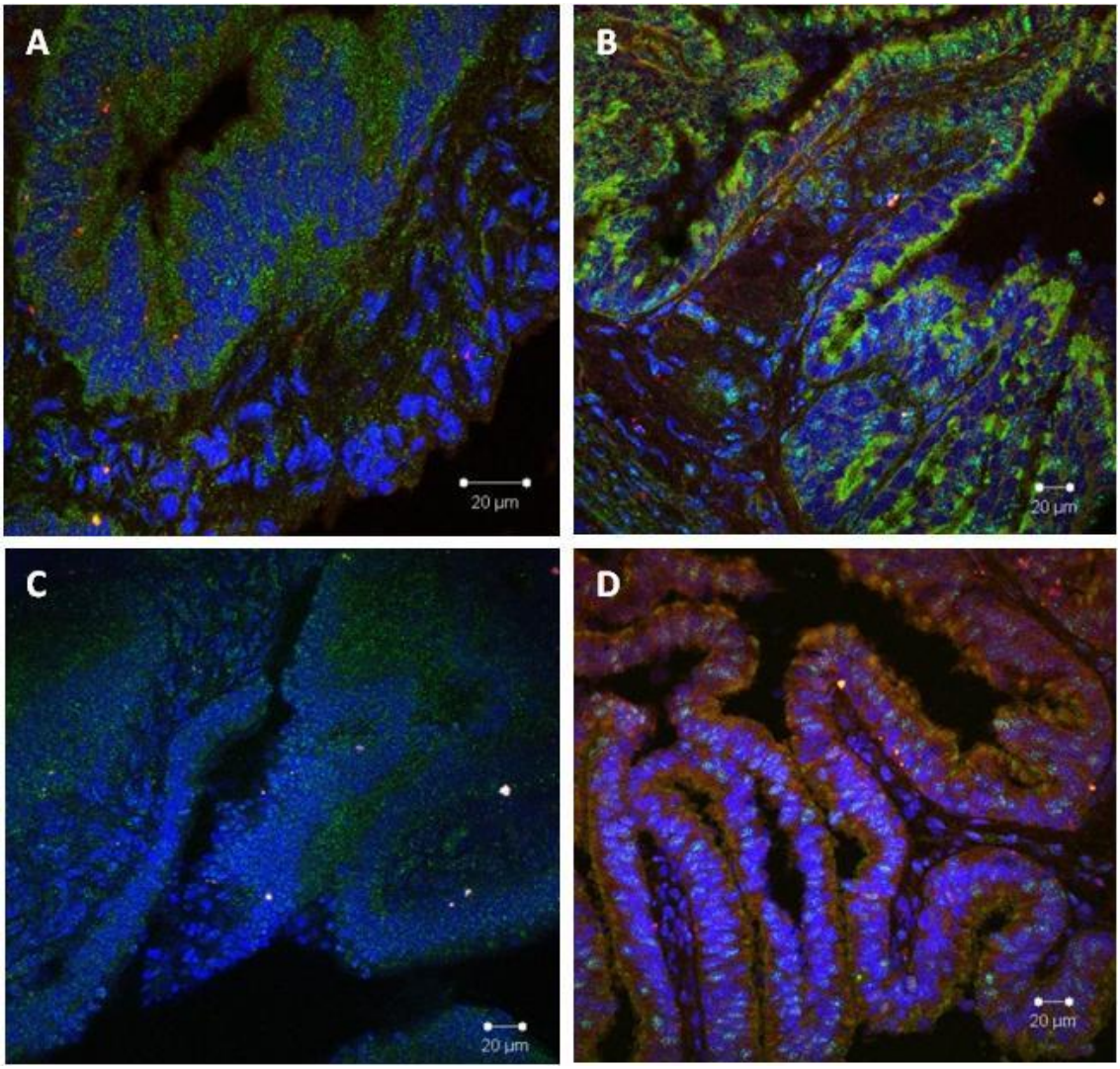

Fig 4.28 Localization of TRPC1 and TRPC6 in permeabilized bovine infundibulum epithelial tissue at stage 1 (4.28, A), stage 2 (4.28, B), stage 3 (4.28, C) and stage 4 (4.28, D) of the estrous cycle. Nuclei are labelled with DAPI (Blue), TRPC1 with Alexa Four 647 FITC conjugated (Red) and TRPC6 with Alexa Flour 488 (Green).

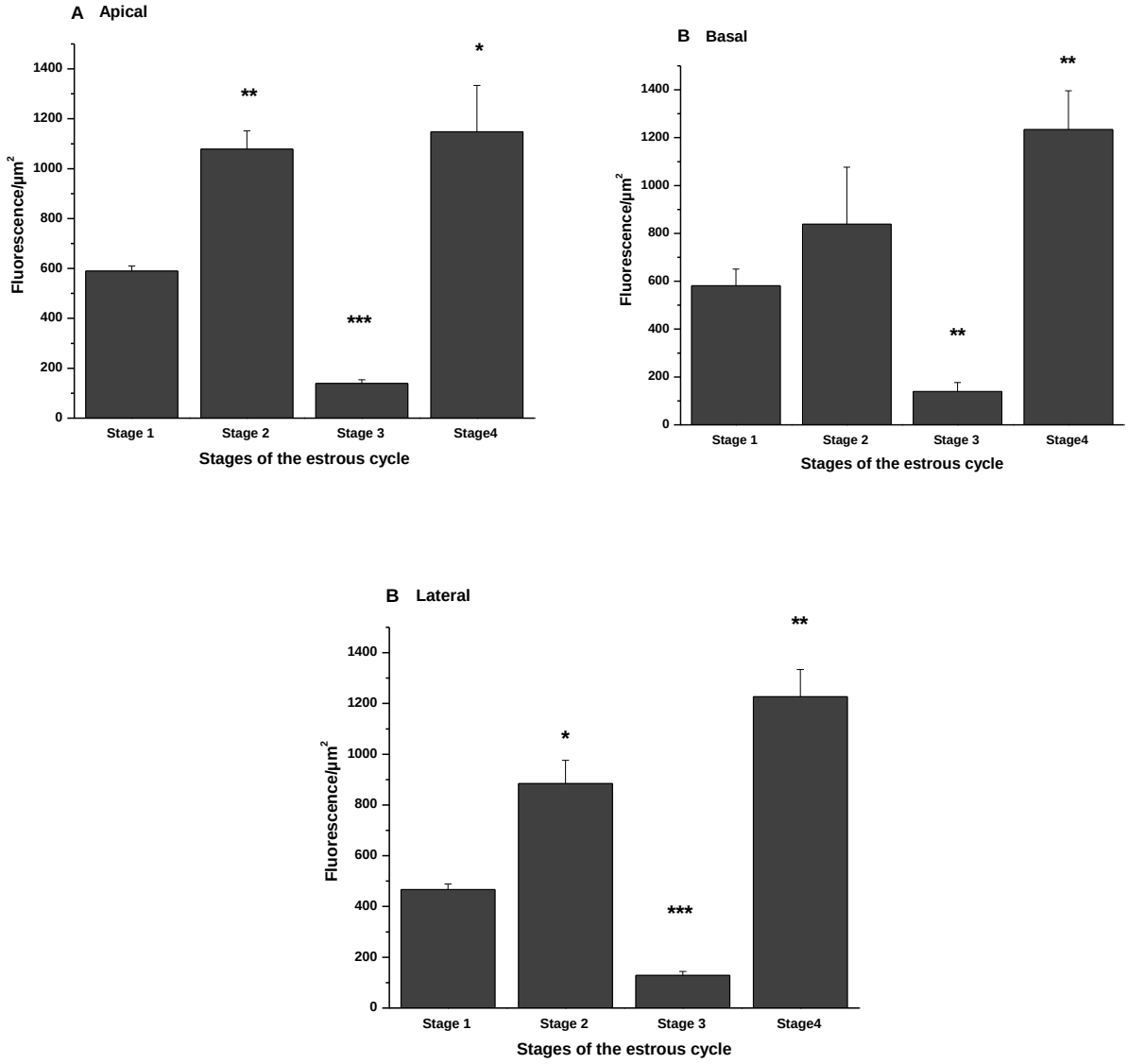

Fig 4.29 Abundance of TRPC1 in permeabilized bovine infundibulum epithelium throughout the estrous cycle on apical (4.29, A), basal (4.29, B) and the lateral (4.29, C) side of the tissue. On the apical side of the tissue, abundance of TRPC1 at stage 2 and 4 was higher than that of the stage 1. However, at stage 3 of the estrous cycle abundance of TRPC1 was lower than that of the stage 1.On the basal side of the tissue, there was no significant difference in abundance of the TRPC1 at stage2 compared to that of the stage 1. Similarly to the apical side, abundance of TROC1 at stage 2 and 4 was higher than that of the stage 1 of the estrous cycle. However, at stage 3 abundance of TRPC1 was decreased compared to that of the stage 1. All data are expressed as a mean of 3 replicates ± 1 standard deviation. (* = $p<0.05$; ** = $p<0.01$; *** = $p<0.001$).

Abundance of TRPC6 channel on the apical side of the permeabilized bovine infundibulum epithelial tissue was 1.66 fold (p= 0.04) higher at stage 2 compared to that of stage 1 of the estrous cycle. At stage 3 of the estrous cycle, abundance of TRPC6 channel was reduced by 0.65 fold (p= 0.01) relative to stage 1. However, abundance of TRPC6 on the apical side of the permeabilized bovine infundibulum epithelium at stage 4 (p= 0.1) was equal to that of stage 1 of the estrous cycle (Fig 4.30, A). On the basal side of the permeabilized bovine infundibulum epithelial tissue, there was no significant difference in abundance of TRPC6 at stage 2 (p= 0.5) compared to stage 1. However, abundance of TRPC6 was decreased by 0.75 (p= 0.001) and 0.68 (p= 0.03) fold at stage 3 and 4 respectively compared to that of stage 1 (Fig 4.30, B). On the lateral side of the permeabilized bovine infundibulum epithelial tissue, abundance of TRPC6 at stage 2 (p= 0.2) was equal to that of stage 1 of the estrous cycle. Abundance of TRPC6 was reduced by 0.73 fold (p= 0.03) at stage 3 relative to stage 1. However, there was no significant difference in abundance of TRPC6 at stage 4 (p= 0.6) compared to stage 1 of the estrous cycle (Fig 4.30, C).

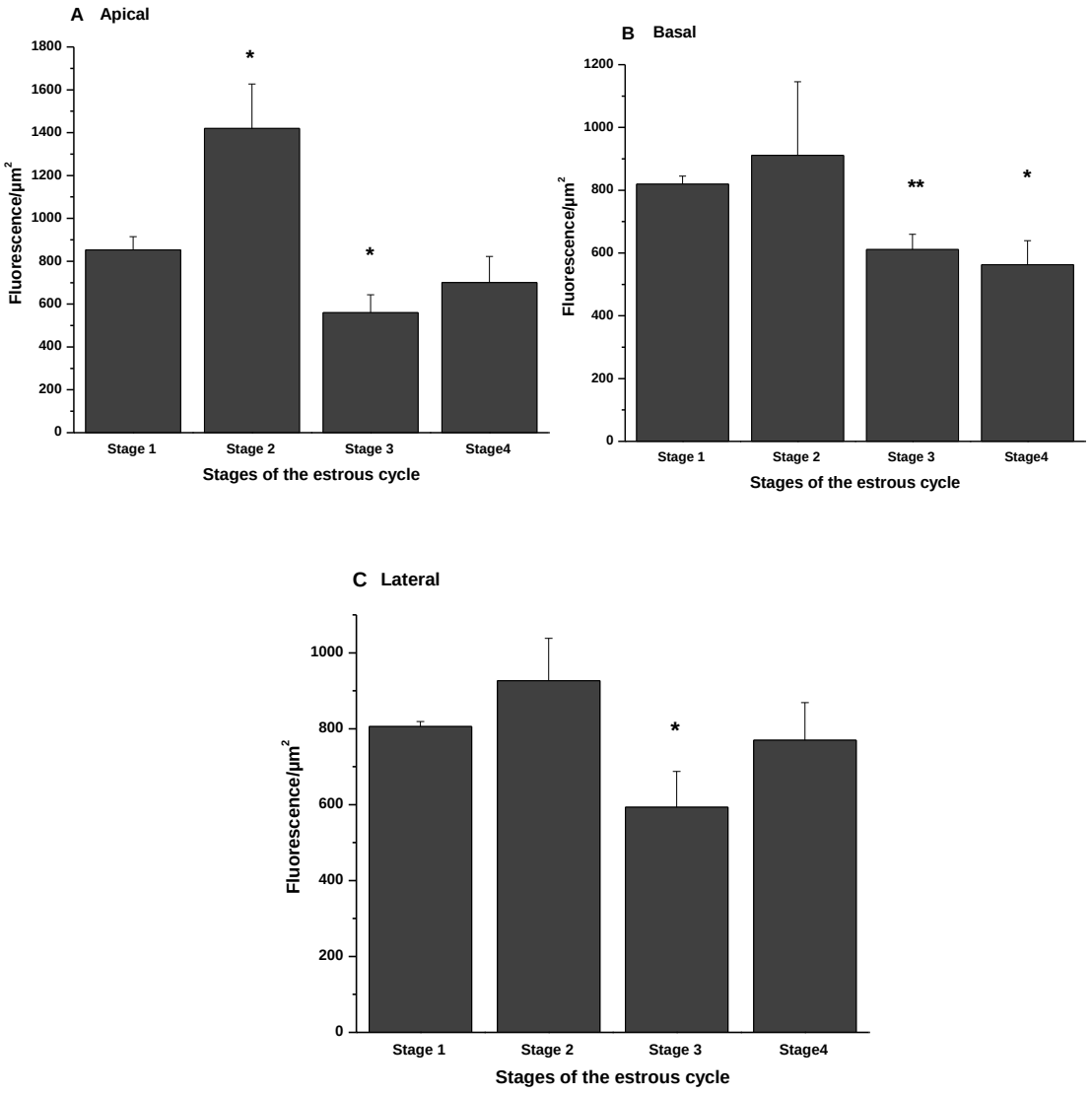

Fig 4.30 Abundance of TRPC6 in permeabilized bovine infundibulum epithelium throughout the estrous cycle in apical (4.30, A), basal (4.30, B) and the lateral (4.30, C) side of the tissue. Abundance pattern of TRPC6 was the same on apical and lateral side of the tissue. On the apical side of the tissue, abundance of TRPC6 at stage 2 of the estrous cycle was higher than that of the stage 1. However, at stage 3 abundance of TRPC6 was decreased compared to that of the stage 1. There was no significant difference in abundance of TRPC6 on apical side of the tissue at stage 4 compared to the of the satge1. On the basal side of the permeabilized bovine infundibulum epithelial tissue, no significant difference was observed in abundance of TRPC6 between stage 1 and 2 of the estrous cycle. However, abundance of TRPC6 at both stage 3 and 4 was lower than that of the stage 1. On the lateral side of the tissue, there was no significant difference in abundance of TRPC6 at stage 2 and 4 compared to that of the stage1. However, abundance of TRPC6 was decreased at stage 3 compared to the stage 1 of the estrous cycle. All data are expressed as a mean of 3 replicates ± 1 standard deviation. (* = $p<0.05$; ** = $p<0.01$; *** = $p<0.001$).

4.1.1.11 Changes in localization and abundance of TRPC1 and TRPC6 in non-permeabilized bovine ampulla epithelium throughout the estrous cycle

`On the apical side of non-permeabilized bovine ampulla epithelial tissue, abundance of TRPC1 at stage 2 (p= 0.4) was equal to that of stage 1. Similarly to stage 2, at stage 3 (p= 0.3) and 4 (p= 0.05) of the estrous cycle abundance of TRPC1 channel was not significantly different compared to stage 1. (Fig 4.32, A). Furthermore, on the basal side of the non-permeabilized bovine ampulla epithelial tissue, abundance of TRPC1 channel at stage 2 (p= 0.2) and 3 (p= 0.3) and 4 (p= 0.08) (Fig 4.32, B) was not significantly different to that of the stage 1 (Fig 4.32, B). On the lateral side of the non-permeabilized bovine ampulla epithelium, abundance of TRPC1 channel was not significantly different at stage 2 (p= 0.08) and 4 (p= 0.2) to that of stage 1 of the estrous cycle. However, at stage 3 of the estrous cycle abundance of TRPC1 was lower by 0.61 fold (p= 0.02) relative to stage 1 of the estrous cycle (Fig 4.32, C).

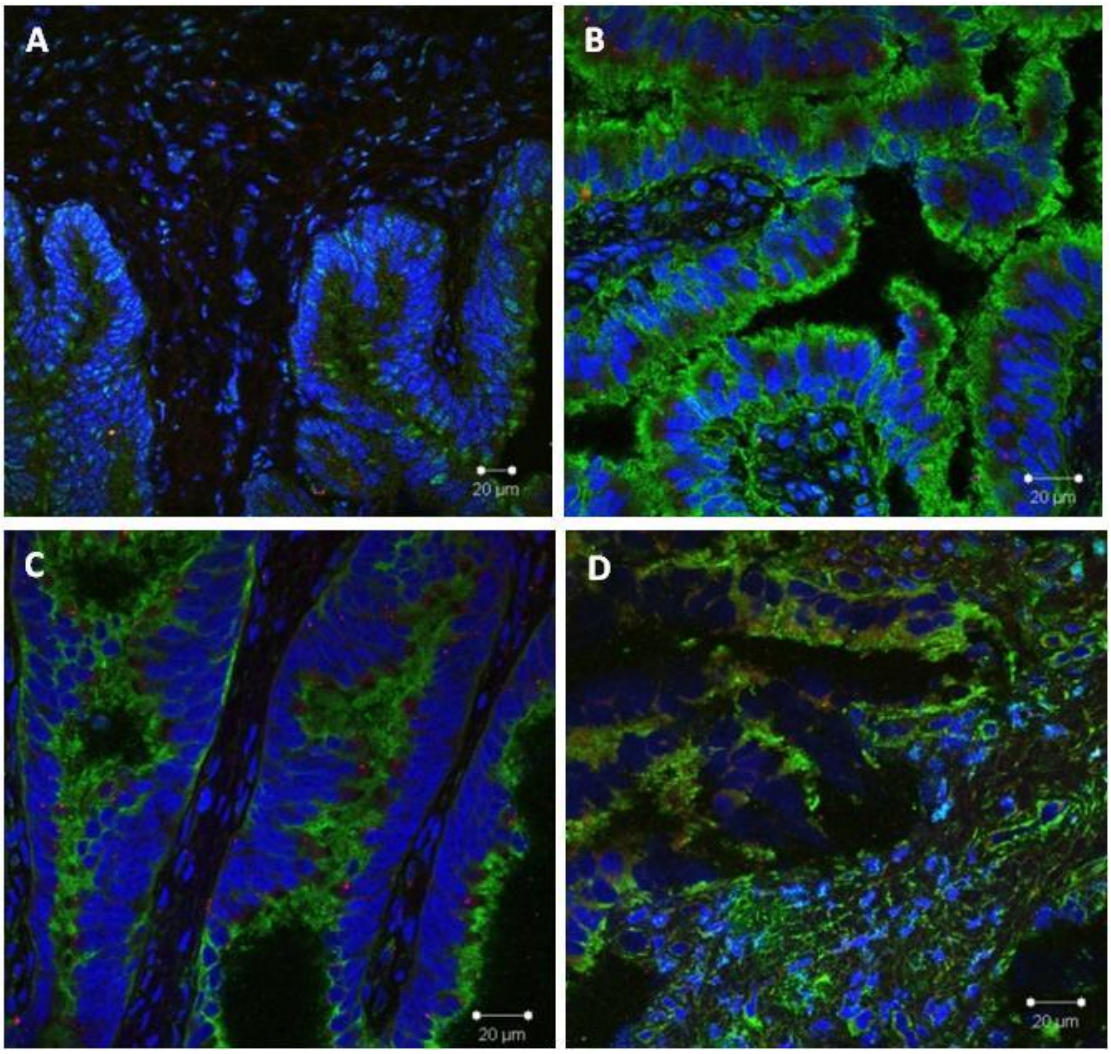

Fig 4.31 Localization of TRPC1 and TRPC6 in non-permeabilized bovine ampulla epithelial tissue at stage 1 (4.31, A), stage 2 (4.31, B), stage 3 (4.31, C) and stage 4 (4.31, D) of the estrous cycle. Nuclei are labelled with DAPI (Blue), TRPC1 with Alexa Four 647 FITC conjugated (Red) and TRPC6 with Alexa Flour 488 (Green).

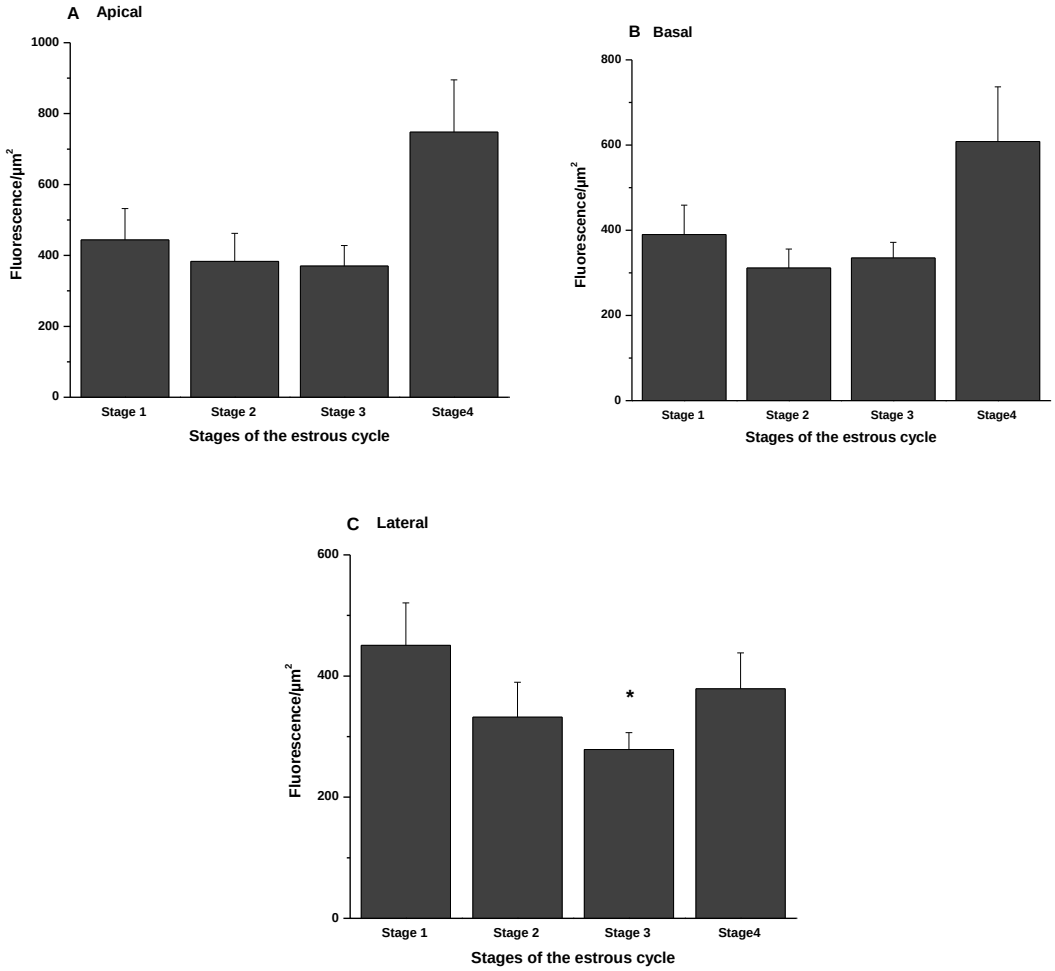

Fig 4.32 Abundance of TRPC1 in non-permeabilized bovine ampulla epithelium throughout the estrous cycle on apical (4.32, A), basal (4.32, B) and the lateral (4.32, C) side of the tissue. On the apical and basal side of the non-permeabilized bovine ampulla epithelial tissue, no significant difference was observed in abundance of TRPC1 at stage 2, 3 and 4 of the estrous cycle compared to that of the stage 1. Furthermore, abundance of TRPC1 at stage 2 and 4 of the estrous cycle on lateral side of the tissue was equal to that of the stage 1. However, abundance of TRPC1 at stage 3 of the estrous cycle was lower than that of the stage 1. All data are expressed as a mean of 3 replicates ± 1 standard deviation. (* = $p<0.05$; ** = $p<0.01$; *** = $p<0.001$).

Abundance of TRPC6 on the apical side of the non-permeabilized bovine ampulla epithelium at stage 2 (p= 0.1) was equal to that of stage 1 of the estrous cycle. However, abundance of TRPC6 channel was increased by 1.3 (p= 0.01) and 1.62 (p= 0.02) fold at stage 3 and 4 respectively compared to stage 1 (Fig 4.33, A). On the basal side of the non-permeabilized bovine ampulla epithelial tissue, abundance of TRPC6 channel at stage 2 (p= 0.1), 3 (p= 0.2), and 4 (p= 0.05) was not significantly different to that of stage 1 (Fig 4.33, B). On the lateral side of the non-permeabilized bovine ampulla epithelial tissue, abundance of TRPC6 was increased by 1.57 fold (p= 0.04) at stage 2 of the estrous cycle compared to stage 1. However, at stage 3 and 4, abundance of TRPC6 was decreased by 0.5 (p= 0.0008) and 0.71 (p= 0.006) fold respectively relative to stage 1 (Fig 4.33, C).

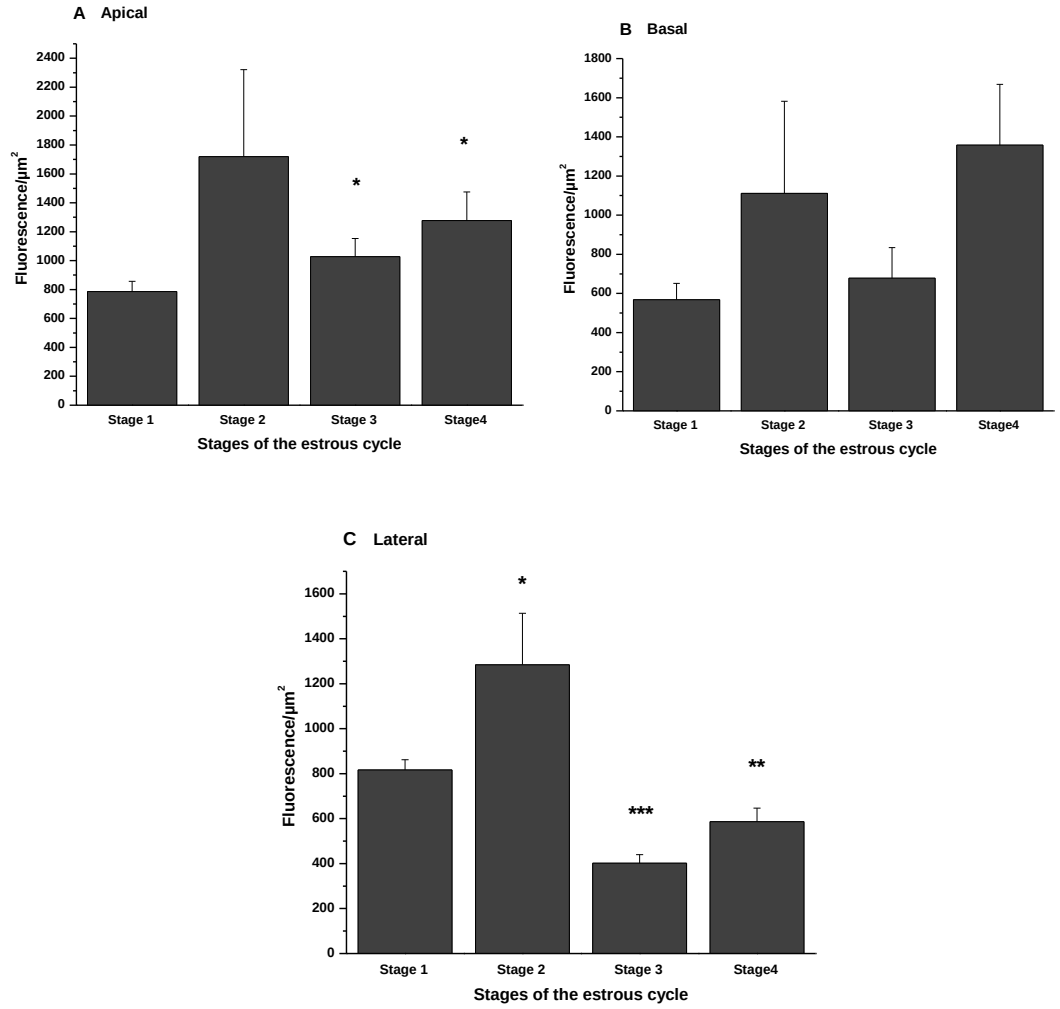

Fig 4.33 Abundance of TRPC6 in non-permeabilized bovine ampulla epithelium throughout the estrous cycle on apical (4.33, A), basal (4.33, B) and the lateral (4.33, C) side of the tissue. On the apical side of the tissue, abundance of TRPC6 at stage 2 was not significantly different to that of the stage 1. However, abundance of TRPC1 was higher at both stage 3 and 4 on the apical side of the tissue compared to that of the stage 1. On the basal side of the non-permeabilized bovine ampulla epithelium, there was no significant difference in abundance of TRPC1 at stage 2, 3 and 4 of the estrous cycle compared to that of the stage 1. However, on the lateral side of the tissue abundance of TRPC1 was increased at stage 2 and decreased at stage 3 and 4 compared to the stage 1 of the estrous cycle. All data are expressed as a mean of 3 replicates ± 1 standard deviation. (* = $p<0.05$; ** = $p<0.01$; *** = $p<0.001$).

4.1.1.12 Changes in localization and abundance of TRPC1 and TRPC6 in permeabilized bovine ampulla epithelium throughout the estrous cycle

Abundance of TRPC1 channels on the apical side of the permeabilized bovine ampulla epithelial tissue was decreased by 0.12 (p= 0.02) and 0.13 (p= 0.02) fold respectively at stage 2 and 4 compared to the stage 1 of the estrous cycle. However, abundance of TRPC1 was the same as that of stage 1 at stage 3 (p= 0.8) of the estrous cycle (Fig 4.35, A). On the basal side of the permeabilized bovine ampulla epithelium, abundance of TRPC1 was reduced by 0.10 (p= 0.02) and 0.14 (p= 0.03) fold respectively at stage 2 and 4 of the estrous cycle compared to that of stage 1. No significant changes in abundance of TRPC1 were observed at stage 3 (p= 0.8) relative to stage 1 of the estrous cycle (Fig 4.35, B). On the lateral side of the permeabilized bovine ampulla epithelial tissue, abundance of TRPC1 was reduced 0.09 (p= 0.01) and 0.16 (p= 0.02) fold at stage 2 and 4 of the estrous cycle respectively compared to stage 1. However, abundance of TRPC1 at stage 3 (p= 0.3) of the estrous cycle was the same as that of stage 1 (Fig 4.35, C).

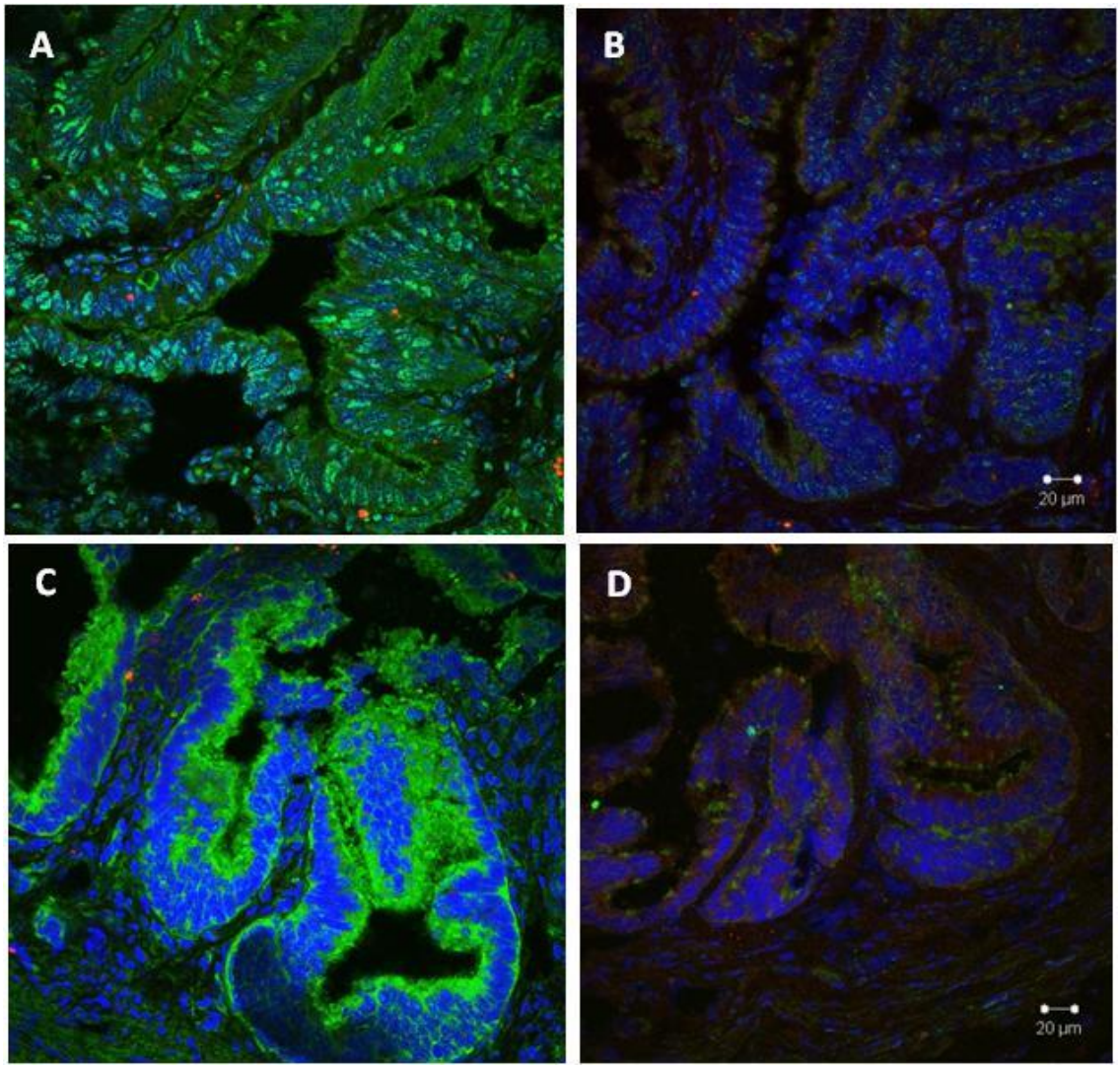

Fig 4.34 Localization of TRPC1 and TRPC6 in permeabilized bovine ampulla epithelial tissue at stage 1 (4.34, A), stage 2 (4.34, B), stage 3 (4.34, C) and stage 4 (4.34, D) of the estrous cycle. Nuclei are labelled with DAPI (Blue), TRPC1 with Alexa Four 647 FITC conjugated (Red) and TRPC6 with Alexa Flour 488 (Green).

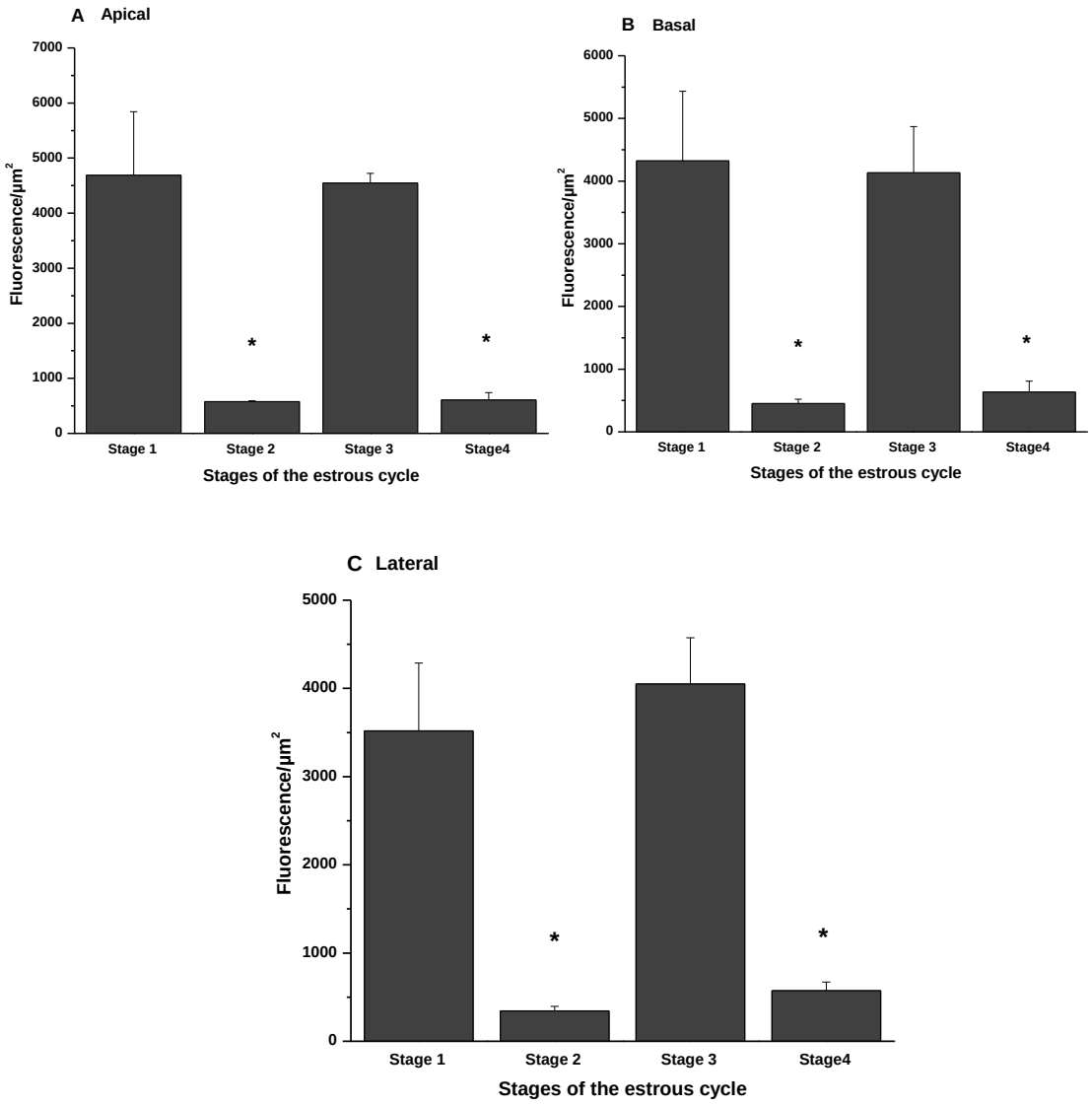

Fig 4.35 Abundance of TRPC1 in permeabilized bovine ampulla epithelium throughout the estrous cycle on apical (4.35, A), Basal (4.35, B) and the lateral (4.35, C) side of the tissue. Abundance of TRPC1 on apical, basal and lateral side of the epithelial tissue of permeabilized bovine ampulla was lower at stage 2 and 4 compared to the stage 1 of the estrous cycle. However, abundance of TRPC1 at stage 3 of the estrous cycle was not significantly different to that of the stage 1. All data are expressed as a mean of 3 replicates ± 1 standard deviation. (* = $p<0.05$; ** = $p<0.01$; *** = $p<0.001$).

On the apical side of the permeabilized bovine ampulla epithelial tissue, abundance of TRPC6 channels was decreased by 0.03 (p= 0.02) and 0.04 (p= 0.02) fold at stage 2 and 4 of the estrous cycle respectively compared to stage 1. In contrast, abundance of TRPC6 was increased by 1.9 fold (p= 0.01) at stage 3 of the estrous cycle relative to stage 1 (Fig 4.36, A). Abundance of TRPC6 channel on the basal side of the permeabilized bovine ampulla epithelial tissue at stage 2 and 4 was decreased by 0.02 (p= 0.003) and 0.04 (p= 0.004) fold respectively compared to stage 1. However, abundance of TRPC6 on the basal side of the permeabilized bovine ampulla epithelial tissue at stage 3 (p= 0.1) was not significantly different compared to stage 1(Fig 4.36, B). On the lateral side of the tissue, abundance of TRPC6 channel was decreased by 0.017 (p= 0.01) and 0.03 (p= 0.01) fold respectively at stages 2 and 4 of the estrous cycle compared to that of stage 1. However, abundance of TRPC6 at stage 3 (p= 0.4) of the estrous cycle was equal to that of stage 1(Fig 4.36, C).

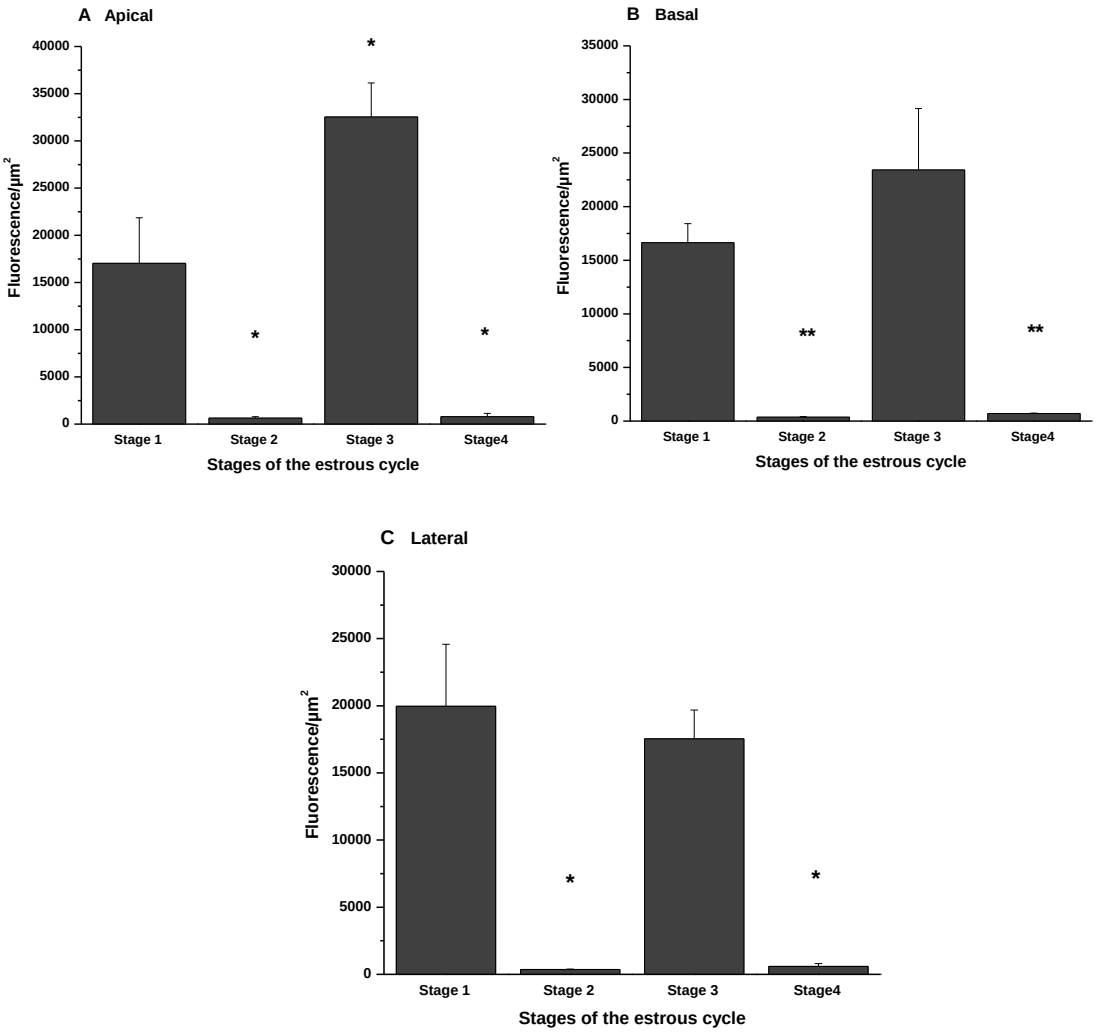

Fig 4.36 Abundance of TRPC6 in permeabilized bovine ampulla epithelium throughout the estrous cycle on apical (4.36, A), basal (4.36, B) and the lateral (4.36, C) side of the tissue. On the apical , basal and lateral side of the permeabilized bovine ampulla epithelial tissue, abundance of TRPC6 was lower at stage 2 and 4 compared to the stage 1 of the estrous cycle. However, abundance of TRPC6 at stage 3 was higher on apical side but not significantly different on none of the basal and lateral side of the tissue compared to the stage 1 of the estrous cycle. All data are expressed as a mean of 3 replicates ± 1 standard deviation. (* = $p<0.05$; ** = $p<0.01$; *** = $p<0.001$).

4.1.1.13 Changes in localization and abundance of TRPC1 and TRPC6 in non-permeabilized bovine isthmus epithelium throughout the estrous cycle

On the apical side of the non-permeabilized bovine isthmus epithelium tissue, abundance of TRPC1 channel was decreased by 0.82 ($p= 0.003$) and 0.54 ($p= 2.95 \times 10^{-6}$) fold at stage 2and 4 of the estrous cycle respectively compared to stage 1. However, abundance of TRPC1 on the apical side of the tissue at stage 3 ($p= 0.06$) was equal to that of stage 1 of the estrous cycle (Fig 4.38, A). On the basal side of the epithelium, abundance of TRPC1 channel was less at stage 2, 3 and 4 by 0.67 ($p= 0.007$), 0.39 ($p= 5.98 \times 10^{-5}$) and 0.21 ($p= 0.001$) fold respectively relative to stage 1 (Fig 4.38, B). On the lateral side of the non-permeabilized bovine isthmus epithelial tissue, abundance of TRPC1 channel was decreased by 0.28 ($p= 3.14 \times 10^{-5}$), 0.29 ($p= 0.0002$) and 0.19 ($p= 0.0004$) fold at stage 2, 3 and 4 of the estrous cycle compared to stage 1(Fig 4.38, C).

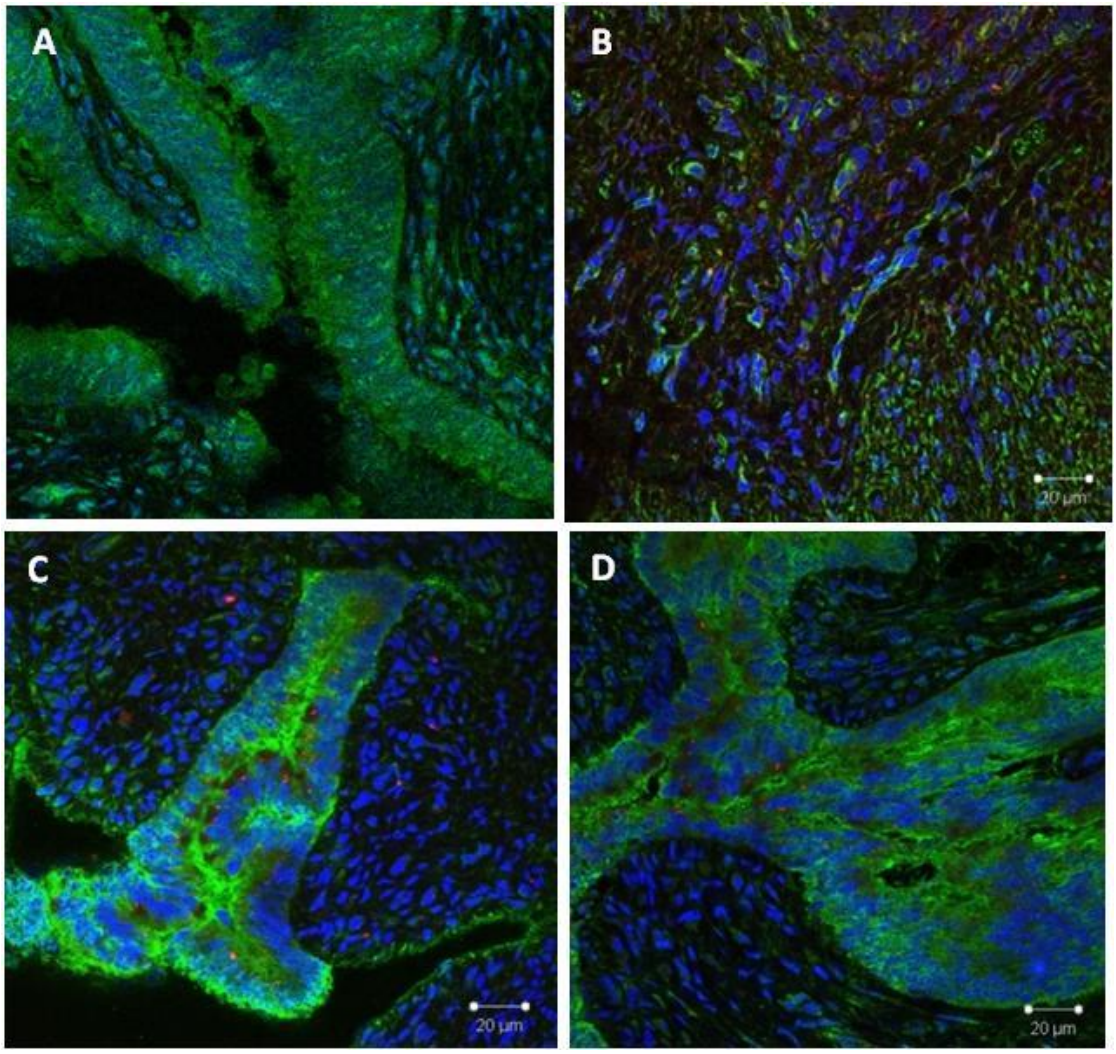

Fig 4.37 Localization of TRPC1 and TRPC6 in non-permeabilized bovine isthmus epithelial tissue at stage 1 (4.37, A), stage 2 (4.37, B), stage 3 (4.37, C) and stage 4 (4.37, D) of the estrous cycle. Nuclei are labelled with DAPI (Blue), TRPC1 with Alexa Four 647 FITC conjugated (Red) and TRPC6 with Alexa Flour 488 (Green).

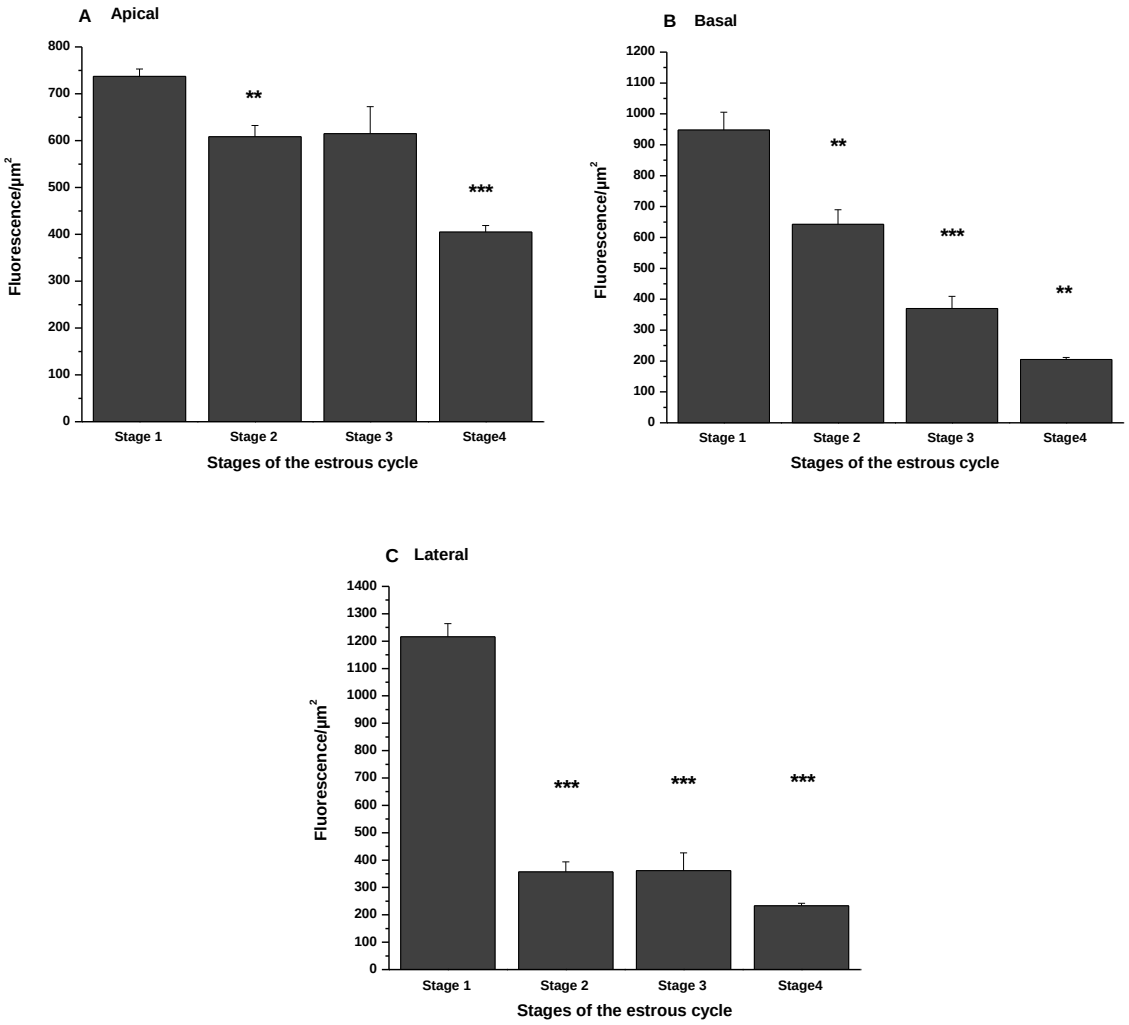

Fig 4.38 Abundance of TRPC1 in non-permeabilized bovine isthmus epithelium throughout the estrous cycle in apical (4.38, A), Basal (4.38, B) and the lateral (4.38, C) side of the tissue. Abundance of TRPC1 on the apical side of the epithelium was the highest at stage 1 and lowest at stage 4. Abundance of TRPC1 at stage 3 was equal to that of the stage 1. A decrease in abundance of TRPC1 was observed at stage 2 compared to the stage 1 of the estrous cycle. On the basal side of the tissue, abundance of TRPC1 was the highest at stage 1 and gradually decreased throughout the estrous cycle and was the lowest at stage 4. On the lateral side of the tissue, abundance of TRPC1 was dramatically higher at stage 1 compared to stage 2, 3 and 4 of the estrous cycle. Abundance of TRPC1 was equal at stage 2 and 3 where it was slightly higher than stage 4 of the estrous cycle. All data are expressed as a mean of 3 replicates ± 1 standard deviation. (* = $p<0.05$; ** = $p<0.01$; *** = $p<0.001$).

On the apical side of the non-permeabilized bovine isthmus epithelial tissue, abundance of TRPC6 channel was highest at stage 1 of the estrous cycle. At stage 2, abundance of TRPC6 was reduced to 0.09 fold (p= 0.04) compared to stage 1. Furthermore, at stages 3 and 4 of the estrous cycle abundance of TRPC6 channel was reduced by 0.19 (p= 0.04) and 0.15 (p= 0.04) fold respectively compared to stage 1 (Fig 4.39, A). On the basal side of the epithelium of the isthmus region, abundance of TRPC6 channel was lower by 0.05 (p= 0.004), 0.12 (p= 0.005) and 0.15 (p= 0.005) fold respectively at stage 2, 3 and 4 relative to stage 1 of the estrous cycle (Fig 4.39, B). Similar to the apical and basal side of the epithelium, abundance of TRPC6 on the lateral side of the epithelium was lower at stage 2, 3 and 4 by 0.025 (p= 0.02), 0.13 (p= 0.03) and 0.058 (p= 0.02) fold respectively compared to stage 1 of the estrous cycle (Fig 4.39, C).

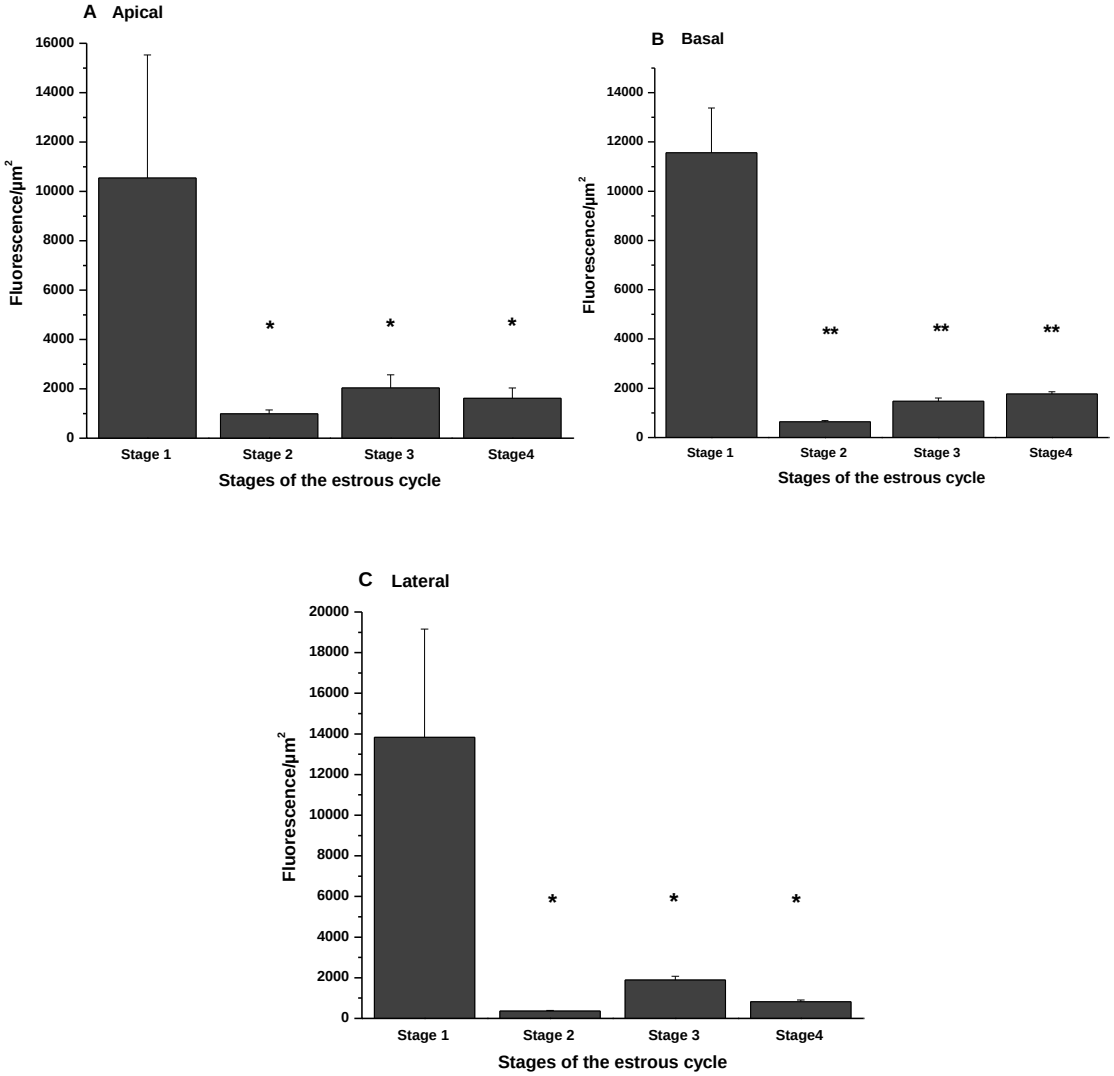

Fig 4.39 Abundance of TRPC6 in non-permeabilized bovine isthmus epithelium throughout the estrous cycle in apical (4.39, A), basal (4.39, B) and the lateral (4.39, C) side of the tissue. On all apical, basal and lateral side of the epithelial tissue, abundance of TRPC6 was highest at stage 1 and lowest at stage 2 of the estrous cycle. Abundance of TRPC6 at stage 3 and 4 was much lower than that of stage 1 on apical, basal and lateral side of the tissue. All data are expressed as a mean of 3 replicates ± 1 standard deviation. (* = $p<0.05$; ** = $p<0.01$; *** = $p<0.001$).

4.1.1.14 Changes in localization and abundance of TRPC1 and TRPC6 in permeabilized bovine isthmus epithelium throughout the estrous cycle

Abundance of TRPC1 channel on the apical side of the permeabilized bovine isthmus epithelial tissue was highest at stage 1 throughout the estrous cycle. Abundance of TRPC1 channel was decreased by 0.16 ($p= 5.71 \times 10^{-5}$), 0.30 (p= 0.0001) and 0.24 (p= 0.0002) fold respectively at stage 2, 3 and 4 of the estrous cycle compared to stage 1 (Fig 4.41, A). On the basal side of the isthmus epithelium, abundance of TRPC1 was reduced by 0.32 fold at stage 2 (p= 0.0006) and 3 (p= 0.0004) and 0.24 fold (p= 0.004) at stage 4 of the estrous cycle relative to stage 1 (Fig 4.41, B). On the lateral side of the permeabilized bovine isthmus epithelial tissue, abundance of TRPC6 was decreased by 0.21 fold at stage 2 ($p= 1.03 \times 10^{-5}$) and 3 ($p= 5.07 \times 10^{-6}$) and 0.16 fold (p= 0.0004) at stage 4 of the estrous cycle compared to stage 1 (Fig 4.41, C).

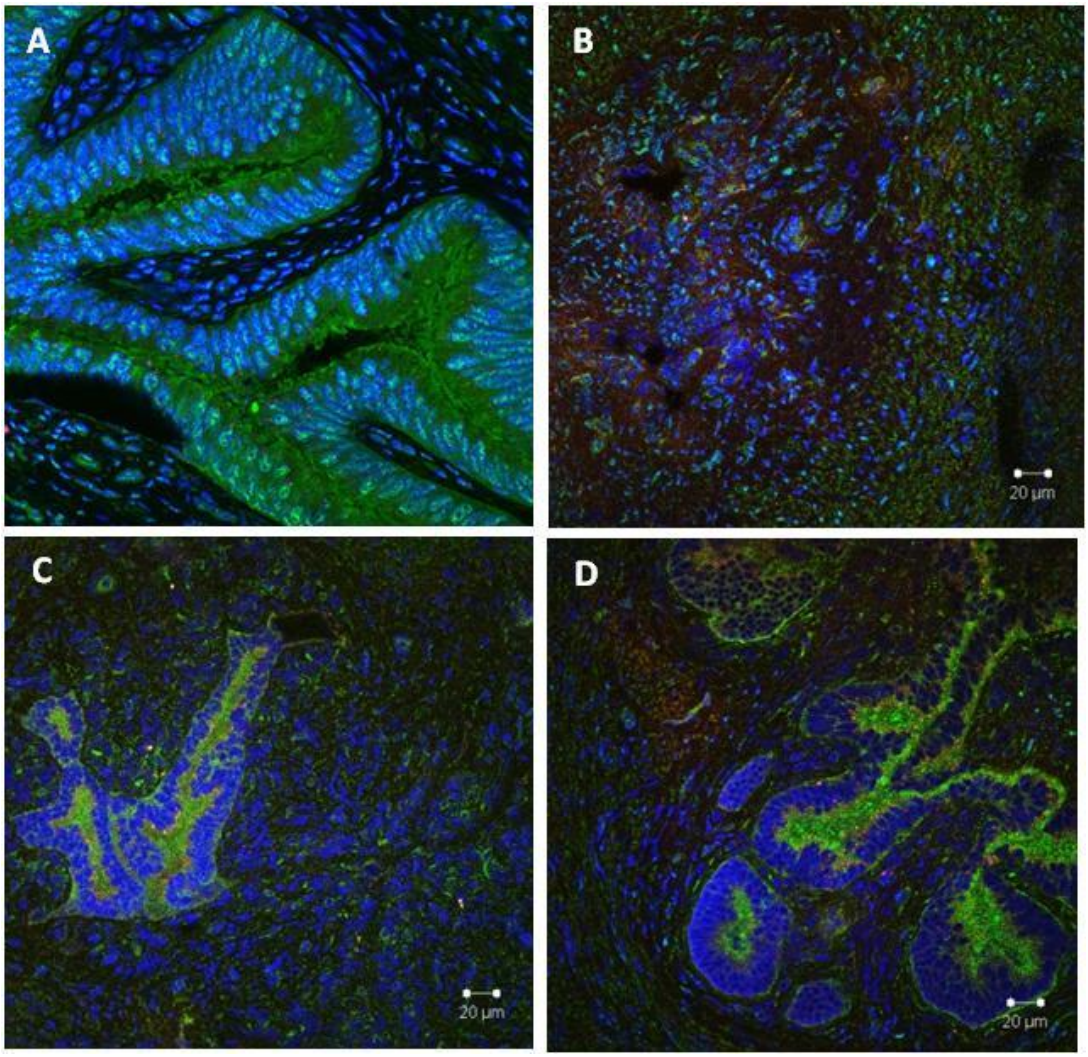

Fig 4.40 Localization of TRPC1 and TRPC6 in permeabilized bovine isthmus epithelial tissue at stage 1 (4.40, A), stage 2 (4.40, B), stage 3 (4.40, C) and stage 4 (4.40, D) of the estrous cycle. Nuclei are labelled with DAPI (Blue), TRPC1 with Alexa Four 647 FITC conjugated (Red) and TRPC6 with Alexa Flour 488 (Green).

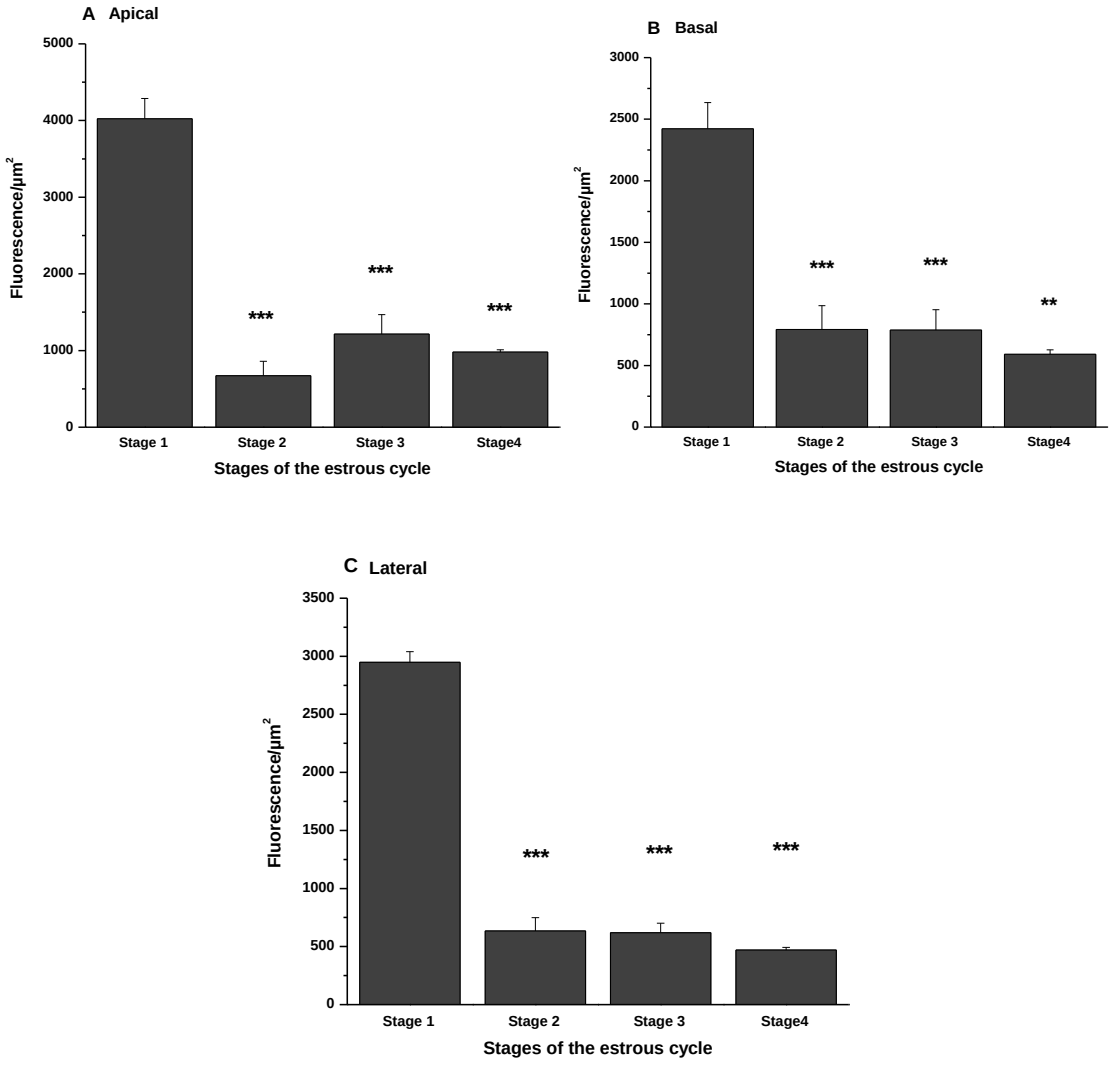

Fig 4.41 Abundance of TRPC1 in permeabilized bovine isthmus epithelium throughout the estrous cycle in apical (4.41, A), basal (4.41, B) and lateral (4.41, C) of the tissue. On the apical side of the tissue TRPC1 was most abundant at stage 1. Abundance of TRPC1 at stage 2, 3 and 4 was much lower than that of stage 1 and the lowest abundance of TRPC1 was observed at stage 2 of the estrous cycle. On the basal and lateral side of the epithelium, abundance of TRPC1 was the highest at stage 1. On the basal and lateral side of the tissue, abundance of TRPC1 at stage 2 and 3 of the cycle was equal and slightly higher than that of stage 4. All data are expressed as a mean of 3 replicates ± 1 standard deviation. (* = $p<0.05$; ** = $p<0.01$; *** = $p<0.001$).

On the apical side of the permeabilized bovine isthmus epithelium, abundance of the TRPC6 channel was reduced by 0.035 (p= 0.003), 0.092 (p= 0.004) and 0.075 (p= 0.004) fold at stage 2, 3 and 4 respectively compared to stage 1 (Fig 4.42, A). On the basal side of the isthmus epithelium, abundance of TRPC6 channel was lower by 0.044 (p= 0.001), 0.064 (p= 0.001) and 0.052 (p= 0.001) fold at stage 2, 3 and 4 of the estrous cycle compared to stage 1 (Fig 4.42, B). On the lateral side of the bovine isthmus epithelium in the permeabilized tissue, abundance of TRPC6 channel was reduced by 0.033 (p= 0.001), 0.034 (p= 0.001) and 0.019 (p= 0.001) fold respectively at stage 2, 3 and 4 of the estrous cycle relative to stage 1 (Fig 4.42, C).

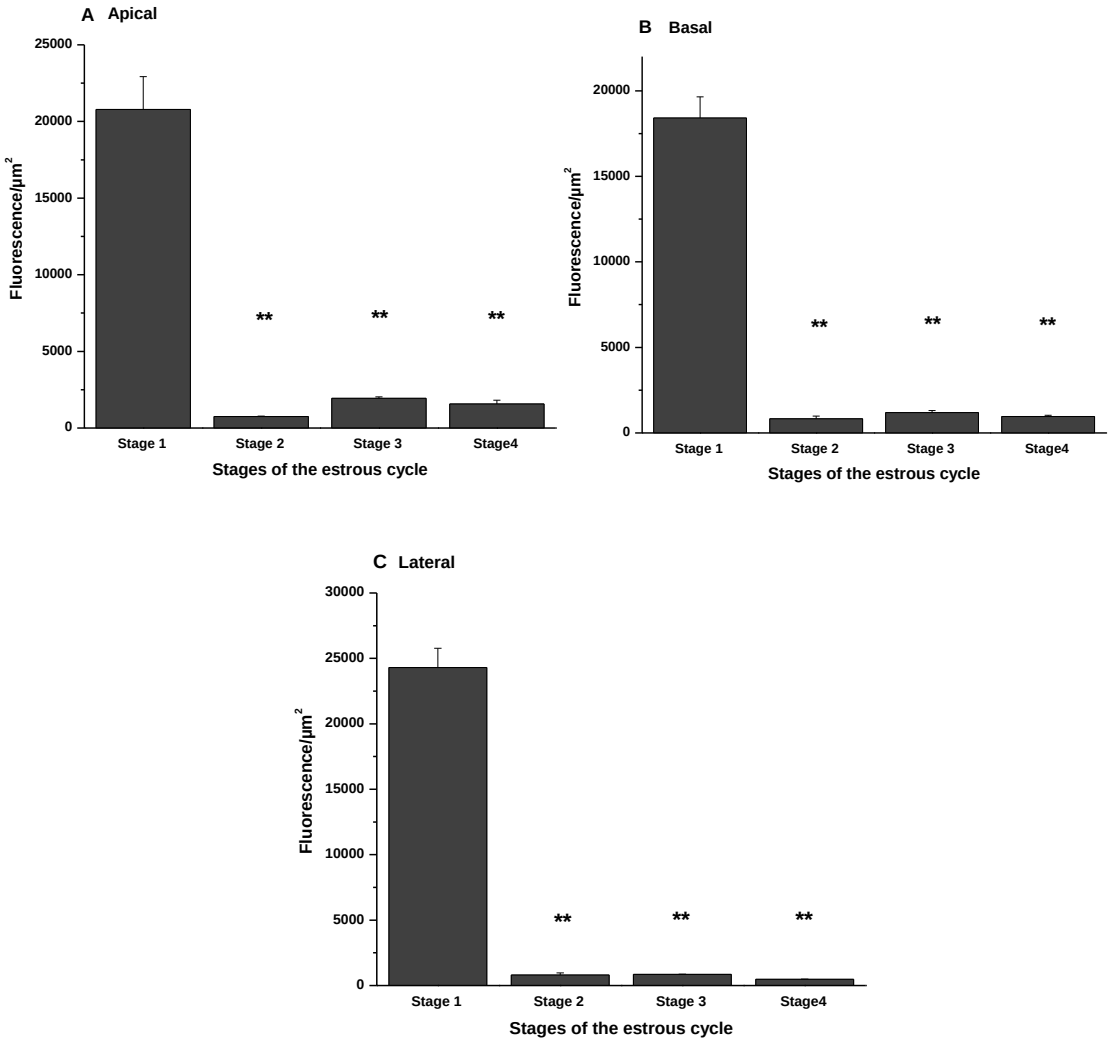

Fig 4.42 Abundance of TRPC6 in permeabilized bovine isthmus epithelium throughout the estrous cycle in apical (4.42, A), basal (4.42, B) and the lateral (4.42, C) side of the tissue. On the apical, basal and lateral side of the tissue, abundance of TRPC6 was extremely higher at stage 1 compared to stage2, 3 and 4 of the estrous cycle. All data are expressed as a mean of 3 replicates ± 1 standard deviation. (* = $p<0.05$; ** = $p<0.01$; *** = $p<0.001$).

4.1.2 Localization of TRPC1 and TRPC6 in bovine uterus throughout the estrous cycle

Localization and abundance of TRPC1 and TRPC6 channels in bovine uterine epithelial tissue throughout the estrous cycle was studied using immunohistochemistry and confocal microscopy techniques.

4.1.2.1 Localization of TRPC1 and TRPC6 in non-permeabilized bovine uterus throughout the estrous cycle

On the apical side of the non-permeabilized bovine uterine epithelial tissue, abundance of TRPC1 channel was lower at stage 2 and 4 by 0.42 ($p= 0.009$) and 0.73 ($p= 0.01$) fold respectively compared to stage 1. However, abundance of TRPC1 on the apical side of the tissue at stage 3 was slightly increased, by 1.37 fold, ($p= 0.009$) relative to stage 1 of the estrous cycle (Fig 4.44, A). On the basal side of the tissue, abundance of TRPC1 channel at stage 2 was decreased by 0.55 fold ($p= 0.01$) compared to stage 1. However, no significant difference was observed in abundance of the TRPC1 on the basal side of the tissue at stage 3 ($p= 0.06$) and 4 ($p= 0.9$) relative to stage 1 of the estrous cycle (Fig 4.44, B). On the lateral side of the non-permeabilized bovine uterine epithelial tissue, abundance of TRPC1 was decreased by 0.61fold ($p= 0.02$) at stage 2 compared to that of stage 1. However, abundance of TRPC1 on the lateral side of the tissue at stage 3 was increased by 1.53 fold ($p= 0.009$) relative to stage 1. Abundance of TRPC1 on the lateral side of the tissue at stage 4 ($p= 0.1$) of the estrous cycle was not significantly different to that of stage 1 (Fig 4.44, C).

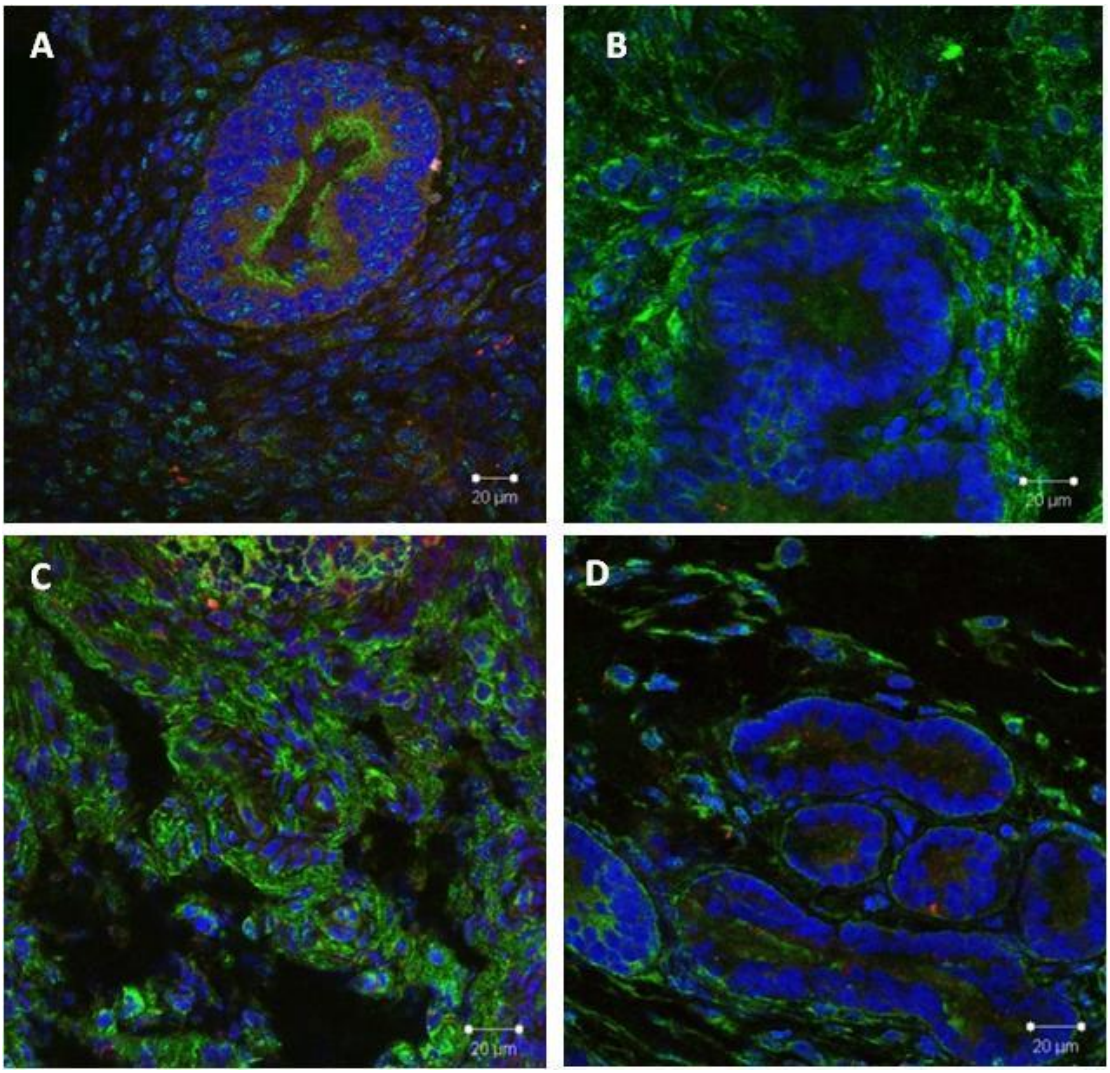

Fig 4.43 Localization of TRPC1 and TRPC6 in non-permeabilized bovine uterine epithelial tissue at stage 1 (4.43, A), stage 2 (4.43, B), stage 3 (4.43, C) and stage 4 (4.43, D) of the estrous cycle. Nuclei are labelled with DAPI (Blue), TRPC1 with Alexa Four 647 FITC conjugated (Red) and TRPC6 with Alexa Flour 488 (Green).

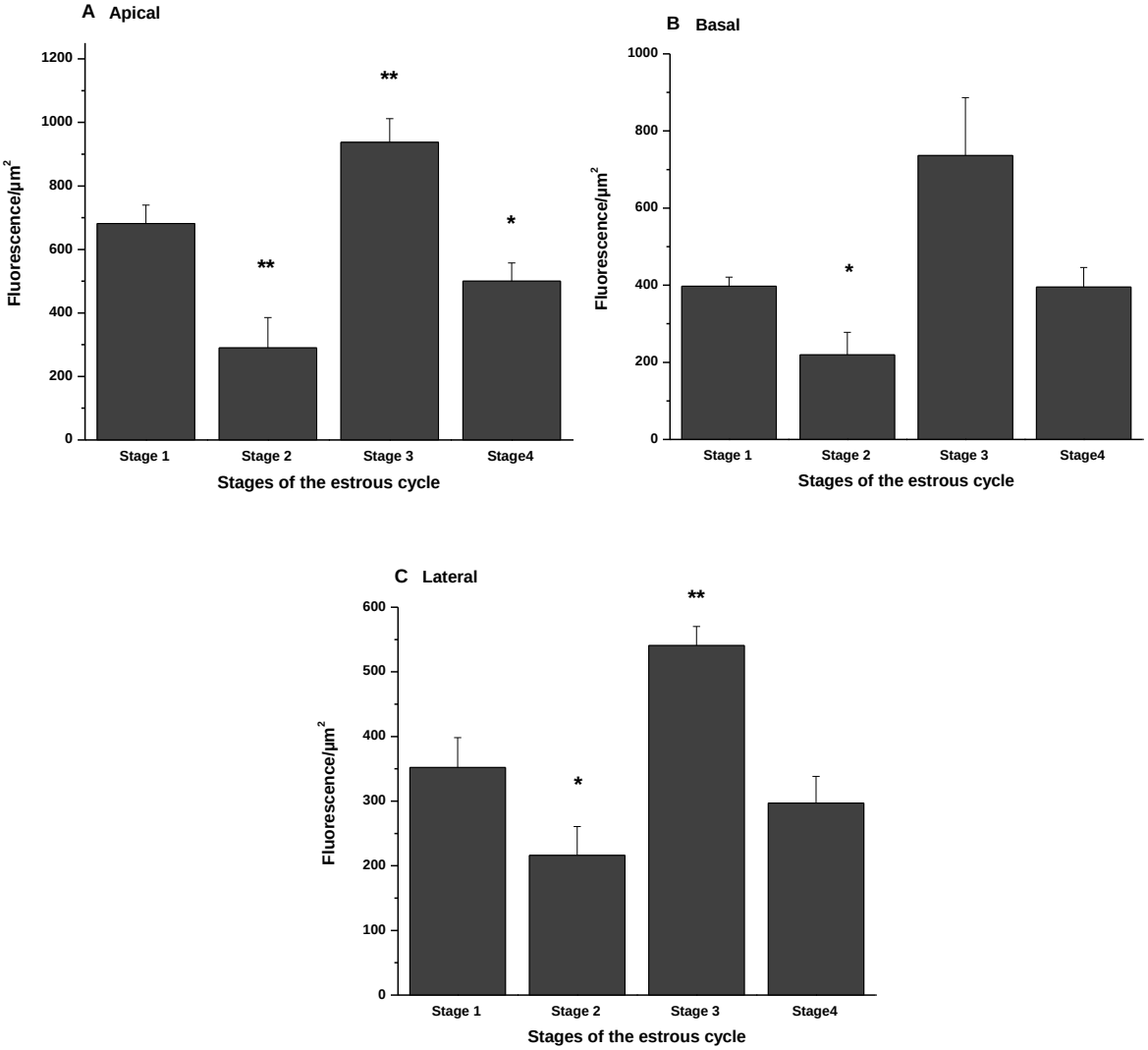

Fig 4.44 Abundance of TRPC1 in non-permeabilized bovine uterine epithelium throughout the estrous cycle in apical (4.44, A), basal (4.44, B) and the lateral (4.44, C) side of the tissue. On the apical side of the non-permeabilized bovine uterine tissue, abundance of TRPC1 was lower at stage 2 and 4 compared to that of the stage 1. However, abundance of TRPC1 at stage 3 was higher than that of the stage 1. On the basal side of the tissue, abundance of TRPC1 at stage 2 was lower than that of the stage 1. However, no significant difference in abundance of TRPC1 at stage 3 and 4 was observed compared to the stage 1 of the estrous cycle. On the lateral side of the tissue, abundance of TRPC1 was lower at stage 2 and higher at stage 3 compared to the stage 1 of the estrous cycle. No significant difference was observed in abundance of TRPC1 at stage 4 relative to stage 1 of the estrous cycle on the lateral side of the tissue. All data are expressed as a mean of 3 replicates ± 1 standard deviation. (* = $p<0.05$; ** = $p<0.01$; *** = $p<0.001$).

Abundance of TRPC6 channel on the apical side of the non-permeabilized bovine uterine epithelial tissue was increased at stage 2, 3 by 1.3 (p= 0.02), 2.99 (p= 0.04) fold respectively compared to stage 1. However, abundance of TRPC6 at stage 4 (p= 0.09) was equal to that of stage 1(Fig 4.45, A). On the basal side of the non-permeabilized bovine uterine epithelium, abundance of TRPC6 channel was increased by 2.41 fold (p= 0.01) at stage 2 compared to that of stage 1. However, abundance of TRPC6 on the basal side of the tissue at stage 3 (p= 0.07) and 4 (p= 0.5) of the estrous cycle was not significantly different to that of stage 1 (Fig 4.45, B). On the lateral side of the non-permeabilized bovine uterine epithelium, abundance of TRPC6 at stage 2 was higher than that of stage 1 by 1.49 (p= 0.02). However, abundance of TRPC6 on the lateral side of the tissue at stage 3 and 4 was not significantly different to that of stage 1 (Fig 4.45, C).

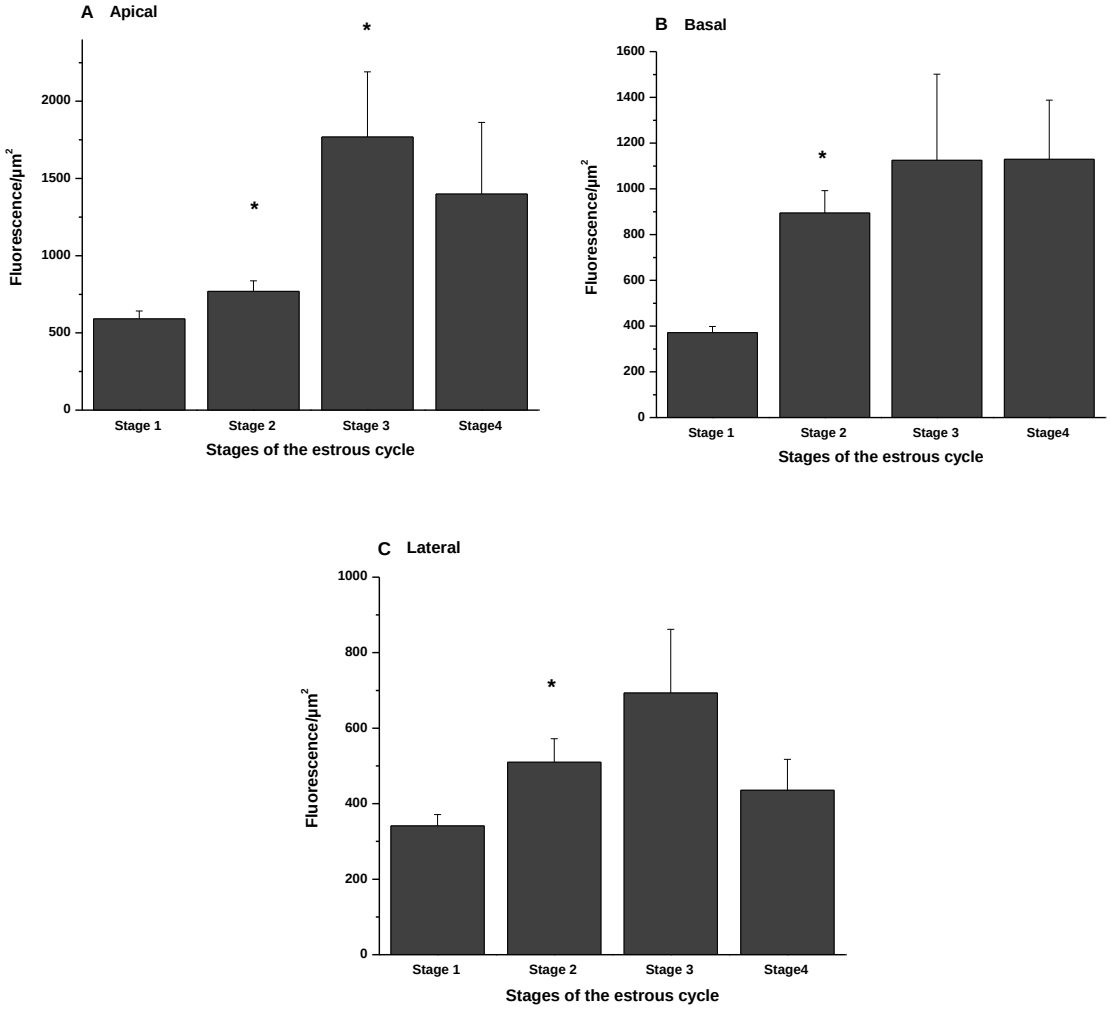

Fig 4.45 Abundance of TRPC6 in non-permeabilized bovine uterine epithelium throughout the estrous cycle in apical (4.45, A), basal (4.45, B) and the lateral (4.45, C) side of the tissue. On the apical side of the non-permeabilized bovine uterine epithelial tissue abundance of was higher at stage 2 and 3 compared of that of the stage 1. However, abundance of TRPC6 at stage 4 was not significantly different to that of the stage 1. On the basal and lateral side of the tissue, abundance of TRPC6 was higher at stage 2 compared to stage 1. However, on both basal and lateral side abundance of TRPC6 at stage 3 and 4 was not significantly different to that of the stage. All data are expressed as a mean of 3 replicates ± 1 standard deviation. (* = $p<0.05$; ** = $p<0.01$; *** = $p<0.001$).

4.1.2.2 Localization and abundance of TRPC1 and TRPC6 in permeabilized bovine uterus throughout the estrous cycle

On the apical side of the permeabilized bovine uterine epithelial tissue, abundance of the TRPC1 channel was increased at stage 2 and 3 by 1.82 (p= 0.02) and 3.21 (p= 5.46 x 10^{-5}) fold respectively compared to that of the stage 1 However, abundance of TRPC1 at stage 4 (p= 0.2) was not significantly different to that of the stage 1 of the estrous cycle(Fig 4.47, A). On the basal side of the epithelium, there was no significant difference in abundance of TRPC1 at stage 2 (p= 0.1) and 4 (p= 0.4) compared to stage 1. However, at stage 3, abundance of TRPC1 was increased by 1.75 fold (p= 0.005) relative to stage 1 of the estrous cycle (Fig 4.47, B). On the lateral side of the tissue at stage 2 (p= 0.1) and 4 (p= 0.5) abundance of TRPC1 was not significantly different to that of the stage1. At stage 3, abundance of TRPC1 on the lateral side of the tissue was increased by 1.33 fold (p= 0.02) relative to stage 1 of the estrous cycle(Fig 4.47, C).

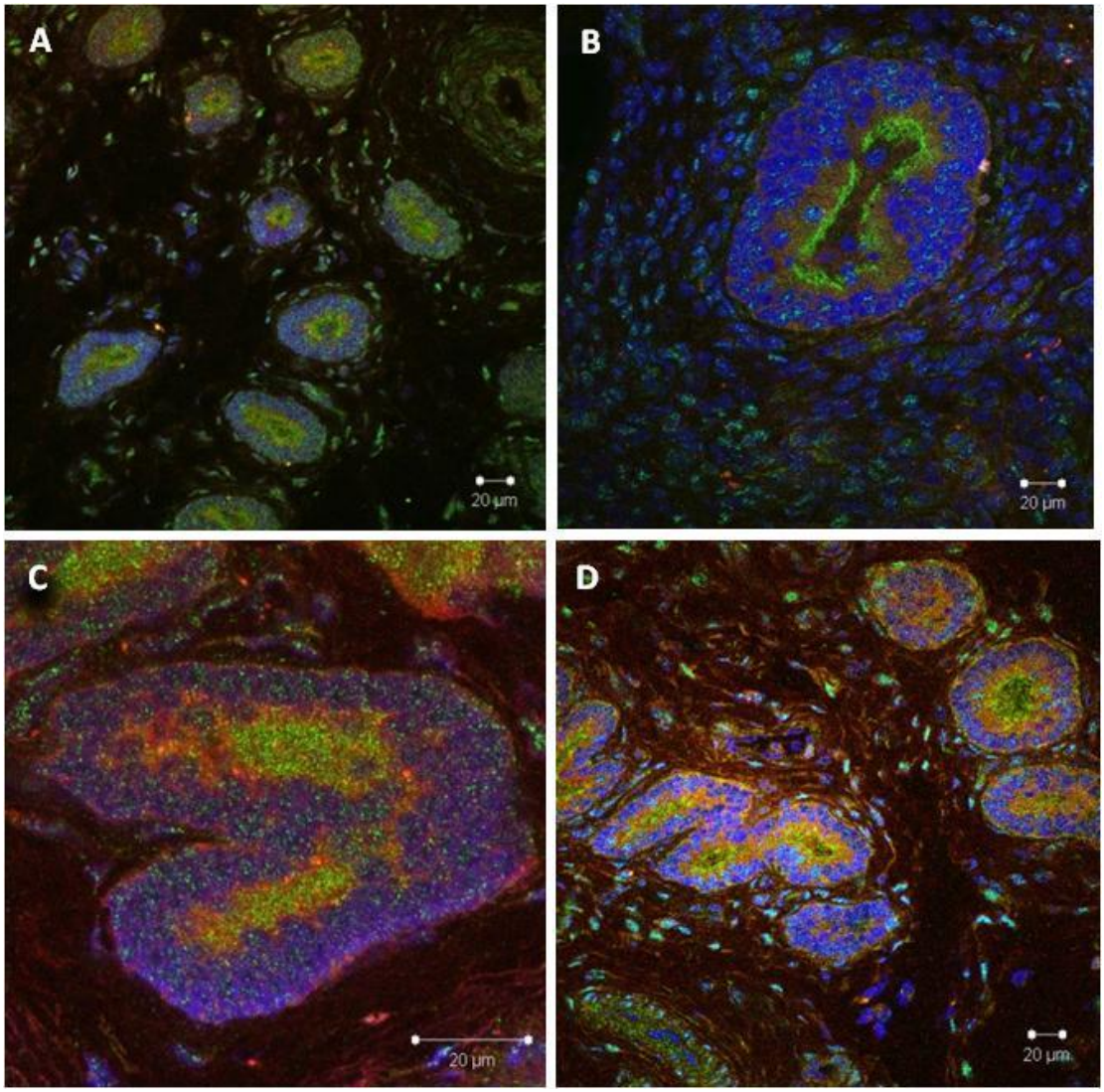

Fig 4.46 Localization of TRPC1 and TRPC6 in permeabilized bovine uterine epithelial tissue at stage 1 (4.43, A), stage 2 (4.43, B), stage 3 (4.43, C) and stage 4 (4.43, D) of the estrous cycle. Nuclei are labelled with DAPI (Blue), TRPC1 with Alexa Four 647 FITC conjugated (Red) and TRPC6 with Alexa Flour 488 (Green).

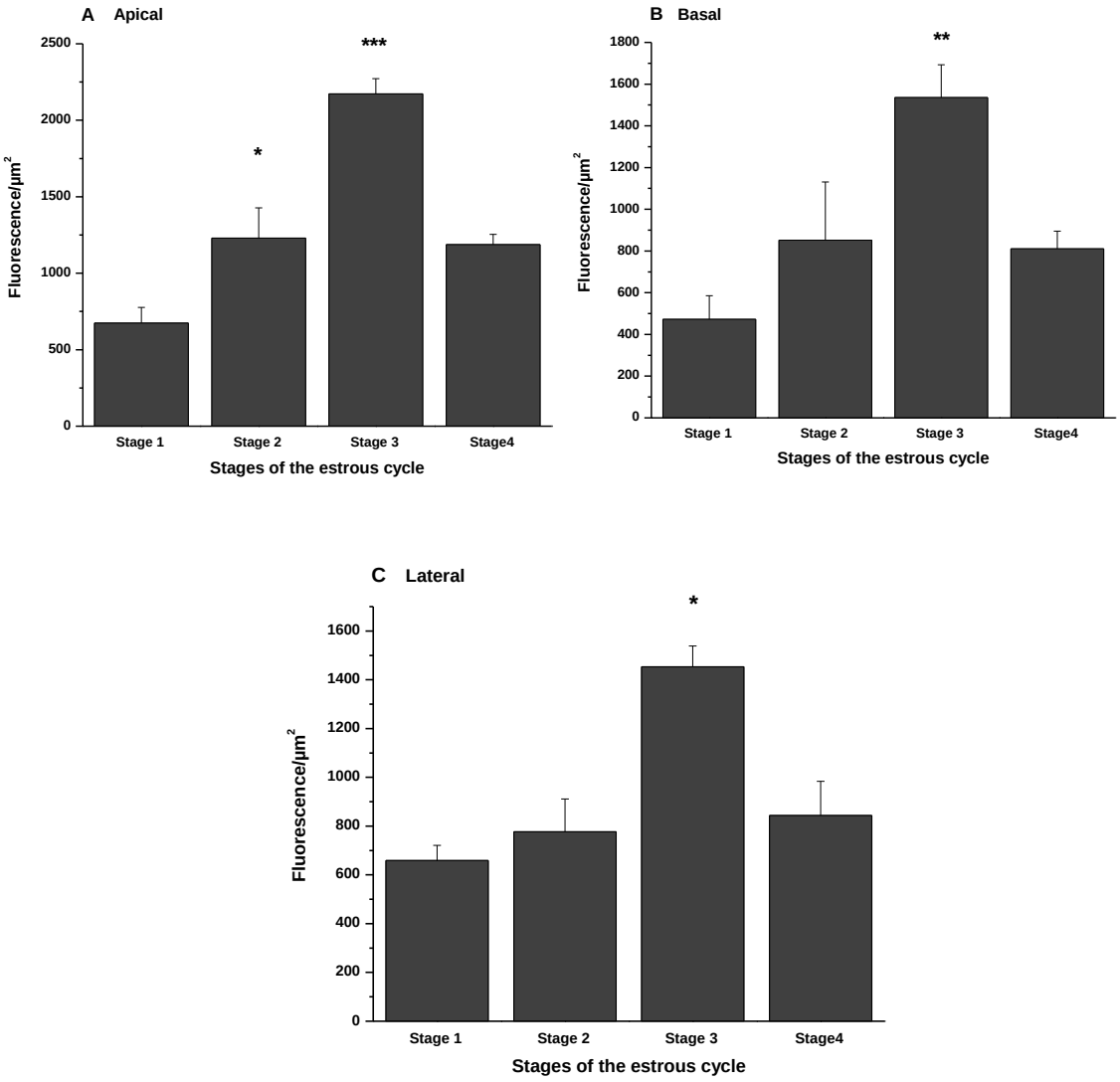

Fig 4.47 Abundance of TRPC1 in permeabilized bovine uterine epithelium throughout the estrous cycle in apical (4.47, A), basal (4.47, B) and the lateral (4.47, C) side of the tissue. On the apical side of the tissue, abundance of TRPC1 was higher at both stage 2 and 3 compared to stage 1 of the estrous cycle. On the basal and lateral side of the tissue, there was not any significant difference in abundance of TRPC1 at stage 2 and 4 compared to the stage 1 of the estrous cycle. The same was the cause in permeabilized bovine uterine epithelium on the apical, basal and lateral side of the tissue. However, at stage 3 abundance of TRPC1 on both basal and lateral side of the tissue was higher than that of the stage 1. All data are expressed as a mean of 3 replicates ± 1 standard deviation. (* = $p<0.05$; ** = $p<0.01$; *** = $p<0.001$).

Abundance of TRPC6 channel on the apical side of the permeabilized bovine uterine epithelial tissue was increased at stage 2 and 3 of the estrous cycle by 3.27 (p= 0.002) and 2.77 (p= 0.01) fold compared to stage 1. There was no significant difference in abundance of TRPC6 on the apical side of the tissue at stage 4 (p= 0.2) compared to stage 1(Fig 4.48, A). On the basal side of the permeabilized uterine epithelium, abundance of TRPC6 channel at stage 2 (p= 0.1) and 4 (p= 0.4) was not significantly different to that of stage 1. However, abundance of TRPC6 on the basal side of the tissue at stage 3 was 1.75 fold (p= 0.005) higher than that of stage 1 (Fig 4.48, B). On the lateral side of the permeabilized bovine uterine epithelial tissue,abundance of TRPC6 at stage 2 and 4 was not significantly different compared to that of stage 1. However, at TRPC6 was more abundant by 1.33 fold (p= 0.02) on the lateral side of the tissue at stage 3 compared to stage 1 of the estrous cycle (Fig 4.48, C).

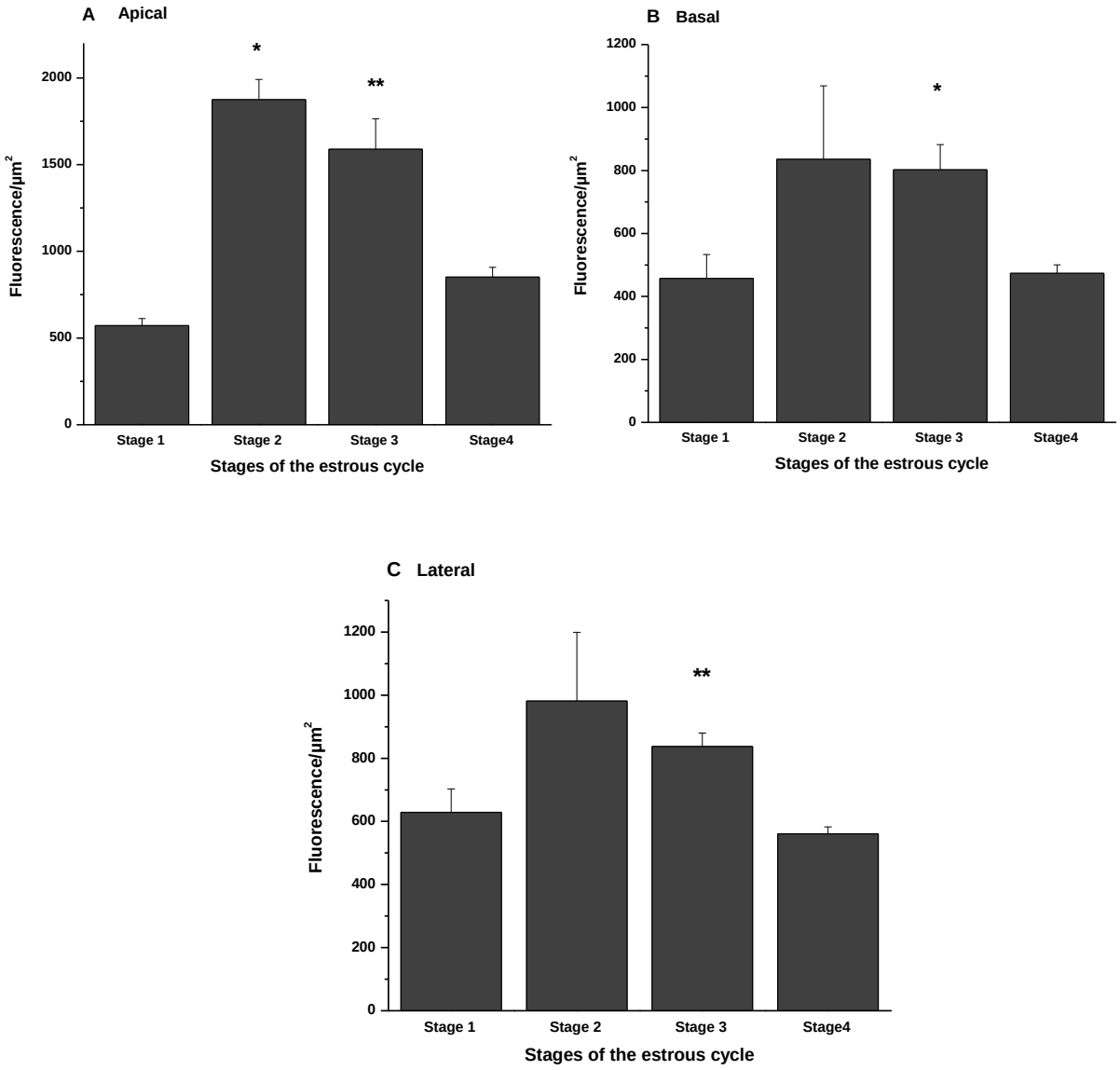

Fig 4.48 Abundance of TRPC6 in permeabilized bovine uterine epithelium throughout the estrous cycle in apical (4.48, A), basal (4.48, B) and the lateral (4.48, C) side of the tissue. On the apical side of the tissue, abundance of TRPC6 at stage 2 and 3 was higher than that of the stage 1. However, abundance of TRPC6 at stage 4 was not significantly different to that of the stage 1. On both the basal and lateral side of the tissue, abundance of TRPC6 at stage 2 and 4 was equal to that of stage 1. However, at stage 3 TRPC6 was more abundant on both basal and lateral side compared to the stage 1 of the estrous cycle. All data are expressed as a mean of 3 replicates ± 1 standard deviation. (* = $p<0.05$; ** = $p<0.01$; *** = $p<0.001$).

4.1.3 Effect of sex hormones on the abundance of TRPC1 and TRPC6 in cultured bovine oviduct epithelial cells throughout the estrous cycle

It was shown in section 3.4 that sex hormones altered the gene expression of TRPCs in Bovine Oviduct Cultured Cells. Immunocytochemistry and confocal microscopy techniques were used to determine if sex hormones could also affect the abundance of TRPC1 and TRPC6 in BOEC.

4.1.3.1 Effect of sex hormones on the distribution of TRPC1 and TRPC6 in non-permeabilized cultured bovine oviduct epithelial cells throughout the estrous cycle

In non-permeabilized Bovine Oviduct Epithelial Cells (BOEC) at stage 1 of the estrous cycle, abundance of TRPC1 was not affected by Est (p= 0.6), FSH/LH (p= 0.9), Prog (p= 0.3) and a combination of Est, Prog, FSH and LH (p= 02) compared to that of the control group. At stage 2, Est (p= 0.2) and FSH/LH (p= 0.5) did not induce any changes in abundance of TRPC1 in non-permeabilized BOEC. However, the Prog (p= 0.004) mixture of Est, Prog, FSH and LH increased the abundance of TRPC1 by 1.95 (p= 0.004) and 1.24 (p= 0.04) fold respectively compared to the control group. At stage 3 of the estrous cycle, abundance of TRPC1 in non-permeabilized BOEC was decreased by 0.65 (p= 0.01) and 0.75 (p= 0.003) fold in cells treated with Est and FSH/LH respectively relative to that of the control group. Prog (p= 0.9) did not alter the abundance of TRPC1 channel in non-permeabilized BOEC compared to the untreated BOEC. However, a combination of Est, Prog, FSH and LH increased the abundance of TRPC1 in non-permeabilized BOEC by 1.4 fold (p= 0.0005) relative to that of the control group. In non-permeabilized BOEC at stage 4 of the estrous cycle, the abundance of TRPC1 channel was not affected byEst (p= 0.3), Prog (p= 0.1), FSH/LH (p= 0.4) and the mixture of all these hormones (p= 0.6) compared to the untreated BOEC(Fig 4. 49, A).

Sex hormones altered the abundance of TRPC6 channel in the non-permeabilized BOEC. At stage 1 of the estrous cycle, Est decrease the abundance of TRPC6 by 0.38 fold (p= 0.002) relative to the untreated group. Furthermore, a 0.6 fold (p= 0.02) decreased in abundance of TRPC6 was observed in the non-permeabilized BOEC treated with FSH and LH. Abundance of TRPC6 in Prog-treated (p= 0.2) non-permeabilized BOEC was not

significantly different compared to the control group. There was no significant difference in abundance of TRPC6 in non-permeabilized BOEC treated with the mixture of Est, Prog, FSH and LH (p= 0.1) relative to the untreated group. At stage 2 of the estrous cycle, Est increased the abundance of TRPC6 channels by 3 fold (p= 0.003) in the non-permeabilized BOEC compared to the untreated group. In FSH/LH-treated BOEC a 1.8 fold (p= 0.01) increase was observed in abundance of TRPC6 channel relative to the control. Prog also increased the abundance of TRPC6 channel by 4.3 fold ($p= 3.8 \times 10^{-5}$) compared to the untreated BOEC. However, in BOEC treated with the mixture of Est, Prog, FSH and LH (p= 0.7) abundance of TRPC6 channels was not significantly different compared to the control group. At stage 3 of the estrous cycle, Est decreased the abundance of TRPC6 in non-permeabilized BOEC by 0.44 fold (p= 0.0006) relative to the control group. Abundance of TRPC6 in non-permeabilized BOEC treated with FSH/LH (p= 0.2) and Prog (p= 0.05) was not significantly different compared to the untreated cells. However, a mixture of Est, Prog, FSH and LH slightly decreased TRPC6 abundance by 0.53 fold (p= 0.001) compared to the untreated group. In non-permeabilized BOEC at stage 4 of the estrous cycle, abundance of TRPC6 channel was decreased by 0.70 fold (p= 0.04) in response to Est compared to the control group . In FSH/LH-treated BOEC (p= 0.1) the abundance of TRPC6 was not significantly different relative to the untreated BOEC. Prog induced a 0.5 fold (p= 0.007) decrease in abundance of TRPC6 channel in non-permeabilized BOEC at stage 4 of the estrous cycle compared to the untreated BOEC. Furthermore, mixture of Est, Prog, FSH and LH reduced the abundance of TRPC6 channels by 0.66 fold (p= 0.04) compared to the control group (Fig 4.49, B).

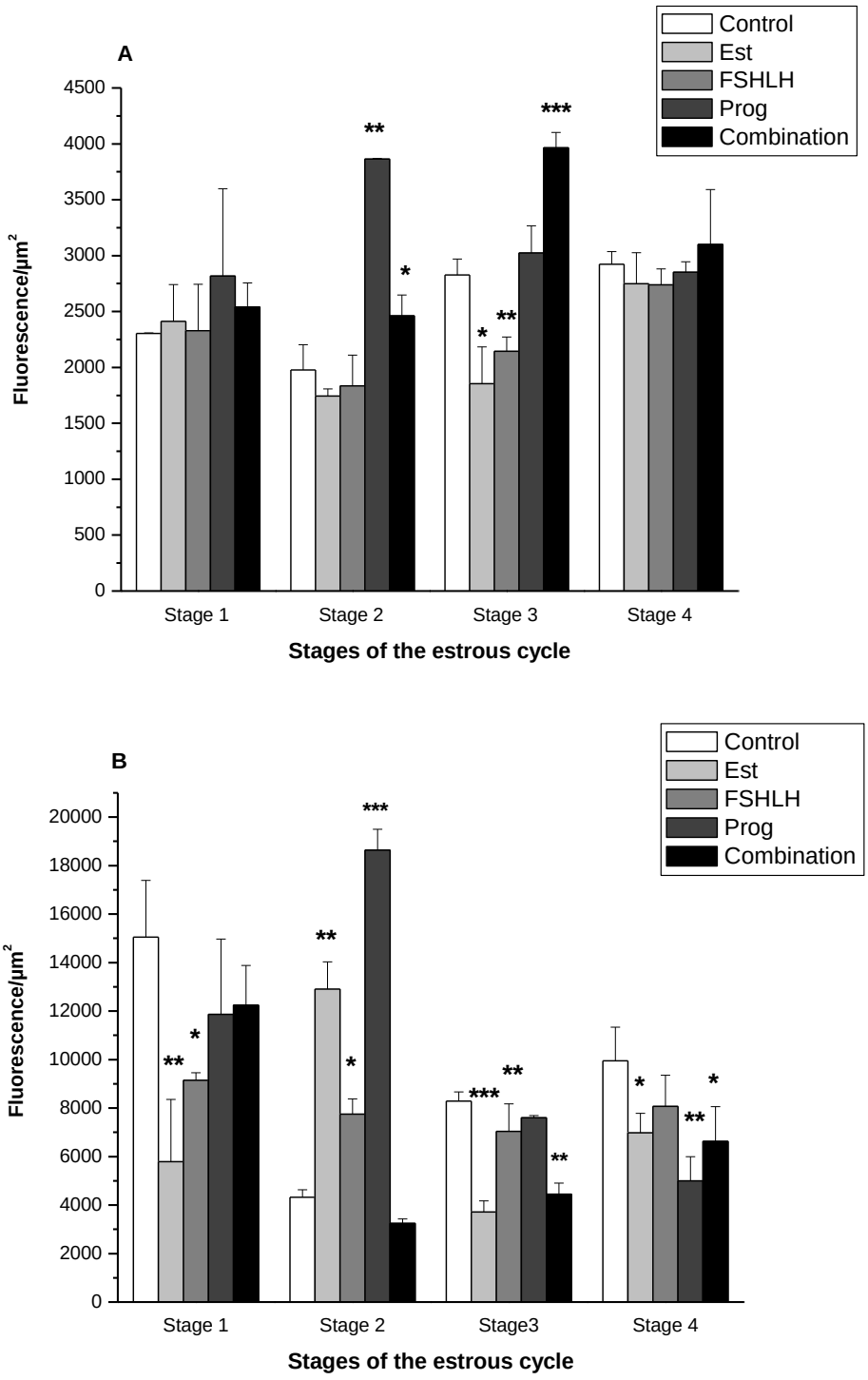

Fig 4.49 Effect of sex hormones on abundance of TRPC1 and TRPC6 channels in non-permeabilized Bovine Oviduct Cultured Cells (BOEC). Abundance of both TRPC1 (4.49, A) and TRPC6 (4.49, B) channels was altered in BOEC treated with sex hormones throughout the estrous cycle. All data are expressed as a mean of 3 replicates ± 1 standard deviation. (* = $p<0.05$; ** = $p<0.01$; *** = $p<0.001$).

4.1.3.2 Effect of sex hormones on the distribution of TRPC1 and TRPC6 in permeabilized cultured bovine oviduct epithelial cells throughout the estrous cycle

In permeabilized Bovine Oviduct Epithelial Cultured Cells (BOEC) abundance of TRPC1 was altered by the sex hormones throughout the estrous cycle. At stage 1 of the estrous cycle, Est reduced the abundance of TRPC1 channels by 0.1 fold ($p= 5.04 \times 10^{-5}$) compared to the untreated group. However, FSH/LH induced a 1.89 fold (p= 0.01) increase in abundance of TRPC1 relative to that of the control group. Furthermore, in Prog-treated BOEC, abundance of TRPC1 channels was increased by 1.4 fold (p= 0.004) compared to the untreated group. A mixture of Est, Prog, FSH and LH (p= 0.5) did not induce any significant changes in abundance of TRPC1 channels in permeabilized BOEC at stage 1 of the estrous cycle. At stage 2, no significant effect was observed in abundance of TRPC1 in BOEC treated with Est (p= 0.1) compared to the control group. However, FSH/LH and a combination of Est, FSH,LH and Prog reduced the abundance of TRPC1 in permeabilized BOEC by 0.82 (p= 0.02) and 0.81 (p= 0.008) fold respectively relative to the untreated BOEC. In BOEC treated with Prog, abundance of TRPC1 was slightly increased by 1.13 fold (p= 0.04) compared to the control group. In permeabilized BOEC at stage 3 of the estrous cycle, abundance of TRPC1 channel was not significantly affected in Est (p= 0.2), FSH/LH (p= 0.1) and Prog (p= 0.3) treated BOEC compared to the untreated group. However, a mixture of Est, FSH, LH and Prog decreased the abundance of TRPC1 by 0.66 fold (p= 0.01) in permeabilized BOEC compared to the control group. At stage 4 of the estrous cycle, abundance of TRPC1 channel in Est (p= 0.09) and FSH/LH (p= 0.1) treated BOEC was not significantly different relative to the untreated BOEC. However, Prog increased abundance of TRPC1 by 1.24 fold (p= 0.03) relative to the untreated BOEC. Furthermore, a mixture of Est, FSH, LH and Prog increased the abundance of TRPC1 channel by 1.4 fold (p= 0.008) in permeabilized BOEC at stage 4 of the estrous cycle compared to the control group (Fig 4.50, A).

The abundance of TRPC6 in permeabilized BOEC at stage 1 of the estrous cycle was reduced by 0.04 fold (p= 0.008) compared to the control group under the effect of Est. However, FSH/LH (p= 0.9) and Prog (p= 0.4) did not induce any significant changes in abundance of TRPC6 relative to the untreated group.

A mixture of Est, FSH, LH and Prog decreased the abundance of TRPC6 channel by 0.6 fold (p= 0.02) compared to the control group. At stage 2 of the estrous cycle, Est reduced the abundance of TRPC6 channel by 0.69 fold (p= 0.01) relative to the control BOEC. In contrast, FSH and LH increased the abundance of TRPC6 by 1.38 fold (p= 0.009) compared to the untreated group. Prog significantly reduced the abundance of TRPC by 0.9 fold (p= 0.04) relative to the untreated group. A combination of Est, Prog, FSH and LH reduced the abundance of TRPC6 channel by 0.13 fold (p= 0.0008) compared to the control group. At stage 3 of the estrous cycle in permeabilized BOEC, Est (p= 0.9) did not induce a significant effect on abundance of TRPC6 channel compared to the untreated BOEC. However, both FSH/LH (p= 0.0003) and Prog (p= 0.002) reduced the abundance of TRPC6 channel by 0.56 and 0.77 fold respectively compared to the control group. Furthermore, a combination of Est, FSH, LH and Prog decreased the abundance of TRPC6 channel by 0.63 fold (p= 0.005) relative to that of the control group. At stage 4 of the estrous cycle, Est (p= 0.05) and FSH/LH increased the abundance of TRPC6 in permeabilized BOEC slightly by 1.31 fold (p= 0.04) compared to the control group. However, Prog induced a decrease by 0.56 fold (p= 0.003) in abundance of TRPC6 compared to the control group. Furthermore, a combination of Est, FSH, LH and Prog decreased the abundance of TRPC6 channel by 0.79 fold (p= 0.04) in permeabilized compared to the untreated BOEC (Fig 4.50, B).

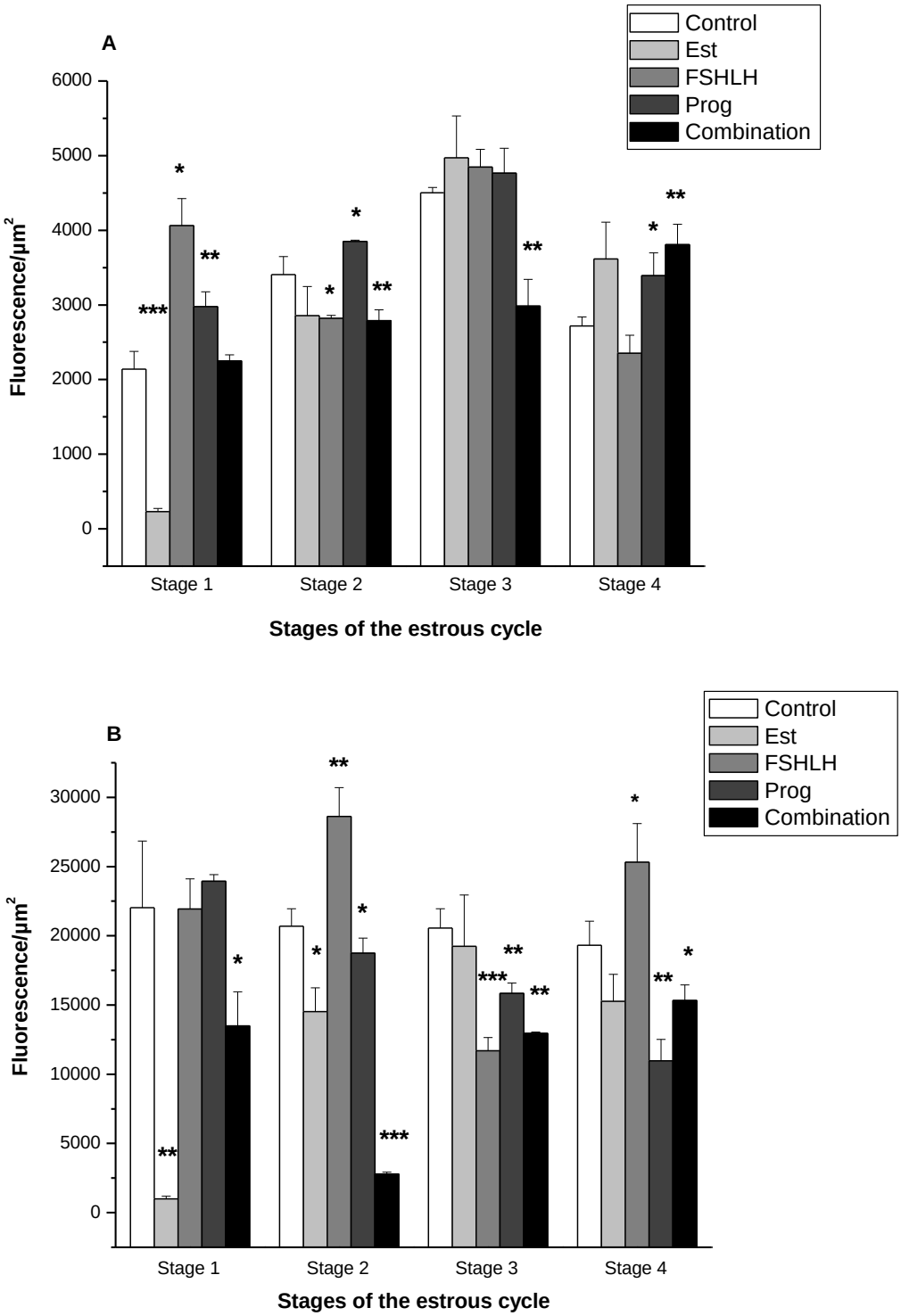

Fig 4.50 Effect of sex hormones on abundance of TRPC1 and TRPC6 channels in permeabilized Bovine Oviduct Epithelial Cultured Cells (BOEC). Abundance of both TRPC1 (4.49, A) and TRPC6 (4.49, B) channels was altered in BOEC treated with sex hormones. All data are expressed as a mean of 3 replicates ± 1 standard deviation. (* = $p<0.05$; ** = $p<0.01$; *** = $p<0.001$).

4.2 Effect of sex hormones on protein expression of TRPC1 and TRPC6 in cultured bovine oviduct epithelial cells throughout the estrous cycle

It was shown in section 3.4 and 4.1.3 that sex hormones are involved in TRPC gene expression regulation, and in the pattern of abundance of TRPC1 and TRPC6 channels in Bovine Oviduct Epithelial Cultured Cells (BOEC). The effect of sex hormones on TRPC1 and TRPC6 protein expression was studied using the western blot technique. As the amount of protein loaded on to each gel was equal (35 μg), the protein expression level of TRPC1 and TRPC6 in BOEC with different treatments could be compared to each other and the control. In BOEC treated with Est, TRPC1 protein expression was lower at stages 1, 2 and 3 compared to the control (Fig 4.51, A and B). Protein expression of TRPC6 was strongly reduced in Est-treated BOEC at all stages of estrous cycle; more significantly at stage 3 and 4 compared to the untreated BOEC (Fig 4.51, A and B). In FSH/LH-treated BOEC, protein expression of TRPC1 was increased at stage 4 of the estrous cycle compared to the control group (Fig 4.51, A and C). In contrast, protein expression of TRPC6 was decreased at stage 1 and increased at stage 3 compared to the control group (Fig 4.51, A and C). In Prog-treated BOEC, protein expression of TRPC1 was slightly reduced at stage 3 compared to the untreated BOEC. However, this decrease was significantly greater than at stage 4 of the estrous cycle compared to the control BOEC (Fig 4.51, A and D). No significant difference was observed in TRPC6 protein expression in Prog-treated BOEC compared to the control group (Fig 4.51, A and D). Protein expression of TRPC1 at all 4 stages of the estrous cycle was significantly decreased in BOEC treated with the mixture of Est, FSH, LH and Prog (Fig 4.51, A and E). In contrast, protein expression of TRPC6 was slightly increased at stage 1 of the estrous cycle in BOEC treated with the mixture of Est, FSH, LH and Prog compared to that of the control BOEC (Fig 4.51, A and E).

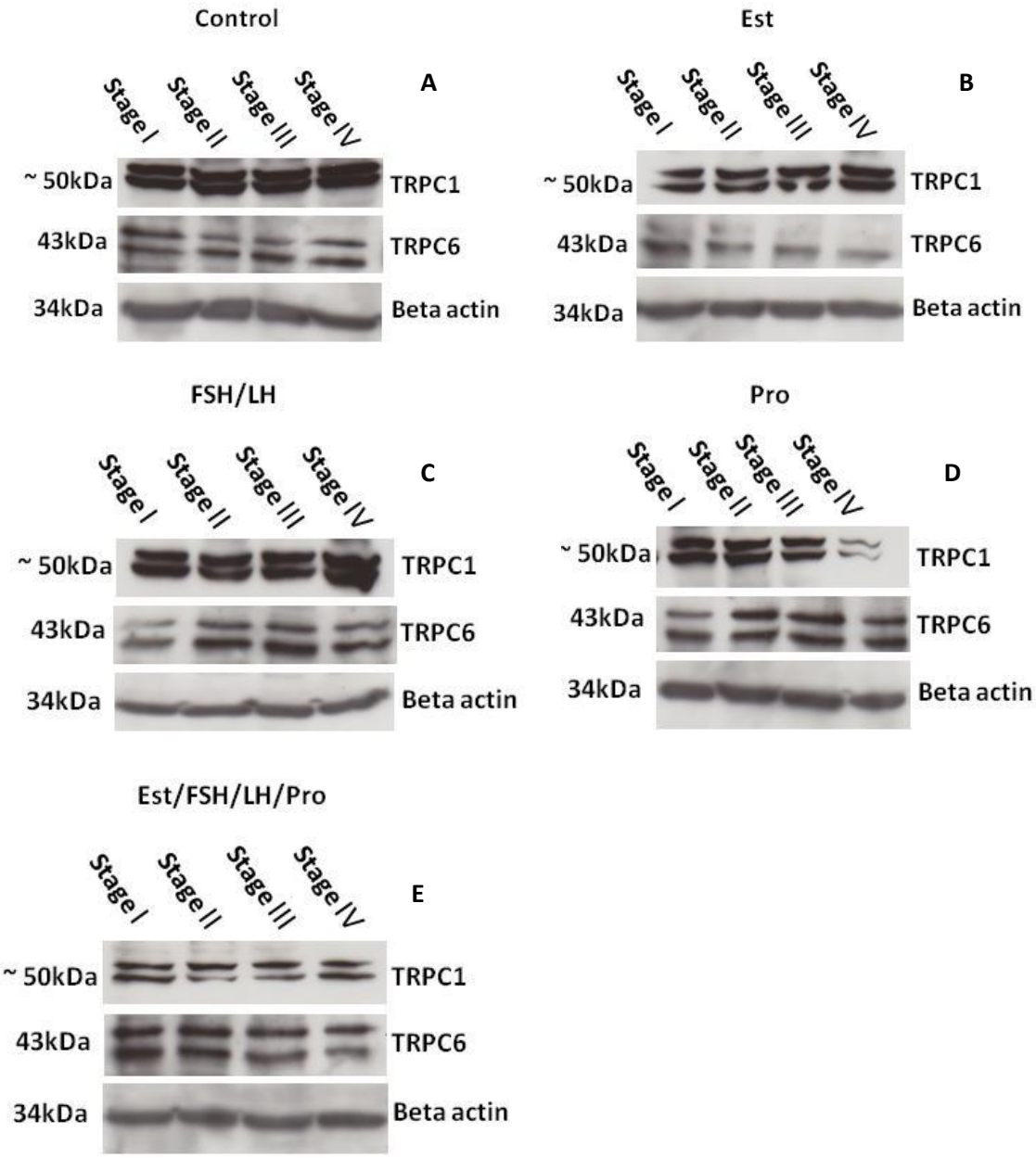

Fig 4.51 Effect of sex hormones on TRPC1 and TRPC6 protein expression in Bovine Oviduct Epithelial Cultured Cells (BOEC). Protein expression level of TRPC1 and TRPC6 was altered by Est (4.51, B), FSH and LH (4.51, C), Prog (4.51, D) and the mixture of Est, FSH, LH and Prog (4.51, E) individually and combined compared to the untreated BOEC (4.51, A). n=1

4.3 Discussion

The data presented in this chapter show that TRPC1 and TRPC6 are localized on the apical, basal and the lateral sides of the cells of the bovine oviduct and uterine epithelial tissue. Generally, TRPC6 is more abundant on the oviduct epithelium compared to TRPC1. In bovine oviduct epithelial tissue abundance of both TRPC1 and 6 on the apical, basal and lateral sides in the infundibulum, ampulla and isthmus regions of the oviduct changes throughout the estrous cycle. These changes in abundance of TRPC1 and TRPC6 follow the same pattern throughout the estrous cycle, however, some differences were observed in the pattern of TRPC1 and 6 abundance on the apical, basal and lateral side of the tissue in the oviduct. For example, changes in membrane abundance of TRPC6 on the apical and basal sides of the infundibulum, ampulla and isthmus epithelium at stage 1 of the estrous cycle were different to that of the lateral side. The difference in abundance of TRPC1 on the apical, basal and the lateral sides of the epithelium might be due to its physiological role in association with STIM and the complex of STIM and Orai proteins (Hong et al., 2011). STIM1 regulates TRPC1, 3, 4, 5 and 6 (Yuan *et al.*, 2007). However, TRPC1, 4 and 5 are gated directly by STIM1 whereas, the regulatory effect of STIM1 on TRPC3 and TRPC6 is via the heteromultimerization of TRPC1-TRPC3 and TRPC4-TRPC6 (Yuan *et al.*, 2007). Therefore, TRPC channels are functional in STIM-dependent and STIM -independent mode indicating their role as Store-Operated Channels (SOC) and Receptor- Operated Channels (ROC). The functional mode of TRPC channels could determine their localization either on the membrane (apical, basal and lateral) or intracellularly.

Although TRPC6 was localized on all sides of the epithelial membrane, its abundance was highest on the apical membrane of both the oviduct and uterine epithelium throughout the estrous cycle. A similar pattern of TRPC6 distribution on both apical and basal membranes was described by Bandyopadhyay et al., (2005) in polarized Madin-Darby canine kidney cells (MDCK) and salivary gland epithelial cells (Bandyopadhyay et al., 2005).

Polarity is a key feature of epithelial tissues and intracellular calcium concentration plays a vital role in the maintenance of this (Schwab et al., 1997; Kimura et al., 2001). It has been clearly shown that TRPC1 is one of the key

players in determining the polarity of Madin–Darby canine kidney-focus epithelial cells (Fabian *et al.*, 2008). Furthermore, in polarized rat podocyte cells the TRPC6 channel was localized on the apical membrane and co-localized with Na^+-K^+-ATPase (NKA) in the basolateral membrane (Goel *et al.*, 2006). NKA is involved in maintaining the resting membrane potential (Lafaire & Schwarz, 1986), cellular ion transport, in particular across the epithelial cells (Sugi *et al.*, 2001), controlling cell volume (Kerr *et al.*, 1982) as well as being a signal transducer (Xie & Cai, 2003). Colocalization of TRPC6 with NKA in basolateral membrane of the rat podocytes suggests the presence of a similar functional unit in the bovine oviduct and uterine epithelial tissue (Goel *et al.*, 2006). It would therefore be interesting in future work to investigate if such an interaction occurs in female reproductive tissue.

Abundance of both TRPC1 and TRPC6 is variable from infundibulum to the isthmus end of the oviduct throughout the estrous cycle and this might indicate the involvement of these channels in various physiological functions of each of infundibulum (oocyte transport) (Talbot *et al.*, 1999), ampulla (fertilization) (Shalgi & Phillips, 1988) and isthmus (spermatozoa reservoir and early embryo transport) (Lefebvre *et al.*, 1995; Kölle *et al.*, 2009) throughout the estrous cycle.

Chapter 5

Physiological role of TRPC channels in calcium homeostasis of bovine oviduct epithelial cells

5.1 Functional role of Transient Receptor Potential (TRP) Channels in Bovine Oviduct Epithelial Cultured Cells (BOEC) throughout the estrous cycle

These experiments were carried out to discover the physiological role of TRPC channels in Bovine Oviduct Epithelial Cultured Cells (BOEC).

Fig 5.1 and 5.2 shows the data collected from experiments to discover whether uptake of calcium by BOEC varies throughout the oestrous cycle due to different expression level of TRPC channels at each stage of the cycle. BOEC of each stage of the estrous cycle were loaded with 10 μM Fura PE 3-AM in calcium free solution as described in section (2.21). Excess dye was removed and the basal intracellular calcium concentration of cells in calcium free solution was measured. Signal collected at 380 nm (F380) represents the amount of the free Fura PE 3-AM and signal collected at 340 nm (F340) emission represents the amount of Fura PE 3-AM bound to intracellular calcium. The ratio of F380/F340 gives the changes in intracellular calcium concentration. Addition of 1.5 mM calcium to the extracellular solution resulted in a significant increase in calcium influx into the cell and consequently an increase in intracellular calcium concentration (Fig 5.1). The data from Fig 5.1 and 5.2 indicate that the calcium influx in stage 2 BOEC was modestly higher by 1.14 fold ($p= 0.001$) relative to that of the stage 1. There is no significant difference in basal calcium uptake in stage 3 BOEC ($p= 0.1$) compared to the stage 1. However in stage 4 BOEC calcium influx was higher by 1.20 fold ($p= 0.0002$) compared to that of stage 1.

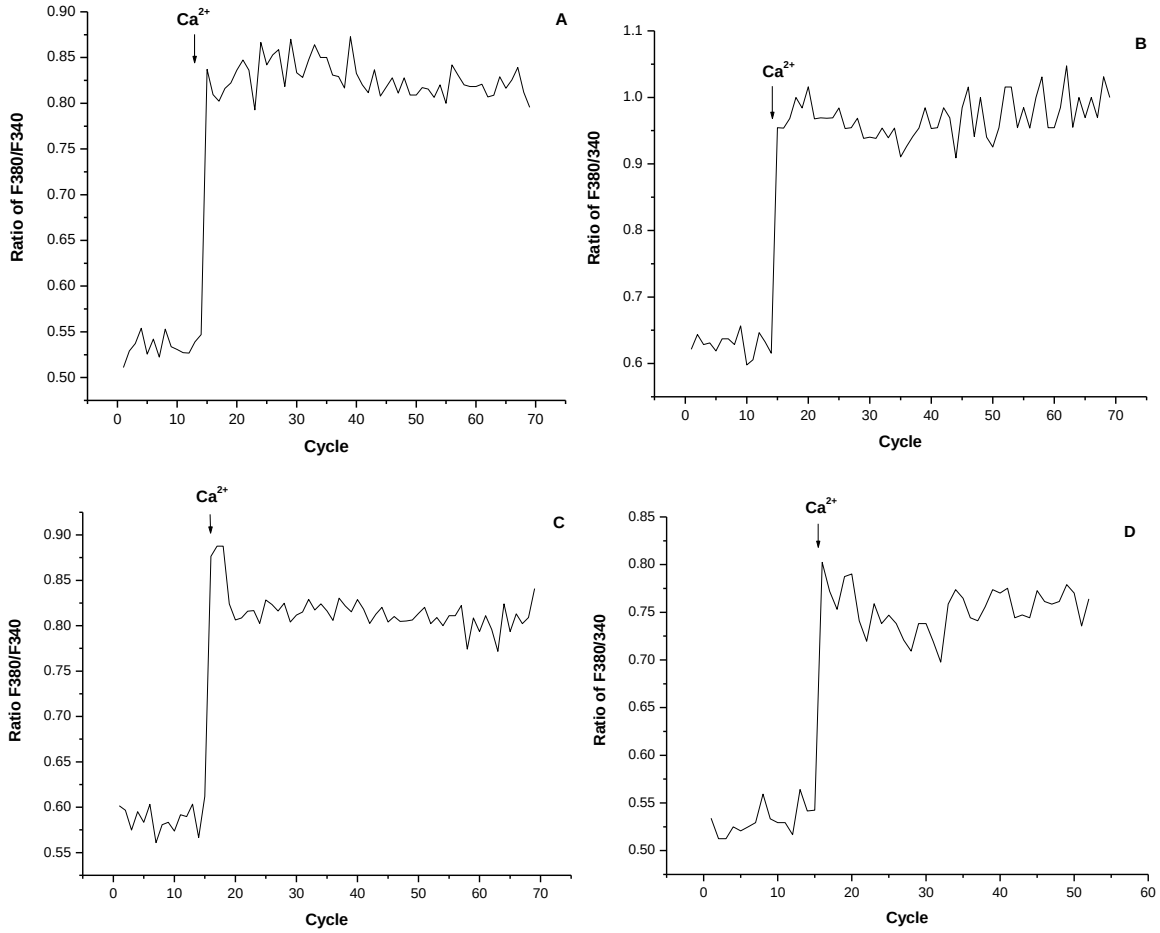

Fig 5.1 Basal calcium intake in Bovine Oviduct Epithelial Cultured Cells (BOEC) throughout the estrous cycle. This figure is an example of data collected from the plate reader. The figure indicates the changes in free Fura PE 3-AM verses Fura PE 3-AM bound to the intracellular calcium when free calcium extracellular was replaced with solution containing 1.5 mM calcium. Changee in basal calcium uptake was measured in BOEC at stage 1 (5.1, A), Stage 2 (5.1, B), Stage 3 (5.1, C) and Stage 4 (5.1, D) of the estrous cycle.

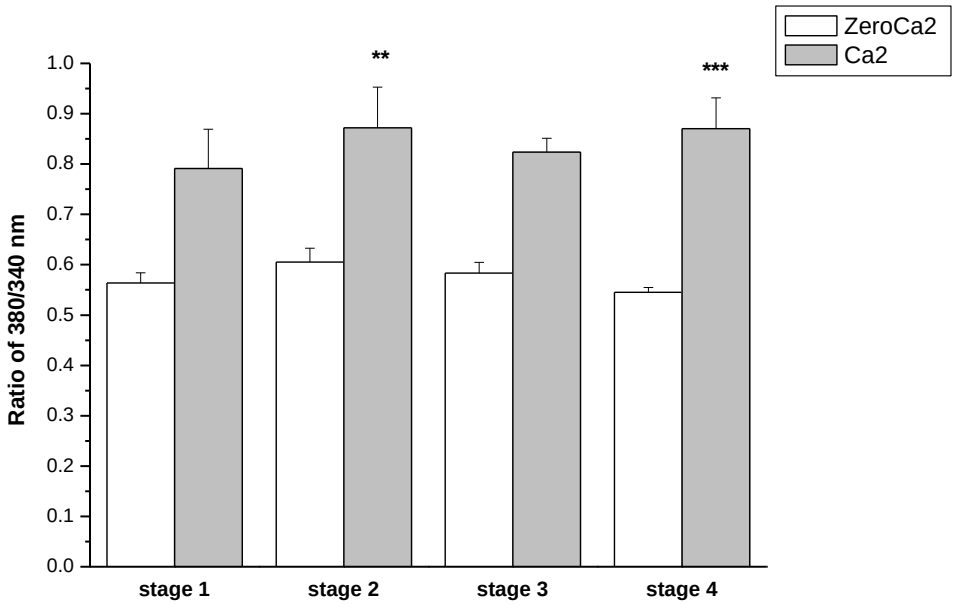

Fig 5.2 Basal calcium intake in Bovine Oviduct Epithelial Cultured Cells (BOEC) harvested from tracts at each stage of the oestrous cycle. This figure shows the mean of the data in Fig 5.1. Increase in $[Ca^{2+}]_i$ occurred by replacing the extracellular Ca^{2+} free solution with solution containing 1.5 mM Ca^{2+} was higher at stage 2 and 4 relative to the stage 1. However, no significant difference was observed in calcium influx in stage 4 BOEC compared to that of the stage 1. All data are expressed as a mean of 6 experiments ± 1 standard deviation. (* = $p<0.05$; ** = $p<0.01$; *** = $p<0.001$).

The data in Fig 5.3 and 5.4 indicate changes in intracellular calcium concentration induced by Hyperforin, a TRPC6 channel activator, and SKF96365, a general TRP channel blocker. Hyperforin did not induce an increase in calcium influx in BOEC at stage 1 of the estrous cycle. Unexpectedly, addition of SKF96365 which is a general TRP channel blocker slightly increased the calcium influx into BOEC by 1.16 fold (p= 0.01) compared to the intracellular calcium ($[Ca^{2+}]_i$) level in BOEC treated with extracellular solution containing 1.5 mM Ca^{2+} and Hyperforin (Fig 5.3, A). However, intracellular calcium concentration was increased by 1.15 fold (p= 0.001) after addition of Hyperforin to the extracellular solution at stage 2 of the estrous cycle compared to $[Ca^{2+}]_i$ of BOEC incubated with extracellular solution containing 1.5 mM Ca^{2+}. The Hyperforin-induced increase in Ca^{2+} influx was abolished by addition of SKF96365 to extracellular solution in BOEC at stage 2 of the estrous cycle and $[Ca^{2+}]_i$ was reduced by 0.89 fold (p= 0.008) compared to that before addition of SKF96365 (Fig 5.3, B). At stage 3 of the estrous cycle, treatment of BOEC with Hyperforin induced an increased in $[Ca^{2+}]_i$ by 1.48 fold (p= 0.003) compared to that of the untreated BOEC. Treatment of stage 3 BOEC with SKF96365 while Hyperforin was still present in the extracellular solution promoted a 0.76 fold (p= 0.01) decrease in $[Ca^{2+}]_i$ relative to that before addition of SKF96365 (Fig 5.3, C). Hyperforin increased the Ca^{2+} influx in BOEC at stage 4 of the estrous cycle by 1.30 fold ($p= 2.78 \times 10^{-7}$) compared to that before Hyperforin treatment. Treatment of stage 4 BOEC with SKF96365 resulted in a decrease in $[Ca^{2+}]_i$ by 0.34 fold ($p= 4.64 \times 10^{-11}$) in comparison to that of the stage 4 BOEC before addition of SKF96365 (Fig 5.3, D). Changes in $[Ca^{2+}]_i$ induced by Hyperforin in stage 2 BOEC was higher by 1.17 fold (p= 0.0008) compared to that of the stage 1 BOEC. The increase in $[Ca^{2+}]_i$ induced by Hyperforin was higher by 1.29 (p= 0.01) and 1.12 (p= 0.0001) fold respectively at in stage 3 and 4 BOEC relative to the stage 1 BOEC. The intracellular calcium concentration in BOEC in response to SKF96365 at stage 2 was lower by 0.76 (p= 0.001), 0.78 ($p= 8.33 \times 10^{-5}$) and 0.29 ($p= 2.77 \times 10^{-6}$) fold respectively at stage 2, 3 and 4 of the estrous cycle (Fig 5.4).

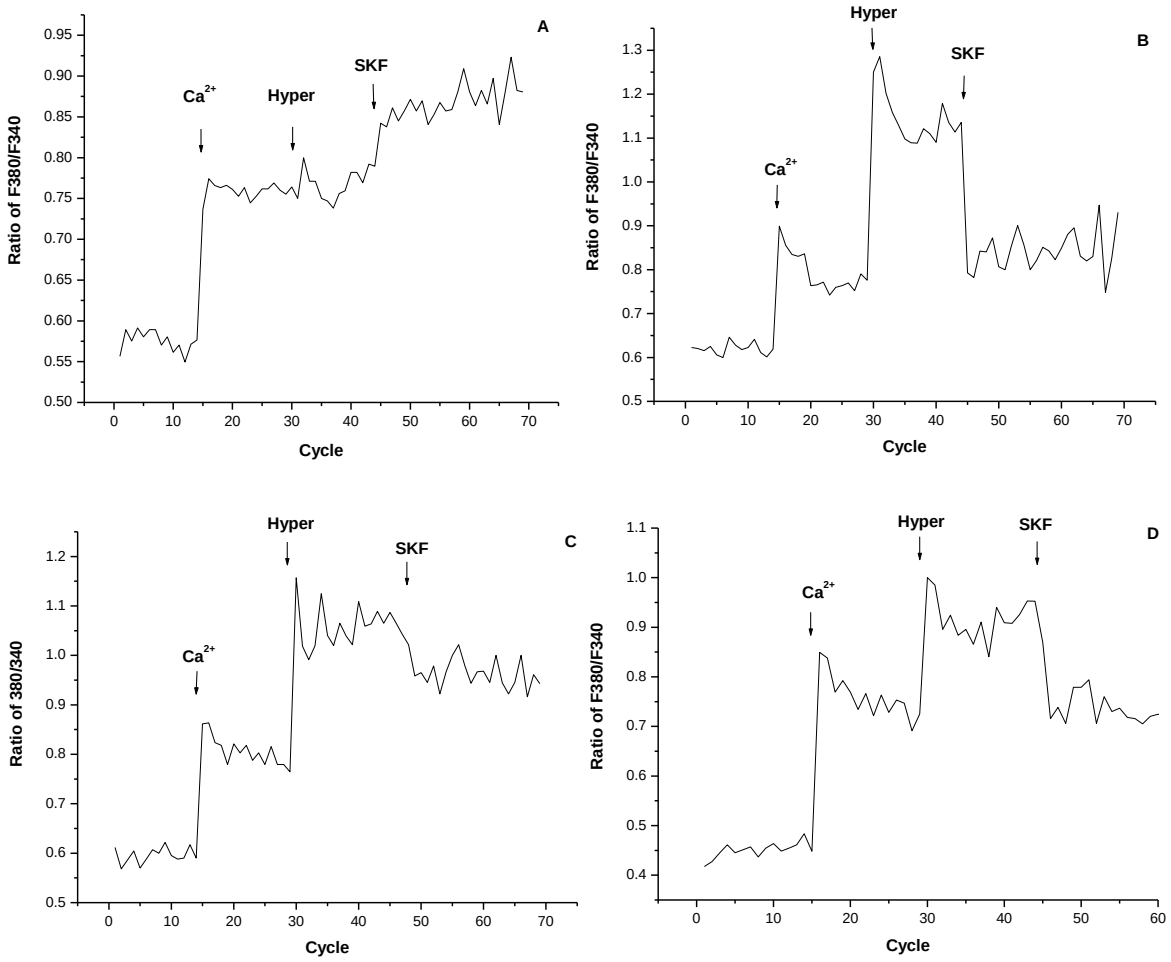

Fig 5.3 Changes in intracellular calcium concentration induced by Hyperforin and SKF96365 in Bovine Oviduct Epithelial Cultured Cells (BOEC) harvested from tracts at each stage of the oestrous cycle. This figure is an example of data collected from the plate reader. Hyperforin induced a small increase in calcium influx at stage 1 (5.3, A) of the estrous cycle. Calcium influx promoted by Hyperforin at stage 2 (5.3, B), stage3 (5.3, C) and stage 4 (5.4, D) of the estrous cycle was stronger than that of stage1 (5.3, A). SKF96365 slightly increased the calcium influx at stage1 (5.3, A) of the estrous cycle. However, intracellular calcium concentration was reduced by SKF96365 at stage 2 (5.3, B), 3 (5.3, C) and stage 4 (5.4, D) of the estrous cycle.

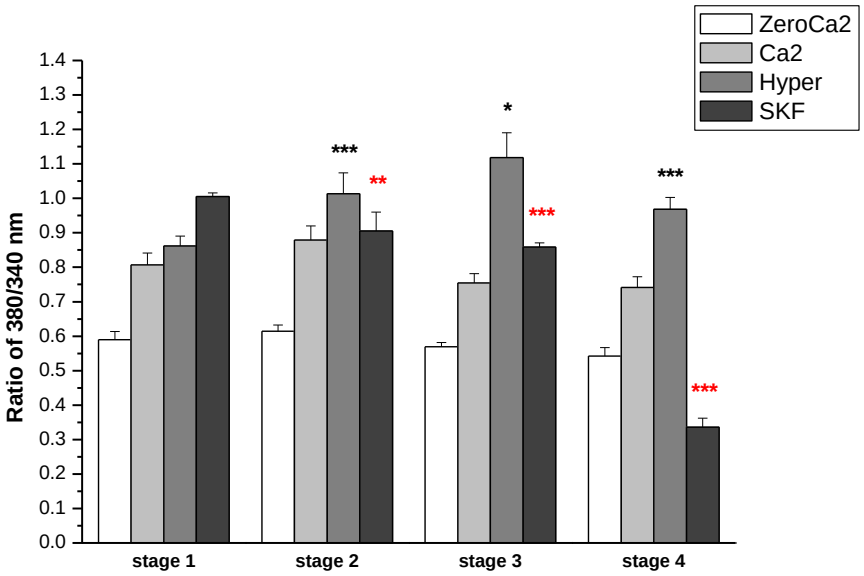

Fig 5.4 Changes intracellular calcium concentration induced by Hyperforin and SKF96365 in Bovine Oviduct Epithelial Cultured Cells (BOEC) throughout the estrous cycle. Hyperforin induced a calcium influx in stage 2, 3 and 4 BOEC but not in stage 1 BOEC. Preliminary activation TRPC6 channel by Hyperforin in BOEC at stage 1 of the estrous cycle resulted in unexpected increase in calcium influx by SKF96365 which is a general TRP channel blocker. However, at stage 2, 3 and 4 of the estrous cycle SKF96365 abolished the Hyperforin-induced increase in intracellular calcium concentration . All data are expressed as a mean of 6 experiments ± 1 standard deviation. (* = $p<0.05$; ** = $p<0.01$; *** = $p<0.001$). * represents the P value, comparing the changes in calcium influx induced by Hyperforin at different stage of the estrous cycle to the stage 1 in BOEC. * represents the P value, comparing the changes in intracellular calcium concentration induced by SKF96365 at different stage of the estrous cycle to the stage 1 in BOEC.

Fig 5.5 and 5.6 show that treatment of BOEC with SKF96365 without activation of TPC6 resulted in an inhibition in Ca2+ influx and decrease in $[Ca^{2+}]_i$ by 0.90 fold (p= 0.006), 0.76 fold (p= 2.93 x 10^{-7}), 0.89 fold (p= 1.66 x 10^{-6}) and 0.63 fold (p= 8.63 x 10^{-5}) at stage 1 (Fig 5.5, A), 2 (Fig 5.5, B), 3 (Fig 5.5, C) and 4 (Fig 5.5, D) of the estrous cycle respectively (Fig 5.6). Changes induced by SKF96365 in stage 2 BOEC was not significantly different (p= 0.2) to that of the stage 1. Furthermore, no significant difference were observed in effect induced by SKF96365 in stage 2 (P= 0.05) and 3 (p= 0.1) BOEC relative to that of stage 1.

Treatment of BOEC incubated in calcium solution containing SKF96365, with Hyperforin resulted in an increase in intracellular calcium concentration at all stages of the estrous cycle (Fig 5.5 and 5.6). Intracellular calcium concentration was increase by 1.46 (1.53 x 10^{-5}), 1.53 (6.54 x 10^{-5}), 1.57 (p= 0.001) and 1.53 (p= 1.95 x 10^{-8}) fold as a consequence of Hyperforin treatment of BOEC at stage 1, 2, 3 and 4 of the estrous cycle respectively (Fig 5.6). No significant difference was observed in BOEC response to Hyperforin at stage 2, 3 and 4 relative to stage 1 of the estrous cycle (Fig 5.6).

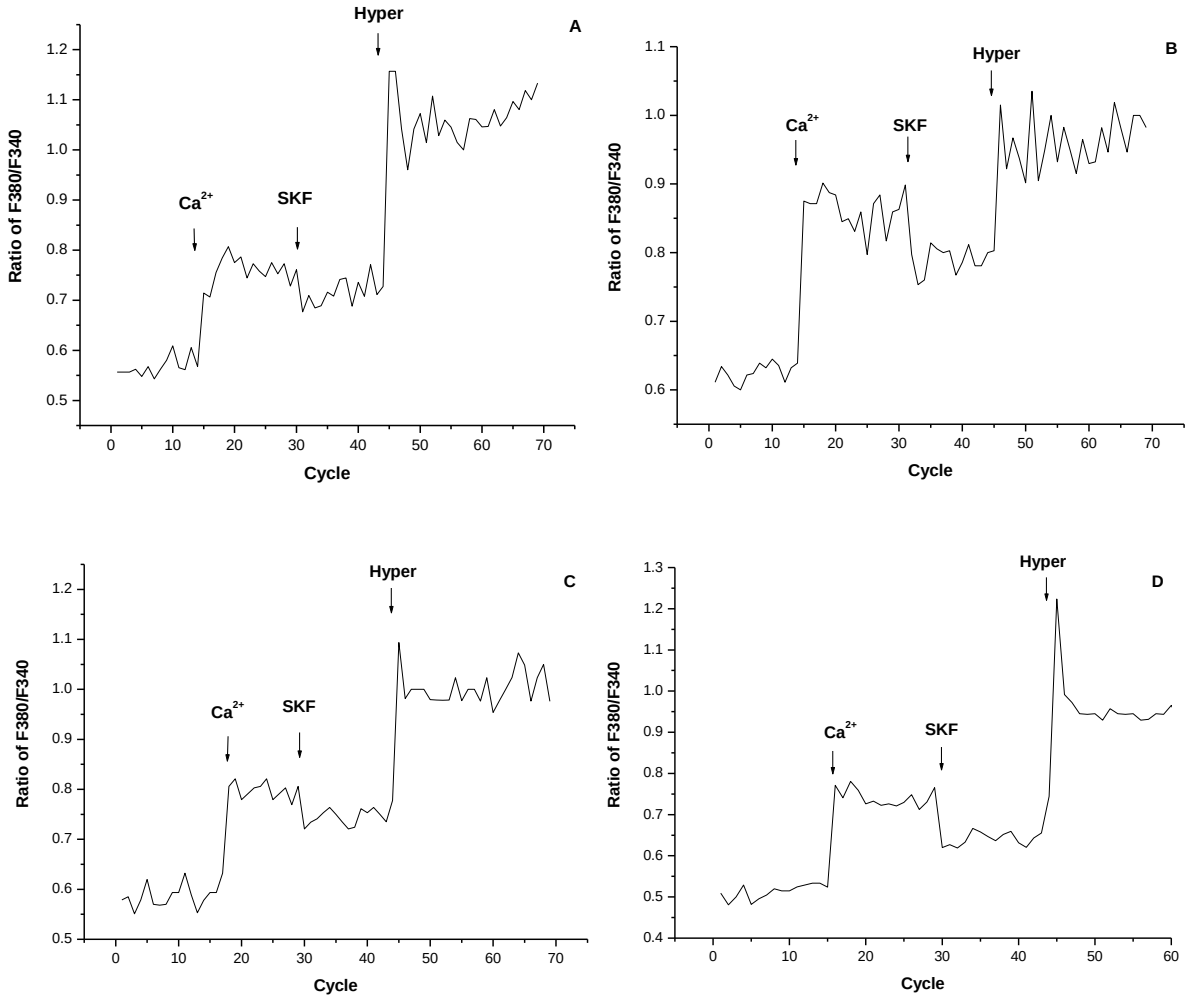

Fig 5.5 Changes in intracellular calcium concentration induced by SKF96365 and Hyperforin in Bovine Oviduct Epithelial Cultured Cells (BOEC) throughout the estrous cycle. This figure is an example of data collected from the plate reader. SKF96365 reduced the intracellular calcium concentration at stage 1 (5.5, A), 2 (5.5, B), 3 (5.5, C) and 4 (5.5, D) of the estrous cycle. Introducing Hyperforin to the extracellular solution led to an increase in intracellular calcium concentration at stage1 (5.5, A), 2 (5.5, B), 3 (5.5, C) and 4 (5.5, D) of the estrous cycle.

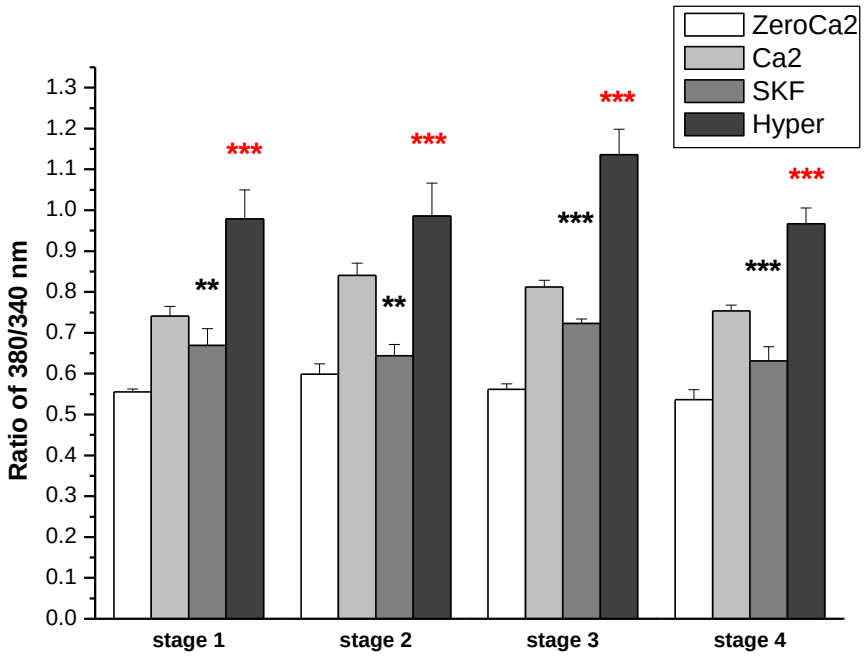

Fig 5.6 Changes in intracellular calcium concentration induced by SKF96365 and Hyperforin in Bovine Oviduct Epithelial Cultured Cells (BOEC) throughout the estrous cycle. SKF96365 reduced the intracellular calcium concentration at all 4 stages of the estrous cycle. Treatment of BOEC with Hyperforin resulted in an increase in calcium influx at stage 1, 2, 3 and 4 of the estrous cycle. However, no significant difference was observed in effect of SKF96365 and Hyperforin at stage 2, 3 and 4 compared to stage 1 of the estrous cycle. All data are expressed as a mean of 6 experiments ± 1 standard deviation. (* = $p<0.05$; ** = $p<0.01$; *** = $p<0.001$). * represents the P value, comparing the changes in calcium influx induced by SKF96365 at different stage of the estrous cycle to the intracellular calcium level before the treatment in BOEC. * represents the P value, comparing the changes in intracellular calcium concentration induced by Hyperforin at different stage of the estrous cycle to the intracellular calcium concentration after SKF96365 in BOEC.

The data in Fig 5.7 and 5.8 indicate the effect of 2.5-Di-t-butylhydroquinone (DBQ) which is sarcoplasmic/endoplasmic reticulum Ca^{2+} -ATPase (SERCA) inhibitor on intracellular calcium. DBQ induced a very small transient increase in intracellular calcium concentration at all stages of the estrous cycle (Fig 5.7). The DBQ-induced transient increase in intracellular calcium concentration at stage 2 was not significantly different (p= 0.6) to that of the stage 1. However, the DBQ-induced effect in BOEC was lower at stage 3 and 4 by 0.75 (p= 0.0003) and 0.49 (p= 1.56×10^{-6}) fold respectively relative to the stage 1. Replacing the Ca^{2+} free solution with extracellular solution containing 1.5 mM Ca^{2+} after depleting the intracellular store resulted in an increase in $[Ca^{2+}]_i$. This increase was not significantly different at stage 2 (P= 0.2), 3 (p= 0.05) and 4 (p= 0.8) compared to the stage1 (Fig 5.7 and 5.8). Addition of SKF96365 to the extracellular solution led to a fall in $[Ca^{2+}]_i$ in BOEC. Effect of SKF96365 was stronger at stage 4 compared to the other stages of the estrous cycle. Effect of SKF96365 was higher at stage 2, 3 and 4 by 1.18 (p= 0.04), 1.28 (p= 0.0002) and 2.09 (p= 6.69×10^{-8}) fold respectively relative at stage 1 (Fig 5.7 and 5.8).

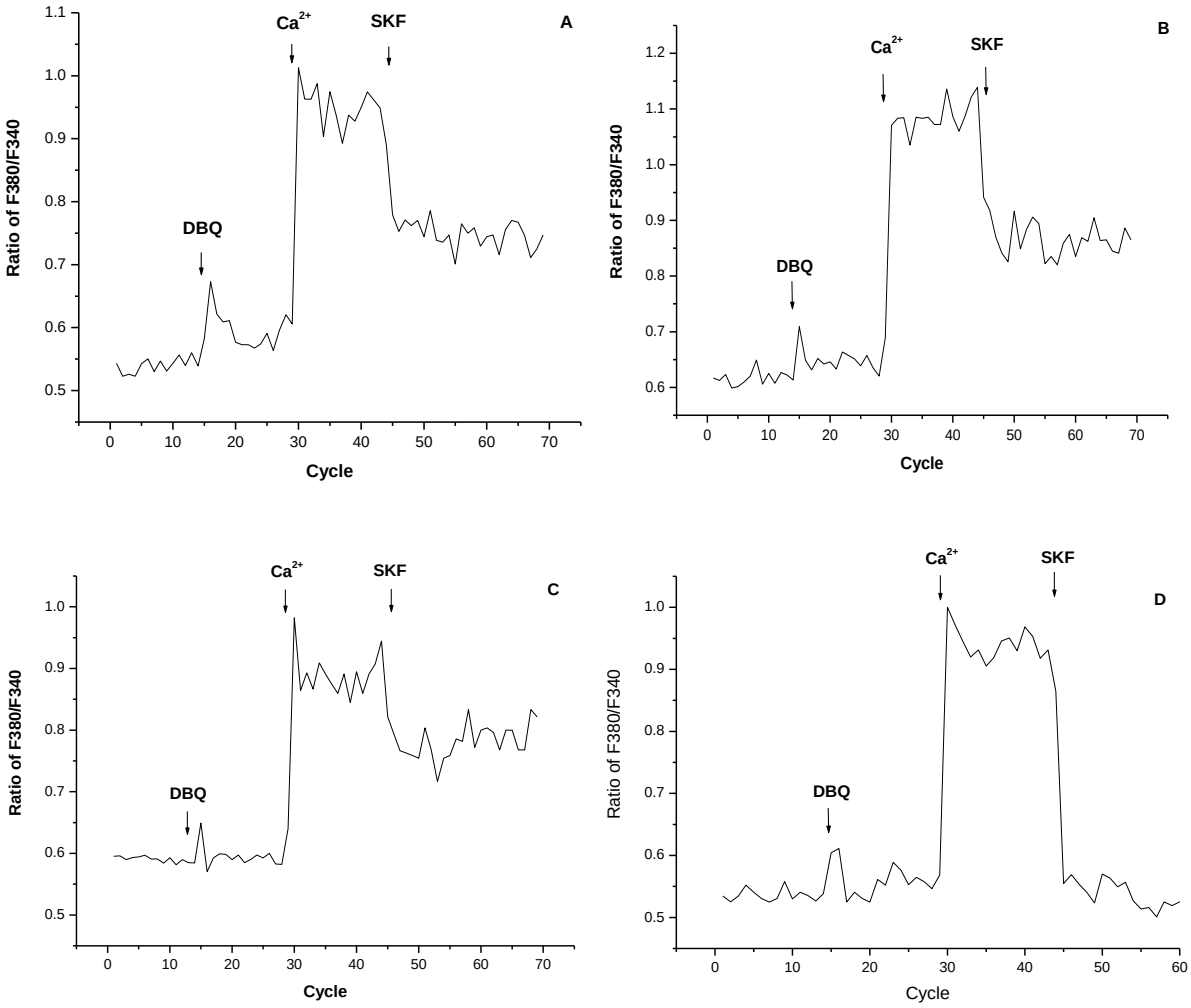

Fig 5.7 Depleting the intracellular calcium store by DBQ enhanced the inhibitory effect of SKF96365 on TRP channels present in Bovine Oviduct Epithelial Cultured Cells (BOEC) throughout the estrous cycle. This figure is an example of data collected from the plate reader. Treatment of BOEC with DBQ induced a small transient increase in intracellular calcium concentration due to the intracellular store depletion. SKF96365 inhibited the calcium influx at all 4 stages of the estrous cycle in BOEC. However, the effect of SKF96365 was much stronger at stage 4 (5.7, D) compared to stage 1 (5.7, A), 2 (5.7, B) and 3 (5.7, C) of the estrous cycle.

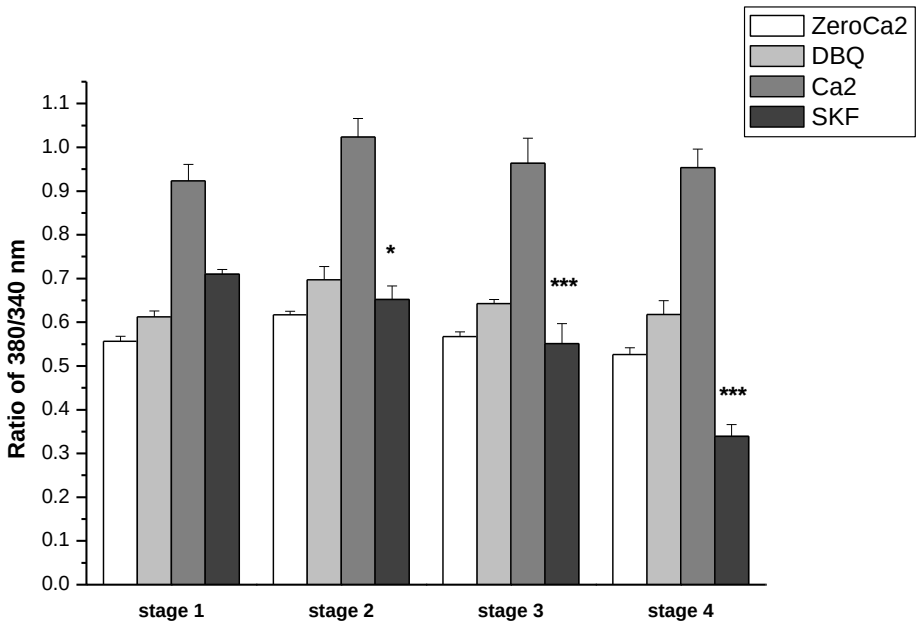

Fig 5.8 Depleting the intracellular calcium store by DBQ enhanced the inhibitory effect of SKF96365 on TRP channels present in Bovine Oviduct Epithelial Cultured Cells (BOEC) throughout the estrous cycle.SKF96365-induced decrease in intracellular concentration was stronger at stage 4 compared to the other stages of the estrous cycle. All data are expressed as a mean of 6 experiments ± 1 standard deviation. (* = p<0.05; ** = p<0.01; *** = p<0.001). * indicates the P value comparing the effect of SKF96365 on calcium influx at stage 2, 3 and 4 relative to that of the stage 1 of the estrous cycle.

5.2 Discussion

The data above indicate that basal calcium influx in stage 2 and 4 BOEC was significantly higher than in stage 1 and 3 (Fig 5.1 and 5.2). However, mRNA expression of all TRPC isoforms present in BOEC, other than TRPC2, were lower at stage 2 and 4 compared to that of stage 1 and 3 of the estrous cycle (Fig 3.3). However, it has been shown previously in chapter 3 and 4 that gene expression does not necessarily equate to functional protein levels. Higher mRNA level at 1 stage could be due to the requirement for a higher amount of functional protein for the next stage. The time gap between the high level of mRNA and high level functional protein could be due to the time required for translation and post-translational modification (PTM). In other work, mRNA of TRPC2 has been detected in bovine testis (Wissenbach *et al.*, 1998). TRPC2 mRNA was also detected in bovine spleen and liver (Wissenbach *et al.*, 1998). Furthermore, TRPC2 is expressed in olfactory epithelium and is possibly involved in a pheromone signalling cascade (Liman *et al.*, 1999). It has also been reported that $G_{\alpha s}$-like G proteins are the G-protein coupled receptors involved in transduction in olfactory epithelium (Schild & Restrepo, 1998). Interestingly, the LH receptor induces it effects via $G_{\alpha s}$-like G protein (Dufau, 1998). This could indicate a possible role of TRPC2 channels in bovine oviduct epithelium calcium homeostasis.

In order to test functionality of the TRP channels, experiments were conducted where cells were exposed to a series of activators and inhibitors. Hyperforin is a TRPC6 specific activator which induced an increase in calcium influx at stage 2, 3 and 4 but not at stage 1 of the estrous cycle (Fig 5.4) indicating that TRPC6 is physiologically active in the bovine oviduct epithelial cells. Hyperforin-induced calcium influx in BOEC was higher at stages 2, 3 and 4 of the estrous cycle compared to that of stage 1. However, the mRNA expression of TRPC6 in BOEC was lower at stages 2 and 4 compared to stages 1 and 3. The apparent discrepancy between the gene expression data and the findings relating to functional activity could be due to different ratios of homotetramer TRPC6 to heterotetramer TRPC3-TRPC6 in BOEC at each stage of the estrous cycle (Hirschler-Laszkiewicz *et al.*, 2009). Furthermore, the association of TRPC6 with STIM and the complex of STIM and Orai (Hong *et al.*, 2011) could also

affect the activation of TRPC6 because of its distinct roles as Store-operated calcium channels (SOC) and Receptor-operated calcium channels (ROC).

SKF96365 is a general TRP channel blocker and surprisingly induced a modest increase in calcium influx in stage 1 BOEC after treatment with Hyperforin which did not induce any effect on intracellular calcium concentration. However, SKF96365 decreased the intracellular calcium concentration in stage 2, 3 and BOEC pre-treated with Hyperforin. Calcium entry into cells may act not only as a second messenger but can also induce membrane depolarization which consequently activates low voltage-activated calcium channels (Perez-Reyes, 2003). Besides blocking TRP channels, SKF96365 is a potent blocker of low voltage-activated t-type calcium channels which have been identified in bovine ciliary epithelial cells (Singh *et al.*, 2010). A Hyperforin-induced increase in intracellular calcium concentration could lead to a membrane depolarization that could activate the low voltage-activated t-type calcium channels. Therefore, it may be concluded that SKF96365 blocks both the TRP isoforms present in BOEC and the low voltage-activated t-type calcium channels. At stage 1, Hyperforin did not affect the intracellular calcium concentration, suggesting that TRPC6 has limited involvement in the calcium homeostasis of stage 1 BOEC regardless to its interaction with other TRPC isoforms or other signalling proteins such as STIM. Therefore, stage 1 BOEC remained polarized after Hyperforin treatment and consequently low voltage-activated t-type calcium channels were not activated. However, to determine the mechanism underlying the SKF96365-induced calcium influx into the stage 1 BOEC after Hyperforin treatment further investigation is required. This could be done by using siRNA to knock-out each TRPC isoforms and study their role in this mechanism. Furthermore, SKF96365-induced activity of low voltage-activated t-type calcium channels could be determined by depolarizing the cell membrane at this stage.

SKF96365 alone induced a decrease in intracellular calcium concentration in BOEC at all 4 stages of the estrous cycle (Fig 5.6). This suggests that some or all TRPC isoforms present in BOEC are physiologically active throughout the estrous cycle. However, inhibition in calcium influx induced by SKF96365 in stage 4 BOEC pre-treated with Hyperforin was stronger than that of the BOEC

not treated with Hyperforin. This could be due to the activation of low voltage-activated t-type calcium channels in BOEC pre-treated with Hyperforin (Singh *et al.*, 2010). After blocking the TRP channels in BOEC with SKF96365, treatment of the cells with Hyperforin still induced an increase in intracellular calcium concentration with could be due to the reversible effect of the SKF96365 (Cherednichenko *et al.*, 2004).

Depletion of the intracellular calcium store with 2.5-Di-t-butylhydroquinone (DBQ) increased the basal calcium intake in BOEC at all 4 stages of the estrous cycle compared to the control group indicating that intracellular store depletion which activates Store-Operated Calcium channels (SOC) is present and active in BOEC. Furthermore, this suggests the possible role of some TRPC isoforms present in BOEC as Store-Operated Calcium channels (SOC) (Chevesich *et al.*, 1997). The role of TRPC channels as SOC has been identified in other epithelial cells such as; TRPC1 in prostate epithelial cells (Vanden Abeele *et al.*, 2003) and TRPC4 in human corneal epithelial cells (Yang *et al.*, 2005). In general, the data presented in this chapter indicate that some or all TRPC isoforms present in BOEC are functionally active, possibly as both Store-operated calcium channels (SOC) and Receptor-operated calcium channels (ROC).

Chapter 6

Role of TRPC channels in female fertility

According to the NHS website around 30% of infertility is related to problems with the woman. Causes of infertility in women are as below:

1. Ovulation disorders which can result in number of conditions;
    - Polycystic ovary syndrome (PCOS)
    - Premature ovarian failure
    - Hyperthyroidism and hypothyroidism
    - Cushing's syndrome
2. Damage or dysfunction of the womb and fallopian tubes which could be due to;
    - Pelvic surgery
    - Cervical surgery
    - Submucosal fibroids
    - Endometriosis
    - Pelvic inflammatroy disease
3. Sterilisation
4. Medicines and drugs
    - Non-steroidal anti-inflammatory drugs (NSAIDs)
    - Chemotherapy
    - Neuroleptic medicines
    - Spironolactone
    - Illegal drugs such as coaine
5. Age

The polycystic ovary which is one of the causes of infertility in women was first described by Stein and Leventhal in 1935 (Stein & Leventhal, 1935) as an important cause of anovulation or irregular ovulation in infertile females. Polycystic ovarian syndrome (PCOS) is a common endocrine disorder with a spectrum of symptoms and signs among different individuals or in an individual over time (Balen *et al.*, 1995). Different features of PCOS are classified into three categories; clinical, endocrine and metabolic. PCOS typically manifests as a combination of severe menstrual disturbance (amenorrhea or oligomenorrhea), hirsutism, acne, alopecia, and recurrent miscarriages (Sagle *et al.*, 1988). The endocrine aspects of this syndrome include hyperandrogenism, elevated level of luteinizing hormone (LH), oestrogen and prolactin. Insulin resistance, obesity, lipid abnormalities and an increased risk of impaired glucose tolerance and type 2 diabetes mellitus are considered as the metabolic aspects of the syndrome (Tsilchorozidou *et al.*, 2004). PCOS might be differentially inherited and its expression is affected by a number of interlinking factors. Genes that could be linked to PCOS are involved in the regulation of ovarian steroidogenesis and those which affect body mass index (BMI) and adiposity. Poor diet and reduced exercise are important environmental factors and PCOS frequently occurs in combination with obesity and insulin resistance. This could be an explanation of the correlation between obesity development and symptom severity in women with PCOS (Barber *et al.*, 2006).

Ther pathogenesis of PCOS has been described by Tsilchorozidou, *et al*. (2004) as, "“A unique defect in insulin action and secretion that leads to hyperinsulinaemia and insulin resistance, a primary neuroendocrine defect leading to an exaggerated LH pulse frequency and amplitude, a defect of androgen synthesis that results in enhanced ovarian androgen production and an alteration in cortisol metabolism resulting in enhanced adrenal androgen production” (Tsilchorozidou *et al.*, 2004).

Insulin resistance occurs due to the low efficiency of insulin in lowering blood glucose level. Insulin resistance is significantly higher in obese PCOS women compared to non-obese PCOS women. This observation indicates that insulin resistance in obese PCOS patients might result from a combination of dual factors; one unique to PCOS and the other obesity specific.

The insulin receptor is a tyrosine kinase receptor (RTK class II). Its activity is increased by autophosphorylation of a tyrosine residue which consequently initiates signal transduction and subsequent actions of insulin. The action of RTK II is inhibited by serine phosphorylation. Excessive serine phosphorylation of insulin receptors leads to inhibit insulin signalling; this represents a potential mechanism of insulin resistance in some PCOS women (Tsilchorozidou *et al.*, 2004). Serine phosphorylation also increases enzymatic activity of androgen biosynthesis, P450c17 (Zhang *et al.*, 1995), which is a single defect and leads both to insulin resistance and hyperandrogenism (Tsilchorozidou *et al.*, 2004).

According to the World Health Organization (WHO) website, recent lifestyle changes have resulted in rising rates of obesity; 1.5 billion adults in 2008, and consequently hyperinsulinemia which in females is important in the pathogenesis of the PCOS. Secretion of androgen from the ovarian stroma is stimulated by insulin. Normal development of ovarian follicles is affected by androgen (Okutsu *et al.*, 2010). Excessive androgens cause adverse effects on follicular growth as well as suppressing apoptosis which permits the survival of follicles which may ordinarily be lost by atresia.

The correlation between hyperinsulinaemia and hyperandrogenism has been shown (Prelevic, 1997). However, most of the evidence suggests hyperinsulinaemia as a primary factor. Pathways leading to androgen production induced by hyperinsulinaemia (Fig. 6.1) include activation of Insulin-like growth factor I receptors (IGF-1 R) of theca cells by insulin at high concentration and insulin-induced enhanced amplitude of LH pulses via stimulation of insulin receptors in pituitary tissue (Tsilchorozidou *et al.*, 2004). Furthermore, circulating levels of IGF-1 are increased by insulin-induced inhibition of hepatic production of IGFBP-1. Hyperinsulinaemia also contributes to hyperandrogenism by inhibiting hepatic synthesis of serum sex hormone-binding globulin (SHBG), which results in an elevation in levels of free androgen and estradiol in the blood stream. There is a striking inverse relation between peripheral insulin and SHBG levels such that SHBG concentration is considered a reliable marker for hyperinsulinaemic insulin resistance (Tsilchorozidou *et al.*, 2004).

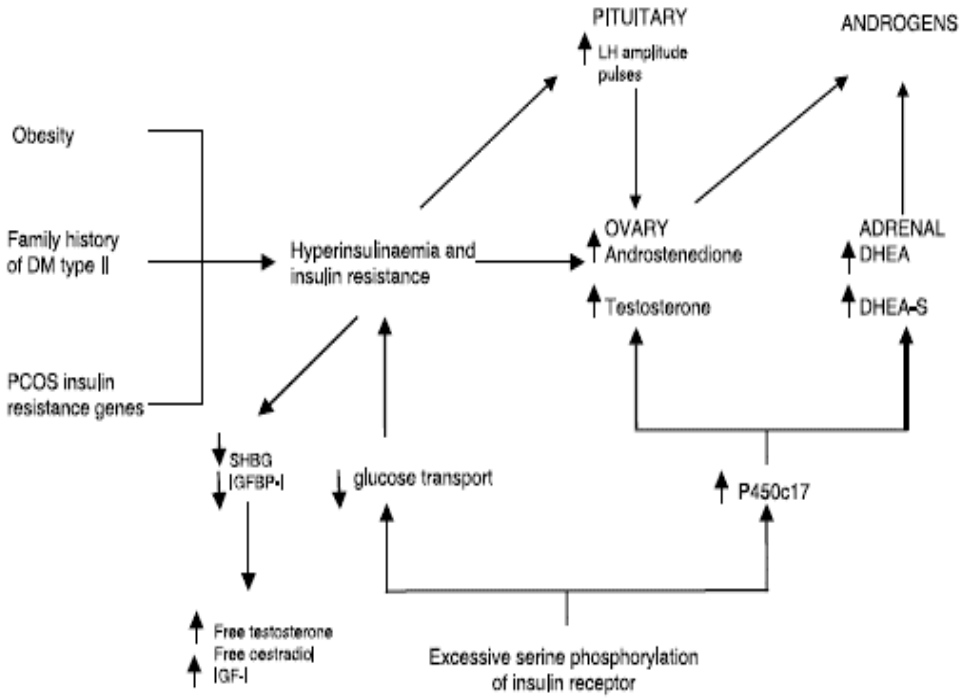

Fig. 6.1 Scheme of proposed interactions leading to excessive androgen level in PCOS (Tsilchorozidou *et al.*, 2004).

Consequently, PCOS is necessarily defined by a range of clinical and biochemical features including disturbed menstrual cycle, elevated serum concentration of LH, testosterone, androstenedione (Franks, 1995) and insulin, obesity, hirsutism, and acne. PCOS has various manifestations and one, all, or any combination of those mentioned could be present in association with polycystic ovaries.

According to the Rotterdam polycystic syndrome consensus workshop group which is cosponsored by the European Society for Human Reproduction and Embryology (ESHRE) and the American Society for Reproductive Medicine (ASRM) diagnosis of PCOS should rely on the presence of at least two of the following 3 symptoms (Azziz, 2006):

1) irregular or absent ovulation, elevated levels of androgenic hormones;
2) enlarged ovaries containing at least 12 follicles each
3) polycystic ovaries (transvaginal ultrasound)

These recommendations form the so-called “Rotterdam Criteria” the accepted standard for diagnosis of PCOS. (Rotterdam ESHRE/ASRM-Sponsored PCOS Consensus Workshop Group., 2004)".

6.1 Expression of the TRPC family in human endometrium

Analysis of TRPC expression in human samples was carried out on archived human endometrium biopsy tissues Hull Royal Infirmary Hospital Archives provided by Prof S.L. Atkin and used according to the REC reference number of 07/Q1104/53.

Expression of TRPC1 (Lane 2), 6 (Lane 6) and 7 (Lane 7) was detected in biopsies collected from human endometrium (fig 6.1). Positive expression of β actin acting as the endogenous control (Fig 6.1, Lane 1) confirmed the success of the PCR reaction. Furthermore, expression of Cytokeratin18 (Fig 6.2, Lane 8), a marker specific to epithelial cells, confirmed that template cDNA was from epithelial cells. The expected size of the PCR products were β actin 211 bp, TRPC1 242 bp, TRPC3 238bp, TRPC4 249bp, TRPC5 255bp, TRPC6 218 bp, TRPC7 240bp and Cytokeratin18 249 bp .

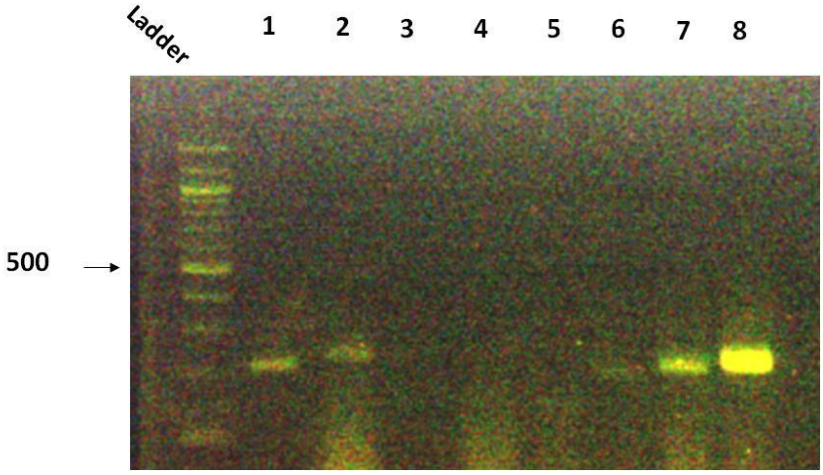

Fig 6.2 Expression of TRPC genes in human endometrium. PCR product was loaded as following: Lane 1; β actin, Lane 2; TRPC1, Lane 3; TRPC3, Lane 4; TRPC4, Lane 5; TRPC5, Lane 6; TRPC6, Lane 7; TRPC7 and Lane 8; Cytokeratin18. PCR Products were electrophoresed on a 2% agarose gel. Band presence indicates positive expression of TRPC 1, 6 and 7 in human endometrium tissue; expression of TRPC3, 4 and 7 was not detected. TRPC2 is a pseudogene in the human. All PCR products were of the predicted size. of β actin: 211 bp, TRPC1: 242 bp, TRPC6: 218 bp, TRPC7: 240bp and Cytokeratin18 : 249 bp .

6.2 TRPC genes and fertility

Expression of the TRPC channels were next examined in endometrial biopsies from women with Polycystic Ovary Syndrome and from women attending for assisted conception through In Vitro Fertilization (IVF). The biopsies from the endometria of women who were unable to conceive but not diagnosed with any physiological problem were used as the control. This group was named Male Factor since the cause of infertility was ascribed to pathology specific to the male, with the female not having compromised fertility. These data are presented in Fig 6.3.

6.2.1 Expression of TRPC genes in endometrium from Polycystic Ovary Syndrome (PCOS) patients

The data in Fig 6.3, A indicate that expression of TRPC1 in the endometrium of PCOS patients was not significantly different ($p= 0.1$) relative to the male factor control. However, expression of both TRPC6 and TRPC7 was up-regulated by 5.63 ($p= 0.01$) and 9.83 (0.04) fold respectively in the endometrium of PCOS patients compared to the male factor controls (Fig 6.3, B and C).

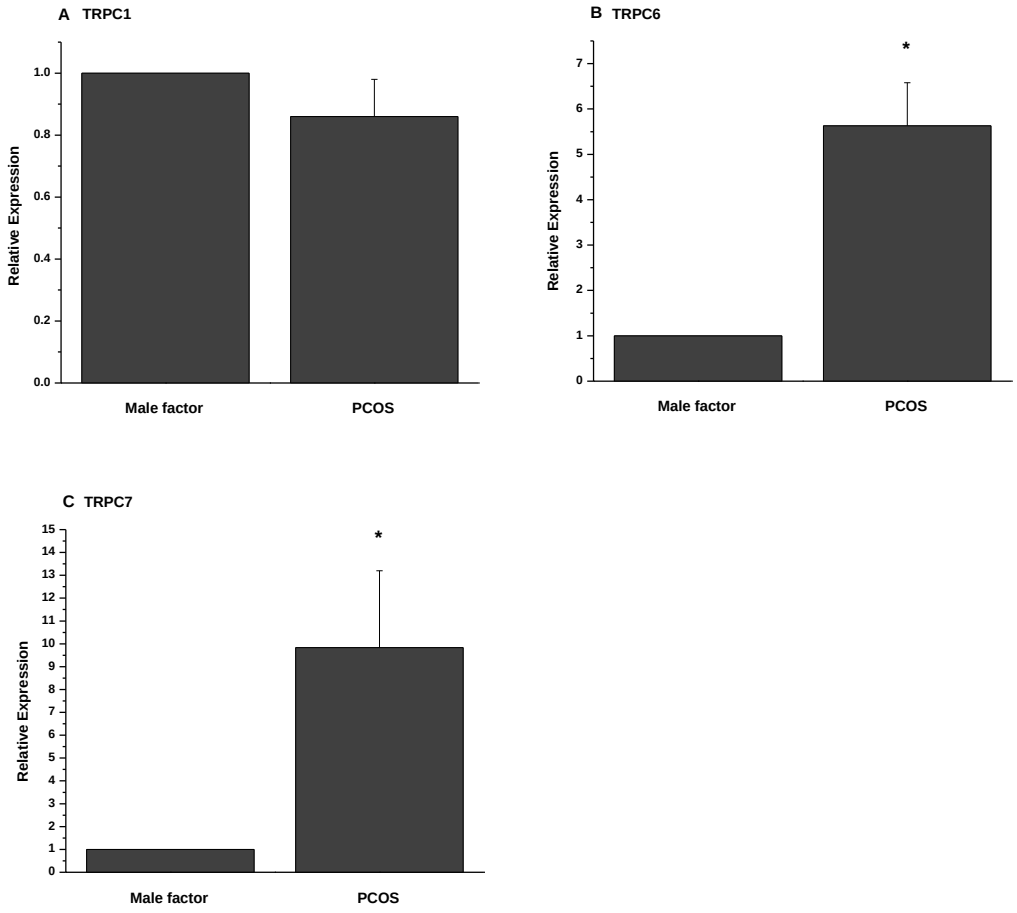

Fig 6.3 Expression of TRPC genes in the endometrium of women with PCOS was different to that of the endometrium of normal women. Expression of TRPC1 in the endometrium of PCOS patients was similar to that of the healthy women (6.3, A). However, TRPC6 and TRPC7 were both up-regulated compared to the control group (Fig 6.3 B and C respectively). All data are expressed as a mean of 3 replicates ± 1 standard deviation. (* = $p<0.05$; ** = $p<0.01$; *** = $p<0.001$).

6.2.2 Expression of TRPC genes in endometrium of IVF patients

The human endometrium biopsies from IVF patients were provided by Dr E. Dickerson and used in accordance with REC approval reference number 07/Q1104/53.

The data from Fig 6.4, A indicate that in endometrium of women attending for In Vitro Fertilization (IVF) on day 21 of the menstrual cycle, expression of TRPC1 was 6.78 fold ($p= 0.009$) higher than that of endometrium from women who were attending for treatment for 'male factor' infertility. Furthermore, expression of TRPC6 was 2.20 fold ($p= 0.01$) higher in endometrium of IVF patients relative to the male factor patients (Fig 6.4, B). However, TRPC7 was dramatically down-regulated to 10% ($p= 0.001$) of its value in the control group (Fig 6.4, C).

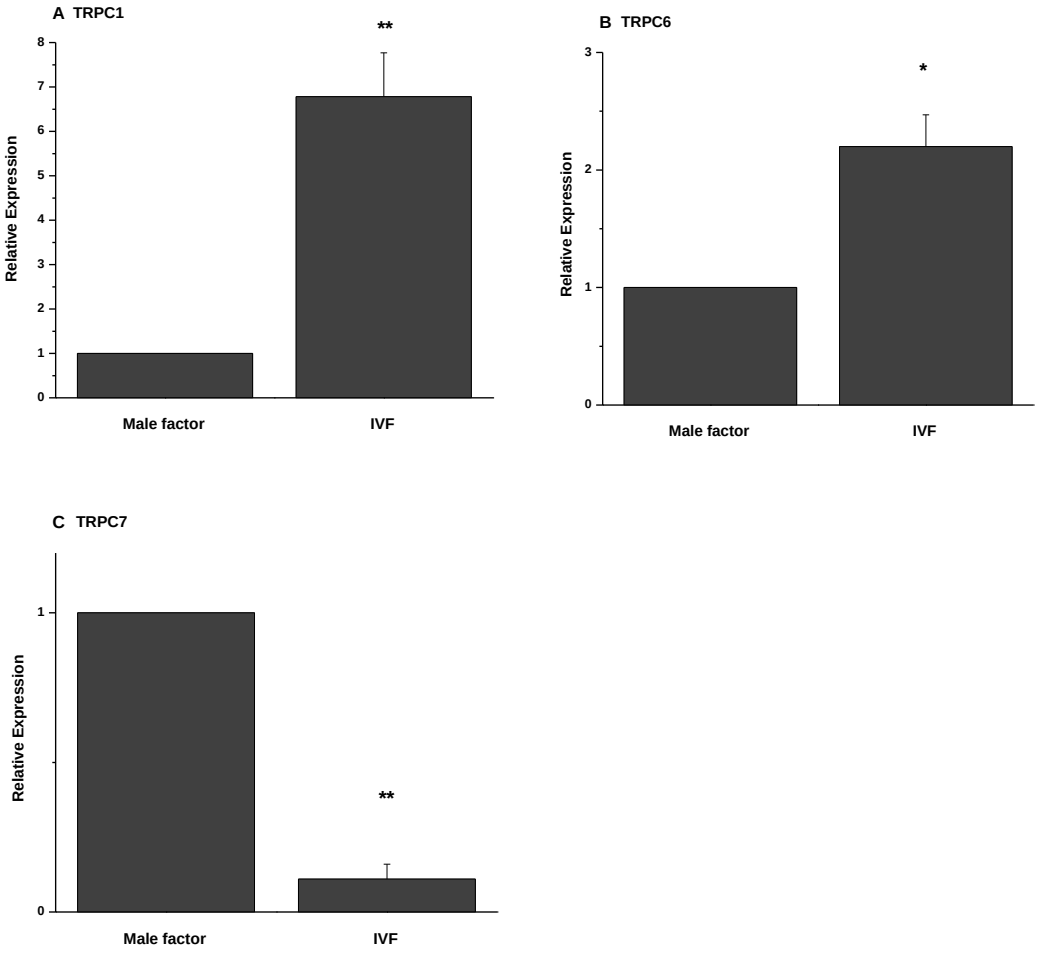

Fig 6.4 Expression of TRPC genes in endometrium of IVF patients was different to that of the endometrium of normal women. Expression level of TRPC1 (Fig 6.4 A) and TRPC6 (Fig 6.4 B) was up regulated in endometrium of IVF patients relative to the male factor. However TRPC7 expression was reduced compared to the control group (Fig 6.4 C). All data are expressed as a mean of 3 replicates ± 1 standard deviation. (* = $p<0.05$; ** = $p<0.01$; *** = $p<0.001$).

6.3 Localization of TRPC channels in human endometrium throughout the menstrual cycle

Semi-quantitative measurements of TRPC1 and TRPC6 throughout the menstrual cycle were carried out in relation to the proliferative phase of the cycle. In non-permeabilized human endometrium tissue, the expression level of TRPC1 channels on cytoplasmic membranes was similar at the proliferative, early secretory ($p= 0.05$) and late secretory ($p= 0.1$) phases of the menstrual cycle. However, at the mid secretory phase, abundance of TRPC1 was lower by 0.41 fold ($p= 0.003$) compared to that of the proliferative phase (Fig 6.5).

Membrane abundance of TRPC6 protein in human endometrium was higher in glandular epithelium at the proliferative phase compared to the rest of the tissue (Fig 6.5, A). However, at early ($p= 0.8$) and mid ($p= 0.1$) secretory phase, abundance of TRPC6 was similar throughout the tissue (Fig 6.5, B and C). At the late secretory phase abundance of TRPC6 was lower by 0.50 fold ($p= 0.04$) relative to that of the proliferative phase (Fig 6.5, D).

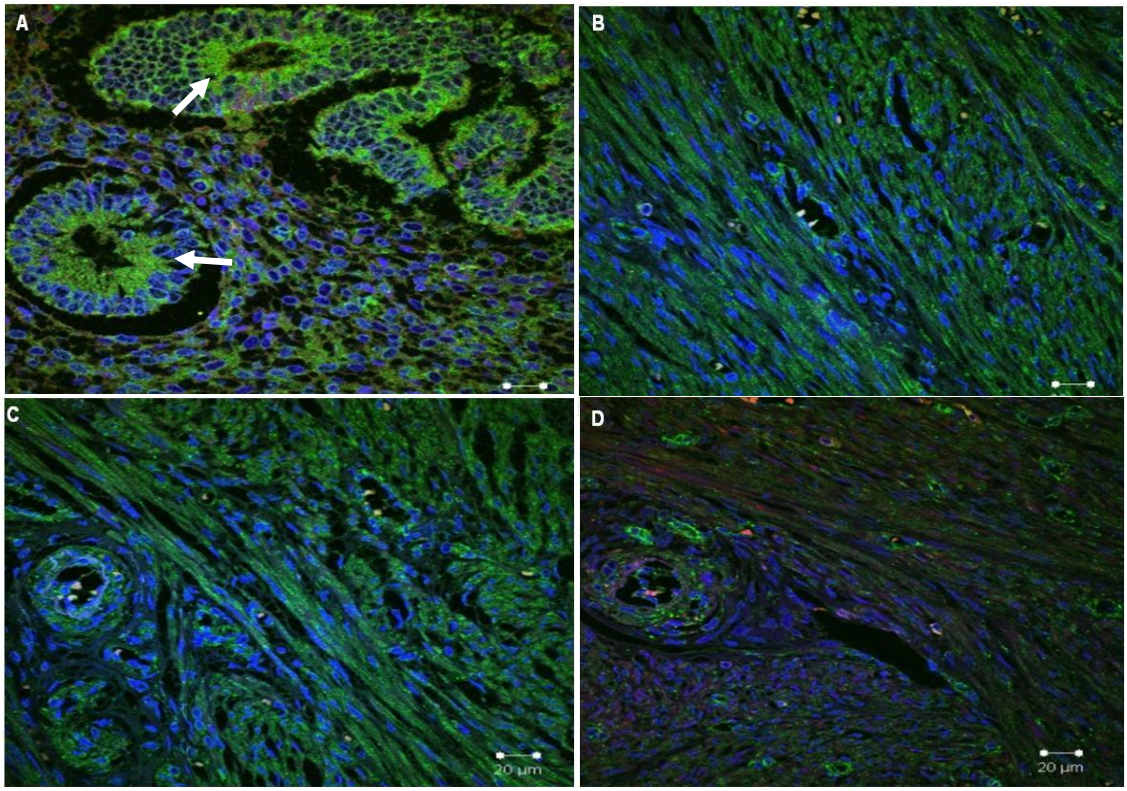

Fig 6.5 Localization of TRPC1 and TRPC6 in non-permeabilized human endometrium throughout the menstrual cycle. Abundance of TRPC1 was similar at proliferative (6.5, A), early secretory (6.5, B) and late secretory (6.5, D) phase. Abundance of TRPC1 was lower at mid secretory phase (6.5, C) compared to other stages of the menstrual cycle. TRPC6 was more abundant in the glandular compartment (shown by arrows) compared to the rest of the tissue in the proliferative phase (6.5, A). At the early secretory (6.5, B), mid secretory (6.5, C) and late secretory (6.5, D) phase, TRPC6 was localized evenly throughout the non-permeabilized human endometrium tissue. Abundance of TRPC6 was equal at proliferative (6.5, A), early (6.5, B) and mid (6.5, C) secretory phase. Abundance of TRPC6 was lowest at late proliferative phase (6.5, D). Nuclei are labeled with DAPI (Blue), TRPC1 with Alexa Four 647 FITC conjugated (Red) and TRPC6 with Alexa Flour 488 (Green).

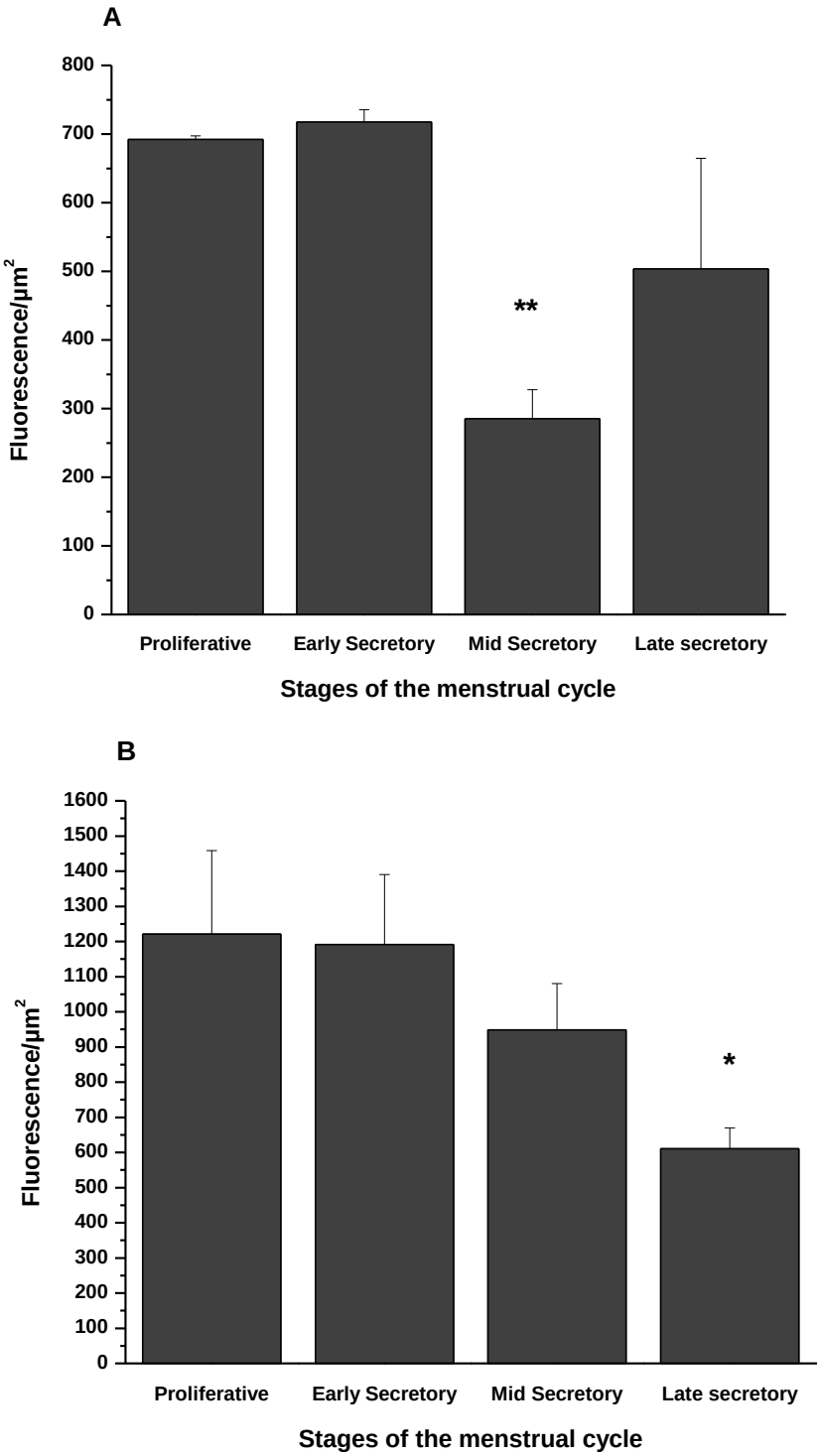

Fig 6.6 Abundance of TRPC1 and TRPC6 in non-permeabilized human endometrium throughout the menstrual cycle. Abundance of TRPC1 was similar at proliferative and early and late secretory phases. However, abundance of TRPC1 was reduced by to half of that proliferative phase at the mid secretory phase of the menstrual cycle (6.6, A). Abundance of TRPC6 was similar at the proliferative, early and mid secretory phases of the menstrual cycle. However, abundance of TRPC6 was reduced to half at the late secretory phase compared to the proliferative phase of the menstrual cycle (6.6, B). All data are expressed as a mean of 3 replicates ± 1 standard deviation. (* = $p<0.05$; ** = $p<0.01$; *** = $p<0.001$).

In the permeabilized human endometrium tissue, abundance of TRPC1 was higher in columnar epithelium compared to the glandular part of the tissue at the proliferative phase of the menstrual cycle (Fig 6.7, A). Abundance of TRPC1 in permeabilized tissue was lower by 0.62 (p= 0.002) and 0.69 (p= 0.008) fold at the early proliferative and late proliferative phases respectively relative to that of the proliferative phase. However, no significant difference was observed in abundance of TRPC1 in permeabilized tissue at mid secretory phase relative to the proliferative phase (Fig 6.8, A).

Abundance of TRPC6 in permeabilized human endometrium was higher in glandular epithelium compared to the columnar epithelium at the proliferative phase as shown by the arrow in Fig 6.7, A. At early and late secretory phase TRPC6 was present at even amounts (Fig 6.7, A, B and D) relative to the proliferative phase. However, abundance of TRPC6 at mid secretory phase in permeabilized human endometrium was even higher by 1.67 fold (p= 0.03) compared to that of the proliferative phase of the menstrual cycle (Fig 6.8, B).

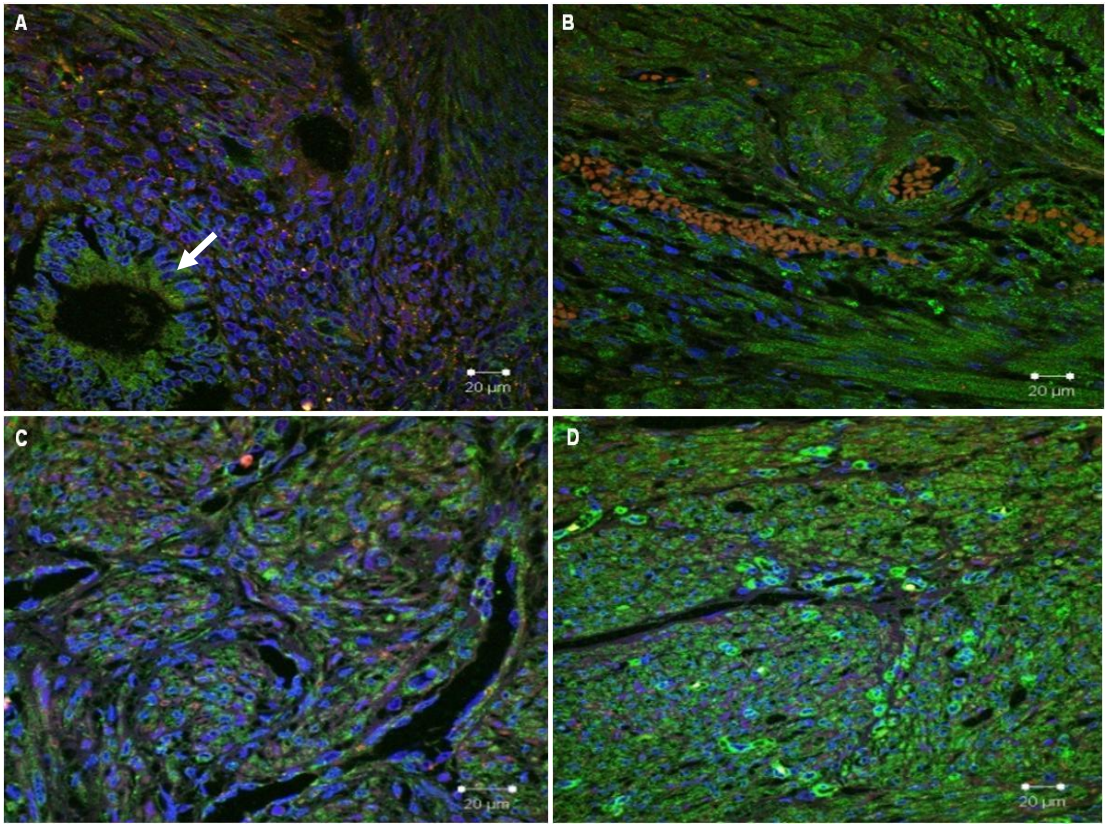

Fig 6.7 Localization and abundance of TRPC1 and TRPC6 in permeabilized human endometrium throughout the menstrual cycle. TRPC1 tended to be more abundant in columnar epithelium compared to glandular cells in permeabilized human endometrium at the proliferative phase of the estrous cycle (6.7 A). However, at the early secretory stage (6.7 B), mid secretory (6.7 C) and late secretory phase (6.7 D) of the menstrual cycle, abundance of TRPC1 was even throughout the tissue. TRPC6 appeared more abundant in the glandular part compared to the rest of the tissue at proliferative phase, shown by an arrow (6.7 A). At early secretory (6.7 B), mid secretory (6.7 C), and late secretory phases (6.7 D) intracellular TRPC6 was localized evenly throughout the permeabilized human endometrium tissue. Nuclei are labelled with DAPI (Blue), TRPC1 with Alexa Four 647 FITC conjugated (Red) and TRPC6 with Alexa Flour 488 (Green).

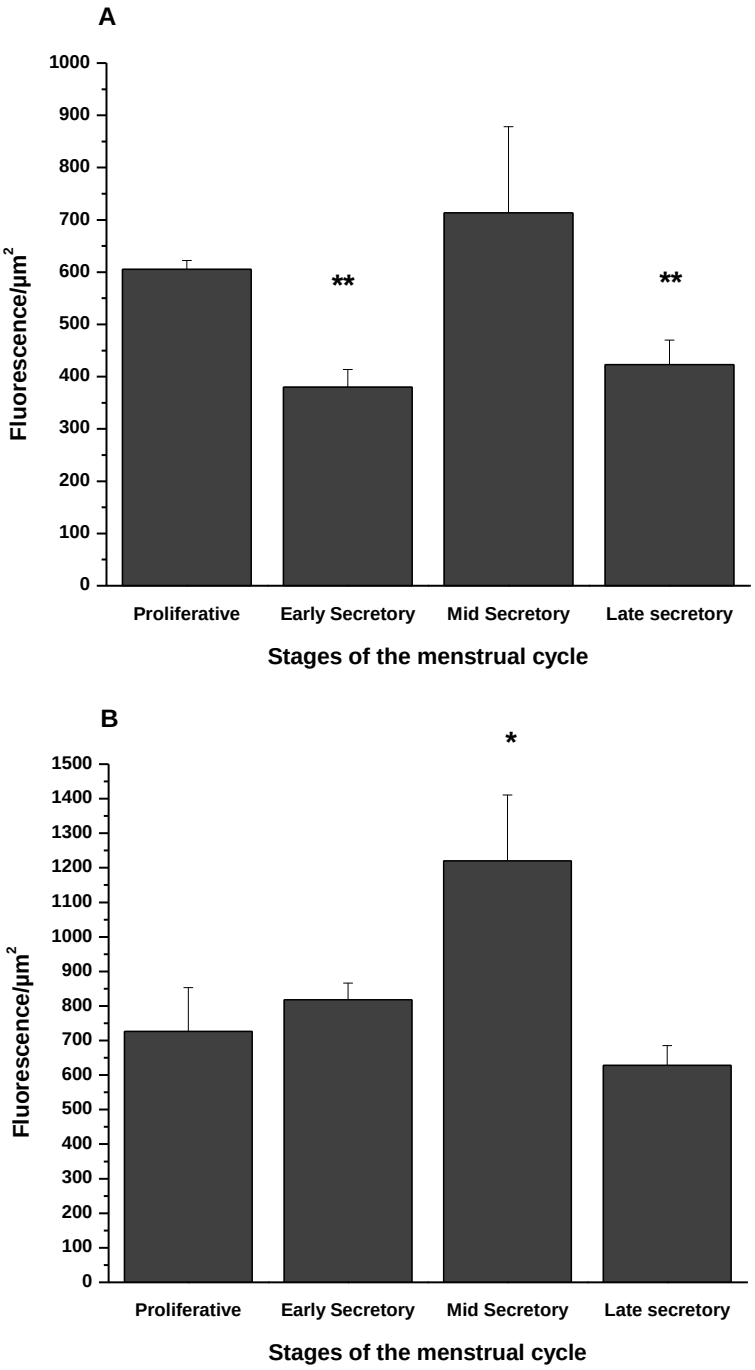

Fig 6.8 Abundance of TRPC1 and TRPC6 in permeabilized human endometrium throughout the menstrual cycle. Abundance of TRPC1 was similar at the proliferative and mid secretory phases. However, lower of TRPC1 was observed at early and late secretory phases (6.8, A). Abundance of TRPC6 was similar in proliferative, early and late secretory phase but higher at mid secretory phase compared to other stages of the menstrual cycle (6.8, B). All data are expressed as a mean of 3 replicates ± 1 standard deviation. (* = $p<0.05$; ** = $p<0.01$; *** = $p<0.001$).

6.4 Discussion

The data presented in this chapter may have significant clinical relevance. The results collected from normal human endometrium indicate that TRPC1, 6 and 7 are expressed (Fig 6.2). Changes in the mRNA expression level of these TRPC isoforms and their physiological role in human endometrium throughout the menstrual cycle could not be studied due to the lack of biopsies. However, changes in mRNA expression of TRPC1, 6 and 7 in the endometrium of patients with Polycystic Ovarian Syndrome as well as endometrium of women attending In Vitro Fertilization (IVF) at day 21 of the menstrual cycle strongly suggest an important role for TRPC channels in human fertility as well as that of the bovine.

Expression of TRPC1 mRNA in endometrium of PCOS patients was not significantly different to that of control tissue. However, mRNA expression level of both TRPC6 and TRPC7 was dramatically increased in endometrium of PCOS patients (Fig 6.3). Between 6-8% percent of women of reproductive age suffer from PCOS (Diamanti-Kandarakis *et al.*, 1999; Asunción *et al.*, 2000; Azziz *et al.*, 2004). Variable clinical presentations are observed in this heterogeneous disorder. However, increased levels of LH and a normal level of FSH are observed in more than 60% of PCOS patients (Blank *et al.*, 2006). Furthermore, the post-ovulatory increase in progesterone secretion is not present in women with PCOS (Blank *et al.*, 2006). In Chapter 3, it was demonstrated that FSH and LH up-regulate the gene expression of TRPC isoforms in BOEC at different stages of the estrous cycle and that progesterone prevents this up-regulatory effect (Fig 3.4-3.8). Furthermore, the mRNA expression level of TRPC isoforms in bovine uterine epithelium was highest at stage 4 of the estrous cycle where progesterone is absent and FSH and LH are at their highest concentration (Fig 3.10). These data suggest a possible up-regulatory role of FSH and LH on mRNA expression of TRPC isoforms in bovine uterine epithelial tissue and endometrium of PCOS patients and the antagonistic activity of progesterone in this process. Examination of TRPC1, 6 and 7 protein expression levels in endometrium of PCOS patients is necessary for further confirmation of these findings.

Expression of TRPC1 and 6 was up-regulated in endometrium of patients attending for IVF compared to that of women without a physiological problem who could not conceive as a result of male partner pathological specification. However, expression of TRPC7 was down-regulated in endometrium of these patients (Fig 6.4). Discovering the mechanism underlying the changes in expression of TRPC1, TRPC6 and TRPC7 in the endometrium of subfertile women who attended for IVF is difficult due to lack of background information about the patients, however, these data do indicate a role for TRPC channels in the epithelial cells of the female reproductive tract.

The examination of changes in TRPC1, 6 and 7 mRNA expression throughout the menstrual cycle was not possible due to difficulties in obtaining human biopsies. However, the protein localization and abundance of TRPC1 and 6 was studied in endometrium of normal women throughout the menstrual cycle. In the glandular epithelium of endometrium, localization of TRPC6 was greater on the apical side. Human endometrium acts as a secretory tissue in the early, mid and late secretory phase (Kabir-Salmani *et al.*, 2005). Evidence for a possible role in this tissue for TRPC channels is provided by the report that G-coupling receptors which are the mediators of TRPC channels are localized on the apical membrane of rat salivary glands and kidney ductal cells (Bandyopadhyay *et al.*, 2005b).

In conclusion, data presented in this chapter indicate an important role of TRPC channels in female reproductive tract, particularly in the epithelium lining the endometrium and fallopian tubes. Furthermore, data collected from human samples confirmed the possibility of a regulatory role of sex hormones on TRPC channel activity.

Chapter 7

Discussion and Conclusion

7. Discussion

The objective of this research was to determine the role of Transient Receptor Potential Canonical channels in female reproductive tract; specifically in the oviduct and uterus. The focus was on epithelial tissue due to its direct interaction with the gametes and embryo (Croxatto, 2002a) as well as its role in providing an optimal environment (Leese *et al.*, 2001) for reproductive processes such as capacitation (Kervancioglu *et al.*, 2000) and fertilization (Kano *et al.*, 1994; Kervancioglu *et al.*, 1997). Intracellular calcium concentration plays a vital role in the physiological function of epithelial cells (Friedman & Gesek, 1995; van de Graaf *et al.*, 2004; Nijenhuis *et al.*, 2005). A variety of channels are involved in calcium homeostasis in epithelial cells, one of which is TRP channels (van de Graaf *et al.*, 2004; Nijenhuis *et al.*, 2005; Menè, 2006; Harteneck & Reiter, 2007; van de Graaf *et al.*, 2007). However, the role of TRP channels as an important superfamily of cation channels has been neglected in the epithelia of female reproductive tract. The focus of the project was on TRPC channels due to their diverse activation pathways as Receptor-Operated Channels (ROC) and Store-Operated Channels (SOC) and physiological function (Xu & Beech, 2001; Clapham, 2003b; Albert *et al.*, 2007). The bovine was used a model for the human due to difficulties in obtaining human biopsies, and the physiological similarities in female reproductive tract and cyclic changes between human and bovine (Navara *et al.*, 1995; Anderiesz *et al.*, 2000; Malhi *et al.*, 2005).

There are several reproductive events after ovulation that are highly calcium dependent. These include: increase in the secretory activity of the epithelial cells lining the oviduct in order to provide an optimal microenvironment for the gametes and the early embryo; increase in the number of ciliated epithelial cells to facilitate the transport of the gametes to the site of the fertilization in the ampullary-isthmus junction (AIJ) as well as helping the movement of the early embryo to the uterus (Hunter, 1994; Croxatto, 2002a). Changes in the intracellular calcium concentration is key in the processes of both secretion (Richardson *et al.*, 1985; Sharma & Rao, 1992; Dickens *et al.*, 1996) and beating frequency of ciliated cells (Salathe, 2006) and TRP channels have been reported to play a role in each process. For example (Uchida & Tominaga, 2011), insulin secretion is mediated by TRPM2 via Cyclic adenosine

diphosphate ribose (cADPR) (Takasawa *et al.*, 1993) and Protein Kinase A (PKA), (Togashi *et al.*, 2006) whereas localization of TRPV4 the base of the cilia in the hamster oviductal epithelial cells (Fernandes *et al.*, 2008) and localization of TRPV4 at the base of cilia in tracheal epithelial cells (Lorenzo *et al.*, 2008) implies a role for these proteins in regulating and stimulating beating frequency of the cilia (Lorenzo *et al.*, 2008)

7.1 TRPC genes expression in epithelial tissue lining female reproductive tract

It was shown in chapter 3 that from seven isoforoms of the TRPC family, TRPC1, 2, 3, 4 and 6 are expressed in both bovine oviduct and uterine epithelial tissue (Fig 3.1 and 3.9). Quantitative measurements of mRNA of TRPC isoforms obtained from each stage of the estrous cycle indicate that the expression level of these isoforms changes throughout the estrous cycle in both the oviduct and uterus (Fig 3.2 and 3.10).

Changes in mRNA expression of TRPC isoforms in bovine oviduct epithelium was different to that of the bovine uterine epithelium throughout the estrous cycle (Fig 3.2 and 3.10). Expression of TRPC1, 2, 3, 4 and 6 in bovine oviduct epithelial tissue was highest at stage 1 where progesterone is the dominant hormone and the concentrations of 17β- estradiol, FSH and LH are very low (Kaneko *et al.*, 1992). However, in uterine epithelial tissue, expression of all the t TRPC isoforms present was highest at stage 4 of the estrous cycle where the concentration of progesterone is very low or absent and 17β- estradiol, FSH and LH are the dominant hormones (Kaneko *et al.*, 1992). Stage 1 (day 1-4) starts immediately after ovulation, when the oocyte is transported into the oviduct. Transport of the oocyte is dependent on the ciliary beat frequency which is calcium-dependant (Schmid & Salathe, 2011). Furthermore, plasma concentration of 17β- estradiol dramatically drops via a reduction in 17β-estradiol production due to the regression of the corpus luteum (CL).

Gene expression of both TRPV5 and TRPV6 is up-regulated by 17β-estradiol in epithelial cells of duodenum. However, the mechanism underlying this up-regulation is not understood (van Abel *et al.*, 2003). The regulatory effect of 17β-estradiol on gene expression of other TRP channel has not been reported. One possible link between 17β-estradiol and regulation of TRPC expression is

the signalling factor nuclear factor-kappa B (NF-ΚB). It has been reported by Valdez and colleagues (2005) that 17β- estradiol stimulates the NF-ΚB activation in bovine granolusa cells (Valdez & Turzillo, 2005). Moreover, It has been reported that FSH triggers the NF-ΚB activity in rat granolusa cells leading to expression of the X-linked inhibitor of apoptosis (XIAP) and inhibition of apoptosis (Valdez & Turzillo, 2005). Furthermore, inhibition of NF-ΚB activation suppresses the FSH-stimulated follicle growth *in vitro* (Wang *et al.*, 2002a). By contrast, progesterone reduces the activation of toll-like receptor 4 (TLR4) and NF-κB signalling pathway in the brain of male rats after subarachnoid hemorrhage (Wang *et al.*, 2011). The promoter region of TRPC1 contains an NF-ΚB binding site (Paria *et al.*, 2004). Furthermore, expression of TRPC1 in human vascular endothelial cells (Paria *et al.*, 2004) and TRPC3 in human airway smooth muscle cells (White *et al.*, 2006) is up-regulated in response to TNF-alpha; which is an activator of NF-ΚB pathway (Findlay *et al.*, 2000). The I kappa B Kinase (IKK) which phosphorylates the NF-ΚB inhibitor (IΚB) is activated by TNF-α. Phosphorylation of IΚB at serine 32 and 36 leads its ubiquitination and degradation by 26S proteasome. This in turn results in the release of the nuclear localization signal of NF-ΚB and translocation of NF-ΚB to the nucleus. Consequently, binding of NF-ΚB to its binding sites on DNA is likely to result in transcription of NF-ΚB-linked proteins such as TRPC1 and TRPC3. However, FSH-induced activation of NF-ΚB is independent of IΚB phosphorylation (Wang *et al.*, 2002b).

At stage 2 and 3 of the estrous cycle, the concentrations of 17β- estradiol and LH are at their lowest level. Several slight increases in FSH concentration (FSH waves) occur throughout stage 2 and 3 of the estrous cycle. An increase in the concentration of Progesterone begins between the end of stage 1 and the beginning of stage 2, reaching a plateau at the end of stage 2 (Gordon, 2003). Progesterone levels drop at the end of stage 3 as the result of regression of the corpus luteum, which is induced by secretion of $PGF_{2\alpha}$ by the endometrium (Schramm *et al.*, 1983). At stage 4 of the estrous cycle, uterine epithelial tissue undergoes proliferation and secretes $PGF_{2\alpha}$ (LaVoie *et al.*, 1975), which is induced by binding of oxytocin to its specific receptor in the endometrium. Oxytocin signalling elicits a rise in inositol phosphates (IPs), key players in the activation pathway for TRPC channels (Clapham, 2003b). Upon activation of

Gq-coupled receptors (Okada *et al.*, 1998; Schaefer *et al.*, 2000) and receptor tyrosine kinases which activate phospholipases C (PLCs), TRP channels might be activated via three pathways; production of diacyglycerol (DAG), hydrolysis of phosphatidylinositol (4,5) bisphosphate and production of inositol (1,4,5) trisphosphate (IP3) (Ramsey *et al.*, 2006). Activation of α subunit of Gq-coupled receptors family leads to stimulation of PLCβ, which in turn results in formation of IP3 and DAG. IP3 binds to the IP3 receptor on the endoplasmic reticulum membrane and promotes calcium release from internal stores. Furthermore, IPs can act as an intracellular calcium concentration regulator (Asselin *et al.*, 1997). DAG is an activator of PKCs (Birnbaumer *et al.*, 1996). Interleukin-1β (IL-1β) is a cytokine that regulates protein synthesis and PGF2α secretion in endometrium (Davidson *et al.*, 1995). Also, IL-1β regulates the expression of TRPC genes in human myometrium (Dalrymple *et al.*, 2004). Furthermore, the role of TRPC isoforms in proliferation such as; TRPC6 (Thebault *et al.*, 2006) and TRPC1 (Fiorio Pla *et al.*, 2005) has already been established. Therefore, IL-1β could have a regulatory effect on endometrium proliferation through TRPC signalling pathways. IL-1β and TNF-α mediate activation of NF-kB in fibroblast-like synoviocytes via IKK-β (Aupperle *et al.*, 1999). The increase in mRNA of the TRPC isoforms present in bovine uterine epithelium at stage 4 of the estrous cycle could be partially related to the effect of IL-1β by a similar mechanism, due to presence of NF-kB binding site in the promoter region of TRPCs such as TRPC1(Paria *et al.*, 2003).

It was interesting to note that the expression pattern of TRPC isoforms in bovine oviduct and uterine epithelial cells maintained in cell culture was different to that of the native tissue. This suggests that a key regulatory factor present in vivo is absent in conventional in vitro culture medium. Given the level of endocrine control of the reproductive cycle, I hypothesised that the sex hormones may play a role in regulating expression of TRP channels. This was based on the observations that sex hormones are the main variable throughout the estrous cycle and were absent in the epithelial culture medium. Further investigation confirmed the hypothesis that sex hormones regulate the gene expression of TRPC isoforms in bovine oviduct and uterine epithelium.

To examine this possibility, BOEC harvested from different stages of the estrous cycle were acutely treated with physiological concentration of sex

hormones (Ginther *et al.*, 2010). A combination of FSH and LH resulted in an up regulation in expression of all TRPC isoforms throughout the estrous cycle. Addition of 17β-estradiol to the mixture of FSH and LH increased the up regulatory effect of FSH and LH for each TRPC isoform throughout the estrous cycle. Each of these have been shown to have a regulatory role on gene expression, for example the regulatory role of 17β- estradiol in gene expression in breast cancer (Charpentier *et al.*, 2000), progesterone-induced gene expression regulation in the endometrium of rhesus moneky (Okulicz & Ace, 1999), role of LH in gene expression regulation in mouse granulosa cells (Carletti & Christenson, 2009) and the regulatory role of FSH in gene expression in pig granulosa primary cells (Bonnet *et al.*, 2006). Furthermore, FSH and LH receptors are expressed in the ovary (Camp *et al.*, 1991), human ovarian surface epithelium and fallopian tube (Zheng *et al.*, 1996), pig fallopian tube (Gawronska *et al.*, 1999) and bovine uterine vein where the LH receptor mRNA and protein level are highest during proestrous and estrous cycle (Shemesh, 2001). It has been reported that 17β-estradiol increases the expression of LH receptors in the epithelium and smooth muscle cells of pig oviduct (Gawronska *et al.*, 1999). The promoter region of LH receptor gene contains three sites for the transcription factor Specificity Protein 1 (SP1) sites (Tsai-Morris *et al.*, 1993). It has been reported that estrogen receptor α (ERα) can interact with SP1 in the promoter of low density lipoprotein receptor (LDLR) gene which leads to activation of LDLR gene transcription by 17b-estradiol in liver hepatoma cells (HepG2) (Li *et al.*, 2001) A similar mechanism might explain the increased up regulatory effect of FSH and LH on TRPC gene expression in BOEC following addition of 17β-estradiol

When Prog was added to the mixture of either FSH and LH or FSH/LH and Est, the up regulatory effect of these combinations on expression of TRPC genes was lost. In cultured murine leydig cells, Prog reduces the mRNA level and function of the LH receptor (El-Hefnawy & Huhtaniemi, 1998). Furthermore, progesterone has an inhibitory effect on activation of toll-like receptor 4 (TLR4) and nuclear factor-kappa B (NF-κB) signalling pathway (Wang *et al.*, 2011). As mentioned above, NF-κB binding site is one of the elements in the promoter of some of TRPC channels such as TRPC1 (Paria *et al.*, 2004) . Enhanced activation of NF-κB by FSH (Wang *et al.*, 2002b)and 17β-estradiol (Valdez &

Turzillo, 2005) and the inhibitory effect of progesterone (Wang *et al.*, 2011) on NF-κB activation could explain the up-regulatory effect of FSH, LH and 17β-estradiol and down-regulatory effect of progesterone on TRPC gene expression in BOEC.

Furthermore, the difference in expression level of some of the TRPC isoforms reported in chapter 3 could be due to expression of their splice variants and possible different regulation pathway; for instance, TRPC1 (Dedman *et al.*, 2004; Dedman *et al.*, 2005) and TRPC4 (Schaefer *et al.*, 2002) with both have several splice variants.

To summarise, TRPC1, 2, 3, 4 and 6 are expressed in both bovine oviduct and uterine epithelium. Expression of these TRPC isoforms changes throughout the estrous cycle. These changes are most likely induced by endocrine changes throughout the estrous cycle as the treatment of BOEC with physiological concentration of Est, FSH, LH and progesterone individually and in combination altered the TRPCs gene expression level in various pattern. Sex hormone possibly induced their effect on TRPC gene expression via TNF-α and NF-κB pathways. To confirm these hypothesis, inhibitors of NF-κB such as SN50 which inhibits the translocation of NF-κB into the nucleus (Wang *et al.*, 2002a) could be used. Expression of TRPC genes could be studied in BOEC treated with NS50 in combination with sex hormones.

7.2 Localization and abundance of TRPC1 and 6 proteins in epithelial tissue lining female reproductive tract

Measuring the Fluorescent intensity of TRPC1 and TRPC6, which are the common TRPC isoforms expressed in both human and bovine endometrium, indicates that TRPC1 and 6 were expressed at the apical, basal and lateral membranes of bovine oviduct epithelium. However, abundance of TRPC6 was generally higher than that of TRPC1. Furthermore, TRPC6 was more abundant on the apical membrane compared to the basal and lateral membranes. This could be due to the direct or indirect physiological role of this TRPC isoforms in secretion in altering the intracellular calcium concentration (Berridge *et al.*, 1998b; Li *et al.*, 2003).

In general, changes in abundance of TRPC1 and TRPC6 were detected in the ampulla and isthmus throughout the estrous cycle, especially their intracellular abundance. The changes in abundance of protein were generally similar to the mRNA level changes detected for these two genes. However, changes in abundance of TRPC1 and TRPC6 in infundibulum did not follow the same pattern as their gene expression throughout the estrous cycle. The infundibulum is a small section of oviduct compared to ampulla and isthmus and the difference observed between the abundance of TRPC1 and TRPC6 channels in infundibulum and their mRNA level in bovine oviduct epithelium could be due to the small amount of mRNA extracted from the infundibulum compared to the ampulla and isthmus. Therefore, the changes in mRNA levels of TRPC1 and TRPC6 in oviduct throughout the estrous cycle mainly reflect those of the ampulla and isthmus but not infundibulum. To re-examine the changes in mRNA level of TRPC1 and TRPC6 in infundibulum, ampulla and isthmus it would be necessary to confirm the difference in abundance of TRPC1 and TRPC6 in different sections of the oviduct throughout the estrous cycle. Due to the lack of research on the role of TRPC channels in epithelia in general and the epithelia lining the female reproductive tract in particular, no literature was found to support or contradict these findings. However, it has been reported that localization of TRPC6 was detected on both the apical and basal sides of epithelial cells, whereas localization of TRPC1 was limited to the basal side of Madin-Darby canine kidney cells (MDCK) and salivary gland epithelial cells. (Bandyopadhyay *et al.*, 2005a). In agreement with the data presented in Chapter 4, TRPC6 was localized on both the apical and basal sides of the epithelial tissue as well as the lateral face of the tissue. In contrast with the report by Bandyopadhyay (2005), localization of TRPC1 in polarized Madin-Darby canine kidney cells (MDCK) and salivary gland epithelial cells was not limited to the basal side of the bovine oviduct/uterine epithelial tissue but was observed on all apical, basal and lateral sides of the tissue. In polarized cells such as epithelial cells, cellular functions which are regulated by calcium are limited to specific microdomains (Muallem & Wilkie, 1999; Petersen, 2000; Bootman *et al.*, 2001; Kiselyov *et al.*, 2002; Kiselyov *et al.*, 2003; Petersen, 2003). These domain-restricted calcium changes have been shown to occur close to the IP3 receptor sites (Sun *et al.*, 1998; Thomas *et al.*, 1998). The apical side of the secretory cells is well-known for local calcium signals

(Petersen *et al.*, 1999) and the oviductal epithelium secrets specific proteins into the oviductal lumen. A group of these proteins are expressed throughout the estrous cycle while secretion of the other group of the proteins by oviductal epithelium is cyclical (Gandolfi *et al.*, 1989). Furthermore, secretion is a well-known feature of the uterine epithelium (Jacobs & Carson, 1993). Apical localization of TRPC6 could be due to its involvement in secretory function of either oviduct or uterine epithelium. Specially, high abundance of TRPC6 on the apical side of the uterine glandular epithelium could confirm this hypothesis.

The epithelial cells in infundibulum are more ciliated compared to the ampulla. The number of ciliated epithelial cells in the isthmus is very low or absent. In the rabbit, secretion of oviductal fluid is greater from the ampulla than the isthmus due to the greater surface area of the epithelial cells in ampulla (Leese, 1983). In the bovine, secretion of oviductal fluid is 10 times greater at estrous where the 17β- estradiol is at its highest concentration throughout the estrous cycle (Roberts *et al.*, 1975). Similarly, in ewes (McDonald & Bellvé, 1969) estradiol triggers the secretion of oviductal fluid, however, progesterone abolishes the estradiol-induced secretion. Non-secretory ciliated epithelial cells undergo hypertrophy, maturation and elongation under the effect of oestrogen (Comer *et al.*, 1998). In contrast, two studies have reported that progesterone induces secretion (Gregoraszczuk *et al.*, 2001), for instance, secretion of dipeptidyl peptidase-IV by endometrium of ewe and cow (Liu & Hansen, 1995). It has been reported that TRP channels are involved in secretion (Uchida & Tominaga, 2011), and Liu et al., (2007) reported that TRPC1 play an important role in the secretion of fluid from salivary gland acinar cells (Liu *et al.*, 2007). Membrane and intracellular abundance of TRPC1 and 6 in different sections of the bovine oviduct was higher in ampulla and isthmus compared to the infundibulum. This could be due to a higher number of non-ciliated secretory epithelial cells in ampulla and isthmus and related to the physiological role of ampulla and isthmus in fertilization (Ellington, 1991) and spermatozoa capacitation (Suarez, 2002).

The difference in abundance of TRPC1 and TRPC6 protein in bovine uterine epithelial tissue at different stages of the estrous cycle was not as dramatic as that of their mRNA level. This difference could be due to post-transcriptional modifications (PTM). However, further investigation is required to clarify the role

of PTM and this could be done by using fluorescent staining of two dimensional gels (Jacob & Turck, 2008).Furthermore, the antibodies used in this research might not be capable of binding to the possible splice variants of TRPC1 and TRPC6 proteins while the mRNA of the possible splice variants could have been detected by the primers used. This could be another reason for differences in the mRNA and protein expression level of TRPC1 and TRPC6 detected in bovine oviduct epithelial cells.

The physiological role of TRPC1 in association with Stromal Interaction Molecule (STIM) and Orai proteins involved in Store-Operated Channels (SOC) complex (Hong *et al.*, 2011) could explain the difference in abundance of these channels on the apical, basal and lateral sides of the oviduct and uterine epithelia. Furthermore, heteromultimerization of TRPC isoforms with each other, which is partially regulated by STIM1 protein, could also affect the localization of these channels (Yuan *et al.*, 2007). Differences in abundance of both TRPC1 and TRPC6 in the bovine oviduct and uterine epithelia throughout the estrous cycle and within the tissue might be due to their various physiological roles which could be a result of the interaction of TRPC channels with other proteins.

7.3 Physiological function of TRPC isoforms in bovine oviduct epithelial cultured cells

Measuring the changes in intracellular calcium concentration using Fura PE 3-AM (calcium dye) indicated that TRPC6 is physiologically active in bovine oviduct epithelial cultured cells. The unexpected response of BOEC to Hyperforin at stage 1 of the estrous cycle, which begins just after ovulation, could be related to the different ratio of homotetramer TRPC6 and heterotetramer TRPC3-TRPC6 in BOEC at this stage of the estrous cycle and the possible difference in the activation pathways of these two protein complexes (Hirschler-Laszkiewicz *et al.*, 2009). Moreover, the physiological association of TRPC6 to STIM and the complex of Orai and STIM (Hong *et al.*, 2011) might affect the channel response to Hyperforin due to the distinct physiological function of TRPC6 channel in the form of Store-operated calcium channels (SOC) or Receptor-operated calcium channels (ROC). However, the role of other TRPC isoforms could not be studied individually due to lack of a specific agonist and antagonist for each TRPC isoforms. Further

investigation is required to address the physiological role of each TRPC isoforms by using siRNA technique to knock out individual isoforms prior to measuring the changes in the intracellular calcium concentration. Furthermore, and as shown in chapter 3, expression level of TRPC isoforms in BOEC is different to that of the intact tissue. Therefore, to provide a better in vitro model, changes in intracellular calcium concentration should be measured in cells treated with physiological concentrations of sex hormones. In addition, as polarity of the epithelial cells is pivotal to their function, measuring the changes in intracellular calcium concentration in polarized cells treated with and without hormones is required to expand our understanding of the physiological role of TRPC channels in the oviduct and uterine epithelia (Chandra *et al.*, 2007). This could be done using transwell permeable supports (Fig 7.1) which permit the cells to take up and secrete molecules on both their apical and basal sides and thereby carry out metabolic activities under more natural conditions, with the cells as a polarized monolayer.

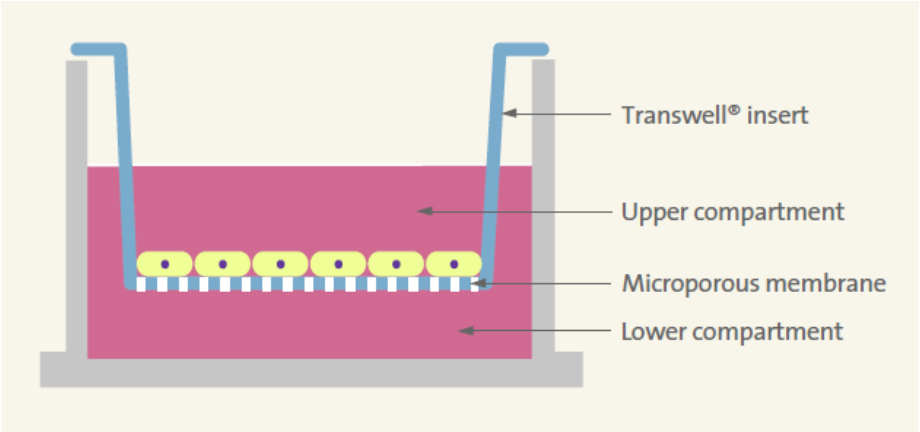

Fig 7.1 Snapwell transwell permeable supports (adapted from Corning, Transwell-guide)

7.4 TRPC channels in human endometrium

To determine the clinical relevance of the data about the role of TRPC channels in epithelial tissue lining the bovine oviduct and uterus, gene expression of TRPC isoforms was studied in endometrium of normal women and women with Polycystic Ovarian Syndrome as well as in endometrium of women at day 21 of the menstrual cycle attending for In Vitro Fertilization (IVF).

Of 7 isoforms of TRPC family, TRPC1, 6 and 7 were expressed in human endometrium. Changes in the expression of TRPC6 and 7 in endometrium of women with PCOS support the idea that FSH and LH, which are elevated in PCOS patients, (Blank *et al.*, 2006) up-regulate the expression of TRPC isoforms, and that progesterone which is absent or present at a very low levels in PCOS patients inhibits the up-regulatory effect of FSH and LH (Blank *et al.*, 2006). This general pattern was observed in *in vitro* studies in Chapter 3. Furthermore, changes in expression level of TRPC1, 6 and 7 in endometrium of women attending for IVF point tantalisingly to a role of TRPC channels in this tissue .

Due to the lack of biopsies of endometrium at different stages of the menstrual cycle, the changes in expression level of TRPC isofoms throughout the menstrual cycle could not be examined. However, localization and abundance of TRPC1 and 6 were studied throughout the menstrual cycle. TRPC1 was more abundant in the epithelium, while TRPC6 was more abundant at the apical membrane of glandular epithelium indicating the possible role of this TRPC isoform in secretion (Li *et al.*, 2003).

7.5 Conclusion and future work

TRPC1, 2, 3, 4 and 6 are expressed in both bovine oviduct and uterine epithelia. The mRNA level of expressed TRPC isoforms in these tissues changes throughout the estrous cycle. Cyclic changes in plasma concentration of sex hormones throughout the estrous cycle may regulate the expression level of TRPC channels. Further investigation is required to determine the mechanisms underlying the regulatory pathways of sex hormones on TRPC channels. TRPC channels are possibly involved in oocyte pick up, sperm capacitation, fertilization and early embryo transport in oviduct and secretion as

they are present throughout the oviduct and uterine epithelia at all 4 stages of the estrous cycle. The TRPC6 channel is physiologically active in bovine oviduct epithelial cultured cells.

Studying the mRNA expression of each of TRPC isoforms and their splice variants in infundibulum, ampulla and isthmus is necessary to determine the relation between the gene and protein expression of each of these isoforms at different stages of the estrous cycle. Furthermore, finding the possible changes in the gene and protein expression level of FSH, LH, Est and Prog receptors would be critical for understanding the regulatory effect of these hormones on gene and protein expression of TRPCs in the epithelial tissues lining the female reproductive tract. Hence, to determine the physiological activation of other TRPC isoforms in oviduct and uterine epithelium, the siRNA technique to knockout individual TRPC isoforms would be useful. Moreover, activity of these channels in polarized epithelial monolayers and in the presence of physiological concentration of sex hormones needs to be studied. More importantly, creating TRPC isoform-deficient mice and studying oocyte maturation, fertilization, early embryo transport, implantation and any other reproductive events would provide a great opportunity for understanding the role of these important calcium channels in mammalian female reproduction.

The expression level of TRPC channels in women attending for IVF was significantly different compared to the control. Further investigation is therefore required to determine the changes in expression level of TRPC isofoms throughout the menstrual cycle. Moreover, determining the association between the mRNA and protein expression of TRPC isoforms in human endometrium and fallopian epithelium throughout the menstrual cycle is important. Finally, the physiological role of TRPC channels in the endometrium needs to be determined using calcium imaging and electrophysiological, including patch clamp, techniques.

References

Abdelgadir SE, Jaeger JR, Oldfield JE, Appell LH & Stormshak F. (1994). Oxytocin synthesis and secretion from bovine corpora lutea exposed in vitro to cycloheximide and colchicine. *Domest Anim Endocrino* **11,** 349-354.

Adeyemo O & Heath E. (1980). Plasma progesterone concentration in Bos taurus and Bos indicus heifers. *Theriogenology* **14,** 411-419.

Ahmed A, Sage SO, Plevin R, Shoaibi MA, Sharkey AM & Smith SK. (1994). Functional platelet-activating factor receptors linked to inositol lipid hydrolysis, calcium mobilization and tyrosine kinase activity in the human endometrial HEC-1B cell line. *J Reprod Fertil* **101,** 459-466.

Albert AP, Saleh SN, Peppiatt-Wildman CM & Large WA. (2007). Multiple activation mechanisms of store-operated TRPC channels in smooth muscle cells. *The journal of Physiology* **583,** 25-36.

Alexander DB & Goldberg GS. (2003). Transfer of biologically important molecules between cells through gap junction channels. *Curr Med Chem* **10,** 2045– 2058.

Anderiesz C, Ferraretti A, Magli C, Fiorentino A, Fortini D, Gianaroli L, Jones GM & Trounson AO. (2000). Effect of recombinant human gonadotrophins on human, bovine and murine oocyte meiosis, fertilization and embryonic development in vitro. *Hum Reprod* **15,** 1140-1148.

Asselin E, Drolet P & Fortier MA. (1997). Cellular mechanisms involved during oxytocin-induced prostaglandin F2alpha production in endometrial epithelial cells in vitro: role of cyclooxygenase-2. *Endocrinology* **138,** 4798-4805.

Asunción M, Calvo RM, San Millán JL, Sancho J, Avila S & Escobar-Morreale HF. (2000). A prospective study of the prevalence of the polycystic ovary syndrome in unselected Caucasian women from Spain. *J Clin Endocrinol Metab* **85,** 2434-2438.

Aupperle KR, Bennett BL, Boyle DL, Tak PP, Manning AM & Firestein GS. (1999). NF-kappa B regulation by I kappa B kinase in primary fibroblast-like synoviocytes. *J Immunol* **163,** 427-433.

Aurbach GD, Marx SJ & Spiegel AM. (1992). *Parathyroid hormone, calcitonin, and the calciferols. In: Wilson JD, Foster DW, eds. Williams textbook of endocrinology*. WB Suanders, Philadelphia.

Azziz R. (2006). Diagnosis of Polycystic Ovarian Syndrome: The Rotterdam Criteria Are Premature. *J of Clinical Endocrinology and Metabolism* **91,** 781-785.

Azziz R, Woods KS, , , Reyna R, Key TJ, Knochenhauer ES & Yildiz BO. (2004). The prevalence and features of the polycystic ovary syndrome in an unselected population. *J Clin Endocrinol Metab* **89,** 2745-2749.

Babich LG, Ku CY, Young HWJ, Huang H, Blackburn MR & Sanborn BM. (2004). Expression of Capacitative Calcium TrpC Proteins in Rat Myometrium During Pregnancy. *Biology of reproduction* **70,** 919-924.

Balen AH, Conway GS, Kaltsas G, Techatraisak K, Manning PJ, West C & Jacobs HS. (1995). Polycystic ovary syndrome: the spectrum of the disorder in 1741 patients. *Hum Reprod* **10,** 2107-2111.

Bandyopadhyay BC, Swaim WD, Liu X, Redman RS, Patterson RL & Ambudkar IS. (2005a). Apical Localization of a Functional TRPC3/TRPC6-Ca^{2+}-Signaling Complex in Polarized Epithelial Cells *The Journal of Biological Chemistry* **280,** 12908–12916.

Bandyopadhyay BC, Swaim WD, Liu X, Redman RS, Patterson RL & Ambudkar IS. (2005b). Apical localization of a functional TRPC3/TRPC6-Ca2+-signaling complex in polarized epithelial cells. Role in apical Ca2+ influx. *J Biol Chem* **280,** 12908-12916.

Barber TM, McCarthy MI, Wass JAH & Franks S. (2006). Obesity and polycystic ovary syndrome. *Clinical Endocrinology* **65,** 137-145.

Barbour GL, Coburn JW, Slatopolsky E, Norman AW & Horast RL. (1981). Hypercalcemia in an anephric patient with sarcoidosis: evidence for extrarenal generation of 1,25-dihydroxyvitamin. *N Engl J Med* **305,** 440-443.

Benais-Pont G, Punn A, Flores-Maldonado C, Eckert J, Raposo G, Fleming TP, Cereijido M, Balda MS & Matter K. (2003). Identification of a tight junction-associated guanine nucleotide exchange factor that activates Rho and regulates paracellular permeability. *J Cell Biol* **160,** 729-740.

Berridge MJ, Bootman MD & Lipp P. (1998a). Calcium--a life and death signal. *Nature* **395,** 645-648.

Berridge MJ, Bootman MD & Lipp P. (1998b). Calcium – a life and death signal. *Nature* **395,** 645-648.

Biner HL, Arpin-Bott MP, Loffing J, Wang X, Knepper M, Hebert SC & Kaissling B. (2002). Human cortical distal nephron: distribution of electrolyte and water transport pathways. *J Am Soc Nephrol* **13,** 836–847.

Birnbaumer L, Zhu X, Jiang M, Boulay G, Peyton M, Vannier B, Brown D, Platano D, Sadeghi H, Stefani E & Birnbaumer M. (1996). On the molecular basis and regulation of cellular capacitative calcium entry: roles for Trp proteins. *PNAS* **93,** 15195-15202.

Blank SK, McCartney CR & Marshall JC. (2006). The origins and sequelae of abnormal neuroendocrine function in polycystic ovary syndrome. *Human Reprod Update* **12,** 351-361.

Blaustein MP, Juhaszova M, Golovina VA, Church PJ & Stanley EF. (2002). Na/Ca exchanger and PMCA localization in neurons and astrocytes: functional implications. *Ann NY Acad Sci* **976,** 356–366.

Blaustein MP & Lederer WJ. (1999). Sodium/calcium exchange: its physiological implications. *Physiol Rev* **79,** 763–854.

Bonnet A, Frappart PO, Dehais P, Tosser-Klopp G & Hatey F. (2006). Identification of differential gene expression in in vitro FSH treated pig granulosa cells using suppression subtractive hybridization. *Reprod Biol Endocrinol* **4,** 35.

Bootman MD, Lipp P & Berridge MJ. (2001). The organisation and functions of local Ca(2+) signals. *J Cell Sci* **114,** 2213-2222.

Borke JL, Caride A, Verma AK, Penniston JT & Kumar R. (1989). Plasma membrane calcium pump and 28-kDa calcium binding protein in cells of rat kidney distal tubules. *Am J Physiol Renal Fluid Electrolyte Physiol* **257,** F842–F849.

Boron WF & Emile LB. (2005). *Medical Physiology (updated Edition)*. Elsevier Saunders, USA.

Boulay G, Brown DM, Qin N, Jiang M, Dietrich A, Zhu MX, Chen Z, Birnbaumer M, Mikoshiba K & Birnbaumer L. (1999). Modulation of Ca(2+) entry by polypeptides of the inositol 1,4,5-trisphosphate receptor (IP3R) that bind transient receptor potential (TRP):

evidence for roles of TRP and IP3R in store depletion-activated Ca(2+) entry. *PNAS* **96,** 14955–14960.

Boulay G, Zhu X, Peyton M, Jiang M, Hurst R, Stefani E & L B. (1997). Cloning and expression of a novel mammalian homolog of Drosophila transient receptor potential (Trp) involved in calcium entry secondary to activation of receptors coupled by the Gq class of G protein. *J Biol Chem* **272,** 29672–29680.

Cai X & Lytton J. (2004). Molecular cloning of a sixth member of the K+-dependent Na+/Ca2+ exchanger gene family, NCKX6. *J Biol Chem* **279,** 5867–5876.

Camp TA, Rahal JO & Mayo KE. (1991). Cellular localization and hormonal regulation of follicle-stimulating hormone and luteinizing hormone receptor messenger RNAs in the rat ovary. *Mol Endocrinol* **5,** 1405-1417.

Carletti MZ & Christenson LK. (2009). Rapid effects of LH on gene expression in the mural granulosa cells of mouse periovulatory follicles. *Reproduction* **137,** 843-855.

Chandra A, Barillas S, Suliman A & Angle N. (2007). novel fluorescence-based cellular permeability assay. *J Biochem Biophys Methods* **70,** 329-333.

Chang AS, Chang SM, Garcia RL & Schilling WP. (1997). Concomitant and hormonally regulated expression of trp genes in bovine aortic endothelial cells. *FEBS Letters* **415,** 335-340.

Channing CP, Schaerf FW, Anderson LD & Tsafriri A. (1980). Ovarian follicular and luteal physiology. *Int Rev Physiol* **22,** 117-201.

Charpentier AH, Bednarek AK, Daniel RL, Hawkins KA, Laflin KJ, Gaddis S, MacLeod MC & Aldaz CM. (2000). Effects of estrogen on global gene expression: identification of novel targets of estrogen action. *Cancer Research* **60,** 5977-5983.

Cherednichenko G, Hurne AM, Fessenden JD, Lee EH, Allen PD, Beam KG & Pessah IN. (2004). Conformational activation of Ca2+ entry by depolarization of skeletal myotubes. *PNAS* **101,** 15793-15798.

Chevesich J, Kreuz AJ & Montell C. (1997). Requirement for the PDZ domain protein, INAD, for localization of the TRP store-operated channel to a signaling complex. *Neuron* **18,** 95-105.

Clapham DE. (2003a). TRP channels as cellular sensors. *Nature* **426,** 517-524.

Clapham DE. (2003b). TRP channels as cellular sensors. *Nature* **426,** 517-524.

Clapham DE, Runnels LW & Strübing C. (2001). The trp ion channel family *Nature Reviews Neuroscience* **2,** 387-396

Clarke CL & Sutherland RL. (1990). Progestin regulation of cellular proliferation. *Andocr Rev* **11,** 266-301.

Comer MT, Leese HJ & Southgate J. (1998). Induction of a differentiated ciliated cell phenotype in primary cultures of Fallopian tube epithelium. *Human Reproduction* **13,** 3114–3120.

Corey DP. (2003). New TRP Channels in Hearing and Mechanosensation. *Neuron* **39,** 585–588.

Croxatto HB. (2002a). Physiology of gamete and embryo transport through the Fallopian tube. *Rerod Biomed Online* **4,** 160-169.

Croxatto HB. (2002b). Physiology of gamete and embryo transport through the fallopian tube. *Reprod Biomed Online* **4,** 160-169.

D'Esposito M, Strazzullo M, Cuccurese M, Spalluto C, Rocchi M, D'Urso M & Ciccodicola A. (1998). Identification and assignment of the human transient receptor potential channel 6 gene TRPC6 to chromosome 11q21-->q22. *Cytogenet Cell Genet* **83,** 46–47.

Dalrymple A, Slater DM, Poston L & RM. T. (2004). Physiological induction of transient receptor potential canonical proteins, calcium entry channels, in human myometrium: influence of pregnancy, labor, and interleukin-1 beta. *J Clin Endocrinol Metab* **89,** 1291-1300.

Davidson JA, Tiemann U, Betts JG & Hansen PJ. (1995). DNA synthesis and prostaglandin secretion by bovine endometrial cells as regulated by interleukin-1. *Reprod Fertil Dev* **7,** 1037-1043.

Dedman AM, Zeng F, Kumar B, Clynes M, Bateson A & Beech DJ. (2005). Regulated alternative splicing of TRPC1 transcripts. In *J Physiol (University of Oxford)*, pp. 568P- PC522.

Dedman AM, Zeng F, McHugh D, Kumar B, Jackson PK, Fountain SJ, Cheong A, Sivaprasadarao A & Beech DJ. (2004). Alternatively spliced transcripts encoding TRPC1 cationic channel in human brain and blood vessels. In *J Physiol (University of Glasgow)*.

Delmas P. (2004). Polycystins: From Mechanosensation to Gene Regulation. *cell* **118,** 145–148.

Diamanti-Kandarakis E, Kouli CR, Bergiele AT, Filandra FA, Tsianateli TC, Spina GG, Zapanti ED & Bartzis MI. (1999). A survey of the polycystic ovary syndrome in the Greek island of Lesbos: hormonal and metabolic profile. *J Clin Endocrinol Metab* **84,** 4006-4011.

Dickens CJ, Comer MT, Southgate J & HJ.Leese HJ. (1996). Human Fallopian tubal epithelial cells in vitro: establishment of polarity and potential role of intracellular calcium and extracellular ATP in fluid secretion. *Human Reproduction* **11,** 212-217.

Dietrich A, Mederos y Schnitzler M, Emmel J, Kalwa H, Hofmann T & Gudermann T. (2003). N-linked protein glycosylation is a major determinant for basal TRPC3 and TRPC6 channel activity. *J Biol Chem* **278,** 47842–47852.

Dietrich JW, Canalis EM, Maina DM & Raisz LG. (1976). Hormonal control of bone collagen synthesis in vitro: effects of parathyroid hormone and calcitonin. *Endocrinology* **98,** 943-949.

Ding YQ, Zhu LJ, Bagchi MK & Bagchi IC. (1994). Progesterone stimulates calcitonin gene expression in the uterus during implantation. *Endocrinology* **135,** 2265-2274.

Dong YL, Vegiraju S, Chauhan M & Yallampalli C. (2003). Expression of calcitonin gene-related peptide receptor components, calcitonin receptor-like receptor and receptor activity modifying protein 1, in the rat placenta during pregnancy and their cellular localization. *Mol Hum Reprod* **9,** 481-490.

Doucet A & Katz AI. (1982). High-affinity Ca-Mg-ATPase along the rabbit nephron. *Am J Physiol Renal Fluid Electrolyte Physiol* **242,** F346–F352.

Downing SJ, Maguiness SD, Tay JI, Watson A & Leese HJ. (2002). Effect of platelet-activating factor on the electrophysiology of the human Fallopian tube: early mediation of embryo-maternal dialogue? *Reproduction* **124,** 523-529.

Dufau ML. (1998). The Luteinizing hormone receptor. *Ann Rev Physiol* **60,** 461-496.

Ebnet. K., Aurrand-Lions. M., Kuhn. A., Kiefer. F., Butz. S., Zander. K., Z.U. M, Brickwedde. M.K., Suzuki. A., Imhof. B.A. & Vestweber. D. (2003). The junctional adhesion molecule (JAM) family members JAM-2 and JAM-3 associate with the cell polarity protein PAR-3: a possible role for JAMs in endothelial cell polarity. *J Cell Sci* **116,** 3879-3891.

Echternkamp SE & Hansel W. (1973). Concurrent changes in bovine plasma hormone levels prior to and during the first postpartum estrous cycle. *Journal of Animal Science* **37,** 1362-1370.

Eduvie LO & Dawuda PM. (1986). Effect of suckling on reproductive activities of Bunaji cows during the postpartum period. *Journal of Agricultural Science (Cambridge)* **107,** 235-238.

El-Hefnawy T & Huhtaniemi I. (1998). Progesterone can participate in down-regulation of the luteinizing hormone receptor gene expression and function in cultured murine Leydig cells. *Mol Cell Endocrinol* **137,** 127-138.

Ellington JE. (1991). The bovine oviduct and its role in reproduction: a review of the literature. *Cornell Vet* **81,** 313-328.

Fernandes J, Lorenzo IM, Andrade YN, Garcia-Elias A, Serra SA, Fernández-Fernández JM & Valverde MA. (2008). IP3 sensitizes TRPV4 channel to the mechano- and osmotransducing messenger 5'-6'-epoxyeicosatrienoic acid. *J Cell Biol* **181,** 143-155.

Findlay JK, Drummond AE, Britt KL, Dyson M, Wreford NG, Robertson DM, Groome NP, Jones ME & Simpson ER. (2000). The roles of activins, inhibins and estrogen in early committed follicles. *Mol Cell Endocrinol* **163,** 81-87.

Fiorio Pla A, Maric D, Brazer SC, Giacobini P, Liu X, Chang YH, Ambudkar IS & Barker JL. (2005). Canonical transient receptor potential 1 plays a role in basic fibroblast growth factor

(bFGF)/FGF receptor-1-induced Ca2+ entry and embryonic rat neural stem cell proliferation. *J Neuroscience* **25,** 2687-26701.

Franks S. (1995). Polycystic Ovary Syndrome. *N Engl J Med* **333,** 853-861.

Friedman J, Au W & Raisz LG. (1968). Responses of fetal rat bone to thyrocalcitonin in tissue culture. *Endocrinology* **82,** 149-156.

Friedman PA, Coutermarsh BA, Kennedy SM & Gesek FA. (1996). Parathyroid hormone stimulation of calcium transport is mediated by dual signaling mechanisms involving protein kinase A and protein

kinase C. *Endocrinology* **137,** 13-20.

Friedman PA & Gesek FA. (1995). Cellular calcium transport in renal epithelia: measurement, mechanisms, and regulation. *Physiol Rev* **75,** 429-471.

Fu Q, Jilka RL, Manolagas SC & O'Brien CA. (2002). Parathyroid hormone stimulates receptor activator of NFkappa B ligand and inhibits osteoprotegerin expression via protein kinase A activation of cAMP-response element-binding protein. *J Biol Chem* **277,** 48868-48875.

Gandolfi F, Brevini TA, Richardson L, Brown CR & Moor RM. (1989). Characterization of proteins secreted by sheep oviduct epithelial cells and their function in embryonic development. *Development* **106,** 303-312.

Garcia NH, Ramsey CR & Knox FG. (1998). Understanding the role of paracellular transport in the proximal tubule. *News Physiol Sci* **13,** 38–43.

Garrod D & Chidgey M. (2008). Desmosome structure, composition and function. *Bioch biophys Acta* **1778,** 572–587.

Garrod D, Chidgey M & North A. (1996). Desmosomes: differentiation, development, dynamics, and disease. *Curr Opin Cell Biol* **5,** 670-678.

Gawronska B, Paukku T, Huhtaniemi I, Wasowicz G & Ziecik AJ. (1999). Oestrogen-dependent expression of LH/hCG receptors in pig Fallopian tube and their role in relaxation of the oviduct. *J Reprod Fertil* **115,** 293-301.

Ginther OJ, Shrestha HK & Beg MA. (2010). Circulating hormone concentrations within a pulse of a metabolite of prostaglandin F2α during preluteolysis and early luteolysis in heifers. *Anim Reprod Sci* **122,** 253-258.

Gkonos PJ, London R & Hendler ED. (1984). Hypercalcemia and elevated 1,25-dihydroxyvitamin D levels in a patient with end-stage renal disease and active tuberculosis. *N Engl J Med* **311,** 1683-1685.

Goel M, Sinkins WG & Schilling WP. (2002). Selective association of TRPC channel subunits in rat brain synaptosomes. *J Biol Chem* **277,** 48303–48310.

Gögelein H, Dahlem D, Englert HC & Lang HJ. (1990). Flufenamic acid, mefenamic acid and niflumic acid inhibit single nonselective cation channels in the rat exocrine pancreas. *FEBS Letters* **268,** 79-82.

González-Mariscal L, Betanzos A, Nava P & Jaramillo BE. (2003). Tigh junction proteins. *Prog Biophys Mol Biol* **81,** 1-44.

Goodenough DA. (1999). Plugging the leaks. *PNAS* **96,** 319-321.

Gopalakrishnan S, Dunn KW & Marrs JA. (2002). Rac1, but not RhoA, signaling protects epithelial adherens junction assembly during ATP depletion. *Am J Physiol Cell Physiol* **283,** C261–C272.

Gordon I. (2003). *Laboratory Production of Cattle Embryos, 2nd Edition*. CABI Publisher, UK, Cambridge.

Graham CE, Collins DC, Robinson H & Preedy JR. (1972). Urinary levels of estrogens and pregnanediol and plasma levels of progesterone during the menstrual cycle of the chimpanzee; relationship to the sexual swelling. *Endocrinology* **91,** 13-24.

Grasberger H, Van Sande J, Hag-Dahood Mahameed A, Tenenbaum-Rakover Y & Refetoff S. (2007). A familial thyrotropin (TSH) receptor mutation provides in vivo evidence that the inositol phosphates/Ca2+ cascade mediates TSH action on thyroid hormone synthesis. *J Clin Endocrinol Metab* **92,** 2816-2820.

Green KJ & Jones JC. (1996). Desmosomes and hemidesmosomes: Structure and function of molecular components. *FASEB J* **10,** 871–881.

Gregoraszczuk EL, Milewicz T, Kolodziejczyk J, Krzysiek J, Basta A, Sztefko K, Kurek S & Stachura J. (2001). Progesterone-induced secretion of growth hormone, insulin-like growth factor I and prolactin by human breast cancer explants. *Gynecol Endocrinol* **15,** 251-258.

Greka A, Navarro B, Oancea E, Duggan A & Clapham DE. (2003). TRPC5 is a regulator of hippocampal neurite length and growth cone morphology. *Nat Neurosci* **6,** 837–845.

Gründker C, Schulz K, Günthert AR & Emons G. (2000). Luteinizing hormone-releasing hormone induces nuclear factor kappaB-activation and inhibits apoptosis in ovarian cancer cells. *J Clin Endocrinol Metab* **85,** 3815-3820.

Hardie RC, Minke, B.,. (1992). The trp gene is essential for a light-activated Ca2+ channel in Drosophila photoreceptors. *Neuron* **8,** 643-651.

Harteneck C & Reiter B. (2007). TRP channels activated by extracellular hypo-osmoticity in epithelia. *Biochem Soc Trans* **35,** 91-95.

Heersche JNM, Marcus R & Aurbach GD. (1974). Calcitonin and the formation of 3`,5` cAMP in bone and kidney. *Endocrinology* **94,** 241-247.

Hirschler-Laszkiewicz I, Tong Q, Conrad K, Zhang W, Flint WW, Barber AJ, Barber DL, Cheung JY & Miller BA. (2009). TRPC3 activation by erythropoietin is modulated by TRPC6. *J Biol Chem* **284,** 4567=4581.

Hoenderop JG DPJ, Bindels RJ, and Willems PH. (1999). Hormone-stimulated Ca2 reabsorption in rabbit kidney cortical collecting system is cAMP-independent and involves a phorbol ester-insensitive PKC isotype. *Kidney Int* **55,** 225–233.

Hoenderop JG, Hartog A, Stuiver M, Doucet A, Willems PH & Bindels RJ. (2000). Localization of the epithelial Ca2+ channel in rabbit kidney and intestine. *J Am Soc Nephrol* **11,** 1171–1178.

Hoenderop JG, Nilius B & Bindels RJ. (2002). Molecular mechanism of active Ca2 reabsorption in the distal nephron. *Annu Rev Physiol* **64,** 529–549.

Hofmann T, Obukhov AG, Schaefer M, Harteneck C, Gudermann T & Schultz G. (1999). Direct activation of human TRPC6 and TRPC3 channels by diacylglycerol. *Nature* **397,** 259–263.

Hofmann T, Schaefer M, Schultz G & Gudermann T. (2000). Transient receptor potential channels as molecular substrates of receptor-mediated cation entry. *J Mol Med* **78,** 14–25.

Hofmann T, Schaefer M, Schultz G & Gudermann T. (2002). Subunit composition of mammalian transient receptor potential channels in living cells. *PNAS* **99,** 7461–7466.

Hong JH, Li Q, Kim MS, Shin DM, Feske S, Birnbaumer L, Cheng KT, Ambudkar IS & Muallem S. (2011). Polarized but differential localization and recruitment of STIM1, Orai1 and TRPC channels in secretory cells. *Traffic* **12,** 232-245.

Huguenard JH. (1998). Low voltage-activated (T-type) Ca2+ channel genes identified. *Trend in Neural Science* **21,** 451-452.

Hunter RHF. (1994). Modulation of gamete and embryonic microenvironments by oviduct glycoproteins. *Mol Reprod Dev* **39,** 176-181.

Ireland JJ, Murphee RL & Coulson PB. (1980). Accuracy of predicting stages of bovine estrous cycle by gross appearance of the corpus luteum.

Ireland JJ, Murphee RL, Coulson PB. *J Dairy Sci* **63,** 155-160.

Jacob AM & Turck CW. (2008). Detection of post-translational modifications by fluorescent staining of two-dimensional gels. *Methods Mol Biol* **446,** 21-32.

Jacobs AL & Carson DD. (1993). Uterine epithelial cell secretion of interleukin-1 alpha induces prostaglandin E2 (PGE2) and PGF2 alpha secretion by uterine stromal cells in vitro. *Endocrinology* **132,** 300-308.

Jimenez-Gonzalez C, Michelangeli F, Harper CV, Barratt CL & Publicover SJ. (2006). Calcium signalling in human spermatozoa: a specialized 'toolkit' of channels, transporters and stores. *Human Reprod Update* **12,** 253-247.

Kabir-Salmani M, Nikzad H, Shiokawa S, Akimoto, Y., & Iwashita M. (2005). Secretory role for human uterodomes (pinopods): secretion of LIF. *Mol Hum Reprod* **11,** 553-559.

Kaltenbach CC, Dunn TG, Kiser TE, Corah LR, Akbar AM & Niswender GD. (1974). Release of FSH amd LH in beef heifers by synthetic gonadotropin releasing hormone. *Journal of Animal Science* **38,** 357.

Kandel ER, Schwartz JH & Jessell TM. (1995). *Principles of Neural Science*. Elsevier, New York.

Kaneko H, Nakanishi Y, Akagi S, Arai K, Taya K, Watanabe G, Sasamoto S & Hasegawa Y. (1995). Immunoneutralization of inhibin and estradiol during the follicular phase of the estrous cycle in cows. *Bio Reprod* **53,** 931-939.

Kaneko H, Watanabe G, Taya K & Sasamoto S. (1992). Changes in peripheral levels of bioactive and immunoreactive inhibin, estradiol-17 beta, progesterone, luteinizing hormone, and follicle-stimulating hormone associated with follicular development in cows induced to superovulate with equine chorionic gonadotropin. *Biol Reprod* **47,** 76-82.

Kano K, Miyano T & Kato S. (1994). Effect of oviductal epithelial cells on fertilization of pig oocytes in vitro. *Theriogenology* **1,** 1061-1068.

Kawashima H, Kraut JA & Kurokawa K. (1982). Metabolic acidosis suppresses 25-hydroxyvitamin D_3-1a-hydroxylase in the rat kidney. *J Clin Investig* **70,** 135-140.

Kero J, Ahmed K, Wettschureck N, Tunaru S, Wintermantel T, Greiner E, Schütz G & Offermanns S. (2007). Thyrocyte-specific Gq/G11 deficiency impairs thyroid function and prevents goiter development. *J Clin Invest* **117,** 2399-2407.

Kervancioglu ME, Saridogan E, Aitken RJ & Djahanbakhch O. (2000). Importance of sperm-to-epithelial cell contact for the capacitation of human spermatozoa in fallopian tube epithelial cell cocultures. *Fertility and Sterility* **74,** 780-784.

Kervancioglu ME, Saridogan E, Atasü T, Camlibel T, Demircan A, Sarikamis B & Djahanbakhch O. (1997). Human Fallopian tube epithelial cell co-culture increases fertilization rates in male factor infertility but not in tubal or unexplained infertility. *Hum Reprod* **12,** 1253-1258.

Kip SN & Strehler EE. (2003). Characterization of PMCA isoforms and their contribution to transcellular Ca2 flux in MDCK cells. *Am J Physiol Renal Physiol Renal Physiol* **284,** F122–F132.

Kip SN & Strehler EE. (2004). Vitamin D3 upregulates plasma membrane Ca2+-ATPase expression and potentiates apico-basal Ca2+ flux in MDCK cells. *Am J Physiol Renal Physiol* **286,** F363–F369.

Kiselyov K, Shin DM, Luo X, Ko SB & Muallem S. (2002). Ca2+ signaling in polarized exocrine cells. *Adv Exp Med Biol* **506,** 175-183.

Kiselyov K, Shin DM & Muallem S. (2003). Signalling specificity in GPCR-dependent Ca2+ signalling. *Cell Signal* **15,** 243-253.

Kleinau G, Jaeschke H, Worth CL, Mueller S, Gonzalez J, Paschke R & Krause G. (2010). Principles and determinants of G-protein coupling by the rhodopsin-like thyrotropin receptor. *PLoS One* **5**.

Kowalczyk AP, Stappenbeck TS, Parry DA, Palka HL, Virata ML, Bornslaeger EA, Nilles LA & Green KJ. (1994). Structure and function of desmosomal transmembrane core and plaque molecules. *Biophys Chem* **50,** 97–112.

Kumar NM & Gilula NB. (1996). The gap junction communication channel. *Cell* **84,** 381–388.

Lajeunesse D, Bouhtiauy I & Brunette MG. (1994). Parathyroid hormone and hydrochlorothiazide increase calcium transport by the luminal membrane of rabbit distal nephron segments through different pathways. *Endocrinology* **134,** 35–41.

LaVoie VA, Poncelet GR, Han DK, Soliday CL, Lambert PW & Moody EL. (1975). Effect of Prostaglandin F2a on the Estrous Cycle, Corpora Lutea and Profesterone Levels of Hysterectomized Cows. *J of Animal Science* **41,** 166-171.

Lawn AM. (1973). The ultrastructure of the endometrium during the sexual cycle. *Adv Reprod Physiol* **6,** 61-95.

The Fallopian Tube in Infertility and IVF Practice

Cambridge University Press UK, Cambridge.

Lee YM, Kim BJ, Kim HJ, Yang DK, Zhu MH, Lee KP, So I & Kim KW. (2003). TRPC5 as a candidate for the nonselective cation channel activated by muscarinic stimulation in murine stomach. *Am J Physiol Gastrointest Liver Physiol* **284,** G604–G616.

Leese HJ. (1983). Studies on the movement of glucose, pyruvate and lactate into the ampulla and isthmus of the rabbit oviduc. *Quarterly Journal of Experimental Physiology* **68,** 89-96.

Leese HJ, Tay JI, Reischl J & Downing SJ. (2001). Formation of Fallopian tubal fluid: role of a neglected epithelium. *Reproduction* **121,** 339-346.

Li C, Briggs MR, Ahlborn TE, Kraemer FB & Liu J. (2001). Requirement of Sp1 and estrogen receptor alpha interaction in 17beta-estradiol-mediated transcriptional activation of the low density lipoprotein receptor gene expression. *Endocrinology* **142,** 1546-1553.

Li S, Westwick J & Poll C. (2003). Transient receptor potential (TRP) channels as potential drug targets in respiratory disease. *Cell Calcium* **33,** 551-558.

Li XF, Kraev AS & Lytton J. (2002). Molecular cloning of a fourth member of the potassium-dependent sodium-calcium exchanger gene family, NCKX4. *J Biol Chem* **277,** 48410–48417.

Li Z, Matsuoka S, Hryshko LV, Nicoll DA, Bersohn MM, Burke EP, Lifton RP & Philipson KD. (1994). Cloning of the NCX2 isoform of the plasma membrane Na+-Ca2+ exchanger. *J Biol Chem* **269,** 17434–17439.

Liman ER, Corey DP & Dulac C. (1999). TRP2: a candidate transduction channel for mammalian pheromone sensory signaling. *PNAS* **96,** 5791-5796.

Lin AY & Rui YC. (1994). Platelet-activating factor induced calcium mobilization and phosphoinositide metabolism in cultured bovine cerebral microvascular endothelial cells. *Biochim Biophys Acta* **1224,** 323-328.

Linck B, Qiu Z, He Z, Tong Q, Hilgemann DW & Philipson KD. (1998). Functional comparison of the three isoforms of the Na+ -Ca2+ exchanger (NCX1, NCX2, NCX3). *Am J Physiol* **274,** 415-423.

Liu WJ & Hansen PJ. (1995). Progesterone-induced secretion of dipeptidyl peptidase-IV (cluster differentiation antigen-26) by the uterine endometrium of the ewe and cow that costimulates lymphocyte proliferation. *Endocrinology* **136,** 779-787.

Liu X, Cheng KT, Bandyopadhyay BC, Pani B, Dietrich A, Paria BC, Swaim WD, Beech D, Yildrim E, Singh BB, Birnbaumer L & Ambudkar IS. (2007). Attenuation of store-operated Ca2+ current impairs salivary gland fluid secretion in TRPC1(-/-) mice. *PNAS* **104,** 17542-17547.

Livak KJ & Schmittgen TD. (2001). Analysis of Relative Gene Expression Data Using Real-Time Quantitative PCR and the 22DDCT Method. *Methods* **25,** 402-408.

Llewelyn CA, Munro CD, Luckins AG, Jordt T, Murray M & Lorenzini E. (1987). Behavioural and ovarian changes during the oestrous cycle in the Boran (Bos indicus). *British Veterinary Journal* **143,** 75-82.

Loffing J, Loffing-Cueni D, Valderrabano V, Klausli L, Hebert SC, Rossier BC, Hoenderop JG, Bindels RJ & Kaissling B. (2001). Distribution of transcellular calcium and sodium transport pathways along mouse distal nephron. *Am J Physiol Renal Physiol* **281,** F1021–F1027.

Lorenzo IM, Liedtke W, Sanderson MJ & Valverde MA. (2008). TRPV4 channel participates in receptor-operated calcium entry and ciliary beat frequency regulation in mouse airway epithelial cells. *Proc Natl Acad Sci* **105,** 12611-12616.

Lowry OH, Rosebrough NJ, Farr AL & Randall RJ. (1951). Protein measurement with the Folin Phenol Reagent. *Journal of Biological Chemistry* **193,** 265-275.

Lussier MP, Cayouette S, Lepage PK, Bernier CL, Francoeur N, St-Hilaire M, Pinard M & Boulay G. (2005a). MxA, a Member of the Dynamin Superfamily, Interacts with the Ankyrin-like Repeat Domain of TRPC. *THE JOURNAL OF BIOLOGICAL CHEMISTRY* **280,** 19393–19400.

Lussier MP, Cayouette S, Lepage PK, Bernier CL, Francoeur N, St-Hilaire M, Pinard M & BoulayG. (2005b). MxA, amember of the dynamin superfamily, interactswith the ankyrin-like repeat domain of TRPC. *J Biol Chem* **280,** 19393–19400.

Malhi PS, Adams GP & Singh J. (2005). Bovine model for the study of reproductive aging in women: follicular, luteal, and endocrine characteristics. *Bio Reprod* **73,** 45-53.

Marion S, Robert F, Crepieux P, Martinat N, Troispoux C, Guillou F & Reiter E. (2002). G protein-coupled receptor kinases and beta arrestins are relocalized and attenuate cyclic 3',5'-adenosine monophosphate response to follicle-stimulating hormone in rat primary Sertoli cells. *Biol Reprod* **66,** 70-76.

Martìn-Padura. I., Lostaglio. S., Schneemann. M., Williams. L., Romano. M., Fruscella. P., Panzeri. C., Stoppacciaro. A., Ruco. L., Villa. A., Simmons. D. & Dejana. E. (1998). Junctional adhesion molecule, a novel member of the immunoglobulin superfamily that distributes at intercellular junctions and modulates monocyte transmigration. *J Cell Biol* **142,** 117-127.

Martin L. (1980). *Estrogens, anti-estrogen and the regulation of cell proliferation*

in the female reproductive tract in vivo. Elsevier, New York,.

Martin L, Das RM & Finn CA. (1973). The inhibition by progesterone of uterine epithelial proliferation in the mouse. *J Endocrinol* **57,** 549-554.

Massheimer V, Boland R & de Boland AR. (1994). Rapid 1,25(OH)2-vitamin D3 stimulation of calcium uptake by rat intestinal cells involves a dihydropyridine-sensitive cAMP-dependent pathway. *Cell Signal* **6,** 299–304.

McDonald MF & Bellvé AR. (1969). Influence of oestrogen and progesterone on flow of fluid from the Fallopian tube in the ovariectomized ewe. *Journal of Reproduction and Fertility* **20,** 51-61.

McKay RR, Szymeczek-Seay CL, Lievremont JP, Bird GS, Zitt C, Jungling E, Luckhoff A & Putney JW Jr. (2000). Cloning and expression of the human transient receptor potential 4 (TRP4) gene: localization and functional expression of human TRP4 and TRP3. *Biochem J* **351,** 735–746.

Mendoza-Rodriguez CA, Merchant-Larois H, Segura-Valdez ML, Moreno-Mendoza N, Cruz ME, Arteaga-Lopez P, Camacho-Arroyo I, Dominguez R & Cerbon M. (2003). c-fos and Estrogen Receptor Gene Expression Pattern in the Rat Uterine Epithelium During

the Estrous Cycle. *Molecular Reproduction and Development* **64,** 379-388.

Menè P. (2006). Transient receptor potential channels in the kidney: calcium signaling, transport and beyond. *J Nephrol* **19,** 21-29.

Menezo Y & Guerin P. (1997). The mammalian oviduct: biochemistry and physiology. *Eur J Obstet Gynecol Reprod Bio* **73,** 97-104.

Mesiano S & Welsh TN. (2007). Steroid hormone control of myometrial contractility and parturition. *Semin Cell Dev Biol* **18,** 321-331.

Mizuno N, Kitayama S, Saishin Y, Shimada S, Morita K, Mitsuhata C, Kurihara H & Dohi T. (1999). Molecular cloning and characterization of rat trp homologues from brain. *Brain Res Mol Brain Res* **64,** 41–51.

Montell C, Birnbaumer L & Flockerzi V. (2002a). The TRP Channels, a Remarkably Functional Family. *Cell* **108,** 595–598.

Montell C, Birnbaumer L, Flockerzi V, Bindels RJ, Bruford EA, Caterina MJ, Clapham DE, Harteneck C, Heller S, Julius D, Kojima I, Mori Y, Penner R, Prawitt D, Scharenberg AM, Schultz G, Shimizu N & Zhu MX. (2002b). A Unified Nomenclature for the Superfamily of TRP Cation Channels. *Molecular Cell* **9,** 229–231.

Montell C, Birnbaumer L, Flockerzi V, Bindels RJ, Bruford EA, Caterina MJ, Clapham DE, Harteneck C, Heller S, Julius D, Kojima I, Mori Y, Penner R, Prawitt D, Scharenberg AM, Schultz G, Shimizu N & Zhu MX. (2002). A unified nomenclature for the superfamily of TRP cation channels. *Mol Cell* **9,** 229–231.

Moreau R, Hamel A, Daoud G, Simoneau L & Lafond J. (2002). Expression of calcium channels along the differentiation of cultured trophoblast cells from human term placenta. *Biol Reprod* **67,** 1473–1479.

Mori Y, Takada N, Okada T, Wakamori M, Imoto K, Wanifuchi H, Oka H, Oba A, Ikenaka K & Kurosaki T. (1998). Differential distribution of TRP Ca2+ channel isoforms in mouse brain. *Neuroreport* **9,** 507–515.

Muallem S & Wilkie TM. (1999). G protein-dependent Ca2+ signaling complexes in polarized cells. *Cell Calcium* **26,** 173-180.

Mundy GR & Guise TA. (1999). Hormonal Control of Calcium Homeostasis. *Clinical Chemistry* **45,** 1347-1352.

Nadler RD, Graham CE, Collins DC & Gould KG. (1979). Plasma gonadotropins, prolactin, gonadal steroids, and genital swelling during the menstrual cycle of lowland gorillas. *Endocrinology* **105,** 290-296.

Navara CS, Simerly C & Schatten G. (1995). Imaging motility during fertilization. *Theriogenology* **44,** 1099-1114.

Nicoll DA, Quednau BD, Qui Z, Xia YR, Lusis AJ & Philipson KD. (1996). Cloning of a third mammalian Na+-Ca2+ exchanger, NCX3. *J Biol Chem* **271,** 24914–24921.

Nijenhuis T, Hoenderop JG & Bindels RJ. (2005). TRPV5 and TRPV6 in Ca(2+) (re)absorption: regulating Ca(2+) entry at the gate. *Pflugers Arch* **451,** 181-192.

Norman AW, Roth J & Orci L. (1982). The vitamin D endocrine system: steroid metabolism, hormone, receptors, and biological response (calcium binding proteins). *Endocr Rev* **3,** 331-366.

North AJ, Bardsley WG, Hyam J, Bornslaeger EA, Cordingley HC, Trinnaman B, Hatzfeld M, Green KJ, Magee AI & Garrod DR. (1999). Molecular map of the desmosomal plaque. *J Cell Sci* **112,** 4325–4336.

Novak E & Everett HS. (1928). Cyclical and other variations in the tubal epithelium. *Am J Obstet Gynecol* **16,** 499-505.

Nozaki M & Ito Y. (1987). Changes in physiological properties of rabbit oviduct by ovarian steroids. *Am J Physiol* **252,** R1059-1065.

Obukhov AG & Nowycky MC. (2004). TRPC5 activation kinetics are modulated by the scaffoldingprotein ezrin/radixin/moesin-binding phosphoprotein-50 (EBP50). *JCellPhysiol* **201,** 227–235.

Ohki G, Miyoshi T, Murata M, Ishibashi K, Imai M & Suzuki M. (2000). A Calcium-activated Cation Current by an Alternatively Spliced Form of Trp3 in the Heart. *THE JOURNAL OF BIOLOGICAL CHEMISTRY* **275,** 39055–39060.

Okada T, Inoue R, Yamazaki K, Maeda A, Kurosaki T, Yamakuni T, Tanaka I, Shimizu S, Ikenaka K, Imoto K & Mori Y. (1999). Molecular and functional characterization of a novel mouse transient receptor potential protein homologue TRP7. Ca2+-permeable cation channel that is constitutively activatedandenhancedby stimulationofGprotein-coupled receptor. *J Biol Chem* **274,** 27359–27370.

Okada T, Shimizu S, Wakamori M, Maeda A, Kurosaki T, Takada N, Imoto K & Mori Y. (1998). Molecular cloning and functional characterization of a novel receptor-activated TRP Ca2+ channel from mouse brain. *J Biol Chem* **273,** 10279–10287.

Okada T, Shimizu S, Wakamori M, Maeda A, Kurosaki T, Takada N, Imoto K & Mori Y. (1998). Molecular cloning and functional characterization of a novel receptor-activated TRP Ca2+ channel from mouse brain. *J Biol Chem* **273,** 10279-10287.

Okulicz WC & Ace CI. (1999). Progesterone-regulated gene expression in the primate endometrium. *Semin Reprod Endocrinol* **17,** 241-255.

Okutsu Y, Itoh MT, Takahashi N & Ishizuka B. (2010). Exogenous androstenedione induces formation of follicular cysts and premature luteinization of granulosa cells in the ovary. *Fertil Steril* **93,** 927-935.

Padinjat R & Andrews S. (2004). TRP channels at a glance. *J Cell Sci* **117,** 5707-5709.

Pak WL, Grossfield, J., Arnold, K.S.,. (1970). Mutants of the visual pathway of Drosophila melanogaster. *nature* **227,** 518-520.

Pappenheimer JR. (1987). Physiological regulation of transepithelial impedance in the intestinal mucosa of rats and hamsters. *J Membr Biol Cell* **100,** 137-148.

Paria BC, Malik AB, Kwiatek AM, Rahman A, May MJ, Ghosh S & Tiruppathi C. (2003). Tumor necrosis factor-alpha induces nuclear factor-kappaB-dependent TRPC1 expression in endothelial cells. *J Biol Chem* **278,** 37195-37203.

Paria BC, Vogel SM, Ahmmed GU, Alamgir S, Shroff J, Malik AB & Tiruppathi C. (2004). Tumor necrosis factor-alpha-induced TRPC1 expression amplifies store-operated Ca2+ influx and endothelial permeability. *Am J Physiol Lung Cell Mol Physil* **287,** L1303-1313.

Pauerstein CJ & Eddy CA. (1979). The role of the oviduct in reproduction; our knowledge and our ignorance. *J Reprod Fertil* **55,** 223-229.

Pedersen SF, Owsianik G & Nilius B. (2005). TRP channels: An overview. *Cell Calcium* **38,** 233-252.

Peng JB, Brown EM & Hediger MA. (2003). Epithelial Ca2 entry channels: transcellular Ca2 transport and beyond. *J Physiol* **551,** 729–740.

Peng JB, Chen XZ, Berger UV, Vassilev PM, Tsukaguchi H, Brown EM & Hediger MA. (1999). Molecular cloning and characterization of a channel-like transporter mediating intestinal calcium absorption. *J Biol Chem* **274,** 22739–22746.

Perez-Reyes E. (2003). Molecular physiology of low-voltage-activated t-type calcium channels. *Physiol Rev* **83,** 117-161.

Peters KE, Bergfeld EG, Cupp AS, Kojima FN, Mariscal V, Sanchez T, Wehrman ME, Grotjan HE, Hamernik DL, Kittok RJ & Kinder JE. (1994). Luteinizing hormone has a role in development of fully functional corpora lutea (CL) but is not required to maintain CL function in heifers. *Bio Reprod* **51,** 1248-1254.

Petersen OH. (2000). The functional organisation of calcium signalling in exocrine acinar cells. *J Korean Med Sci* **15,** S44-45.

Petersen OH. (2003). Localization and regulation of Ca2+ entry and exit pathways in exocrine gland cells. *Cell Calcium* **33,** 337-344.

Petersen OH, Burdakov D & Tepikin AY. (1999). Polarity in intracellular calcium signaling. *BioEssays* **21,** 851-860.

Peterson GL. (1979). Review of the Folin phenol Quantitayion Method of Lowry, Rosebrough, Farr, and Randall. *Analytical Biochemistry* **100,** 201-220.

Philipp S, Cavalie A, Freichel M, Wissenbach U, Zimmer S, Trost C, Marquart A, Murakami M & Flockerzi V. (1996). A mammalian capacitative calcium entry channel homologous to Drosophila TRP and TRPL. *EMBO J* **15,** 6166-6171.

Philipp S, Hambrecht J, Braslavski L, Schroth G, Freichel M, Murakami M, Cavalie´ A & Flockerzi V. (1998). A novel capacitative calcium entry channel expressed in excitable cells. *The EMBO Journal* **17,** 4274–4282.

Philipson KD & Nicoll DA. (2000). Sodium-calcium exchange: a molecular perspective. *Annu Rev Physiol* **62,** 111–133.

Plant TD & Schaefer M. (2003). TRPC4 and TRPC5: receptor-operated Ca2+-permeable nonselective cation channels. *Cell Calcium* **33,** 441–450.

Prelevic GM. (1997). Insulin resistance in polycystic ovary syndrome. *Curr Opin Abstet Gynnecol* **9,** 193-201.

Preuss KD, No¨ller JK, Krause E, Go¨bel A & Schulz I. (1997). Expression and Characterization of a trpl Homolog from Rat. *BIOCHEMICAL AND BIOPHYSICAL RESEARCH COMMUNICATIONS* **240,** 167–172.

Quamme GA. (1980). Effect of calcitonin on calcium and magnesium transport in rat nephron. *Am J Physiol* **238,** E573-E578.

Ramsey IS, Delling M & Clapham DE. (2006). An introduction to TRP channels. *Annu Rev Physiol* **68,** 619-647.

Randel RD. (1980). Total serum estrogens before and after estrus in Brahman, Brahman x Hereford and Hereford heifers. *Journal of Animal Science* **51**.

Riccio A, Mattei C, Kelsell RE, Medhurst AD, Calver AR, Randall AD, Davis JB, Benham CD & Pangalos MN. (2002). Cloning and functional expression of human short TRP7, a candidate protein for store-operated Ca2+ influx. *J Biol Chem* **277,** 12302–12309.

Riccio A , Medhurst AD , Mattei C, Kelsell RE, Calver AR , Randall AD, Benham CD & Pangalosa MN. (2002). m RNA distribution analysis of human TRPC family in CNS and peripheral tissues. *Molecular Brain Research* **109,** 95-104.

Richardson PS, Mian N & Balfre K. (1985). The role of calcium ions in airway secretion. *Br J clin Pharmac* **20,** 275s-279s.

Roberts GP, Parker JM & Symonds HW. (1975). Proteins in the luminal

fluid from the bovine oviduct. *Journal of Reproduction and Fertility* **45,** 301-313.

Rotterdam ESHRE/ASRM-Sponsored PCOS Consensus Workshop Group. (2004). Revised 2003 consensus on diagnostic criteria and long-term health risks related to polycystic ovary syndrome. *Fertil Steril* **81,** 19-25.

Rychkov G & Barritt GJ. (2007). TRPC1 Ca2+-Permeable Channels in Animal Cells. *HEP* **179,** 23–52.

Sagle M, Bishop K, Ridley N, Alexander FM, Michel M, Bonney RC, Beard RW & Franks S. (1988). Recurrent early miscarriage and polycystic ovaries. *British Medical Journal* **297,** 1027-1028.

Salathe M. (2006). Regulation of mammalian ciliary beating. *Annu Rev Physiol* **69,** 401-422.

Sanborn BM. (2000). Relationship of ion channel activity to control of myometrial calcium. *J Soc Gynecol Investig* **7,** 4-11.

Schaefer M, Plant TD, Obukhov AG, Hofmann T, Gudermann T & Schultz G. (2000). Receptor-mediated regulation of the nonselective cation channels TRPC4 and TRPC5. *J Biol Chem* **275,** 17517–17526.

Schaefer M, Plant TD, Obukhov AG, Hofmann T, Gudermann T & Schultz G. (2000). Receptor-mediated regulation of the nonselective cation channels TRPC4 and TRPC5. *J Biol Chem* **275,** 17517-17526.

Schaefer M, Plant TD, Stresow N, Albrecht N & Schultz G. (2002). Functional differences between TRPC4 splice variants. *J Biol Chem* **277,** 3752–3759.

Schams DF, Hofer E, Schallenberger E, Hartl M & Karg H. (1974). Pattern of luteinizing hormone (LH) and follicle stimulating hormone (FSH) in bovine blood plasma after injection of a synthetic gonadotropin-releasing hormone (GnRH). . *Theriogenology* **1,** 137.

Schild D & Restrepo D. (1998). Transduction mechanisms in vertebrate olfactory receptor cells. *Physiol Rev* **78,** 429-466.

Schmid A & Salathe M. (2011). Ciliary beat co-ordination by calcium. *Biol Cell* **103,** 159-168.

Schmidt A, Heid HW, Schafer S, Nuber UA, Zimbelmann R & Franke WW. (1994). Desmosomes and cytoskeletal architecture in epithelial differentiation: Cell type-specific plaque components and intermediate filament anchorage. *Eur J Cell Biol* **65,** 229–245.

Schramm W, Bovaird L, Glew ME, Schramm G & McCracken JA. (1983). Corpus luteum regression induced by ultra-low pulses of prostaglandin F2 alpha. *Prostaglandins* **26,** 347-364.

Shalgi R & Phillips DM. (1988). Motility of rat spermatozoa at the site of fertilization. *Biol Reprod* **39,** 1207-1213.

Sharma SC & Rao AJ. (1992). Role of calcium in secretion of chorionic gonadotropin by first trimester human placenta. *Indian Journal of Experimental Biology* **30,** 1105-1110.

Shemesh M. (2001). Actions of gonadotrophins on the uterus. *Reproduction* **121,** 835-842.

Sherwood L. (2008). *Human Physiology From Cells to Systems*. Yolanda Cossio, Canada.

Singh A, Hildebrand ME, Garcia E & Snutch TP. (2010). The transient receptor potential channel antagonist SKF96365 is a potent blocker of low-voltage-activated T-type calcium channels. *Br J Pharmacol* **160,** 1464-1475.

Slater M, Barden JA & Murphy CR. (2000). The purinergic calcium channels P2X1,2,5,7 are down-regulated while P2X3,4,6 are up-regulated during apoptosis in the ageing rat prostate. *Histochem J* **32,** 571-580.

Söhl G & Willecke K. (2004). Gap junctions and the connexin protein family. *Cardiovasc Res* **62,** 228-232.

Sossey-Alaoui K, Lyon JA, Jones L, Abidi FE, Hartung AJ, Hane B, Schwartz CE, Stevenson RE & Srivastava AK. (1999). Molecular Cloning and Characterization of TRPC5 (HTRP5), the Human Homologue of a Mouse Brain Receptor-Activated Capacitative Ca21 Entry Channel. *Genomics* **60,** 330–340.

Stauffer TP, Hilfiker H, Carafoli E & Strehler EE. (1993). Quantitative analysis of alternative splicing options of human plasma membrane calcium pump genes. *J Biol Chem* **268,** 25993–26003.

Stein IF & Leventhal ML. (1935). Amenorrhoea associated with bilateral polycystic ovaries. *American Journal of Obstetrics anf Gynecology* **29,** 181-191.

Strehler EE & Zacharias DA. (2001). Role of alternative splicing in generating isoform diversity among plasma membrane calcium pumps. *Physiol Rev* **81,** 21-50.

Stru¨bing C, Krapivinsky G, Krapivinsky L & Clapham DE. (2003). Formation of Novel TRPC Channels by Complex Subunit Interactions in Embryonic Brain. *THE JOURNAL OF BIOLOGICAL CHEMISTRY* **278,** 39014–39019.

Strubing C, Krapivinsky G, Krapivinsky L & Clapham DE. (2001). TRPC1 and TRPC5 Form a Novel Cation Channel in Mammalian Brain. *Neuron* **29,** 645–655.

Strubing C, Krapivinsky G, Krapivinsky L & Clapham DE. (2003). Formation of novel TRPC channels by complex subunit interactions in embryonic brain. *J Biol Chem* **278,** 39014–39019.

Suarez SS. (2002). Formation of a reservoir of sperm in the oviduct. *Reprod Domest Anim* **37,** 140-143.

Suda T, Takahashi N & Martin TJ. (1992). Modulation of osteoclast differentiation. *Endocr Rev* **13,** 66-80.

Sun XP, Callamaras N, Marchant JS & Parker I. (1998). A continuum of InsP3-mediated elementary Ca2+ signalling events in Xenopus oocytes. *J Physiol* **509,** 67-80.

Suss-Toby E SZ, Minke B,. (1991). Lanthanum reduces the excitation efficiency in fly photoreceptors. *THE JOURNAL OF GENERAL PHYSIOLOGY* **98,** 849-868.

Takahashi N, Yamana H, Yoshiki S, Roodman GD, Mundy GR, Jones SJ, Boyde A & Suda T. (1988). Osteoclast-like cell formation and its regulation by osteotropic hormones in mouse bone marrow cultures. *Endocrinology* **122,** 1373-1382.

Takasawa S, Nata K, Yonekura H & Okamoto H. (1993). Cyclic ADP-ribose in insulin secretion from pancreatic beta cells. *Science* **259,** 370-373.

Talbot P, Geiske C & Knoll M. (1999). Oocyte pickup by the mammalian oviduct. *Mol Biol Cell* **10,** 5-8.

Tesarik J & Sousa M. (1996). Mechanism of calcium oscillations in human oocytes: a two-store model. *Mol Hum Reprod* **2,** 383-386.

Thebault S, Flourakis M, Vanoverberghe K, Vandermoere F, Roudbaraki M, Lehen'kyi V, Slomianny C, Beck B, Mariot P, Bonnal JL, Mauroy B, Shuba Y, Capiod T, Skryma R & Prevarskaya N. (2006). Differential role of transient receptor potential channels in Ca2+ entry and proliferation of prostate cancer epithelial cells. *Cancer Research* **15,** 2038-2047.

Thomas D, Lipp P, Berridge MJ & Bootman MD. (1998). Hormone-stimulated calcium puffs in non-excitable cells are not stereotypic,but reflect activation of different size channel clusters and variable recruitment of channels within a cluster. *J Biol Chem* **173,** 27130-27136.

Tibbetts TA, Mendoza-Meneses M, O'Malley B. W. & Conneely OM. (1998). Mutual and Intercompartmental Regulation of Estrogen Receptor and Progesterone

Receptor Expression in the Mouse Uterus. *Biology of reproduction* **59,** 1143-1152.

Tiemann U & Hansen PJ. (1995). Steroidal and growth factor regulation of [3H]thymidine incorporation by cultured endosalpingeal cells of the bovine oviduct. *In Vitro Cell Dev Biol Anim* **31,** 640-645.

Tiemann U, Neels P, Küchenmeister U, Walzel H & Spitschak M. (1996). Effect of ATP and platelet-activating factor on intracellular calcium concentrations of cultured oviductal cells from cows. *J Reprod Fertil* **108,** 1-9.

Tinel H, Denker HW & Thie M. (2000). Calcium influx in human uterine epithelial RL95-2 cells triggers adhesiveness for trophoblast-like cells. Model studies on signalling events during embryo implantation. *Mol Hum Reprod* **6,** 1119-1130.

Togashi K, Hara Y, Tominaga T, Higashi T, Konishi Y, Mori Y & Tominaga M. (2006). TRPM2 activation by cyclic ADP-ribose at body temperature is involved in insulin secretion. *EMBO J* **225,** 1804-1815.

Tsai-Morris CH, Xie X, Wang W, Buczko E & Dufau ML. (1993). Promoter and RegulatorRy egions of the Rat LuteinizingH ormone receptor gene. *J Biol Chem* **268,** 4447-4452.

Tsilchorozidou T, Overton C & Conway GS. (2004). The pathophysiology of polycystic ovary syndrome. *Clinical Endocrinology* **60,** 1-17.

Uchida K & Tominaga M. (2011). The role of thermosensitive TRP (transient receptor potential) channels in insulin secretion. *Endocr J*.

Valdez KE & Turzillo AM. (2005). Regulation of nuclear factor-kappaB (NF-kappaB) activity and apoptosis by estradiol in bovine granulosa cells. *Mol Cell Endocrinol* **243,** 66-73.

van Abel M, Hoenderop JG, van der Kemp AW, van Leeuwen JP & Bindels RJ. (2003). Regulation of the epithelial Ca2+ channels in small intestine as studied by quantitative mRNA detection. *Am J Physiol Gastrointest Liver Physiol* **285,** G78-85.

van de Graaf SF, Bindels RJ & Hoenderop JG. (2007). Physiology of epithelial Ca2+ and Mg2+ transport. *Rev Physiol Biochem Pharmacol* **158,** 77-160.

van de Graaf SF, Boullart I, Hoenderop JG & Bindels RJ. (2004). Regulation of the epithelial Ca2+ channels TRPV5 and TRPV6 by 1alpha,25-dihydroxy Vitamin D3 and dietary Ca2+. *J Steroid Biochem Mol Biol* **89-90,** 303-308.

Vanden Abeele F, Shuba Y, Roudbaraki M, Lemonnier L, Vanoverberghe K, Mariot P, Skryma R & Prevarskaya N. (2003). Store-operated Ca2+ channels in prostate cancer epithelial cells: function, regulation, and role in carcinogenesis. *Cell Calcium* **33,** 357-373.

Vannier b, Peyton M, Boulay G, Brown D, Qin N, Jiang M, Zhu X & Birnbaumer L. (1999). Mouse trp2, the homologue of the human trpc2 pseudogene, encodes mTrp2, a store depletion-activated capacitative Ca21 entry channel. *Proc Natl Acad Sci USA* **96,** 2060–2064.

Velasquez LA, Aguilera JG & Croxatto HB. (1995). Possible role of platelet-activating factor in embryonic signaling during oviductal transport in the hamster. *Biol Reprod* **52,** 1302-1306.

Venkatachalam K & Montell C. (2007). TRP Channels. *The Annual Review of Biochemistry* **76,** 387-417.

Venkatachalam K, Zheng F & Gill DL. (2003). Regulation of canonical transient receptor potential (TRPC) channel function by diacylglycerol and protein kinase C. *J Biol Chem* **278,** 29031–29040.

Verhage HG, Bareither ML, Jaffe RC & Akbar M. (1979). Cyclic changes in ciliation, secretion and cell height of the oviductal epithelium in women. *Am J Anat* **156,** 505-521.

Walker RL, Hume JR & Horowitz B. (2001). Differential expression and alternative splicing of TRP channel genes in smooth muscles. *Am J Physiol Cell Physiol* **280,** C1184–C1192.

Wang H, Eriksson H & Sahlin L. (2000). Estrogen Receptors αλπηα and beta in the Female Reproductive Tract of the Rat During

the Estrous Cycle. *Biology of reproduction* **63,** 1331-1340.

Wang Y, Chan S & Tsang BK. (2002a). Involvement of inhibitory nuclear factor-kappaB (NFkappaB)-independent NFkappaB activation in the gonadotropic regulation of X-linked inhibitor of apoptosis expression during ovarian follicular development in vitro. *Endocrinology* **143,** 2732-2740.

Wang Y, Chan S & Tsang BK. (2002b). Involvement of inhibitory nuclear factor-kappaB (NFkappaB)-independent NFkappaB activation in the gonadotropic regulation of X-linked inhibitor of apoptosis expression during ovarian follicular development in vitro. *Endocrinology* **143,** 2732-2740.

Wang Y, Zhang J, Yi XJ & Yu FS. (2004). Activation of ERK1/2 MAP kinase pathway induces tight junction disruption in human corneal epithelial cells. *Exp Eye Res* **78,** 125-136.

Wang Z, Zuo G, Shi XY, Zhang J, Fang Q & Chen G. (2011). Progesterone administration modulates cortical TLR4/NF-κB signaling pathway after subarachnoid hemorrhage in male rats. *Mediators Inflamm* **2011**.

Wangemann P, Wittner M, Di Stefano A, Englert HC, Lang HJ, Schlatter E & Greger R. (1986). Cl(-)-channel blockers in the thick ascending limb of the loop of Henle. Structure activity relationship. *Pflugers Arch* **407,** S128-141.

Webb AR & Holick MF. (1988). The role of sunlight in the cutaneous production of vitamin D_3. *Ann Rev Nutr* **8,** 375-399.

Weinstein AM & Windhager EE. (2001). The paracellular shunt of proximal tubule. *J Membr Biol* **184,** 241-245.

Wes PD, CHEVESICH J, JEROMIN A, ROSENBERG C, STETTEN G & MONTELL C. (1995). TRPC1, a human homolog of a Drosophila store-operated channel. *PNAS* **92,** 9652-9656.

White TA, Xue A, Chini EN, Thompson M, Sieck GC & Wylam ME. (2006). Role of transient receptor potential C3 in TNF-alpha-enhanced calcium influx in human airway myocytes. *Am J Respir Cell Mol Biol* **35,** 243-251.

Wissenbach U, Schroth G, Philipp S & Flockerzi V. (1998). Structure and mRNA expression of a bovine trp homologue related to mammalian trp2 transcripts. *FEBS Letters* **429,** 61-66.

Wray S, Jones K, Kupihayanant S, Li Y, Mathew A, Monir-Bishty E, Noble K, Pierce SJ, Quenby S & Shmygol AV. (2003). Calcium signaling and uterine contractility. *J Soc Gynecol Investig* **10,** 252-264.

Xu SZ, Zeng F, Boulay G, Grimm C, Harteneck C & Beech DJ. (2005). Block of TRPC5 channels by 2-aminoethoxydiphenyl borate: a differential, extracellular and voltage-dependent effect. *British Journal of Pharmacology* **145,** 405–414.

Xu SZ & Beech DJ. (2001). TrpC1 Is a Membrane-Spanning Subunit of Store-Operated Ca2+ Channels in Native Vascular Smooth Muscle Cells. *Circulation Research* **88,** 84-87.

Xu SZ, Zeng F, Boulay G, Grimm C, Harteneck C & Beech DJ. (2005). Block of TRPC5 channels by 2-aminoethoxydiphenyl borate: a differential, extracellular and voltage-dependent effect. *Br J Pharmacol* **145,** 405-414.

Yang H, Mergler S, Sun X, Wang Z, Lu L, Bonanno JA, Pleyer U & Reinach PS. (2005). TRPC4 knockdown suppresses epidermal growth factor-induced store-operated channel activation and growth in human corneal epithelial cells. *J Biol Chem* **280,** 32230-32237.

Yániz, J. L.,, Lopez-Gatius F, Santolaria P & Mullins KJ. (2000). Study of the functional anatomy of bovine oviductal mucosa. *The Anatomical Record* **260,** 268-278.

Yildirim E, Dietrich A & Birnbaumer L. (2003). The mouse C-type transient receptor potential 2 (TRPC2) channel: Alternative splicing and calmodulin binding to its N terminus. *PNAS* **100,** 2220–2225.

Yildirim E, Kawasaki BT & Birnbaumer L. (2005). Molecular cloning of TRPC3a, an Nterminally extended, store-operated variant of the humanC3 transient receptor potential channel. *PNAS* **102,** 3307-3311.

Yu AS, Boim M, Hebert SC, Castellano A, Perez-Reyes E & Lytton J. (1995). Molecular characterization of renal calcium channel beta-subunit transcripts. *Am J Physiol Renal Fluid Electrolyte Physiol Rev* **268,** F525–F531.

Yuan JP, Zeng W, Huang GN, Worley PF & Muallem S. (2007). STIM1 heteromultimerizes TRPC channels to determine their function as store-operated channels. *Nat Cell Biol* **9,** 636-645.

Zeng F, Xu SZ, Jackson PK, McHughD, KumarB, Fountain SJ & Beech DJ. (2004). HumanTRPC5 channel activated by a multiplicity of signals in a single cell. *J Physiol* **559,** 739–750.

Zerwekh JE & Breslau NA. (1986). Human placental production of 1a,25-dihydroxyvitamin D3: biochemical characterization and production in normal subjects and patients with pseudohypoparathyroidism. *J Clin Endocrinol Metab* **62,** 192-196.

Zhang L & SaffenD. (2001). Muscarinic acetylcholine receptor regulation of TRP6 Ca2+ channel isoforms.Molecular structures and functional characterization. *J Biol Chem* **276,** 13331–13339.

Zhang LH, Rodriguez H, Ohno S & Miller WL. (1995). Serine phosphorylation of human P450c17 increases 17,20-lyase activity: implications for adrenarche and the polycystic ovary syndrome. *PNAS* **92,** 10619-10623.

Zhang Z, Tang J, Tikunova S, Johnson JD, Chen Z, Qin N, Dietrich A, Stefani E, Birnbaumer L & Zhu MX. (2001). Activation of Trp3 by inositol 1,4,5-trisphosphate receptors through displacement of inhibitory calmodulin froma common binding domain. *PNAS* **98,** 3168–3173.

Zheng J, Fricke PM, Reynolds LP & Redmer DA. (1994). Evaluation of growth, cell proliferation, and cell death in bovine corpora lutea throughout the estrous cycle. *Biol Reprod* **51,** 623-632.

Zheng W, Magid MS, Kramer EE & Chen YT. (1996). Follicle-stimulating hormone receptor is expressed in human ovarian surface epithelium and fallopian tube. *Am J Pathol***,** 47-53.